# LITHOFACIES, PROVENANCE, AND DIAGENESIS OF JURA-CRETACEOUS STRATA OF THE NORTHERN BOWSER BASIN, BRITISH COLUMBIA

by

HARRISON OWEN COOKENBOO

B.Sc., Duke University, 1981
M.Sc., The University of British Columbia, 1989

A THESIS SUBMITTED IN PARTIAL FULFILLMENT OF THE REQUIREMENTS FOR THE DEGREE OF DOCTOR OF PHILOSOPHY

in

THE FACULTY OF GRADUATE STUDIES

(Department of Geological Science)

We accept this thesis as conforming

to the required standard

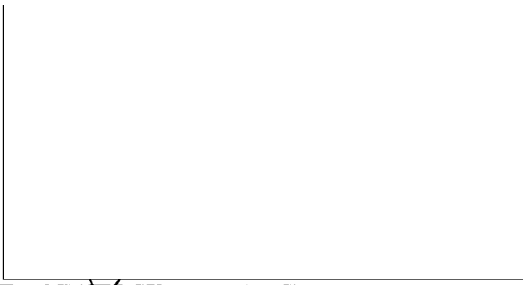

THE UNIVERSITY OF BRITISH COLUMBIA

October 1993

In presenting this thesis in partial fulfilment of the requirements for an advanced degree at the University of British Columbia, I agree that the Library shall make it freely available for reference and study. I further agree that permission for extensive copying of this thesis for scholarly purposes may be granted by the head of my department or by his or her representatives. It is understood that copying or publication of this thesis for financial gain shall not be allowed without my written permission.

(Signature) _____

Department of Geological Sciences

The University of British Columbia
Vancouver, Canada

Date 15 October 1993

DE-6 (2/88)

## ABSTRACT

Lithofacies, provenance, and diagenetic studies of more than 3 km of Late Jurassic to mid-Cretaceous silicilastic sediments exposed in the northern Bowser Basin (northern British Columbia) record the tectonic development of the Canadian Cordillera. Strata are divided into the undivided Bowser Lake Group and overlying Currier, McEvoy, and Devils Claw formations Lithofacies include marine mudstone, coarsening upward mudstone, fining upward sandstone, coarsening upward sandstone, chert pebble conglomerate, and coal. Common lithofacies associations are interpreted as a progression (from older to younger) of shallow marine, lower delta plain, upper delta plain, and alluvial braid-plain depositional environments. A subsidence model based on sediment compaction and isostatic load accounts for the necessary accommodation space.

The composition of the sandstone suggests an obducted island arc and oceanic crust as provenance. Three petrofacies have been identified by modal analysis of framework grains. Petrofacies 1 (P1), which occurs in undivided Bowser Lake Group and Currier Formation strata, ($Q_tFL$ = 34-14-52; $Q_mFL_t$ = 9-14-77) is volcanic lithic rich with subequal to minor chert, minor monocrystalline quartz (generally <10%), and 10-25 % feldspar. Petrofacies 2 (P2) occurs in lower McEvoy Formation, and has higher concentrations of chert reflecting a recycled component in the sandstones, but also retains significant portions of volcanics ($Q_tFL$ = 62-5-33; $Q_mFL_t$ = 5-5-89). Petrofacies 3 (P3) occurs in the upper McEvoy and Devils Claw formations, and is chert rich like P2, with less volcanic lithics and a small but significant portion of metamorphic lithic fragments ($Q_t$=64%, F=5%, L=31%; $Q_m$=7%, F=5%, $L_t$=88%). Paleocurrent directions indicate transport from northeast to southwest.

Microprobe analysis of detrital chromian spinel accessory grains demonstrates alpine type peridotite occurs in the provenance. No spinels typical of mid-ocean ridge or Alaskan type complexes were found. The petrofacies and chromian spinel chemistry are consistent with a provenance from island arc and marginal basin lithosphere obducted onto the western margin of North America.

Diagenetic history of the sediments provides insight into depositional and post depositional

processes in the basin. Seven stages of cement paragenesis are recognized in the sandstones: 1) chlorite; 2) illite; 3) kaolinite; 4) dead oil; 5) quartz; 6) chlorite dissolution; and 7) calcite. Estimated precipitation temperatures begin below 80°C for chlorite, and increase to approximately 100°C to 200°C for quartz, and to above roughly 200°C for calcite. Fluid inclusions in quartz cements support such temperature estimates. The succession of cements is interpreted to record replacement of original connate seawater by acid pore waters derived from organic matter maturation that were forced out by compaction of the interbedded muds. Carbon isotopes in carbonate concretions from the mudstones are consistent with formation during a late stage of methanogenesis. Oxygen isotopes from the same concretions suggest pore fluids in the muds at the time of formation were meteoric to brackish waters typical of cool temperate climates. Organic maturation was modelled by using vitrinite reflectance values from interbedded coals and mudstones, and assuming progressive heating as inferred from the sandstone cement paragenesis. Results of the model indicate that a high paleogeothermal gradient, similar to some back arc basins, best explains the diagenetic history of the northern Bowser Basin.

Constraints from the lithofacies, provenance, and pore water evolution studies suggest the Bowser Basin began as a deep marine basin which was filled by sediment derived from island arc and marginal basin crust obducted earlier onto the western margin of North America.

## TABLE OF CONTENTS

## LIST OF FIGURES

LIST OF TABLES

# ACKNOWLEDGEMENT

Completion of this dissertation has only been possible due to the cooperative and indulgent efforts of numerous friends and colleagues. First, I must acknowledge the support provided by my thesis supervisor Dr. R. M. Bustin, who untiringly read and re-read both this and my earlier Master's thesis. Next, I am happy to have an opportunity to thank M. Dawson of the Institute of Sedimentary and Petroleum Geology, B. Ryan of the British Columbia Ministry of Mines and Energy Resources, E. Swanbergson of Gulf Minerals, and G. Cave of Esso Minerals, who graciously provided logistical support for parts of my field work, and helpfully discussed vagaries of Bowser Basin coal occurrences. Finally, I thank inclusively all the staff (especially Brian Cranston), faculty and my fellow graduate students who provided advice, assistance, and instruction too many times to acknowledge individually, but without whom my research would have been stymied.

Partial funding for this research originated from NSERC (grant A7337 to R. M. Bustin), the Geological Survey of Canada, Esso Minerals, and the British Columbia Ministry of Energy, Mines and Petroleum Resources, and we thank each organization for their support. Electron microprobe analyses were made at the University of British Columbia, using facilities supported by NSERC infrastructure grant #9924. Valuable insights into the chemistry of chromian spinel were provided by conversations with J. K. Russell, G. T. Nixon, and P. R. Roeder. J. Grigsby, A. R. Basu, and an anonymous reviewer provided constructive comments to an earlier version of the detrital chromian spinel chapter, for which I am particularly grateful.

Dedicated and intrepid field assistance was provided by C. Bryan, M. Gant, E. Bergeson and A. Toma, and equally dedicated lab assistance and organization was provided by D. Jacklin.

# PREFACE

Presentation of this dissertation is in the format of four stand-alone chapters, following common practice at the University of British Columbia and most other universities. In order to reduce the repetition that is inevitable with this format, the geologic setting and stratigraphy sections have been deleted from chapters 2, 3, 4 and 5, and are combined under one heading in the introductory chapter (chapter 1). In accordance with the University of British Columbia regulations, I briefly describe below my contribution to published portions of this thesis. Chapter 4, in slightly edited form, has been submitted to the Journal of Sedimentary Petrology for review under the title "Detrital chromian spinel compositions used to reconstruct the tectonic setting of provenance: implications for orogeny in the Canadian Cordillera" by H. O. Cookenboo, R. M. Bustin, and K. R. Wilks. As principal author, I attest that I am responsible for all aspects of the concept, data collection, interpretation and writing of the article, with the exception of running the microprobe during data collection, which was done by Dr. Wilks.

Appendix 1 consists of a formal discussion of MacLeod and Hills (1990). This discussion entitled "Conformable Late Jurassic (Oxfordian) to Early Cretaceous strata, northern Bowser Basin, British Columbia: a sedimentological and paleontological model: Discussion." was published in 1991 in the Canadian Journal of Earth Sciences, (volume 28, p. 1497-1502) with Drs. R. M. Bustin and I. W. Moffat as co-authors. As senior author, I wrote the discussion, conceived the arguments, and drew the conclusions. Drs. Moffat and Bustin initiated stratigraphic work in the Groundhog Coalfield that ultimately led to our age constraints, including collection of the pivotal ammonite data mentioned in the discussion, and additionally provided valuable editorial contributions to the final document.

# CHAPTER 1

## INTRODUCTION

Sediments are multifaceted records of geologic history. Intrabasinal conditions prior to and during sedimentation are preserved by the succession of lithofacies and depositional environments. For example, cratonic basins commonly begin with alluvial sequences followed by lacustrine, evaporite and shallow to deep marine successions, depending on extent of rifting, climate, and rate of sediment accumulation. Extrabasinal conditions are reflected in the provenance record, which depends largely on sediment composition and paleoclimate, both preceding and during deposition. Syn- to post- depositional tectonic conditions within the basin are recorded by authigenic minerals, organic maturation, and structural deformation.

The broad range of geologic data available from sediments makes their study indispensable to understanding evolution of the Canadian Cordillera. Sediments most relevant to orogeny in the Canadian Cordillera are those deposited within or adjacent to the Cordillera, during orogeny and accretion. Such syn-orogenic basins occurred in the Intermontane Belt of the Canadian Cordillera, where they are located between the two principal metamorphic and plutonic belts, the Coast Plutonic Complex to the west and the Omineca Belt to the east. The largest of the Intermontane Belt basins is the Bowser Basin of northern British Columbia, which is the subject of this thesis.

The problem addressed by this thesis is to use detailed sedimentology of northern Bowser Basin strata to constrain postulated accretionary and orogenic processes that resulted in formation of the Cordillera. The basis of this study are forty-nine stratigraphic sections that were measured and described in the vicinity of the Groundhog coalfield in the northern Bowser Basin. Samples collected from those sections were later analyzed in the laboratory by methods including transmitted and reflected light microscopy, scanning electron microscopy, electron microprobe, fluid inclusion microthermometry, micro Fourier transform infrared spectroscopy, x-ray diffraction, stable isotope geochemistry, vitrinite reflectance, and computer modelling of organic maturation. Three principal approaches were employed

in this study: 1) description of lithofacies and interpretation of depositional environments leading to a plausible model of basin origin and development; 2) quantification of sandstone composition leading to a description of provenance and a model of tectonic origin for the sediment source rocks; and 3) diagenetic studies to constrain pore water evolution, leading to a well-constrained thermal maturation model for the basin.

Lithofacies in the northern Bowser Basin are described in detail in Chapter 2. The lithofacies are derived from detailed measurement and description of 49 stratigraphic sections selected on the basis of exposure and continuity as determined from air photos. The depositional environment model builds upon earlier stratigraphic work which established a general trend to shallower marine deposition upward from the base of the Bowser Basin strata, into overlying deltaic and alluvial plain strata of the Groundhog Coalfield (Malloch, 1914; Buckham and Latour, 1950; Eisbacher, 1974; Bustin and Moffat, 1983; Moffat, 1985; Cookenboo, 1989; Ricketts, 1990). In this study, lithofacies and lithofacies associations are interpreted to represent marine shelf, prodelta, delta, and alluvial plain depositional environments. In addition, the succession of lithofacies associations indicates a depositional history which involved a deep marine basin filled first by progressively shallower marine deposits, and subsequently by near sea-level deposition of deltaic, delta plain, and alluvial braid-plain sediments.

Chapter 3 describes the methods and results of a provenance study based on modal analysis of the sandstones. This study extends provenance interpretations originating in the early part of this century, which associated the abundant chert pebbles with chert rich strata of the Cache Creek terrane located north of the Bowser Basin (Malloch, 1914; Eisbacher, 1981). The most significant observation in this study is that the sandstones are lithic rich, changing from dominantly volcanic lithic fragments in older strata, to dominantly chert in overlying younger strata. These changing compositions are split into three petrofacies, and each petrofacies is interpreted in terms of likely composition of its provenance. Petrofacies 1 was derived from obducted island arc and oceanic crust. Petrofacies 2 was derived from similar source rocks, but increased chert content suggests an additional component of recycled sediments. Petrofacies 3 is interpreted as derived from obducted island arc and oceanic crust, with a large recycled

component and an additional small but significant component of metamorphic and plutonic source.

A question remaining from the framework grain modal analysis is - what kind of oceanic crust is included in the provenance? This question is addressed in Chapter 4 by using microprobe analyses of detrital chromian spinels that occur as accessory grains in most northern Bowser Basin sandstones. Chromian spinel compositions are distinct for a number of ultramafic petrogenetic origins, including stratiform complexes, Alaskan type peridotites, back-arc basins, and mid-ocean ridges. Detrital spinel compositions in Bowser Basin sandstones are most compatible with an unmetamorphosed island arc and marginal basin crust origin, and suggest that mid-ocean ridge or Alaskan-type complexes did not contribute (at least significantly) to the northern Bowser Basin.

Chapter 5 describes pore water evolution in northern Bowser Basin sediments based on observations of sandstone cement paragenesis, mudstone concretion mineralogy, and stable isotope geochemistry. Previous analyses of basin maturation have centred on vitrinite reflectance studies (Bustin and Moffat, 1983; Moffat, 1985; Bustin, 1984; Bustin and Moffat, 1989) which yield interpreted maximum temperatures, but are ambiguous as to whether maximum temperatures were reached early as a function of progressive heating during burial, or later in response to possible tectonic events. Diagenetic observations in this study enhance the maturation models based on vitrinite reflectance alone by clarifying thermal history and pore water evolution prior to the sediments reaching maximum temperatures. Seven stages of sandstone cement paragenesis were found: 1) chlorite; 2) illite; 3) kaolinite; 4) dead oil; 5) quartz; 6) chlorite dissolution; and 7) calcite. From these sandstone cement stages, pore water evolution is interpreted as initially saline to brackish marine water being replaced first by acid waters and migrating oil associated with organic maturation, and later by alkaline waters following thermal breakdown of organic acids at roughly 200°C. The successive cement stages and interpreted pore water evolution are consistent with progressive heating during burial to temperatures in excess of 200°C. Geochemistry of mudstone cements, as preserved in carbonate concretions, suggests interbedded organic rich muds were the source of the acid pore waters, derived probably by dewatering during burial compaction. Thermal maturation modelling consistent with the pore water history and

vitrinite reflectance values suggests burial in a very high paleogeothermal gradient regime (60° to 65° C/km).

## GEOLOGIC SETTING AND STRATIGRAPHY

Sedimentary strata examined in this study were deposited in the Bowser Basin, which is the largest basin in the Intermontane Belt of the Canadian Cordillera. The Bowser Basin is located in northern British Columbia between the two principal metamorphic and plutonic belts of the Canadian Cordillera, the Coast Plutonic Complex to the west and the Omineca Belt to the east (Fig. 1-1). The study area is located in the northern part of the Bowser Basin, approximately coincident with the traditional and informal limits of the Groundhog Coalfield (Fig. 1-2). The sediments were deposited during the Middle Jurassic through Early (and perhaps earliest Late) Cretaceous, and today are bound on all sides by older volcanic and plutonic rocks except at the eastern margin where younger sediments of the Sustut Basin cover the Bowser Basin. The northern and southern limits of Bowser Basin clastics are the Stikine (north) and Skeena (south) arches. Although the present limits of the Basin are defined sharply, only an eastern boundary is known during deposition, and the basin may have been open to the west (Ricketts, 1990).

Clastic sedimentation in the Bowser Basin was initiated during the Middle Jurassic with deep-water turbidites and shales of the Bowser Lake Group (Tipper and Richards, 1976). Progressively shallower marine facies were deposited until the Late Jurassic when interbedded shallow marine, deltaic, and fluvio-deltaic facies began accumulating. The youngest sediments preserved in the Bowser Basin are fluvial and fluvio-deltaic strata deposited during the Early to mid-Cretaceous. The minimum total thickness of Bowser Basin strata, calculated by adding data in Ricketts (1990) to measurements from the study area is in excess of 5 kilometres (Cookenboo and Bustin, 1990). The true total thickness could significantly exceed this minimum estimate, due to complex structural development following

Figure 1-1: Location of the study area in the Bowser Basin and adjacent features of the Canadian Cordillera.

Figure 1-2: Stratigraphic exposures measured in this study are located near the Groundhog Coalfield, within the northern Bowser Basin.

deposition. These sediments were subsequently buried by as much as three to five kilometres (Bustin, 1984) of now eroded rocks. The eroded beds were presumably at least in part equivalent to Upper Cretaceous and Tertiary alluvial strata preserved east of the Bowser in the Sustut Basin. An angular unconformity separates Sustut rocks from clastic and volcaniclastic rocks equivalent to the lower part of the Bowser Basin section (Eisbacher, 1974).

Structural deformation in the Bowser Basin has included at least two and possibly three phases of deformation beginning in the Early to mid-Cretaceous (Moffat, 1985; Moffat and Bustin, 1993). This complex deformational history has led to an estimated 35% to 45% shortening across the basin (Moffat, 1985; Evenchick, 1991).

Basement rocks are not exposed in the study area. Along the southern margin of the basin, however, thick island arc volcanic sequences of the Upper Triassic Takla Group and Lower to Middle Jurassic Hazelton Groups underlie clastic marine strata which comprise the base of the Bowser Basin section (Tipper and Richards, 1976). Hazelton Group volcanics are also exposed along the northeastern basin margin where they are separated from the clastic Bowser Basin strata by a relatively thin (<250 metres) volcaniclastic and thin bedded siltstone unit termed the Spatsizi Group (Thomson *et al.*, 1986). Pillow basalts and basinal sediments of the Lower to Middle Jurassic Salmon River Formation and older strata are exposed at the western margin of the basin (Lewis *et al.*, 1993).

A window to older basement rocks exists at Oweegee Dome near the western margin of the Bowser Basin (Fig. 1-1), where Greig (1991) reports Paleozoic limestones and cherts exposed beneath Hazelton and earlier Mesozoic volcanic strata. No older basement is known.

### *Stratigraphy in the study area*

Four lithostratigraphic units are recognized in the study area (Cookenboo and Bustin, 1989). From oldest to youngest, they are undivided Bowser Lake Group, and the Currier, McEvoy and Devils Claw Formations (Fig. 1-3). Formal definitions and detailed descriptions of the Currier,

Figure 1-3: Stratigraphic column. Lithostratigraphic units used in this study are listed under the heading "Northern Bowser Basin".

McEvoy, and Devils Claw Formations are provided in Cookenboo and Bustin (1989), with extensions and further information resulting from three subsequent years of fieldwork described in Cookenboo and Bustin (1990a), Cookenboo and Bustin (1990b), and Cookenboo and Bustin (1991). Summary descriptions of the stratigraphic units and nomenclature used in this thesis are given below, based on integration of Cookenboo and Bustin (1989) with subsequent years fieldwork as described in the fieldwork summaries mentioned above Cookenboo and Bustin (1990a), Cookenboo and Bustin (1990b), and Cookenboo and Bustin (1991) and Cookenboo (1989). Age of the stratigraphic units are derived from data presented in Bustin and Moffat (1983), Moffat (1985), Moffat *et al.* (1988), Cookenboo and Bustin (1989), MacLeod and Hills (1990) and Cookenboo (1989). A fuller discussion of the ages is presented in Cookenboo et al. (1991: Appendix 1), but conservatively the McEvoy can be called Early Cretaceous and possibly in part middle Albian in age.

The base of the exposed section in the sampled area is termed undivided Bowser Lake Group in this thesis, and consists of a dark grey to black marine mudstone unit that coarsens in the upper part to include prodelta sandstones and siltstones. Thickness is poorly constrained because the base is not known, but estimates range upwards of 2000 metres (Moffat, 1985). The upper part of this unit contains *Buchia concentrica*, which suggests an age of late Oxfordian to early Kimmeridgian (Poulton *et al.*, 1991). Progressively older marine beds north of the study area suggest that undivided Bowser Lake Group is as old as the Middle Jurassic (Poulton *et al.*, 1991). Similar dark grey to black marine mudstones of the Ashman Formation in the southern Bowser Basin span the late Bajocian to the top of the early Oxfordian (Tipper and Richards, 1976). The undivided Bowser Lake Group in the study area is largely equivalent in lithology and age to the Ashman Formation, but because of inconsistencies in usage of the term 'Ashman Formation' in different parts of the basin (Cookenboo and Bustin, 1991), and a lack of demonstrated continuity with the Ashman Formation strata in the southern Bowser Basin, the less specific name 'undivided Bowser Lake Group' is used in this thesis.

The Currier Formation consists of as much as 1000 m of interbedded shales, siltstones, sandstones, coals and authigenic carbonate layers (Cookenboo and Bustin, 1989; 1990a) that overlie the

marine beds of the undivided Bowser Lake Group. The Currier Formation is exposed from south of Maitland Creek at the northeast edge of the study area to the Groundhog Range in the south (Fig. 1-2). Based on the ammonite *Amoeboceras* collected from the lower portion of the coal bearing section (Moffat *et al.*, 1988), and Late Jurassic dinoflagellate suites (Rouse, written communication, 1989) the Currier Formation is suggested to be in part Late Jurassic. MacLeod and Hills (1990) suggest the Currier Formation may be in part earliest Cretaceous as well, based on their recovery of latest Jurassic species of *Buchia* from beneath coal-bearing strata, and probably Neocomian the astariid bivalve *Herzogina* from within the formation.

The McEvoy Formation consists of 600 m to approximately 1000 m of fluvio-deltaic siltstones and shales with minor sandstones, thin coals, authigenic carbonate layers, and conglomerates (Bustin and Moffat, 1983; Cookenboo and Bustin, 1989; Cookenboo and Bustin, 1990a; Cookenboo and Bustin, 1990b; and Cookenboo and Bustin, 1991). The McEvoy Formation is exposed between the Skeena and Nass rivers from south of Mount Klappan in the north to Devils Claw Mountain in the south. Strata exposed south of Sweeney Creek and between the Nass River and Konigus Creek are also assigned to the McEvoy Formation, and in this area the formation may be as much as 1500 m thick Cookenboo and Bustin, (1990b). The McEvoy lacks marine body fossils but has been dated based on palynoassemblages as late Barremian or Aptian to late middle Albian (Moffat *et al.*, 1988; Cookenboo and Bustin, 1989). Plant macrofossils have been used recently to suggest an earlier (pre-Albian) Cretaceous age (MacLeod and Hills, 1990) for the McEvoy Formation.

The Devils Claw Formation consists of up to 600 m of fluvio-deltaic and coastal plain strata characterized by thick pebble and cobble conglomerates, with associated coarse sandstones and minor siltstones and shales. Exposure of the Devils Claw Formation is limited to the area the Skeena and Nass rivers south of Mount Klappan and north of Devils Claw Mountain (Fig. 1-2). The conglomeratic strata of the Devils Claw overlie the McEvoy Formation, and are Albian (Early Cretaceous) to perhaps earliest Late Cretaceous (Cenomanian; Moffat *et al.*, 1988; Cookenboo and Bustin, 1989).

No younger strata are preserved above the Devils Claw Formation. To the east and south east of the study area, alluvial strata of the Sustut Group (reported age range of mid-Cretaceous to Paleocene) unconformably overlie rocks of the Bowser Lake Group (Eisbacher, 1974).

## REFERENCES

Buckham, F., and Latour, B. A., 1950. The Groundhog coalfield, British Columbia. Geological Survey of Canada, Bulletin 16, 82 p.

Bustin, R. M., 1984. Coalification levels and their significance in the Groundhog Coal field, north-central British Columbia. International Journal of Coal Geology, v. 4, p. 21-44.

Bustin, R. M., and Moffat, I. 1983. Groundhog Coalfield, British Columbia: reconnaissance stratigraphy and structure. Bulletin of Canadian Petroleum Geology, 31: 231-245.

Bustin, R. M., and Moffat, I. W., 1989. Semianthracite, anthracite and meta-anthracite in the central Canadian Cordillera: their geology, characteristics and coalification history. International Journal of Coal Geology, v. 13, p. 303-326.

Cookenboo, H. O., 1989. Lithostratigraphy, palynostratigraphy, and sedimentology of the northern Skeena Mountains and their implications to the tectonic history of the Canadian Cordillera. MSc. thesis, University of British Columbia, Vancouver British Columbia. 131 p.

Cookenboo, H. O., and Bustin, R. M., 1989. Jura-Cretaceous (Oxfordian to Cenomanian) stratigraphy of the north-central Bowser Basin, northern British Columbia: Canadian Journal of Earth Sciences, v. 26, p. 1001-1012.

Cookenboo, H. O., and Bustin, R. M. 1990a. Stratigraphy of coal occurrences in the Bowser Basin. *in* Geological Fieldwork 1989. British Columbia Ministry of Energy, Mines and Petroleum Resources, Paper 1990-1, pp. 473-477.

Cookenboo, H. O., and Bustin, R. M. 1990b. Lithostratigraphy of the northern Skeena Mountains, British Columbia: Current Research, Part F, Geological Survey of Canada Paper 90-1F, p. 151-156.

Cookenboo, H. O., and Bustin, R. M. 1991. Coal-bearing facies in the northern Bowser Basin (104A, H): British Columbia Ministry of Energy, Mines and Petroleum Resources, Geological Fieldwork 1990, Paper 1991-1, p. 415-418.

Cookenboo, H. O., Bustin, R. M., and Moffat, I. W., 1991. Conformable Late Jurassic (Oxfordian) to Early Cretaceous strata, northern Bowser Basin, British Columbia: a sedimentological and paleontological model: Discussion. Canadian Journal of Earth Sciences, v. 28, p. 1497-1502.

Eisbacher, G. H., 1974. Sedimentary and tectonic evolution of the Sustut and Sifton Basins, north-central British Columbia. Geological Survey of Canada Paper 73-31, 57 p.

Eisbacher, G., 1981. Late Mesozoic - Paleogene Bowser Basin molasse and Cordilleran tectonics, western Canada, *In* Miall, A. D. (ed.), Sedimentation and Tectonics. Geological Association of Canada, Special Paper 23, p. 125-151.

Evenchick, C. A., 1991. Geometry, evolution and tectonic framework of the Skeena fold belt, north central British Columbia. Tectonics, v. 10, p. 527-546.

Greig, C. J., 1991. Stratigraphic and structural relations along the west-central margin of the Bowser Basin, Oweegee and Kinskuch areas, northwestern British Columbia. Geological Survey of Canada Current Research Part A, Paper 91-1A, P. 197-205.

Lewis, P. D., Thompson, J. F. H., Nadaraju, G., R. G. Anderson, and G. G. Johnson, 1993. Lower and Middle Jurassic stratigraphy in the Treaty Glacier area and geological setting of the Treaty Glacier alteration system, northwestern British Columbia. Geological Survey of Canada Current Research Part A, Paper 93-1A, p. 75-86.

MacLeod, S. E., and Hills, L. V. 1990. Conformable Late Jurassic (Oxfordian) to Early Cretaceous strata, northern Bowser Basin, British Columbia: A sedimentological and paleontological model. Canadian Journal of Earth Sciences, v. 27, p. 988-998.

Malloch, G. S., 1914. Groundhog coal field. Summary report of the Geological Survey Department of Mines, p. 69 to 101.

Moffat, I. W. 1985. The nature and timing of deformational events and organic and inorganic metamorphism in the northern Groundhog Coalfield: implications for the tectonic history of the Bowser Basin. Ph.D thesis, University of British Columbia, Vancouver, B.C.

Moffat, I. W., and Bustin, R. M., 1993. Deformational history of the Groundhog Coalfield, northeastern Bowser Basin, British Columbia: styles, superposition and tectonic implications. Bulletin of Canadian Petroleum Geology, v. 41, p. 1-16.

Moffat, I. W., Bustin, R. M., and Rouse, G. E. 1988. Biochronology of selected Bowser Basin strata: tectonic significance. Canadian Journal of Earth Sciences, v. 25 p. 1571-1578.

Poulton, T. P., Callomon, J. H., and Hall, R. L., 1991. Bathonian through Oxfordian (Middle and Upper Jurassic) marine macrofossil assemblages and correlations, Bowser Lake Group, west-central Spatsizi map area, northwestern British Columbia. Current Research, Part A, Geological Survey of Canada Paper 91-1A, p. 59-63.

Ricketts, B. D. 1990, A preliminary account of sedimentation in the lower Bowser Lake Group, northern British Columbia, *In* Current Research, Part F, Geological Survey of Canada, Paper 90-1F, p. 145-150.

Thomson, R. C. Smith, P. L. and Tipper, H. W. 1986. Lower to Middle Jurassic (Pliensbachian to Bajocian) stratigraphy of the northern Spatsizi area, north-central British Columbia. Canadian Journal of Earth Sciences, v. 23, p. 1963-1973.

Tipper, H. W. and Richards, T. A., 1976. Jurassic stratigraphy and history of north-central British Columbia. Geological Survey of Canada, Bulletin 270, 73 p.

# CHAPTER 2

# LITHOFACIES IN THE NORTHERN BOWSER BASIN, BRITISH COLUMBIA: FILLING OF A DEEP MARINE BASIN AND SUBSEQUENT ISOSTATIC ADJUSTMENT

## ABSTRACT

Thick Jura-Cretaceous siliciclastic strata of the northern Bowser Basin contain a record of Cordilleran orogeny that can be understood, in part, by analyzing their lithofacies and reconstructing depositional history. The strata examined in this study belong to four stratigraphic units exposed in the vicinity of the Groundhog coalfield. The units are, from oldest to youngest, undivided Bowser Lake Group strata, and the Currier, McEvoy, and Devils Claw formations. Lithofacies recognized in this study are defined on grain size, biotic features, bedding geometry, sedimentary structures, and composition (for conglomerates). They consist of marine mudstone, black to dark gray claystone, coarsening upward mudstone, fining upward sandstone, coarsening and thickening upward sandstone, chert pebble conglomerate, and coal. Associations of lithofacies differ in each of the four stratigraphic units exposed in the northern Bowser Basin: 1) marine facies association (undivided Bowser Lake Group); 2) lower delta plain facies association (Currier Formation); 3) upper delta plain facies association (McEvoy Formation) and 4) alluvial braid plain facies association (Devils Claw Formation). As the designations imply, these four lithofacies associations are interpreted as having genetic significance, and the vertical succession reflects development of the basin.

The succession of lithofacies associations records filling of a pre-existing deep marine basin, first with thick basinal and slope sediments (exposed outside the study area), followed by more than 3000 m of `near sea-level' (shallow marine to deltaic to coastal plain) sediments. Calculation of compaction and lithostatic loading effects demonstrate that merely filling a pre-existing marine basin more than 3000 m deep is sufficient mechanism to explain the origin of the Bowser Basin and subsequent creation of accommodation space necessary for the entire near sea-level stratigraphic column. By this model, compaction and lithostatic loading of the marine basin fill create accommodation space near sea-level that is filled first by shallow marine shelf sediments, later by delta plain sediments, and finally by alluvial braid plain sediments. This constitutes a sediment driven model that requires no other tectonic factors,

such as thrust fault loading, to explain the subsidence of the basin.

## INTRODUCTION

Sediment accumulation closely reflects tectonic setting. Cratonic sedimentary basins tend to accumulate shallow water and/or subaerial sediments relatively slowly. Many foreland basins accumulate thick shallow marine to alluvial sediments in response to tectonic thrust loading. Continental margin basins, in contrast to both foreland and cratonic basins, may accumulate siliciclastic sediments in depositional environments as diverse as deep ocean fans to subaerial alluvial fans as rapidly as sediment supply allows. Because sedimentation is directly controlled by tectonic conditions, understanding lithofacies and lithofacies successions may permit inferences to be made concerning tectonic controls on the basin.

The purpose of this chapter is to provide lithofacies descriptions and interpretations of depositional environments for the siliciclastic succession that in turn forms the basis of inferences about the tectonic setting of the basin.

## FACIES DESCRIPTIONS

Measured exposures were divided into facies based on their lithologic and biologic components, and some of the facies were further divided into subfacies (Fig. 2-1). The facies and subfacies are described below for each of the four stratigraphic units in the study area (Chapter 1). Because some facies occur in more than one unit some repetition is inevitable. An interpretation of the depositional history follows the facies descriptions for each unit.

Terminology used in descriptions of fine-textured sediments vary widely in the literature. In this study, terminology is based on Blatt *et al.*, (1972) and Collinson and Thompson (1989). Mudstone is applied to lithified sediments in which clays and silts are mixed between 1/3 and 2/3, or more generally in unspecified amounts. Claystone is applied more precisely to lithified sediments dominated

Figure 2-1: Facies described in text (subfacies in parentheses). Within each formation heading, the facies are listed in approximate order of decreasing abundance.

| STRATIGRAPHIC UNIT: | FACIES: |
|---|---|
| **Devils Claw Formation** | Fining Upward Chert Pebble-Cobble Conglomerate (FUCPCC)<br>Coarsening Upward Mudstone (CUM)<br>Black claystone (BC homogeneous + carbonaceous)<br>Thin coal |
| **McEvoy Formation** | Coarsening Upward Mudstone (CUM)<br>Black claystone (BC homogeneous + carbonaceous)<br>Fining Upward Sandstone (FUS)<br>Coarsening and Thickening Upward Sandstone (CUS)<br>Chert Pebble-Cobble Conglomerate (CPCC)<br>Thin coal |
| **Currier Formation** | Black claystone (BC laminated + homogeous + carbonaceous)<br>Fining Upward Sandstone (FUS)<br>Coarsening and Thickening Upward Sandstone (CUS)<br>Interbedded claystone, siltstone and very fine sandstone (ICSS)<br>Thick coal<br>Chert Pebble Conglomerate- well sorted (CPCws) |
| **undivided Bowser Lake Group** | Marine Mudstone (MM)<br>Coarsening and Thickening Upward Sandstone (CUS)<br>Fining Upward Sandstone (FUS) |

by (>2/3) clay, and siltstone is applied to lithified sediments that appear in the field to be dominated by (>2/3) silt.

## UNDIVIDED BOWSER LAKE GROUP

Undivided Bowser Lake Group crops out surrounding the Groundhog coalfield, and was examined in 10 sections (Fig. 2-2), including four sections in which the contact with the overlying Currier Formation was encountered. The thickest apparently continuous stratigraphic section measured was 617 m (section 49 located south of the Klappan River Fig. 2-2 and 2-3). The total thickness of the undivided Bowser Lake Group is poorly constrained because no base to the unit occurs in the study area. Similar facies that probably correlate with those described below occur to the north of the study area (Ricketts, 1990; Poulton *et al*, 1991), west of the Klappan River (Evenchick and Green, 1990), at Notchtop Peak in the Slamgeesh Mountains (Jeletzky, 1976; Cookenboo and Bustin, 1990), and along the southern margin of the Bowser Basin (Tipper and Richards, 1976; Richards and Jeletzky , 1974). The age of the unit ranges from late Bajocian to the end of the early Oxfordian in the southern part of the Bowser Basin (Tipper and Richards, 1976), and to as young as late Oxfordian or early Kimmeridgian in the northern part of the basin (Poulton *et al.*, 1991).

The undivided Bowser Lake Group strata exposed in the study area are characterized by three facies described below (Fig. 2-1). The dominant facies are marine mudstone and coarsening and thickening upward sandstones. The third and relatively minor facies is fining upward sandstone.

### *Marine mudstone facies*

The marine mudstone (MM) facies consists of recessive weathering, dark blue-black claystone; silty claystone in light to medium brown laminae; and thin interbeds of siltstone or very fine sandstone. The MM facies is typically 10s to 100s of metres thick, and is pervasively burrowed by a variety of trace fossils (abundant *Helminthopsis* (Fig. 2-4), with less abundant *Teichichnus*, *Chondrites*, *Zoophycus*, *Skolithos*, and *Rhizocorallium*). The brown laminae are normally graded from 3 to 10 cm thick, with the

Figure 2-2: Geological map based on sections measured in this study. Sections numbers are the same as used in text.

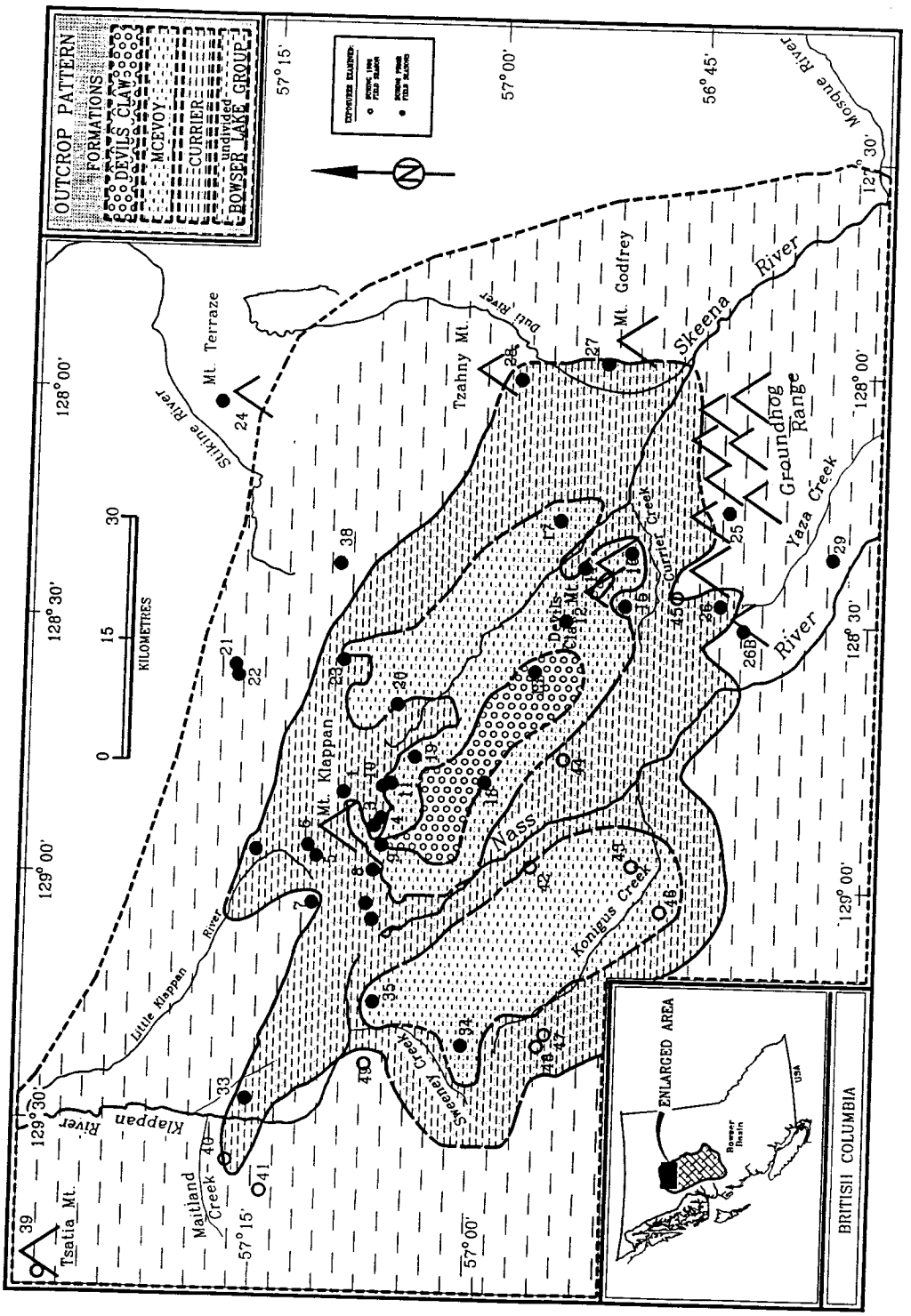

Figure 2-3: Marine mudstones are interbedded with coarsening upward sandstones in section 49, an interpreted succession of repeatedly stacked prodelta to delta front lobes.

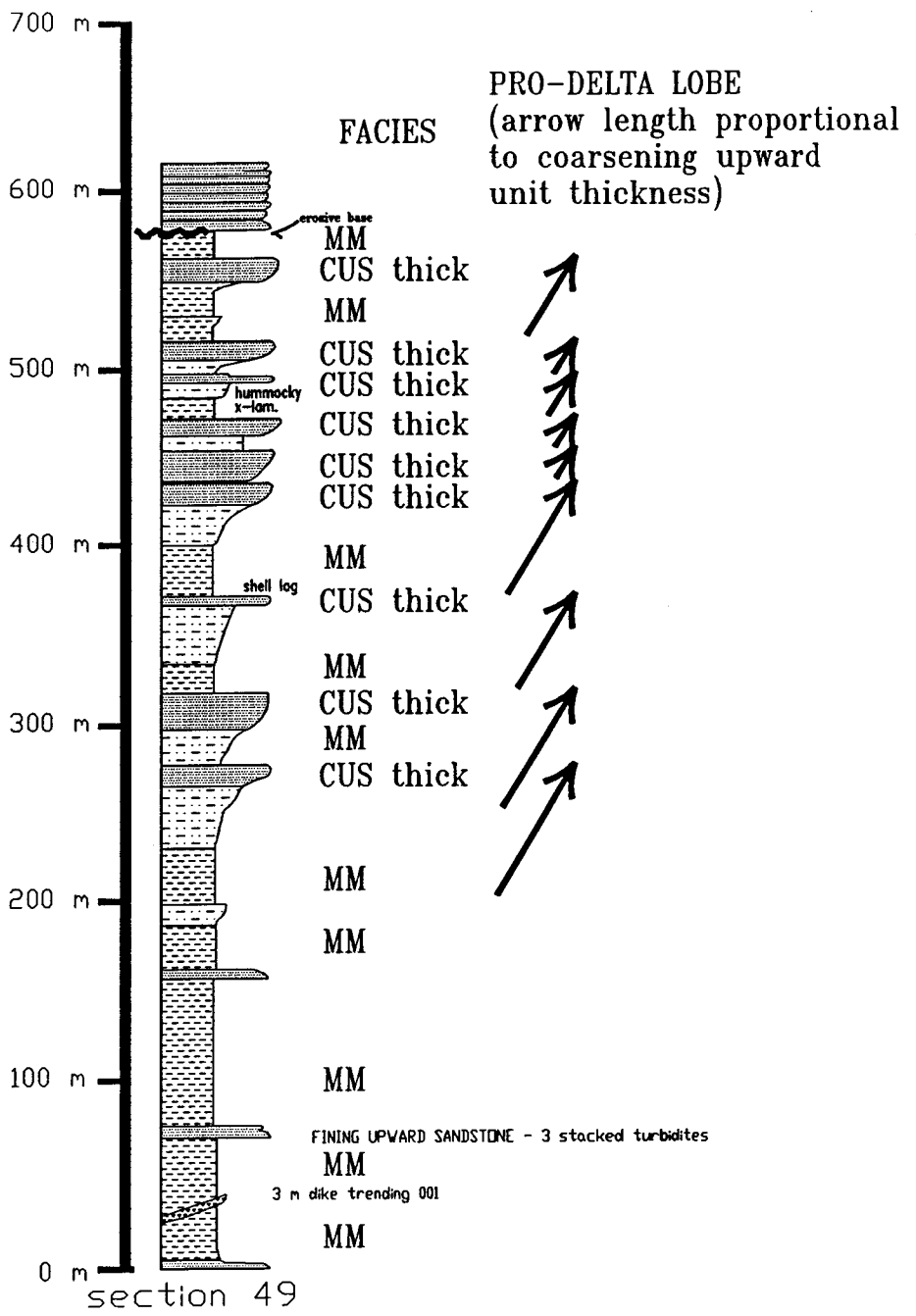

Figure 2-4: Bedding surface of marine mudstone facies from the undivided Bowser Lake Group extensively burrowed by *Helminthopsis*.

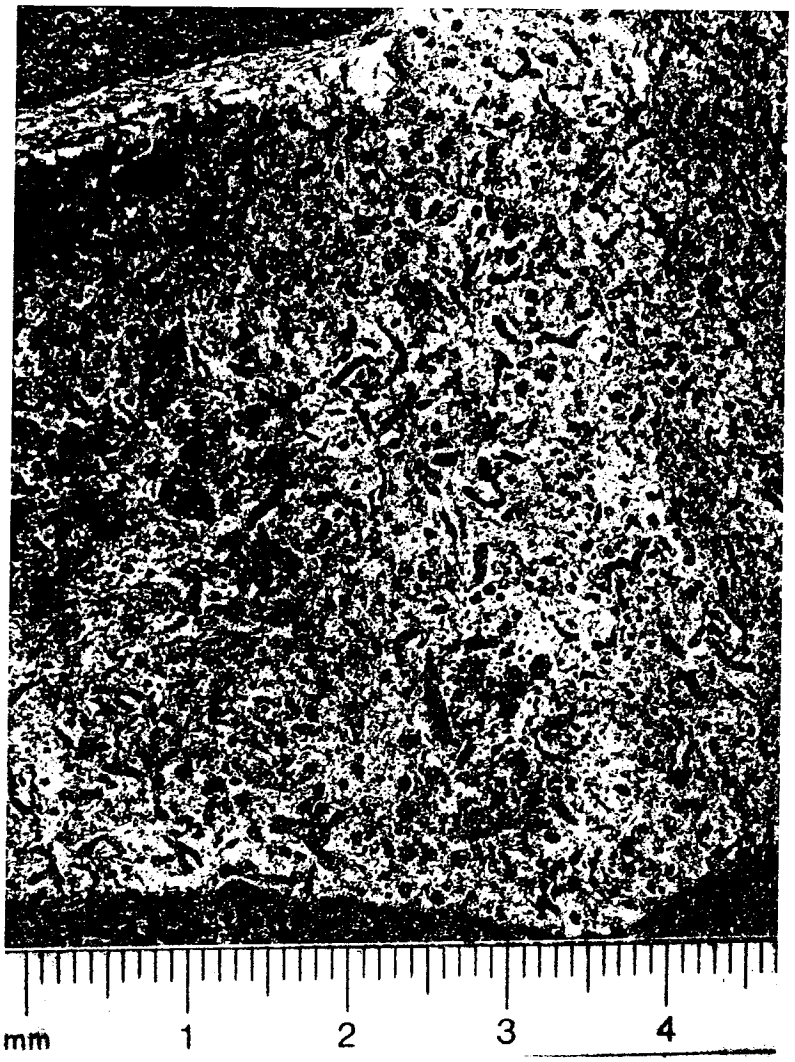

basal portion (up to 50%) of each layer composed of sharp based, normally graded sandstone or siltstone, which locally is rippled or finely cross laminated. The basal sandstone or siltstone is covered by claystone, which is commonly thoroughly bioturbated by *Helminthopsis*. A general trend in the MM facies is change from pervasively burrowed mudstone in stratigraphically low exposures to mudstone with fewer trace fossils higher in the section. As intensely burrowed mudstones become rare, ripples within interbedded sandstones become abundant, and hummocky cross beds occur rarely. Normally graded silt- or sandstone layers are regularly spaced within each marine mudstone bed, but spacing varies from one normally graded layer per 2 metres to as many as five in 15 cm in different areas. The thickness of the normally graded layers is also nearly constant within a single bed, but varies from thin laminae less than 0.5 cm thick to thin beds as much as 5 cm thick in different areas. Interbedded normally graded layers are generally thicker and more abundant in the upper portions of the MM facies. In addition to being generally coarser, normally graded layers in the upper portion of the MM facies commonly exhibit abundant ripples and contain relatively few trace fossils, in contrast to the lower portions of the MM facies in which ripples are rare, and biogenic structures abundant (Fig. 2-5). Marine invertebrate fossils are common in MM facies of the Bowser Basin, and plant debris is mostly absent. Yellow-brown weathered authigenic ferroan dolomite layers spaced 10 to 20 m vertically apart occur near the upper limit of MM occurrence.

### *Coarsening Upward Sandstone*

The coarsening and thickening upward sandstone facies (CUS) consists of resistant, light to medium brown weathered, sandstone and siltstone (grey to dark grey on fresh surfaces) that occurs in composite and generally parallel thin to thick beds. Grain size increases upward with bed thickness, from very fine to fine grained in thin beds near the base up to fine and less commonly medium grained sandstone near the top. Typically, the base is gradational with underlying mudstones and near the base, siltstone interbeds make up as much as 50% of the bed. In contrast, the top contact is sharp and siltstone interbeds become thin and rare near the top. The overall thickness of CUS in the undivided Bowser Lake Group, from the gradational base to the sharp upper contact, ranges from 8 up to 40 m. Symmetrical

Figure 2-5: Normally graded sandy siltstone layers separated by blue-black shale. These layers are typical of extensively burrowed, normally graded siltstone and sandstone layers from the marine mudstone facies.

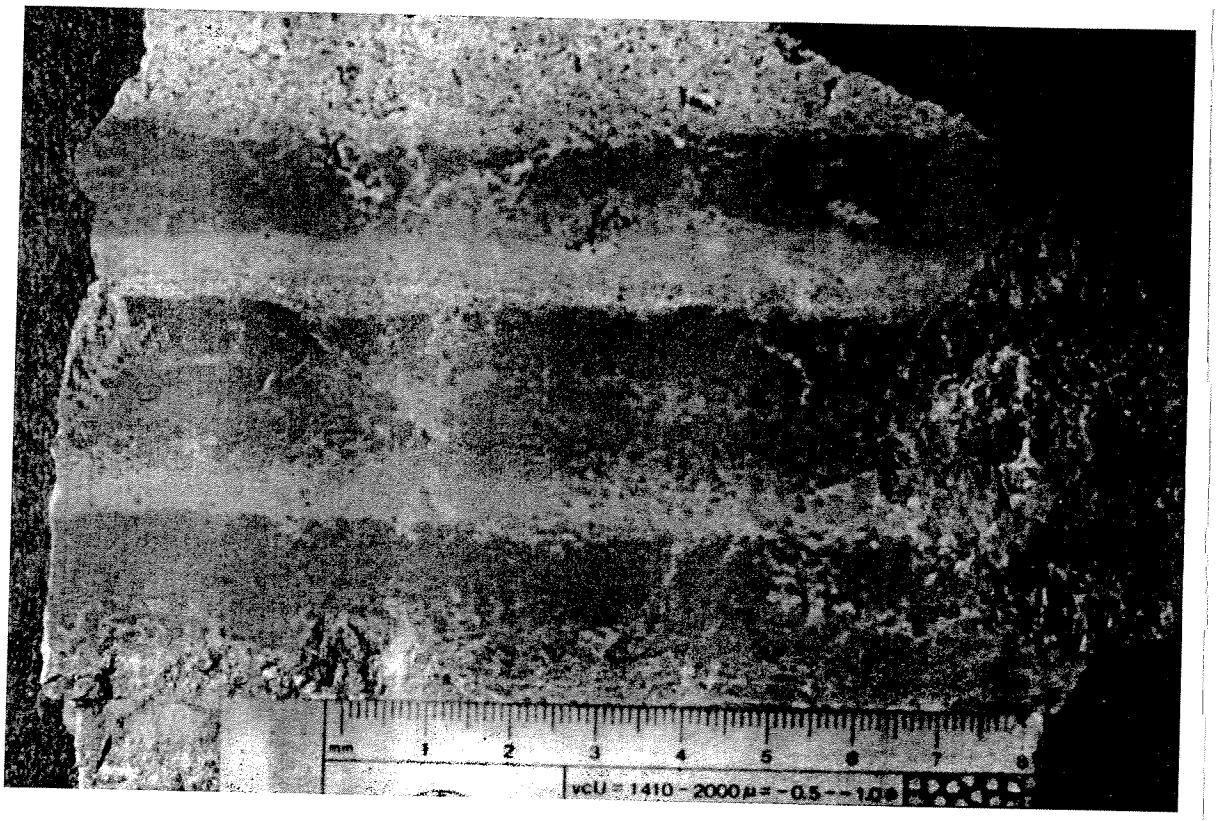

ripples (wave ripples) are common in the thinly bedded sandstones near the base of CUS. Trough cross beds occur in the thick upper sandstones in some coarsening upward units. Along the northeast margin of the study area (sections 22 and 38 in figure 2-2), some CUS contain disarticulated shell beds, and concentrations of chert pebbles (less than 5 cm diameter) in layers near their upper contacts. Some of these chert pebble layers define low angle (less than 10°) cross beds which dip to the southwest (towards the basin). Such shell and pebble layers are rare in sections 25, 26, 45 and 49 to the southwest (locations given in figure 2-2). CUS is associated with invertebrate-bearing mudstones in adjacent facies of undivided Bowser Lake Group. Thick CUS generally lack leaf fossils or other coarse plant debris, either within the facies or in adjacent mudstones.

*Fining upward sandstone facies*

Fining upward sandstone facies in the undivided Bowser Lake Group ($FUS_{marine}$) consists of fine and medium grained sandstone near the usually erosive basal contact, commonly with lode casts, and fines upward to very fine sandstone near the gradational, or less commonly sharp, upper contact. The sandstone is well sorted, and near the base, beds are structureless, up to 2 m thick, and commonly contain rounded rip-up clasts of mudstone that in some beds are as large as boulders. The very fine grained sandstone near the top of each $FUS_{marine}$ is commonly rippled. Siltstone or claystone layers occur gradationally above the very fine sandstone. Locally, $FUS_{marine}$ units occur stacked as many as three times.

*Depositional environments of undivided Bowser Lake Group facies:*

The stacked normally graded layers that comprise most of the marine mudstone facies are similar in form to the tempestites described by Aigner (1985) in modern and ancient sediments, and were probably similarly deposited from suspension by bottom currents possibly related to storms. Similar normally graded thin sands also originate from the Yukon Delta during rapidly waning flow following extreme storm surge, and have spread more than 100 km offshore across the shallow shelf of the Norton Sound, Alaska (Nelson, 1982). The graded sand layers of Norton Sound described by Nelson (1982)

exhibit distal to proximal increases in thickness, bioturbation, coarseness, and current structures similar to the vertical changes in MM facies of the Bowser Basin.

The relative paucity of trace fossils in the upper portions of MM facies is consistent with a stressed biologic community, suggesting rapid sediment aggradation and possibly brackish water conditions (Pemberton and MacEachern, 1992). The decrease in trace fossil abundance and increase in current and oscillatory sediment structures in MM facies from low in the undivided Bowser Lake Group to near the top of the unit suggest shallowing upward from outer shelf (below wave base) to shallow shelf (above wave base) deposition. In light of this repeated shallowing trend and the fact that deltaic facies overlie the MM facies (as described later in this chapter), it is likely that MM was deposited as prodelta shelf muds seaward of a prograding delta system.

The MM facies is gradationally overlain by thick CUS, which represent sands that have prograded into shallow shelf environments. Given their great thickness and areal extent, the sands were probably delivered by distributaries of a major delta system. The CUS are a continuation of the coarsening and shallowing trend that was noted in the MM facies, and probably represent the delta mouth bar depositional environment (c.f. Coleman, 1982). The sands have been reworked by waves to varying degrees, as evidenced by the shell lags and pebble layers, with the most intense reworking confined to the eastern edge of the study area. Low angle cross bedding defined by pebble layers and dipping towards the basin suggest beach deposits, and indicates that some of the thick CUS became at least briefly emergent. However, lack of terrestrial plant fossils suggests that emergence, where it occurred, was ephemeral. Although deposited as distributary mouth bars, wave reworking has changed the sands to delta front bars, shoals and barrier islands or spits.

Fining upward sandstones in the undivided Bowser Lake Group occur as interbeds in the MM facies (where it is associated with invertebrate fossils, and extensive bioturbation) and in the upper parts of CUS. The lode casts common at the base, the thick structureless lower sandstone layer (commonly containing rip-up clasts), finer and commonly rippled upper sandstone layers, and marine association

suggest that the FUS interbedded with MM was deposited by turbidity currents in inner- to outer shelf environments. These FUS may have been redeposited from the delta front to offshore positions, similar to the thinner normally graded sands that are abundant in MM facies. FUS associated with the upper portions of thick CUS are probably unreworked distributary channel deposits similar to those described from the Rhone Delta (Oomkens, 1970).

The upward trend to shallower water depths in the undivided Bowser Lake Group within the study area is the culmination of a regional marine shallowing trend that began in the Middle Jurassic with initial Bowser Lake Group deposition. Initial Bowser Lake Group sediments were deposited in slope and submarine fan environments (Ricketts, 1990) where they overlie deep basinal marine claystones of the Middle Jurassic (Lower Bajocian) Quock Formation (uppermost Spatsizi Group; Thomson, *et al.*, 1986). By the time undivided Bowser Lake Group sediments exposed in the study area were deposited, slope environments had been succeeded by deep to shallow shelf environments, which in turn were overlain by deltaic deposits as described below. The progressive change from deep basinal deposits to slope facies and finally upward to shelf and shallow marine environments is interpreted as a record of shelf construction. The shelf was constructed by filling a pre-existing ocean or marginal sea basin.

## CURRIER FORMATION

The Currier Formation was encountered in 20 sections, four of which contain the contact with the underlying undivided Bowser Lake Group, and four of which contain the contact with the overlying McEvoy Formation (Fig. 2-2). The thickness of the Currier Formation is roughly 1000 m (Cookenboo and Bustin, 1990b), although no continuous sections of the entire formation are known. The Currier Formation is the main coal-bearing unit of the Groundhog coalfield and is exposed from Maitland Creek in the north to the Groundhog Range in the south.

Six facies (one divided into three subfacies) are recognized in the Currier Formation (Fig. 2-1) and described below. The most abundant facies are black claystone (homogeneous, carbonaceous, and laminated subfacies), interbedded claystone-siltstone-very fine grained sandstone, fining upward

sandstone, and coarsening and thickening upward sandstone. Volumetrically minor facies include thick coal, and well-sorted chert pebble conglomerate.

*Black claystone facies*

The black claystone (BC) facies consists of recessive-weathering, variably silty, black to dark gray, thin to thick bedded claystone. This facies is characterized by abundant terrigenous organic matter including leaf fossils, petrified wood, coal and disseminated plant debris, and a lack of marine invertebrates. In addition, a diverse assemblage of spores, pollen and dinoflagellate cysts have been recovered from some claystone samples (Rouse, personal communication, 1989). The BC facies comprises three subfacies recognizable in the field:

**1) Homogeneous black to dark gray claystone subfacies.** Homogeneous black to dark gray claystone ($BC_{homogeneous}$) commonly 3 to 10 metre thick is the most common subfacies. It consists of variably silty claystone, and contains abundant and varied leaf remains. Few trace fossils are seen in outcrop, but slabbed and polished samples commonly reveal pervasive *Helminthopsis* burrows. Interbeds of fine sandstone lenses 30 to 50 cm thick of limited lateral extent (less than 10 to 20 m) occur within the beds of $BC_{homogeneous}$ beds. Thick $BC_{homogeneous}$ beds commonly are gradationally overlain by laminated claystone or siltstone, and underlain by carbonaceous claystone. This subfacies commonly contains carbonate concretion layers which weather yellow-brown and usually occur at the tops of beds. Most of the concretions are composed of ferroan dolomite, and some contain cores of siderite. The yellow-brown layers commonly have very well preserved leaf fossils on their surfaces, and appear to be coalesced concretions.

**2) Carbonaceous black claystone subfacies ($BC_{carbonaceous}$).** Carbonaceous black claystone subfacies ($BC_{carbonaceous}$) is similar to the homogeneous black claystone subfacies, but is distinctly more organic rich, with abundant plant fossils and occasional coaly layers. Many carbonaceous claystones that directly overlie coals (roof shales) have been analyzed for palynology, and contain a wide variety of pollen, spores, and dinoflagellate cysts. This facies commonly grades into homogeneous

claystone or coal.

**3) Laminated black claystone subfacies ($BC_{laminated}$).** The laminated black claystone subfacies ($BC_{laminated}$), consists of black claystone and parallel laminae of buff to yellowish brown siltstone. The laminae usually range between 3 and 15 mm thick for each claystone-siltstone pair, and are normally graded. The laminated facies is up to 3 metres thick, and commonly lacks both macro- and microfossils, although surrounding beds tend to be rich in plant remains.

*Interbedded claystone, siltstone and very fine grained sandstone*

Interbedded claystone, siltstone and very fine grained sandstone facies (ICSS) occurs as a gradational, thin to thick bedded facies in the Currier Formation, and dominates some exposures of the upper part of the formation. This facies consists of gradational beds of claystone overlain by siltstone and/or very fine grained sandstone, that occur in composite units between 0.5 and 20 m thick. Claystone is similar to the black claystone described above, and is only included in this facies where gradationally in contact with beds of siltstone or very fine grained sandstone. Locally, ICSS coarsens upward in claystone-to-siltstone-to very fine sandstone successions, similar to coarsening upward mudstones in the McEvoy Formation (described below).

*Fining upward sandstone facies (FUS)*

In the Currier Formation, the FUS facies is most commonly 1 to 3.5 m thick, although thicker FUS (up to 20 m) also occur. Similar to the undivided Bowser Lake Group, FUS in the Currier Formation is resistant, weathers dark gray and light brown (gray to dark gray on fresh surfaces), and is composed of well sorted very fine, fine and medium grained sandstone. FUS fines upward from a usually erosive basal contact to a gradational or less commonly sharp upper contact. In the Currier Formation, FUS is generally laterally continuous at outcrop scale with only minor down-cutting visible. Rounded rip-up clasts of mudstone pebbles are common near the base where the sandstone is usually fine grained, structureless, and thick bedded. Beds are usually structureless, but planar cross bed sets 50 to

75 cm thick occur rarely in the basal portion of the fining upward sandstone. Groove casts up to 10 cm across are common on the base of FUS where well exposed. Higher in the fining upward sandstones, grain size is finer, and planar or trough cross beds sets less than 50 cm thick are common.

*Coarsening upward sandstones*

Coarsening and thickening upward sandstones (CUS) are common in the Currier Formation. In the lower Currier Formation, CUS are similar to those described above for the undivided Bowser Lake Group, except that in the Currier they are commonly capped by $BC_{carbonaceous}$ and/or coals (including the thickest coals of the Groundhog coalfield). For example, in sections 27, 28, 33, 41, 44 and 47 located along the limits of Currier Formation exposure (cross-section figure 2-6; and location map figure 2-7), the first thick coal occurs 10 to 20 m above $CUS_{thick}$. In some sections, this transition of marine facies to terrestrial coals is repeated over stratigraphic intervals of 150 to 300 m, suggesting stacked delta lobes prograding into shallow marine waters. Section 33 (Fig. 2-8), for example, has 10 m of coal-bearing strata above an 18 m thick coarsening upward sandstone in the lower 50 to 100 m of the section, and another coal-bearing section (two seams of 1.5 and 1 m thickness) 300 m higher in the section, again within 20 m above a 10 m thick coarsening upward sandstone.

In the upper portions of the Currier Formation, thinner CUS occur ranging between 2 to 7 m thick. These differ from thick CUS in the lower Currier Formation and underlying Bowser Lake Group strata because they are generally associated with abundant plant remains and rare or absent invertebrate fossils, and may have rooted upper contacts.

*Chert pebble conglomerate*

Chert pebble conglomerate (CPC) is a minor facies in the Currier Formation. The conglomerates are typically clast supported, and most are between 5 and 20 m thick. Clasts are rounded, well sorted pebbles generally 1 to 3 cm in diameter, and the maximum observed pebble

Figure 2-6: Cross-section of Currier Formation strata. Relative stratigraphic positions of sections are poorly constrained. Interpreted positions are based on facies character (mainly presence or absence of thick coals) and relative proximity of each section to marine facies of the undivided Bowser Lake Group below and fluvio-deltaic facies of the McEvoy Formation above.

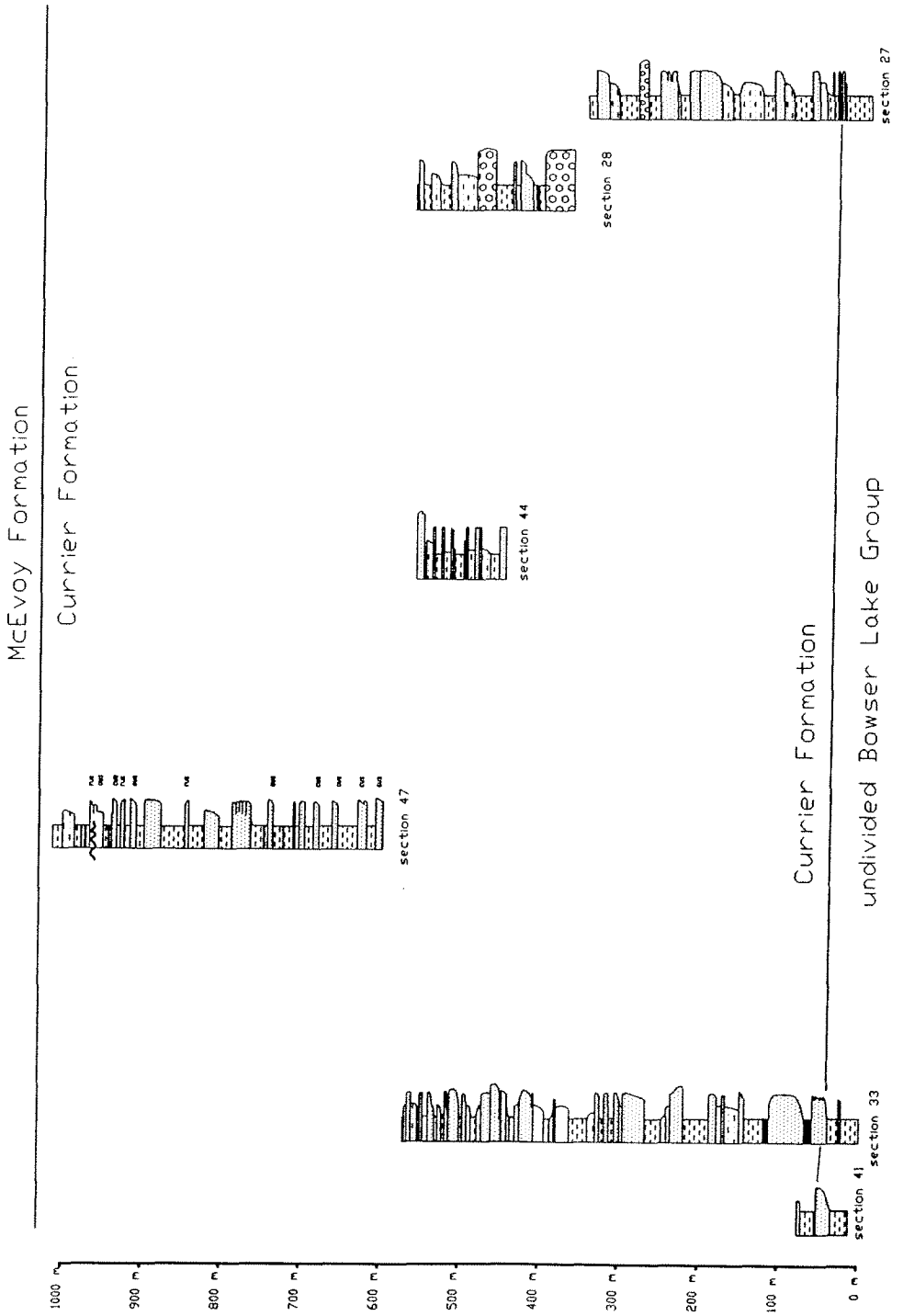

Figure 2-7: Location map for Currier Formation cross-section (Fig. 2-6).

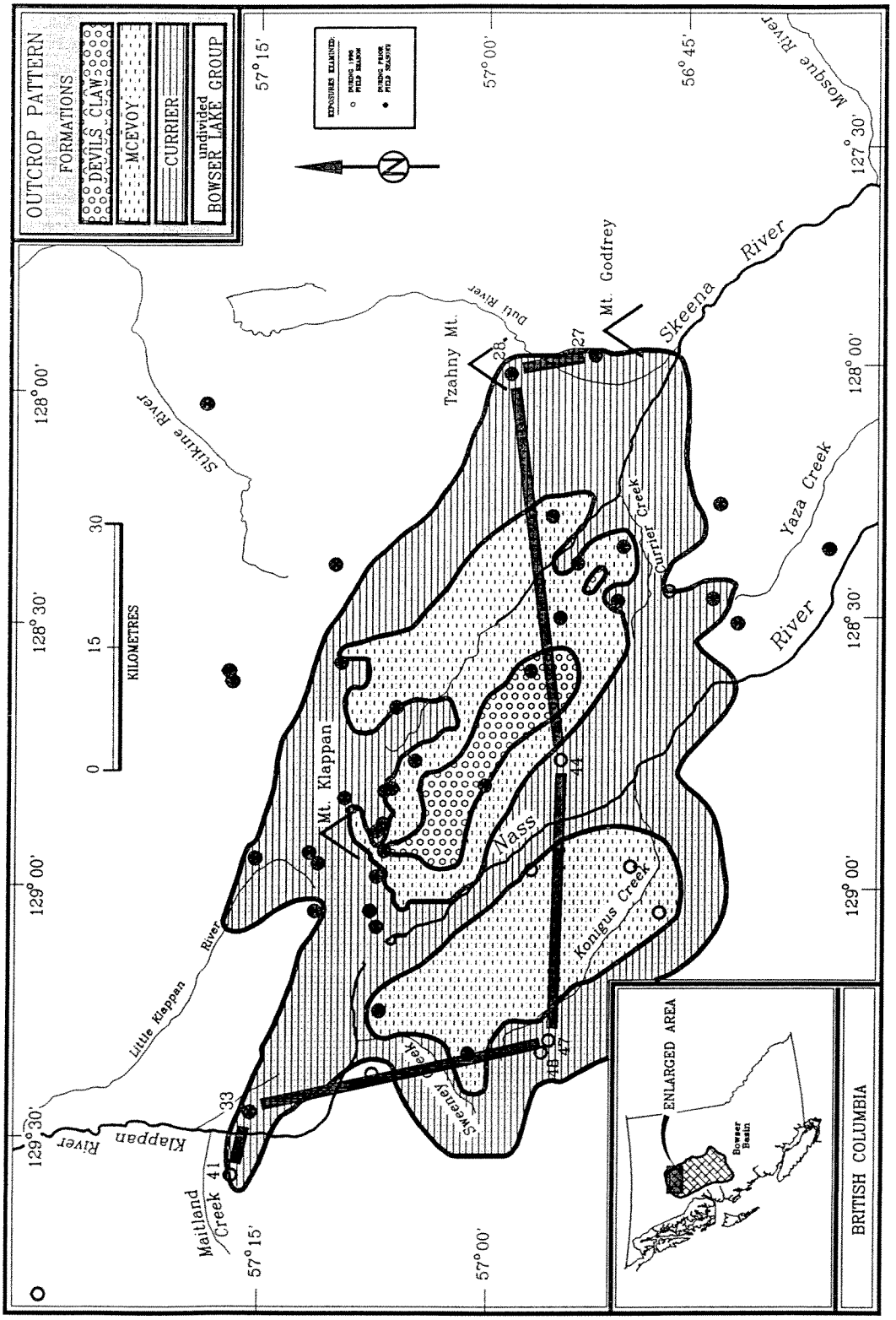

Figure 2-8: Marine mudstones interfinger with coarsening upward sandstones capped by thick coals in the lower Currier Formation (section 33 located east of the Klappan River).

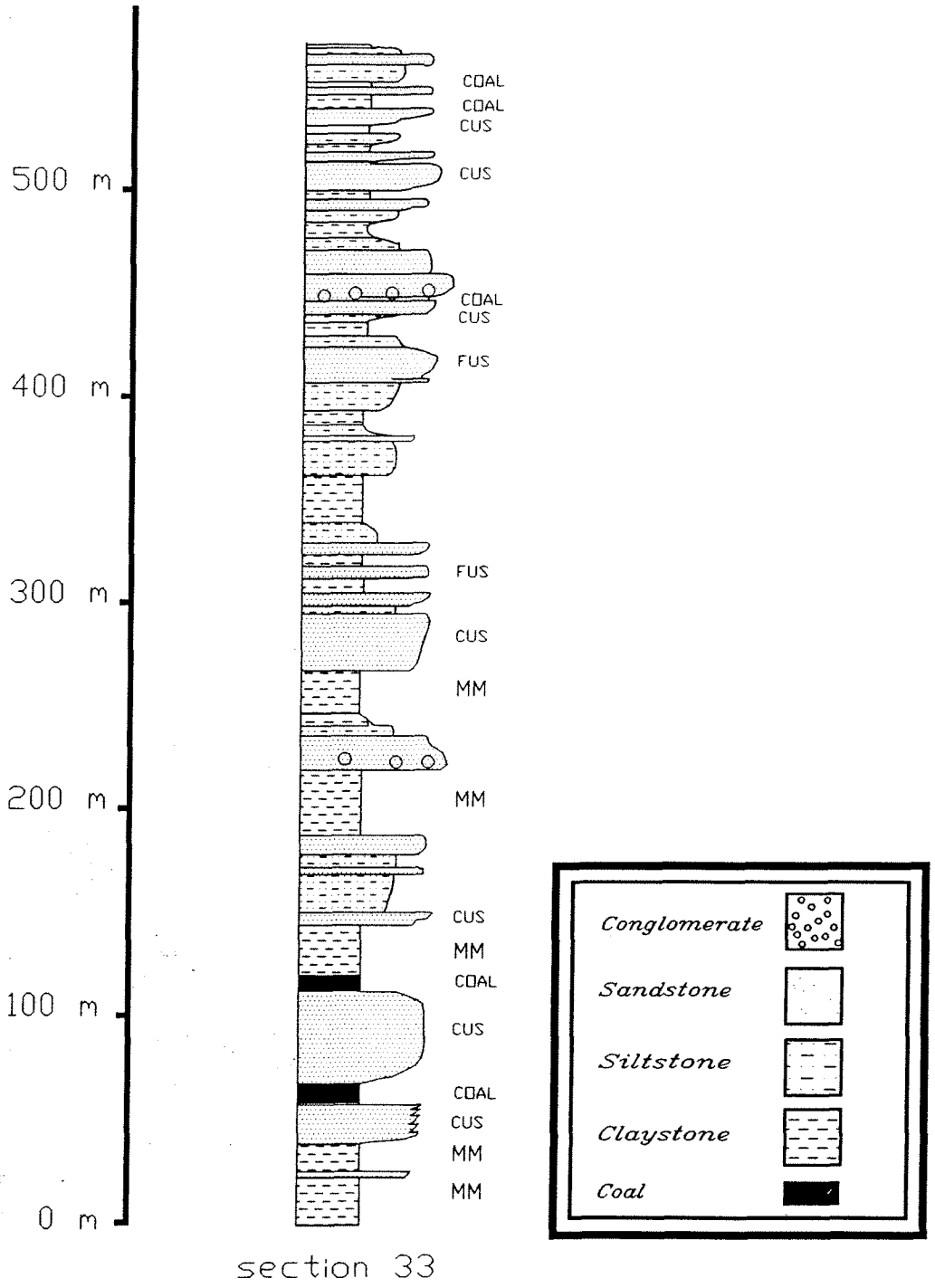

size is 7 cm. The clasts are more than 95% chert, and occur in colors of gray, green, and black. The conglomerates form laterally extensive sheets 1 kilometre or more across most outcrops, but show local thickening in channels.

In some exposures, thick pebble conglomerate grades laterally into sandstone channels. An example of such lateral gradation is well exposed south of Mt Klappan (section 3). Here, a 15 m thick conglomerate composed of pebbles generally less than 2 cm in diameter grades over a distance of 150 m to the west into fine grained sandstone. Still farther to the west this unit exhibits a sharp basal contact that cuts more than 2 m down into the surrounding mudstones.

### *Thick coal*

Coals in the Currier Formation are commonly associated with carbonaceous claystones and direct overlie CUS. The thickest coals occur in the lower Currier Formation, where coals up to 3 to 5 m thick have been reported from north of Mount Klappan (Gulf Canada LTD open file reports, 1984, 1987) and near Currier Creek (Bustin and Moffat, 1983). Two poorly exposed seams 8 to 10 m thick were encountered east of the Klappan River (section 33, Fig. 2-8; Cookenboo and Bustin, 1990b). The thick seams east of the Klappan River directly overlie coarsening upward sandstones that in turn overlie marine mudstones. Seams less than 1 m thick occur in the upper Currier Formation where they are associated with thin CUS and not associated with marine mudstones. Some of these thinner coals are rooted in underlying CUS.

Currier Formation coal is anthracite to meta-anthracite in rank (Chapter 5), and commonly contains framboidal or disseminated pyrite, and diagenetic veins of calcite and quartz.

### *Depositional environments of the Currier Formation*

The Currier Formation occurs stratigraphically above, and in its lowest parts interfingered with, the pro-delta muds and delta front sands that characterize the underlying undivided Bowser Lake Group. As might be expected in such a stratigraphic context, the Currier Formation facies are consistent with

prograding deltaic deposition. Thick FUS and CUS facies in the lower Currier Formation occur at the transition from marine to partly terrestrial deposition. The thick FUS, with their sharp, at least locally erosive base, well sorted texture, and fining upward nature, probably represent channel deposits of major distributary channels. As with the CUS in the upper part of the undivided Bowser Lake Group, the thick CUS of the lower Currier Formation were deposited as delta mouth bars delivered to the delta front by the distributary channels inferred from the FUS facies. In contrast to the underlying marine strata, thick CUS in the lower Currier Formation became emergent for significant periods. This emergence is demonstrated most directly by the occurrence of thick coals above many of the CUS, whose plant precursors required an emergent substrate to grow upon. Furthermore, the fine grained and organic rich character of the black claystone facies that commonly occurs above the marine to terrestrial transition is consistent with accumulation in protected waters, such as form shoreward of emergent delta front barrier bars and islands. The laminated black claystone facies, which is largely restricted to the Currier Formation, and is commonly associated with $BC_{homogeneous}$ and coarsening upward mudstones is similar to laminated deposits are known from the central parts of tropical and temperate deltaic lakes and lagoons (Tye and Coleman, 1989). Such a depositional environment is consistent with delta deposition in water bodies of large surface area that are subsequently filled by fine grained crevasse splay or lacustrine delta deposits (Tye and Coleman, 1989). Such large water bodies, including interdistributary lakes and lagoons are common in lower delta plain environments.

The stacked coarsening upward cycles, first formed in the underlying marine strata (e. g. section 49, Fig. 2-3), and continuing during the accumulation of the Currier Formation (e. g. section 33, Fig. 2-8) suggests deposition by lobes of a repeatedly large prograding delta system. The delta lobes are formed in a cycle, as demonstrated in the Mississippi Delta (Fig. 2-9). The cycle begins with initial progradation and deposition of deltas front sands followed by abandonment and subsidence, leading next to wave reworking of barrier sands and lagoon fill deposits, and finally to marine inundation and development of shallow marine conditions (Fig. 2-9). This entire cycle of delta lobe evolution is

Figure 2-9: Four steps of delta lobe progradation, subsidence, innundation and re-establishment. Simplified from Bhattacharya and Walker (1992), based on data from Boyd and Penland (1988).

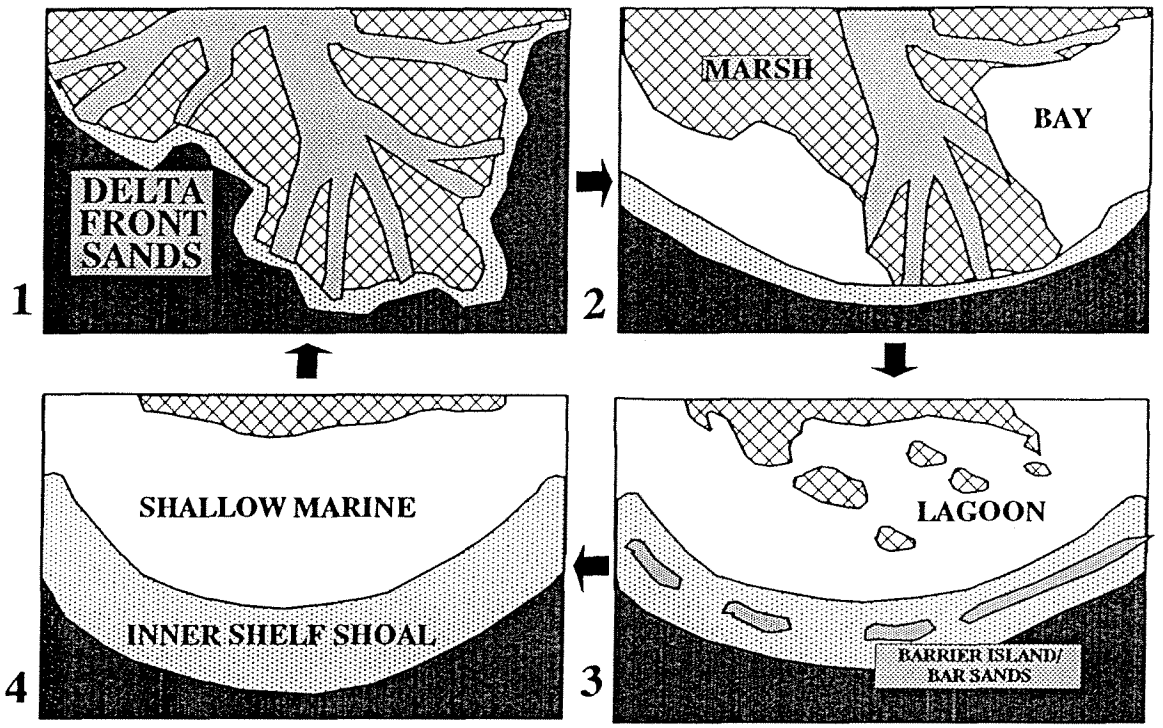


Simplified from Bhattacharya and Walker (1992)
after data from Boyd and Penland (1988).

typically preserved in Currier Formation, suggesting subsidence was rapid compared to the rate of sediment supply.

The thin FUS (1 to 3.5 m thick) and CUS (2 to 7 m thick) facies that are common in the upper Currier Formation were deposited by smaller scale fluvial systems than the thick FUS and CUS of the lower Currier Formation. These thin FUS and CUS are interpreted as crevasse splay or subdelta channel and mouth bar deposits that filled in protected lagoons and interdistributary bays formed shoreward of the delta front. This interpretation is consistent both with the inferred smaller size of fluvial system, and with the abundance of leaf fossils and the general lack of marine macrofossils in the upper Currier Formation. Preservation of sediments deposited mostly shoreward of the delta front during later Currier time suggests the shoreline had prograded west of Konigus Creek, out of the study area. Such preferential preservation of shallow water, marginal marine deposits also implies that subsidence in the study area had diminished relative to sedimentation rate (i.e., less accommodation space was created per unit of delivered sediment) by the time the upper Currier Formation was deposited.

## MCEVOY FORMATION

The McEvoy Formation was examined in 9 sections between the headwaters of the Skeena and Nass rivers, three of which contain the contact with the underlying Currier Formation, and 2 of which contain an exposed contact with the overlying Devils Claw Formation (Fig. 2-2). The thickness of the McEvoy Formation exceeds 780 m between the Skeena and Nass rivers. East of the Skeena River at Distingue Mountain (location given in figure 2-2), 670 m of McEvoy Formation strata were measured, but no upper or lower contact was encountered. Lithologically similar strata with a composite thickness of as much as 1500 m were examined in 5 sections east of the Nass River and south of Sweeney Creek and are tentatively assigned to the McEvoy Formation. Part of this section may be time correlative with the Devils Claw Formation, but it lacks the thick conglomerates by which the Devils Claw Formation is defined.

Coarsening upward mudstone and chert pebble-cobble conglomerate are the most characteristic

facies of the McEvoy Formation. These two facies and the usually thin coals are described in detail below. Black claystone, fining upward sandstone, and coarsening upward sandstone also occur in the McEvoy Formation. The latter three facies are not further described below because they have essentially the same characteristics described earlier for BC, FUS, and CUS facies in the Currier Formation, with the following exceptions: $BC_{laminated}$ was not found in McEvoy Formation sections, and CUS is limited to thin examples with no associated marine facies.

*Coarsening upward mudstone facies (CUM)*

Coarsening upward mudstone (CUM) is the dominant facies of the McEvoy Formation. CUM consists of moderately recessive beds of claystone and siltstone with interbeds of silty very fine to fine grained sandstone. A typical coarsening upward unit begins with black claystone (which may be carbonaceous or coaly near the base) which has a sharp basal contact. The black claystone gradationally coarsens upward into siltstone, which in turn coarsens upward into very fine sandstone (locally coarsening further to fine grained sandstone near the top). The sandstone usually has an abrupt upper contact that may be rooted, and is commonly overlain by another coarsening upward mudstone. A typical CUM unit is composed of approximately 70% siltstone, and roughly equal parts claystone and sandstone accounting for the rest. However, a range of claystone-siltstone-sandstone ratios exists, from some composed only of claystone and siltstone to others composed dominantly of siltstone and sandstone. This facies weathers dark gray to brownish gray and contains abundant leaf fossils, wood, and plant debris. Many of the best preserved leaf fossils are found on surfaces of authigenic carbonate interbeds, most commonly located at the siltstone to claystone transition. Invertebrate fossils are lacking and trace fossils are rare.

CUMs range from 1 to 8 m thick, and are commonly stacked as many as 6 or 7 times in succession without being broken by another facies. In section 12 (Fig 2-10; location given in figure 2-2), a McEvoy Formation exposure west of the Skeena River, the thickness of CUMs decreases

Figure 2-10: Cliff face exposure composed of mostly CUM facies, from the lower part of section 12 in the McEvoy Formation. Stratigraphic column for section 12 illustrated in figure 2-11.

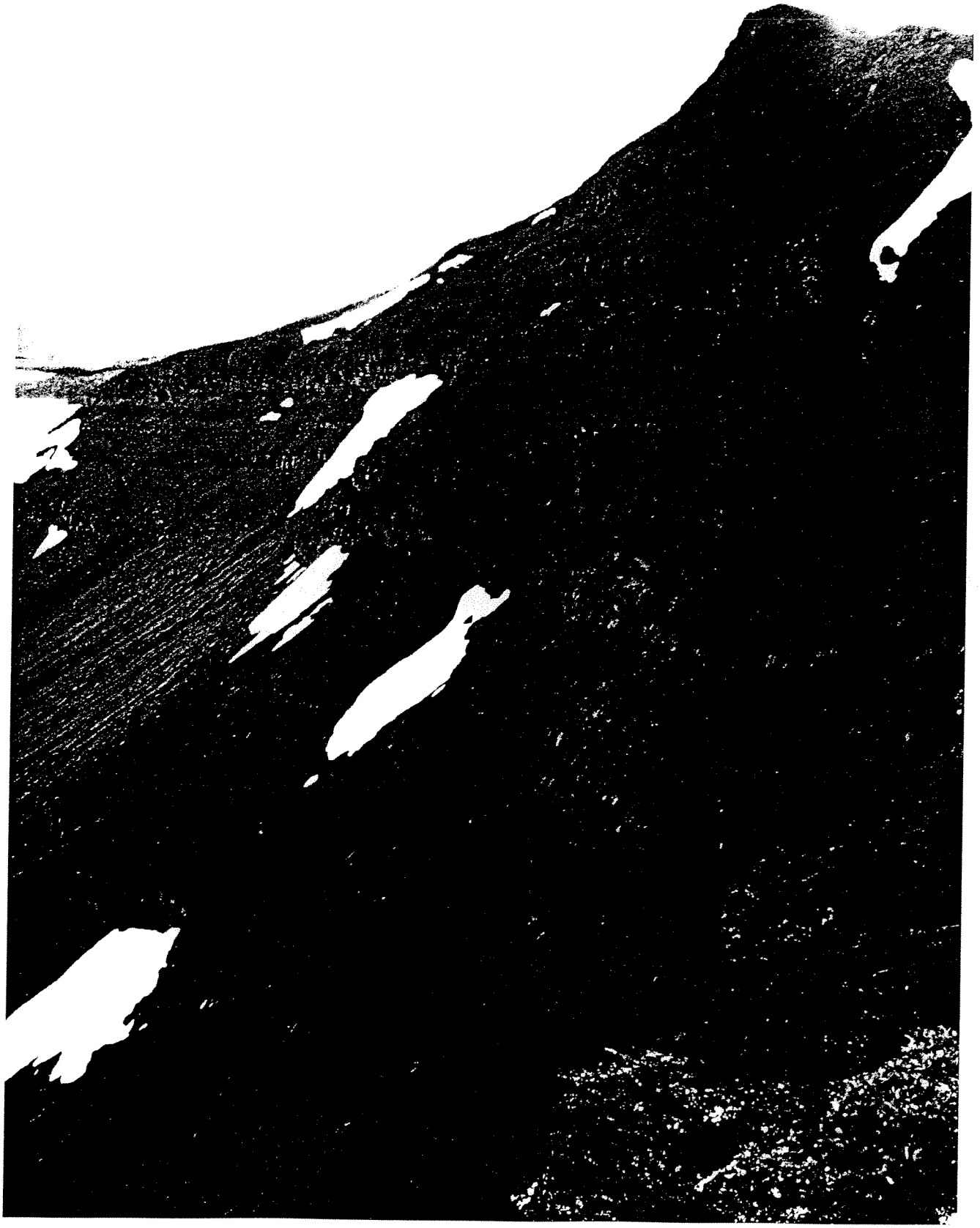

upwards in two successive trends (Fig. 2-11). The lower trend has CUMs near the base 5 m thick that thin to 1 to 2 m each 200 m higher. This thinning upwards trend is overlain by another thinning upwards trend 80 m thick that varies from 8 m CUMs near the base to 3 to 3.5 m thick CUMs at the top. Although they vary widely in thickness in different locales and stratigraphic levels, adjacent CUMs from a single exposure tend to be of approximately equal thickness.

### *Chert Pebble-Cobble Conglomerate*

Conglomerate in the McEvoy Formation is generally thicker, coarser and more laterally extensive than in the Currier Formation. Most conglomerate beds are between 10 and 15 m thick, and some can be traced in outcrop for more than 2 kms. Clasts are more than 95% chert pebbles and cobbles, with maximum observed clast size of 10 cm. Three of the thickest and most laterally extensive of the conglomerates occur in 200 m thick zone near the middle of the McEvoy Formation. Two of these three conglomerates occur in successions similar to the fining upward conglomerate facies described for the Devils Claw Formation later. Beds are typically clast supported, with a matrix of medium to fine sand and no preferred grain orientation observed. Locally, some conglomerates grade to pebbly sandstone, and basal contacts are erosive.

### *Coal*

Coal in the McEvoy Formation east of the Nass River consists mostly of thin seams ($< 0.5$ m) and discontinuous coaly layers that commonly occur in carbonaceous claystone. Some of these thin coals are rooted in sandstones or siltstones that form the top of underlying coarsening upward sequences (CUM or thin CUS facies). Coal is semianthracite to anthracite rank, with most vitrinite reflectance values (random reflectance in oil) between 2.1% and 2.9% (Chapter 5).

West of the Nass River and south of Sweeney Creek (sections 34 and 35 in figure 2-2), six seams of 1 to 3 m thickness occur within 300 m of strata that are interpreted to be a generally finer grained facies of the McEvoy Formation than that previously describe in the type area of the Klappan

Figure 2-11: Stacked coarsening upward mudstones from section 12 in the McEvoy Formation.

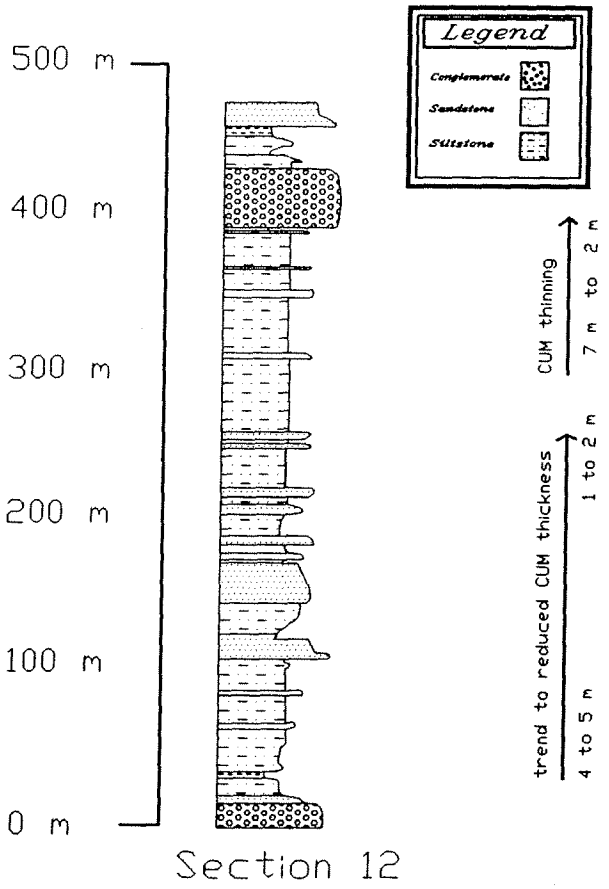

and Groundhog coalfields east of the Nass River (Cookenboo and Bustin, 1989). Coal in the Sweeney Creek area is semianthracite rank., with a measured vitrinite reflectance value of $Ro_{rand}$=2.2%. to 2.%.

*Depositional environments of the McEvoy Formation*

The dominant facies of the McEvoy Formation is coarsening upward mudstone (CUM). A close modern analog for this facies (with excellent preservation potential) is the upward-coarsening lacustrine delta of Lake Fausse Pointe which formed on the upper delta plain of the Mississippi River. As described by Tye and Coleman (1989), the Lake Fausse delta is a 1.5 to 3 m thick coarsening upward succession of clay, silty clay, silty very-fine grained sand, and fine grained sand that has rapidly aggraded and prograded (approximately 100 years since initiation) over organic-rich backswamp clays. Tye and Coleman (1989) also point out that such upward-coarsening sequences tend to be stacked in repeated units, and three such upward-coarsening units are stacked in the Lake Fausse area in the 30 m of Holocene sediments. Notably, most of the vertical sediment aggradation in the Lake Fausse area occurred during the rapid delta building events, but most of the time is represented by slowly accumulating backswamp deposits. CUM facies in the study area probably accumulated mostly on the upper delta plain but diverse dinocysts assemblages (Rouse, written communication, 1989) recovered from carbonaceous claystones ($BC_{carbonaceous}$) collected near the base of some CUMs in the McEvoy Formation suggest that the bodies of water filled in by these facies were bays at least intermittently connected to the sea.

Similar CUMs that occur alone or in repetitively stacked units in ancient rocks have also been identified as crevasse splay deposits in Cretaceous coal bearing strata of the Rocky Mountains (Flores, 1985). Like the coarsening up units described by Flores (1985), CUMs in the study area are associated with fining upward sandstones (1-3.5 m version), which are interpreted as crevasse splay channels (see above) and thick black claystone facies deposited in backswamp and lagoon environments. Unlike the Rocky Mountain strata, coals associated with CUMs in the study area are thin and argillaceous.

Fining upward sandstones occur in a wide range of thicknesses, suggesting the presence of both major distributary channels and smaller crevasse channels, as were interpreted for the Currier Formation.

Coarsening upward sandstones, however, are consistently relatively thin (2 to 7 m) in the McEvoy Formation, suggesting that deep bodies of water were lacking.

Compared to the underlying Currier Formation, where the entire cycle of delta lobe evolution is repeatedly preserved, the McEvoy Formation contains mostly upper delta plain deposits, and the delta front is not preserved in the study area (Fig. 2-9). Because no delta front sediments occur, marine inundation between sediment aggradation events was incomplete (assuming continual subsidence), and thus sediment filled the accommodation space that was created by subsidence more quickly than during Currier Formation accumulation. Therefore, subsidence rates were lower relative to sedimentation rate for the McEvoy Formation than the Currier Formation.

The chert pebble-cobble conglomerates of the McEvoy Formation are probably channel deposits of the same fluvial system that deposited thick FUS. The great lateral extents of these conglomerates suggests that the fluvial channels migrated unimpeded across the inferred upper delta plain. The increasing abundance and coarseness of conglomerates in the McEvoy Formation compared to the Currier Formation indicates that the fluvial system became more competent through time at delivering gravels to the study area. Theoretical modelling by Paola (1988), supported by recent field studies (Heller and Paola, 1992; Gordon and Heller, 1993), indicates that conglomerates composed of resistant clasts (such as the oligomict chert conglomerates of the northern Bowser Basin conglomerates) tend to prograde farther into a basin as a result of slower subsidence rate. The conglomerates, therefore, support the conclusion that subsidence was relatively slow in the study area during deposition of the McEvoy Formation.

## DEVILS CLAW FORMATION

The Devils Claw Formation was examined in 2 sections between the Nass and Skeena rivers, and both sections contain the contact with the underlying McEvoy Formation (Fig. 2-12 and Fig. 2-13).

Figure 2-12: Cross-section of Devils Claw formation exposures described in text. Lines between stratigraphic columns correlate conglomerates at the base of fining upward successions. Section locations are given in map figure 2-13.

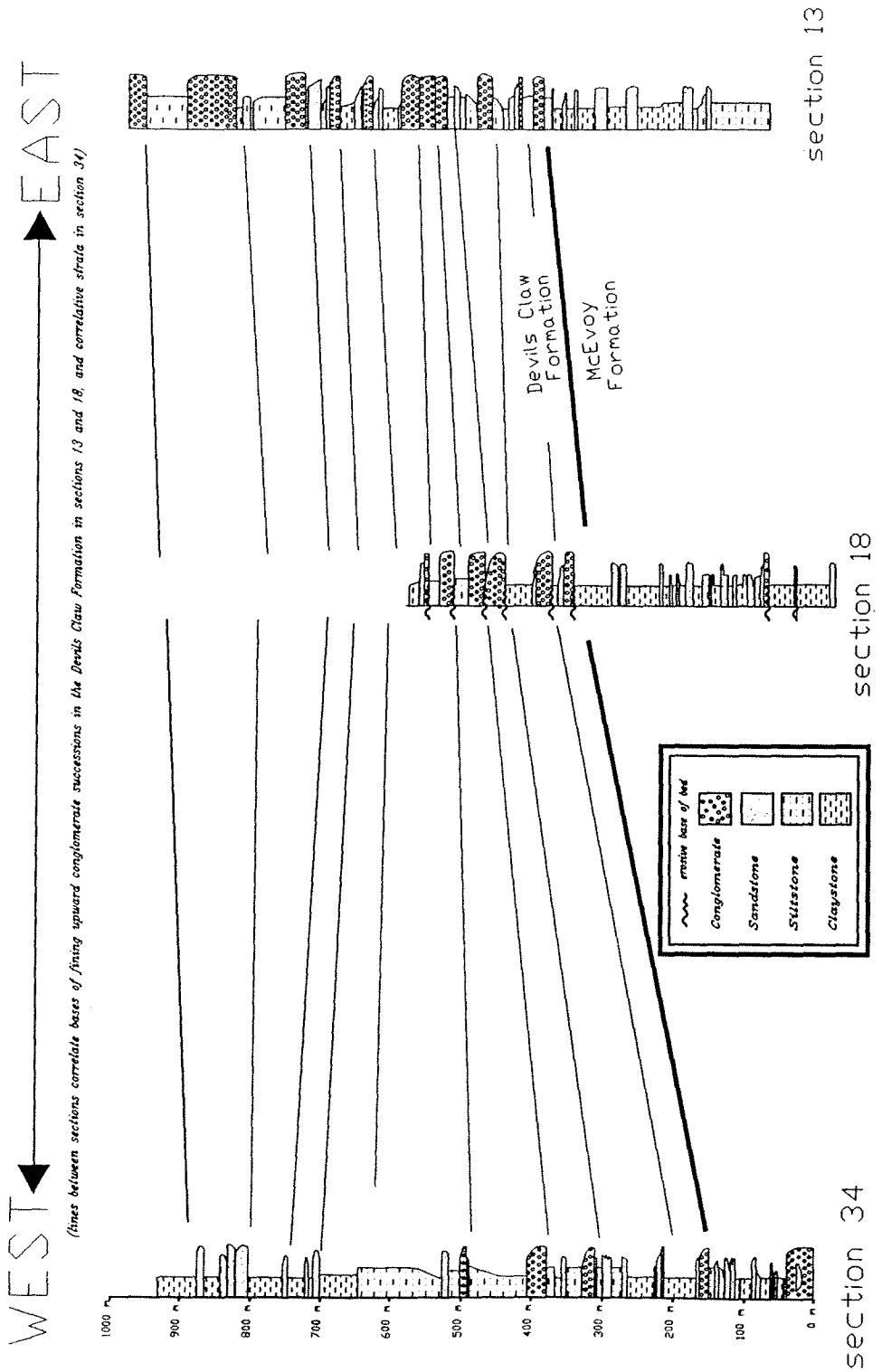

Figure 2-13: Location map for Devils Claw Formation cross-section (Fig. 2-12)

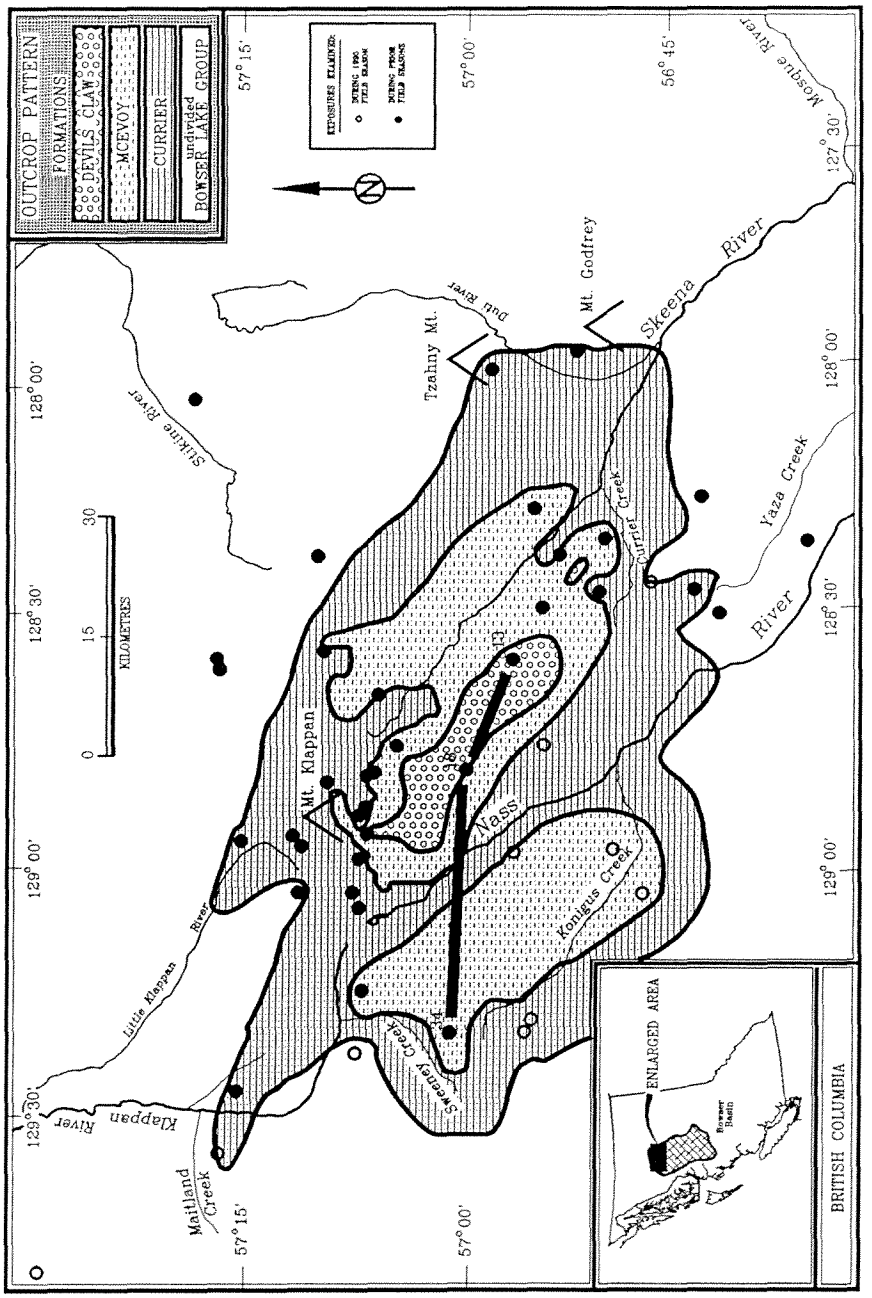

The maximum measured thickness of Devils Claw strata is 600 m but no younger strata are preserved above the top of the section and therefore the total depositional thickness is not known.

Claystone, mudstone, sandstone and thin coal facies broadly similar to those in the McEvoy formation also occur in the Devils Claw Formation. However, the stratigraphic distribution is more regular in the Devils Claw Formation than in either the Currier or McEvoy formations: facies in the Devils Claw Formation are stacked repeatedly in a pronounced fining upward pattern, beginning at the base with a conglomerate and commonly grading upward to carbonaceous claystone (and in some locales thin coal). The pronounced fining upward tendency leads to the different lithologies being described below as a single facies characteristic of the Devils Claw Formation. Coarsening upward mudstones and chert pebble-cobble conglomerates similar to those described for the McEvoy Formation (not in well defined fining upward successions) also occur as minor components of the Devils Claw Formation, most commonly in the lower part of the formation.

*Fining upward chert pebble-cobble conglomerate (FUPCC)*

Pebble-cobble conglomerate occurs with sandstone, siltstone, clay-rich mudstone and occasional thin coal in repeatedly stacked, fining upward units through most of the Devils Claw Formation. Individual fining upward units range from 25 to 30 m thick, and conglomerate generally forms between 20 and 70% of the fining upward unit. Overlying the conglomerate, there is gradational change to medium to fine grained sandstone, siltstone, and carbonaceous shale. Coals up to 1 m thick cap some fining upward units. Although dominated by chert pebble-cobble conglomerate, this facies (FUPCC) differs from others described in this chapter in being composed of many different lithologies. However, the pronounced tendency of these lithologies to occur in the same fining upward succession through most of the Devils Claw strata justifies consideration of these multiple lithologies as a single facies.

Conglomerate forms the base of each FUPCC facies, and occurs in laterally continuous beds that tend to form the resistant cliffs which characterize most Devils Claw Formation exposures. Air photo interpretation indicates continuity of individual beds may be on the order of 5 to 10 km (Cookenboo,

1989). The bases of the conglomerates are locally erosive, cutting down more than 3 m into underlying fine sediments over a lateral distance of less than 50 m. Scours 50 cm to 1 m deep occur in some of these erosive bases. The beds are usually normally graded, with cobbles concentrated near the base.

The conglomerate is composed of clast supported chert pebbles and cobbles up to 15 cm in longest dimension. Like the conglomerates from older units, clasts are more than 95% well rounded, gray, green and black chert, and most are spherical, although roller shapes also occur. Most beds exhibit no preferred clast orientation, although large scale trough cross bedding occurs in some beds in sets more than 3 m thick. The cross bed sets are composed of layers approximately 20 cm thick that fine upward, with cobbles concentrated in the lower 10 cm, and are concave up.

The fining upward conglomerate facies is best exposed in section 18 on a ridge west of the Nass River (figs. 2-12 and 2-13). Here 11 fining upward sequences, each from 22 to 28 m thick, occur stacked vertically in the Devils Claw Formation. From the base of the Devils Claw Formation upwards, six conglomerates occur over an upward interval of 185 m, with only minor CUM facies separating some of the fining upward sequences. At least five more fining upward successions occur higher in the section, but are not accessible due to steepness. Observations from a distance indicate that the sharp based and gradational fining upward pattern continues upward from conglomerate in these successions. An additional conglomerate occurs in the upper McEvoy Formation, 300 m below the Devils Claw Formation. In each unit, the chert pebble-cobble conglomerate occurs at the base, and comprises from 40% to 90% of each fining upward sequence. Cobbles as large as 15 cm in their longest dimension are concentrated near the erosive base, where scour marks are common. Higher in the conglomerate, cobbles become rare or absent as pebbles increase, and sandstone interbeds become more abundant. Above the conglomerate, sandstones grade upwards from thick bedded medium grained with planar and trough cross beds, to fine, very fine and finally silty sandstone. The silty sandstone grades into siltstone, which in turn grades into mudstone and carbonaceous claystone, and in one area the fining upward sequence is topped by coal. The most striking aspect of FUPCC in this exposure is the regularity and completeness of each fining upward sequence (conglomerate-sandstone-mudstone-carbonaceous claystone and rarely

coal). In addition, only minor quantities of other facies are preserved in this section.

In section 13 located in the Devils Claw Formation west of the Skeena River (Figs. 2-12 and 2-13), cliffs of FUPCC dominate the upper 450 m of exposure (Fig. 2-14). Conglomerates occur in five fining upward sequences 19 to 30 metres thick, similar to those in section 18. Maximum observed clast dimension is 13 cm in roller shaped cobbles. Two other conglomerates are much thicker (64 and 68 metres thick each). These very thick conglomerates are interpreted as stacked fining upward conglomerates in which the fine grained beds separating the conglomerates are missing due to subsequent erosion, rather than a fundamental difference in sedimentary processes. The 64 metre thick conglomerate is well exposed, and exhibits three fining upward divisions of 18, 21 and 24 m thickness, separated by sandstone or pebbly conglomerate interbeds, and thus is a composite bed of three fining upward conglomerates. The 68 m conglomerate is poorly exposed (partially talus covered).

Near the base of section 13, lens shaped pebble conglomerates (maximum observed clast size of 5 cm) occur that cut sharply down as much as 6 m into surrounding fine grained facies (mostly CUM). These conglomerates are not parts of fining upward successions and are up to 17 m thick, and are limited to the lowest 50 m of the Devils Claw Formation.

The third section measured with abundant FUCPCC is located south of the headwaters of Sweeney Creek (section 34 in figures 2-12 and 2-13). In this exposure, eleven fining upward pebble-cobble conglomerates 2 to 38 metres thick occur over a stratigraphic interval of 850 metres. The defining characteristics of erosive base, cobbles (maximum observed clast size 7 to 9 cm) concentrated near the base, associated plant-bearing facies, and fining upward succession of overlying beds are all similar to sections 18 and 13, but here the conglomerates are generally thinner. Interbedded sandstones, mudstones and occasional coal separating the conglomerates dominate the section.

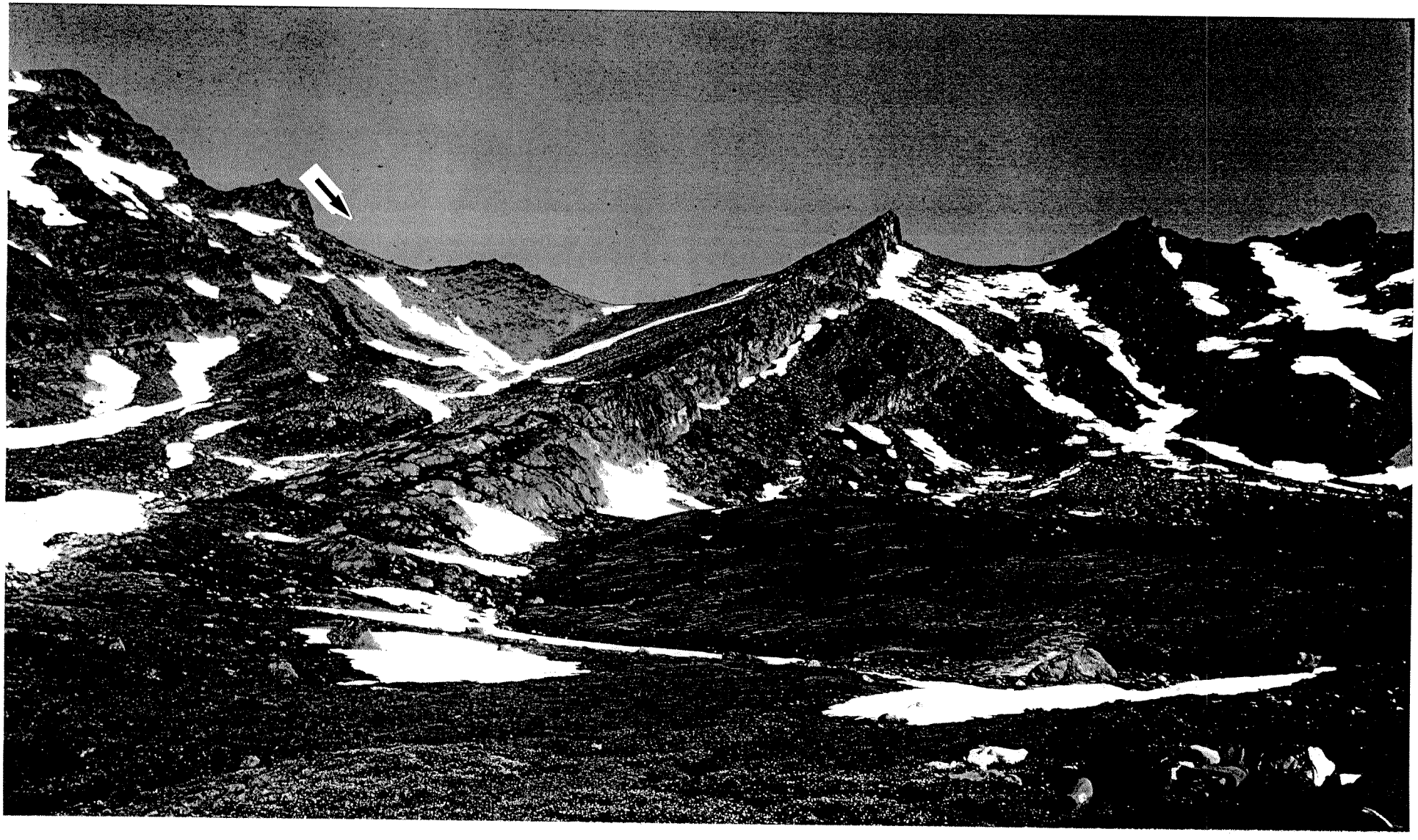

Figure 2-14: The upper 420 m of section 13 exposed on an east west trending ridge line west of the Skeena River. The more resistant cliffs are conglomerates, as are some of the less resistant strata. The upper part of cliffs to the west (left side of field of view) were unreachable, and suggest that significantly more strata may occur in the Devils Claw Formation than the 600 m maximum measured in this section.

The three exposures described above exhibit a distinct trend from east to west (sections 13 to 18 to 34; cross-section figure 2-12; location map figure 2-13) of increasing deposition and/or preservation of fine grained fluvial facies between conglomerate beds. Structural complexity and sparse paleontological control make bed to bed correlations tentative in widely separated sections such as these, but as shown in cross-section (Fig. 2-12; location map Fig. 2-13), sections 18 and 13 both contain the McEvoy to Devils Claw contact, and can be confidently correlated lithologically. Section 34 may also be correlative, but because of structural separation, lower overall concentration of conglomerate (17% of the section), and the increased fluvial fine grained facies, this correlation remains uncertain. Limited paleontological control supports the facies based correlation, as do the low vitrinite reflectance values, assuming only burial related coalification (Moffat, 1985; Fig. 2-12).

*Depositional environments of the Devils Claw Formation*

The Devils Claw Formation is dominated by conglomerate facies. Near the base of the formation, lens shaped chert pebble conglomerates cut down sharply into fine grained facies, suggesting creation of ravinement surfaces in the underlying McEvoy Formation. Creation of such ravinement surfaces may be related to relative drops in sea-level, and consequent increase in overall channel slope (Reynolds *et al.*, 1991).

Above these lens-shaped conglomerates, fining upward chert pebble-cobble conglomerate facies dominates more 500 m of strata. The erosive bases, normal grading, and fining upward character suggest fluvial deposition, similar to the processes inferred for deposition of McEvoy Formation conglomerates. In the Devils Claw Formation, however, fine grained facies are mostly absent. The three sections illustrated in cross-section figure 2-12 suggest increased basinward deposition and/or preservation of sediments transported by a gravelly fluvial system, similar to the proximal-distal relationship summarized by Miall (1985) for the Scott, Donjek and South Saskatchewan rivers. The analogy with the three rivers listed above is imperfect, however, because the great lateral extent of Devils Claw conglomerates suggest that the fluvial system was largely unbound by valley walls. Given the stratigraphic context overlying

(and to some extent mixing with) upper delta plain deposits of the McEvoy Formation, an alluvial braidplain may best describe the Devils Claw depositional environment. Following the model of Paola (1988) mentioned earlier to explain the progradation of McEvoy Formation conglomerates, the Devil Claw Formation may have accumulated during a period of slow basin subsidence, leading to progradation of oligomict chert conglomerate relatively far into the basin.

## SUMMARY OF DEPOSITIONAL HISTORY

Sedimentation began in the study area with accumulation of middle to outer shelf muds and turbidites during the Middle to earliest Late Jurassic. The initial shelf sediments are distal prodelta deposits that prograded over Bajocian to Callovian (Middle Jurassic) deep basin to slope deposits exposed north and east of the study area (Ricketts, 1990), and they mark the change from primarily aggradational sediment accumulation that characterized the Bowser Basin since its inception in the Early to Middle Jurassic, to mainly progradational sediment accumulation that characterizes the remainder of Bowser Basin history through the mid-Cretaceous. Each prograding delta lobe filled the available accommodation space to near sea-level, as shown by the occurrence of current structures and wave reworking in thick CUS in the upper portions of the undivided Bowser Lake Group. Successive prograding lobes are recorded by the stacked coarsening upward mudstone to sandstone sequences, and each lobe filled accommodation space as it was created, implying continual subsidence of the underlying strata. The tendency of stacked coarsening upward successions to become thinner higher in the stratigraphic column suggests progressive change in the balance between sedimentation rate and subsidence. A progressive reduction of subsidence rate through time is consistent with the sediment compaction and isostatic adjustment model of accommodation space creation described in a later section of this chapter (p. 50). An increase in sedimentation rate could cause similar progradation, and cannot be excluded.

Overlying the marine strata, Currier Formation facies record further progradation of the delta during the Late Jurassic and possibly Early Cretaceous. Extensive peats formed above delta front barrier

sands and gave rise to the thick lower Currier Formation coals. A complex of crevasse splay, lagoon fill, and distributary channel deposits accumulated behind the delta front sands. These deltaic deposits repeatedly built up to subaerial delta plains, and just as repeatedly subsided again (Fig. 2-15). As in the underlying undivided Bowser Lake Group strata, the thickness of coarsening upward successions generally diminishes up in the stratigraphic column. Further reduction of subsidence rate, is therefore inferred during Currier Formation accumulation.

Deposits of the McEvoy Formation overlying the Currier Formation suggest further delta progradation during the mid-Cretaceous. Sediments accumulated by repeated aggradation of fluvial deposits on a relatively slowly subsiding delta plain. The relative slow subsidence of the delta plain could indicate a further reduction in subsidence rate, or an equivalent increase in sedimentation rate. Some indications of an increase in sedimentation rate exist. Sandstone framework grain composition is more chert rich (compositionally mature) in the McEvoy Formation than in the Currier Formation, suggesting that recycled alluvial plain equivalents to the Currier Formation may have been added to the provenance of the lower McEvoy Formation (Chapter 3). Addition of easily eroded alluvial plain sediments to the provenance is consistent with an increase in sedimentation rate. Furthermore, erosion of basin margin sediments is confirmed by the sub-Sustut Group unconformity east of the study area reported by Eisbacher (1974). This unconformity may correlate with the depositional hiatus between the Currier and McEvoy Formations inferred from palynological data (Rouse, written communication, *in* Cookenboo and Bustin, 1989).

Chert pebble to cobble conglomerates become more abundant higher in the McEvoy, and dominate the overlying Devils Claw Formation. The conglomerates are interpreted as a record of progradation of alluvial braidplain facies over the older deltaic strata. The highly resistant nature of chert clasts, and the oligomict nature of the conglomerate are, as mentioned earlier, consistent with progradation into a slowly subsiding basin (Paola, 1988, Gordon and Heller, 1993).

Figure 2-15: Diagrammatic representation of deltaic depositional environments typical of the Currier Formation prograding over shallow marine shelf deposits of the undivided Bowser Lake Group.

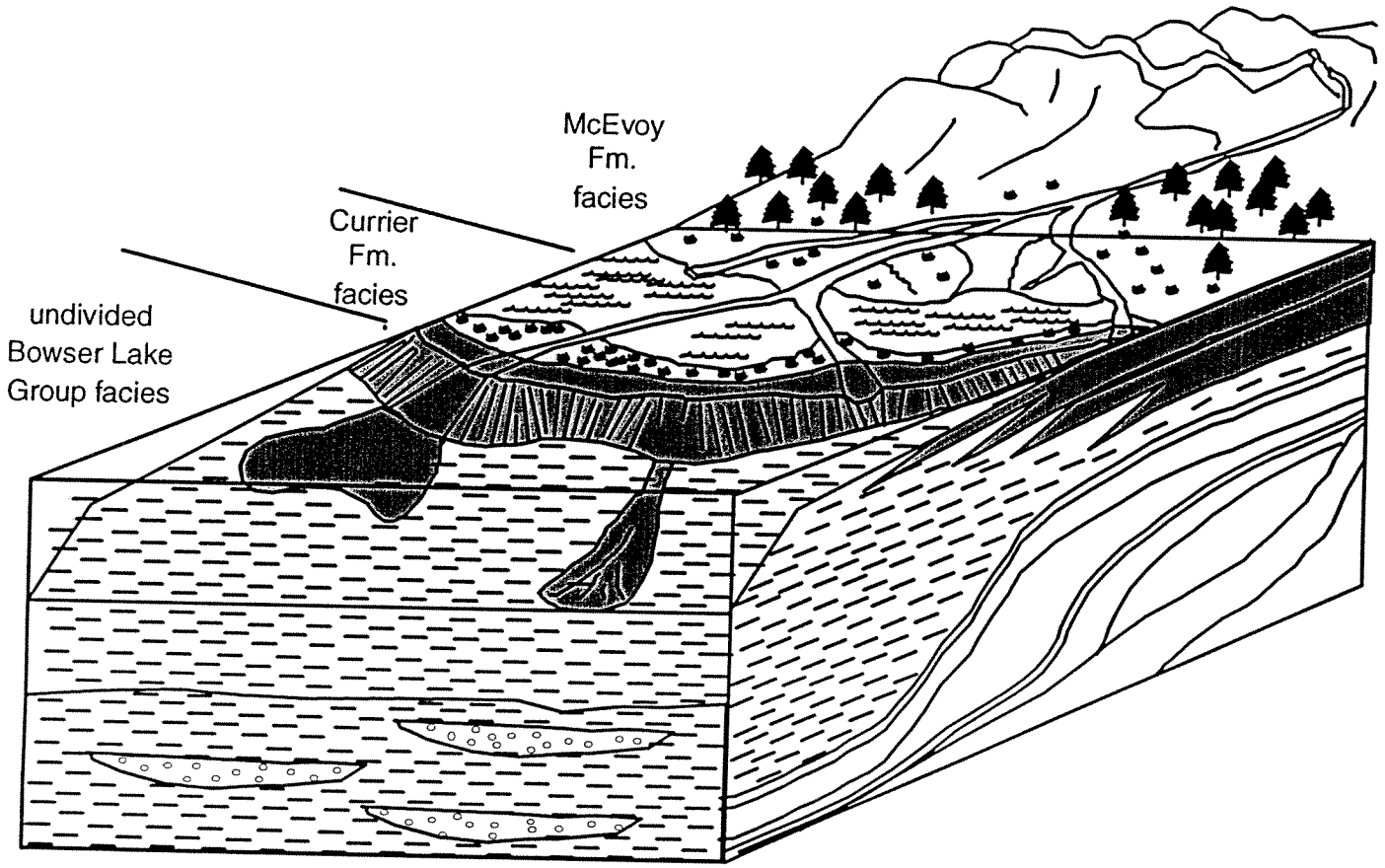

During accumulation of the upper McEvoy and Devils Claw Formations, therefore, subsidence rate was probably decreasing. Sedimentation in the Bowser Basin ceased some time after Devils Claw accumulation, and during the Late Cretaceous, some of the Bowser Basin strata were eroded and transported into the Sustut basin to the east (Eisbacher, 1974; Bustin and McKenzie, 1989).

## CLIMATE

Climate affects many sedimentologic processes, but the record left by climate effects is subtle and difficult to quantify from the rock record. However, understanding climate is of great importance to paleogeographic reconstructions, and therefore it is worth considering the sedimentologic evidence available in a qualitative attempt to reconstruct paleoclimate for the northern Bowser Basin. The most obvious sedimentologic evidence concerning climate in the northern Bowser Basin is the presence of coal in all facies associations above the undivided Bowser Lake Group. Variation in coal seam thickness and abundance in different facies associations, however, is controlled by changing depositional processes, not necessarily climate change. Clearly, coal implies humid climatic conditions. Modern peat accumulations are favoured in two regions where precipitation exceeds evaporation: the tropics, (between 13°N and 7°S latitude); and the temperate zone (north and south of 38° latitude), where moist air in the Hadley cell descends as rain (Sellers, 1965 *in* Ziegler *et al.*, 1987). Paleogeographic reconstructions of coal deposits on a worldwide basis confirm that most coals were deposited within either the tropic or temperate zones (Habicht, 1979). Other features allow distinction between tropical and temperate zone origin for northern Bowser Basin sediments. Most important is the presence of conspicuous tree rings comprised mostly of earlywood with a sharp and thin transition to latewood (Fig. 2-16) in the abundant fossil wood. Additionally, earlywood cell walls are thin and their tracheid cross-sectional areas are large. Conspicuous tree rings form in response to seasonal growth and are pervasive in temperate zone woods, but are commonly lacking or faintly developed in tropical woods (Creber and Chalconer, 1985). The large thin walled tracheids are comparable to modern conifers not commonly exposed to freezing, and suggest mild winters (Spicer, 1989). False rings also occur in Bowser Basin wood, suggesting drought conditions during some growing seasons

Figure 2-16: Silicified transverse section of fossil wood from the Currier Formation, showing abundant early wood and a sharp change to late wood. Field of view is 4 mm in long dimension.

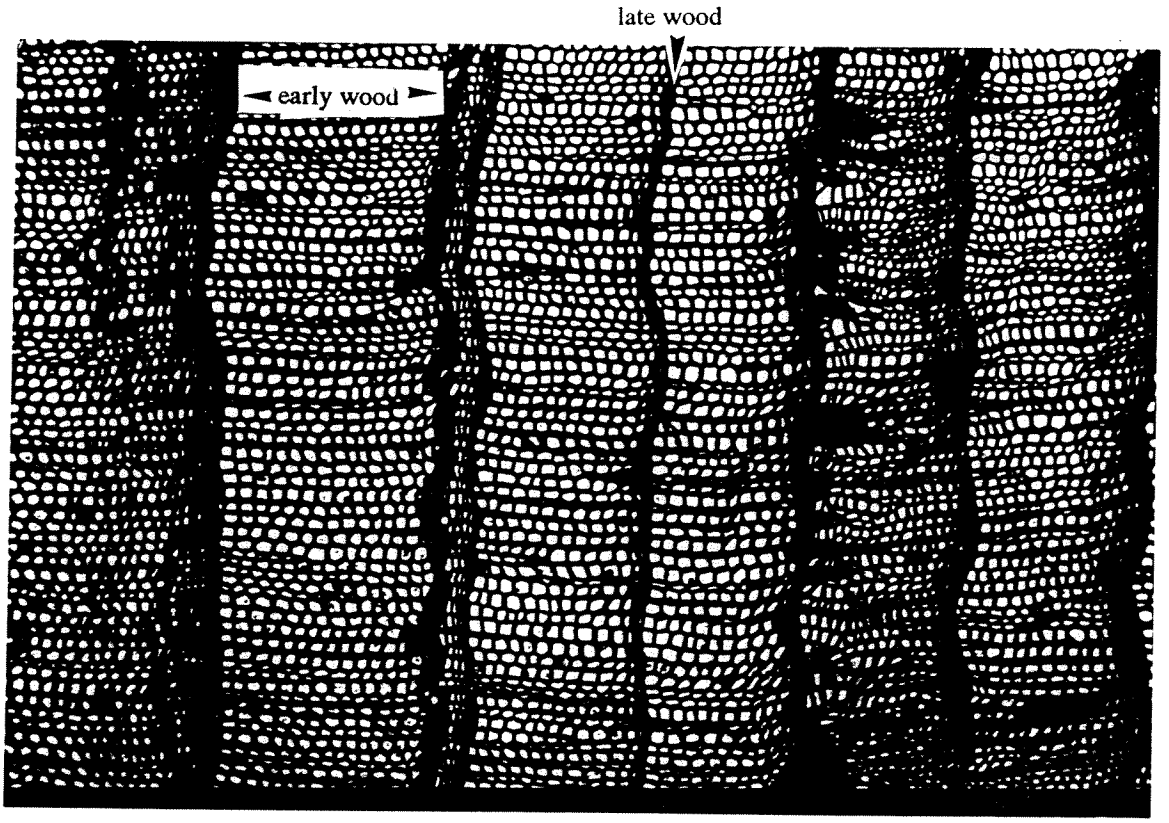


(summer months), although other causes of false rings such as waterlogging, fire or insect attack cannot be eliminated (Spicer, 1989; Spicer and Parrish, 1990). The combination of coals and conspicuous tree rings, therefore, points to a humid temperate climate for the northern Bowser Basin.

An extensive collection of Bowser Basin leaf fossils has been described by MacLeod and Hills (1990). From their work, it is clear that composition of the flora remained relatively stable throughout Bowser Basin sediment accumulation, and that the described flora compares well to worldwide occurrences of humid temperate floras from other Upper Jurassic and Lower Cretaceous strata. In addition, *Nilssonia*, an important component of the Bowser Basin flora, has been shown to be a deciduous plant (Kimura and Sekido, 1975). Deciduous plants, like conspicuous tree-rings, suggest a seasonal climate. The leaf fossils, therefore, support a humid, seasonal temperate climate during Bowser Basin sedimentation.

Further evidence for a cool temperate rather than equatorial or sub-tropical climate is provided

by stable O isotope ratios in carbonate mudstone concretions (Chapter 5). The $d^{18}O$ values suggest concretion precipitation from meteoric or mixed meteoric and marine waters similar to those of present day coastal British Columbia and Alaska.

In contrast, climate of the continental interior appears to have changed during this period. Macroflora assemblages from strata east of the Cordillera change from the Late Jurassic to the end of the Early Cretaceous. One of the prominent changes is the introduction of angiosperm leaf fossils in some mid-continent assemblages in the early Albian. The early angiosperms are thought to have been colonizers of stressed environments, which may have been more common in the interior due to tectonically induced climatic change. For example, Ruddiman and Kutzbach (1991) have demonstrated that late Tertiary uplift of large areas of the Cordillera had caused drying of the North American continental interior and summer drying of the California coast, but not northwest along the coast to Alaska. Similar orogenic separation during the late Mesozoic may have produced a seasonally dry and stressed climate in the continental interior (Lamberson, *et al.*, in preparation), while the Bowser Basin climate remained humid and stable.

## SEDIMENT COMPACTION AND ISOSTATIC LOADING AS MECHANISMS OF BOWSER BASIN FORMATION

Subsidence is required in order to accommodate the thick shallow marine, deltaic, and other near sea-level coastal plain facies in the northern Bowser Basin. A plausible cause for the subsidence is provided by the mechanisms of sediment compaction and isostatic loading, which are inevitably involved in creating subsidence in any large sediment pile such as the Bowser Basin. By assuming Airy isostatic adjustment, and adopting geologically reasonable values for sediment thickness, compaction, and density, a model of the amount of subsidence attributable to sediment compaction and isostatic adjustment is calculated below (Fig. 2-17).

Figure 2-17: Calculation parameters and results for isostatic load plus sediment compaction model of Bowser Basin tectonic development. Total of compaction plus load equals predicted subsidence of basin (created accommodation space) due to sediment accumulation. Following procedures described in Allen and Allen (1990).

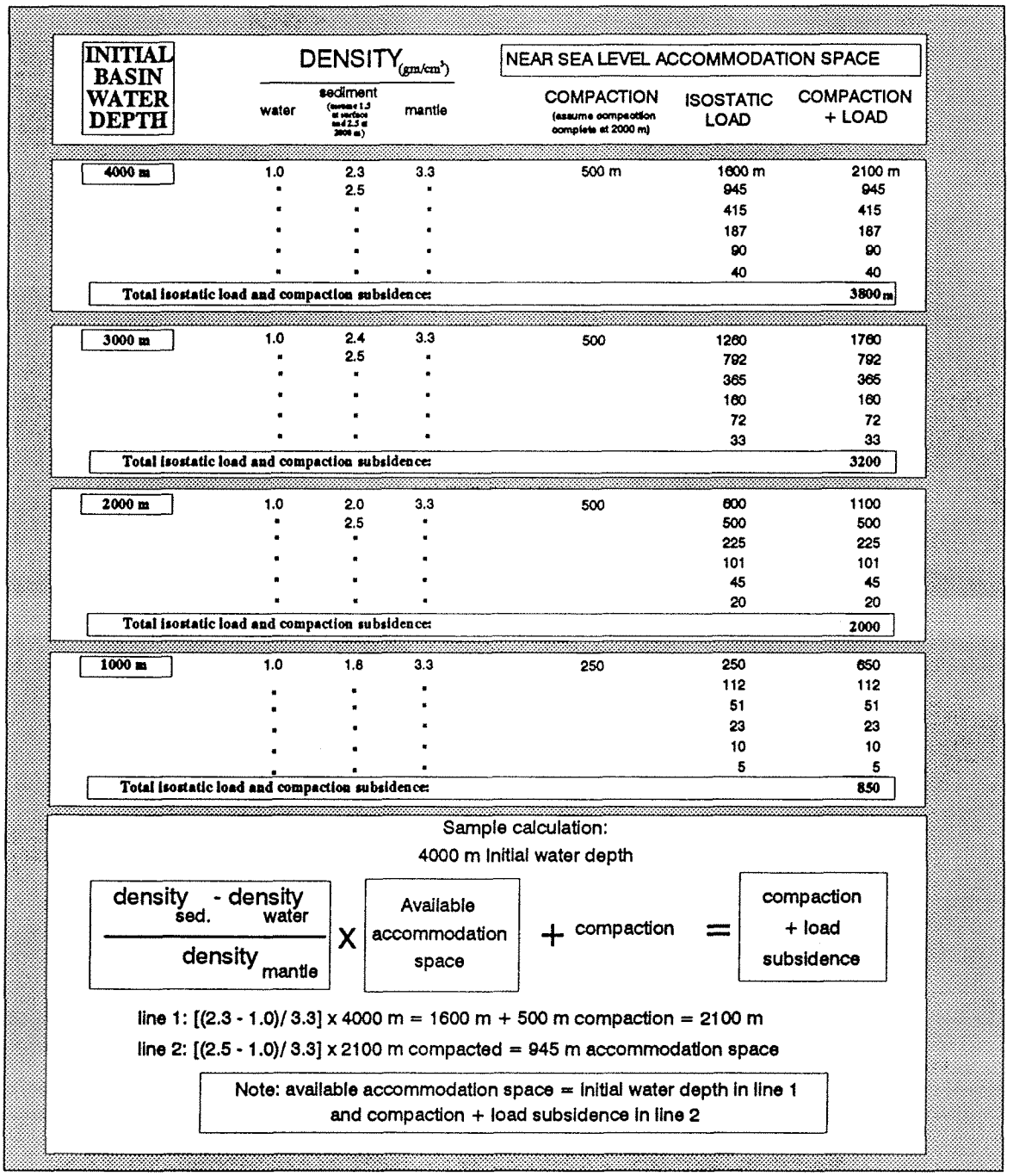

| INITIAL BASIN WATER DEPTH | DENSITY (gm/cm³) water | sediment (increase 1.3 at surface to 2.5 at 2000 m) | mantle | NEAR SEA LEVEL ACCOMMODATION SPACE: COMPACTION (assume compaction complete at 2000 m) | ISOSTATIC LOAD | COMPACTION + LOAD |
|---|---|---|---|---|---|---|
| 4000 m | 1.0 | 2.3 | 3.3 | 500 m | 1600 m | 2100 m |
| | | 2.5 | | | 945 | 945 |
| | | | | | 415 | 415 |
| | | | | | 187 | 187 |
| | | | | | 90 | 90 |
| | | | | | 40 | 40 |
| Total isostatic load and compaction subsidence: | | | | | | 3800 m |
| 3000 m | 1.0 | 2.4 | 3.3 | 500 | 1260 | 1760 |
| | | 2.5 | | | 792 | 792 |
| | | | | | 365 | 365 |
| | | | | | 160 | 160 |
| | | | | | 72 | 72 |
| | | | | | 33 | 33 |
| Total isostatic load and compaction subsidence: | | | | | | 3200 |
| 2000 m | 1.0 | 2.0 | 3.3 | 500 | 600 | 1100 |
| | | 2.5 | | | 500 | 500 |
| | | | | | 225 | 225 |
| | | | | | 101 | 101 |
| | | | | | 45 | 45 |
| | | | | | 20 | 20 |
| Total isostatic load and compaction subsidence: | | | | | | 2000 |
| 1000 m | 1.0 | 1.8 | 3.3 | 250 | 250 | 650 |
| | | | | | 112 | 112 |
| | | | | | 51 | 51 |
| | | | | | 23 | 23 |
| | | | | | 10 | 10 |
| | | | | | 5 | 5 |
| Total isostatic load and compaction subsidence: | | | | | | 850 |

Sample calculation:

4000 m initial water depth

$$\frac{\text{density}_{\text{sed.}} - \text{density}_{\text{water}}}{\text{density}_{\text{mantle}}} \times \text{Available accommodation space} + \text{compaction} = \text{compaction + load subsidence}$$

line 1: [(2.3 - 1.0)/ 3.3] x 4000 m = 1600 m + 500 m compaction = 2100 m

line 2: [(2.5 - 1.0)/ 3.3] x 2100 m compacted = 945 m accommodation space

Note: available accommodation space = initial water depth in line 1 and compaction + load subsidence in line 2

The most significant initial condition for a basin filling model is the starting depth of the Bowser Basin, which is only loosely constrained. However, lithofacies clearly indicate Bowser Basin deposition began in a deep marine environment (Ricketts, 1990). Support for an initial deep marine setting comes from: 1) provenance studies which place the Bowser Basin adjacent to obducted oceanic terranes (Chapters 3 and 4); 2) thermal maturation modelling, which requires high paleogeothermal gradients consistent with oceanic basement (Chapter 5); and 3) the deep basinal character of presumably underlying Spatsizi Group sediments (Thomson, *et al.*, 1986). Considering the long-recognized fundamental tectonic division of most of the earth's surface into oceanic basins greater than 4000 m deep or continental platforms within 100 m of sea-level (c.f. Wegener, 1929), an initial depth as great as 4000 m may be reasonable. Because of uncertainties, however, subsidence models are calculated for initial basins depths of 4000 m, 3000 m, 2000 m, and 1000 m. Other assumptions, including mantle, crustal, and sediment densities, thickness of stratigraphic units and amount of compaction are detailed in the subsidence calculation described in figure 2-17. From these calculations, an initial water depth of 4000 m leads to creation of approximately 3800 m of accommodation space near sea-level, enough to account for accumulation of the entire preserved near sea-level stratigraphic section in the Bowser Basin, plus another 700 m of strata burying the Devils Claw Formation. Three thousand metres initial water depth leads to 3200 m accommodation space, just enough to account for accumulation of the preserved near sea-level strata. Two thousand metres initial water depth creates 2000 m accommodation space, which is sufficient to explain accumulation of the undivided Bowser Lake Group, Currier Formation, and half of the McEvoy Formation. One thousand metres initial water depth leads to only 850 m accommodation space, which can account for accumulation of only MFA and the lower Currier Formation. Based on these calculations, it can be concluded that initial water depths greater than 3000 m adequately account for the subsidence required by the preserved near sea-level sedimentary strata in the northern Bowser Basin, merely as a result of isostatic adjustment and sediment compaction. From another perspective, unless the pre-existing basin was shallower than 3000 m, there is no need to invoke tectonic mechanisms other than compaction and isostatic adjustment, such as the thrust loading suggested by Ricketts *et al.* (1993), to account for Bowser Basin sediment accumulation.

Subsidence and sediment accumulation in the Bowser Basin implies uplift and erosion of the sediment source area. As described above and in chapters 3 and 4, the provenance consisted of obducted island arc and marginal marine lithosphere located north and east of the Bowser Basin. Sandstone petrofacies in successive stratigraphic units, furthermore, suggest that the provenance evolved to greater diversity of rock types during later McEvoy and Devils Claw Formation accumulation. The causes of continual provenance uplift are likely myriad. Isostatic rebound as a result of erosion of material destined for the Bowser Basin probably contributed to the uplift. The erosion implied by sediment accumulation in the Bowser Basin may therefore have contributed to the tectonic evolution of the Western Canadian Cordillera.

# REFERENCES

Aigner, T. 1985. Storm depositional systems, dynamic stratigraphy in modern and ancient shallow marine sequences. *In* Friedman, G. M., Neugebauer, H. J., and Seilacher, A. (*eds.*), Lecture Notes in Earth Sciences. Springer Verlag, Berlin. 174 p.

Allen. P. A. and Allen, J. R., 1990. Basin Analysis. Blackwell Scientific Publications, Cambridge, Massachusetts. 451 p.

Bhattacharya, J. P. and Walker, R. G., 1992. Deltas, *In* Walker, R. G., and James, N. P, (*eds.*) Facies Models: response to sea level change. Geological Association of Canada p. 157-177.

Blatt, H., Middleton, G., and Murray, R., 1972. Origin of Sedimentary Rocks. Prentice-Hall Inc., Englewood Cliffs, New Jersey. 634 p.

Boyd, R., and Penland, S., 1988. A geomorphic model for Mississippi delta evolution: Gulf Coast Association of Geological Societies, Transactions, v. 38, p. 443-452

Bustin, R. M., and McKenzie, K. J., 1989. Stratigraphy and depositional environments of the Sustut Group, southern Sustut Basin, northcentral British Columbia. Bulletin of Canadian Petroleum Geology, v. 31, p. 231-245.

Collinson, J. D., and Thompson, D. B., 1989. Sedimentary Structures. Unwin Hyman, Boston. 207 p.

Cookenboo, H. O. 1989. Lithostratigraphy, palynostratigraphy, and sedimentology of the northern Skeena Mountains and their implications to the tectonic history of the Canadian Cordillera. M.Sc. thesis, University of British Columbia, Vancouver British Columbia. 131 p.

Cookenboo, H. O., and Bustin, R. M. 1990. Lithostratigraphy of the northern Skeena Mountains, British Columbia: Current Research, Part F, Geological Survey of Canada Paper 90-1F, p. 151-156.

Coleman, J. M., 1982. Deltas. International Human Resources Development Corporation. Boston. 124 p.

Creber, G. T. and Chalconer, W., 1985. Tree growth in the Mesozoic and Early Tertiary and the reconstruction of Palaeoclimates. Palaeogeography, Palaeoclimatology, Palaeoecology, v. 52, p. 35-60.

Eisbacher, G. H., 1974. Sedimentary and tectonic evolution of the Sustut and Sifton Basins, north-central British Columbia. Geological Survey of Canada Paper 73-31, 57 p.

Evenchick, C. A., and Green, G. M., 1990. Structural style and stratigraphy of southwest Spatsizi map area, British Columbia. In Current Research, Part F, Geological Survey of Canada, Paper 90-1F, p. 135-144.

Flores, R. M., 1985. Coal deposits in Cretaceous and Tertiary fluvial systems of the Rocky Mountain Region. *In* Flores, R. M., Etheridge, F. G., Miall, A. D., Galloway, W. E. and Fouch, T. D. (*eds.*), Recognition of fluvial depositional systems and their resource potential. Society of Economic Paleontologists and Mineralogists Short Course Notes v. 19, p. 167-216.

Gordon, I., and Heller, P. L., 1993. Evaluating major controls on basinal stratigraphy, Pine Valley, Nevada: implications for syntectonic deposition. Geologic Society of America Bulletin, v. 105, p. 47-55.

Gulf Canada Resources Limited 1987. Lost Fox property. British Columbia Ministry of Energy, Mines and Petroleum Resources, Open File Report 723.

Gulf Canada Resources Limited 1984. Mount Klappan property. British Columbia Ministry of Energy, Mines and Petroleum Resources, Open File Report 111.

Habicht, J. K. A., 1979. Paleoclimate, paleomagnetism, and continental drift. Studies in Geology v. 9, 16 p.

Heller, P. L. and Paola, C., 1992. The large-scale dynamics of grain-size variation in alluvial basins, 2: Application to syntectonic conglomerate. Basin Research, v. 4, p. 91-102.

Jeletzky, O. L., 1976. Preliminary report on stratigraphy and depositional history of Middle to Upper Jurassic strata in McConnell Creek map-area (94D west half), British Columbia. *In* Report of Activities, Part A, Geological Survey of Canada, Paper 76-1A, p. 63-67.

Kimura, T. and Sekido, S., 1975. *Nilssoniocladus* n. genus (*Nilssoniaceae* n. fam), newly found from the early Lower Cretaceous of Japan. Palaeontographica Abt. B., v. 153, p. 111-118.

Lamberson, M. L., Bustin, R. M., Pratt, K. C., and Kalkreuth, W., in prep. The formation of inertinite-rich peats in the mid-Cretaceous Gates Formation: implications for the interpretation of mid-Albian history of paleowildfire.

MacLeod, S. E., and Hills, L. V. 1990. Conformable Late Jurassic (Oxfordian) to Early Cretaceous strata, northern Bowser Basin, British Columbia: A sedimentological and paleontological model. Canadian Journal of Earth Sciences, v, 27, p. 988-998.

Moffat, I. W. 1985. The nature and timing of deformational events and organic and inorganic metamorphism in the northern Groundhog Coalfield: implications for the tectonic history of the Bowser Basin. Ph.D thesis, University of British Columbia, Vancouver, B.C.

Miall, A. D. 1985. Multiple-channel bedload rivers. *In* Flores, R. M., Etheridge, F. G., Miall, A. D., Galloway, W. E. and Fouch, T. D. (*eds.*), Recognition of fluvial depositional systems and their resource potential. Society of Economic Paleontologists and Mineralogists Short Course Notes v. 19, p. 83-100.

Nelson, C. H., 1982. Modern shallow-water graded sand layers from storm surges, Bering shelf: a mimic of Bouma sequences and turbidite systems. Journal of Sedimentary Petrology, v. 52, p. 537-545.

Paola, C., 1988. Subsidence and gravel transport in alluvial basins. *In* K. L. Kleinspehn, and C. Paola (*eds.*), New Perspectives in Basin Analysis. Springer-Verlag, New York. p. 231-243.

Pemberton and MacEachern, 1992. Trace fossil facies models: environmental and allostratigraphic significance. *In* Walker, R. G. and James, N. P. (*eds.*), Facies Models, Geological Association of Canada, p. 47 -72.

Poulton, T. P. , Callomon, J. H., and Hall, R. L., 1991. Bathonian through Oxfordian (Middle and Upper Jurassic) marine macrofossil assemblages and correlations, Bowser Lake Group, west-central Spatsizi map area, northwestern British Columbia. Current Research, Part A, Geological Survey of Canada Paper 91-1A, p. 59-63.

Reynolds, D. J., Steckler, M. S., and Coakley, B. J., 1991. The role of sediment load in sequence stratigraphy: the influence of flexural isostasy and compaction. Journal of Geophysical Research, v. 96, p. 6931-6949.

Richards T. A. and Jeletzky, O. L, 1974. A preliminary study of the Upper Jurassic Bowser Assemblage in the Hazelton west half map-area, British Columbia (93M-W 1/2). Geological Survey of Canada Paper 75-1A, p. 31-36.

Ricketts, B. D. 1990, A preliminary account of sedimentation in the lower Bowser Lake Group, northern British Columbia, in Current Research, Part F, Geological Survey of Canada, Paper 90-1F, p. 145-150.

Ricketts, B. D., Evenchick, C. A., Anderson, R. G., and Murphy, D. C., 1993. Bowser Basin, northern British Columbia: constraints on the timing of initial subsidence and Stikinia-North America terrane interactions. Geology, v. 20, p. 1119-1122.

Ruddiman, W. E. and Kutzbach, J. E., 1991. Late Cenozoic uplift and climate change. Transactions of the Royal Society of Edinburgh: Earth Sciences, v. 81, p. 301-319.

Sellers, W. D., 1965. Physical Climatology. The University of Chicago Press.

Spicer, R. A., 1989. Physiological characteristics of land plants in relation to environment through time.

Transactions of the Royal Society of Edinburgh: Earth Sciences, v. 80, p. 321-329.

Spicer, R. A., and Parrish, J. T., 1990. Latest Cretaceous woods of the central North Slope, Alaska. Palaeontology, v. 33, Part 1, p. 225-242.

Thomson, R. C. Smith, P. L. and Tipper, H. W. 1986. Lower to Middle Jurassic (Pliensbachian to Bajocian) stratigraphy of the northern Spatsizi area, north-central British Columbia. Canadian Journal of Earth Sciences, v. 23, p. 1963-1973.

Tipper, H. W. and Richards, T. A., 1976. Jurassic stratigraphy and history of north-central British Columbia. Geological Survey of Canada, Bulletin 270, 73 p.

Tye, R. S. and Coleman, J. M., 1989. Depositional processes and stratigraphy of fluvially dominated lacustrine deltas: Mississippi delta plain. Journal of Sedimentary Petrology, v. 59, p. 973-996.

Wegener, A., 1929. The origin of continents and oceans. Fourth edition. Dover Publishing, Inc., New York. 246 p.

Ziegler, A. M., Raymond, A. L., Gierlowski, T. C., Horrell, M. A. Rowley, D. B. and Lottes, A. L., 1987. Coal, climate, and climate, and terrestrial productivity: the present and early Cretaceous compared. *In* Scott, A. C. (*ed.*), Coal and Coal-bearing Strata: Recent Advances, Geological Society Special Publication v. 32, p. 25-49.

# CHAPTER 3

## RECORD OF OROGENY IN MESOZOIC SANDSTONES OF THE BOWSER BASIN

### ABSTRACT

Three compositionally distinct, lithic-rich petrofacies occur in Upper Jurassic and Lower Cretaceous sandstones of the northern Bowser Basin. Petrofacies 1 (P1; $Quartz_{total}$ ($Q_t$) =34%, Feldspar (F) =14%, Lithics (L) =52%; $Quartz_{monocrystalline}$ ($Q_m$) =9%, F=14%, $Lithic_{total}$ ($L_t$) =77%) is volcanic lithic rich with subequal to minor chert, minor monocrystalline quartz (generally <10%), and 10 to 25% feldspar. P1 is found in the oldest samples studied from Currier Formation and older Bowser Lake Group sandstones. Stratigraphically above P1, sandstones are chert rich, and contain fewer volcanic lithic components. Petrofacies 2 ($Q_t$=62%, F=5%, L=33%; $Q_m$=5%, F=5%, $L_t$=89%) is rich in chert and poor in feldspar, and has a strong volcanic lithic component and few metamorphic grains like P1. P2 has been found only in the lower McEvoy Formation. The most chert rich samples come from the upper McEvoy and overlying Devils Claw Formations, the youngest stratigraphic units exposed in the northern Bowser Basin, and are designated petrofacies 3 (P3) in this study. Petrofacies 3 (P3; $Q_t$=64%, F=5%, L=31%; $Q_m$=7%, F=5%, $L_t$=88%) is dominantly chert, with a lesser volcanic lithic content. P3 also has lower feldspar content than P1, and a small but significant component (<10%) of metamorphic lithic fragments. Chromite and serpentine are accessory minerals found in all petrofacies. Altered muscovite occurs in P3.

The provenance for P1 is interpreted as obducted sea floor and island arc terranes. P2 is interpreted having the same source, but with the addition of recycled P1 sediments. P3, like P2, combines first cycle ocean floor and island arc provenance with recycled sediments of the same type (such as are preserved in P1). Recycled sediments present in P2 and P3 suggest that uplift of the basin margins may have occurred after deposition of Currier Formation and older Bowser Lake Group (P1), and prior to accumulation of the lower McEvoy Formation (P2). A partly metamorphic and plutonic source for middle McEvoy through Devils Claw formation (P3) may record early stages of dissection of

the island arc that earlier provided the source of P1 and P2.

Independent geological and sedimentological evidence suggest that change in climate, relief, mechanical abrasion or burial diagenesis are unlikely to have significantly affected sandstone compositions.

Comparison with reports of other Cordilleran sandstones demonstrate that chert and volcanic lithic rich sandstones are widespread features of Mesozoic Cordilleran basins. The widespread similarities suggest similar provenance tectonic setting, and that an extensive region of obducted oceanic terranes centered today around the Omineca geanticline was the sediment source for these basins.

## INTRODUCTION

One of the most profound geologic events of the Mesozoic was the rifting of the Atlantic Ocean. This rifting broke apart Pangea and caused the American Continents to override great expanses of Pacific ocean floor. In the process, island arcs were accreted, marginal seas were closed, and the western continental margin developed into the extended orogenic belt of the Cordillera (Coney *et al.*, 1980). Climate patterns, depositional systems and even the evolution of life were all significantly changed by events resulting from rifting of the Atlantic. Record of this paroxysm remains preserved in sedimentary basins both adjacent to and removed from the active orogenic belt. Detailed study of the sedimentary record is called for because of its potential to illuminate the major orogenic events of Mesozoic geologic history.

Intermontane basins contain the most detailed records of the development of the Mesozoic orogenic belt by virtue of their central location within the Cordillera. However, basins within the Intermontane Belt of the Canadian Cordillera are complexly deformed, and of little economic interest, and have therefore received less detailed study than their sedimentary record deserves. In contrast, the Western Canada Sedimentary Basin (WCSB) east of the Canadian Cordilleran orogenic belt has been studied in detail due to its prolific hydrocarbon potential and relatively undisturbed stratigraphy.

Petrographic characterization of Upper Jurassic and Lower Cretaceous sandstones exposed in the northern portion of the Bowser Basin, largest of the basins of the Intermontane Belt of western Canada, was undertaken in an attempt to read part of the record of Cordilleran orogeny. Point-count data and observations of accessory grains are presented herein, and form the basis for interpretations of sandstone provenance. Comparison of the Bowser Basin data with other data sets, including Dickinson and Suczek's (1979) worldwide compendium, sheds light on Cordilleran tectonic development, and allows some inferences to be made concerning events directly related to the Mesozoic rifting of the Atlantic ocean.

## PREVIOUS WORK ON PROVENANCE

Most previous work concerning the provenance of Bowser Basin sediments has concentrated on conglomerate pebble compositions and current directions. Eisbacher (1981), following earlier work of Malloch (1914), related chert pebbles to erosion of Cache Creek Group strata exposed to the north and northeast in the Atlin terrane, and makes brief reference to Bowser Lake Group sandstones composed of approximately 50% volcanic fragments, 40% chert, and 10% quartz. Such pebbles have yielded radiolaria as young as Early to Middle Jurassic (Pliensbachian to Bajocian; Cordey, pers. comm. *cited in* Ricketts and Evenchick, 1991), consistent with the youngest known strata of the Cache Creek Group (Cordey et al., 1987). Paleocurrent directions reported by Eisbacher (1981) and supported by data in Cookenboo (1989) indicate a generally northeastern source area. More recently, Green (1991) reported that almost exclusively chert pebble conglomerate of grey, black and green clast colour occurs in the undivided marine Bowser Lake Group strata exposed north of (and presumably stratigraphically below) rocks sampled in this study. Pebble counts made in the study area reveal similarly oligomict conglomerates of all shades of white, grey, green and black chert.

Isotope ratios have been employed to produce a novel type of provenance data. Neodymium isotopes from Jurassic Bowser Basin clastic strata indicate a predominantly juvenile magma source with minor but steadily increasing content of continental material higher in the section (Samson, *et al.*, 1989).

This isotopic data is consistent with an island arc source mixed either with a few percent continental material or a larger fraction of intermediate material (Samson, *et al.*, 1989).

## COUNTING PROCEDURE

Grains were point-counted by the traditional method which considers each grain individually, using a step size greater than particle size. Well to very well sorted medium grained sandstones were counted to reduce the influence of grain size. A small number of sandstones with mean apparent grain diameter outside the medium sand (250 to 500 $\mu$m) size class were also counted, and are denoted by asterisk in data presentation. The data should be directly comparable with other data derived by use of the Gazzi-Dickinson point count method, because in the northern Bowser Basin, lithic fragments are consistently very finely crystalline, and do not contain a significant proportion of sand-sized crystals (larger than 62.5 $\mu$m).

At least three hundreds grains were counted per sample, with grains assigned to one of nine categories as described in Table 1. Three hundred counts per thin section leaves significant error margins at the 99% confidence level, especially when considering percentages of less abundant components. For example a count of 15 out of 300 (5%) has error margins at 99% confidence levels of plus 3% and minus 2%, i.e. there is a 99% chance that the actual population has between 3 and 8% of whatever component was counted. To halve the 99% confidence interval for a 5% component to between 4 and 6.5% requires increasing the count by four times to 1200 grains (Cheeney, 1982).

Burial compaction has severely altered many sandstones, especially from the lower part of the Bowser Basin section, where concavo/convex and sutured grain contacts and stylolitization attributable to pressure solution are common. As a result, samples exhibiting signs of extreme compaction were avoided for point-counting. Samples preferred for point-counting were those (relatively rare) that exhibit pore-filling cementation which preserved depositional texture. The best such examples of pore-filling cementation are those that contain a poikilitic calcite cement or isopachous chlorite cement which preserve original grain geometry.

Samples from the deepest portion of the stratigraphic column in the Bowser Basin tend to be more affected by burial compaction, and many such samples are unsuitable for provenance determination. Pervasive alteration, replacement by calcite, and pressure solution effects, all become more pronounced with increasing depth in the section. Such effects are most destructive in fine and very fine grain sandstones, and the overall finer grain nature of Currier and older Bowser Lake Group rocks severely limits sample selection. In the oldest rocks examined, provenance signal becomes obscured by development of slatey fabric in many grains. This fabric is recognizable by preferred alignment of birefringent clay minerals and can be pervasive in the most deeply buried samples. This alteration may mark the depth of burial limits to which provenance signal is decipherable in the Bowser Basin.

Accessory grains with potential tectonic significance were noted during thin section examination. Compositions were later confirmed if necessary by examination with combined scanning electron microscopy and energy dispersive x-ray (SEM-EDS) system. Chromian spinel is the best example of such a tectonically significant accessory mineral identified in this study. Further study of chromian spinels from some of these sandstones involving microprobe analysis of chemical compositions is detailed in Chapter 4 of this thesis.

Feldspars were tentatively classified based on twinning styles during point-counting. Reference sections were stained for potassium feldspar using sodium cobaltinitrite. Both methods showed that no potassium feldspar was present in most samples. Due to a lack of significant potassium feldspar content (except in certain stratigraphic intervals as discussed later), no further effort was deemed useful in attempting to refine the percentages of plagioclase versus potassium feldspar.

### *Grain types counted*

**Chert:** Grains called chert in this study are micro- or cryptocrystalline quartz with no visible feldspar phenocrysts. Chert occurs in colors ranging from clear to brown in thin section, and is more or less argillaceous, forming a continuum with siliceous mudstone (argillite), counted as lithic sedimentary fragments. Crystallites are typically intergrown and sutured, and average less than 30 $\mu$m in diameter.

Distinction between chert and siliceous mudstone is made on the criteria of overall low birefringence, and high resistance to compaction deformation for grains counted as chert. This definition of chert differs somewhat from Dickinson (1985), who counts all argillaceous siliceous grains as lithic sedimentary fragments. We believe counting argillaceous chert sand grains as chert conforms better to terminology applied outside sandstone provenance studies, such as in works referring to bedded chert or conglomerate pebbles (e.g. Pollack, 1987; Sugitani *et al.*, 1991).

**Volcanic lithic fragments:** Volcanic lithic fragments are generally finely crystalline with included microlites of fine grain plagioclase lathes and a trachytic texture (Fig. 3-1). Less commonly volcanic lithic fragments contain quartz phenocrysts. Grains are more or less altered to chlorite. Very fine grained micro- or cryptocrystalline grains were called volcanic lithic fragments if direct indications of volcanic origin such as plagioclase lathes or other microlites were identified. Chloritized grains were counted as volcanic lithic fragments if any internal volcanogenic texture was recognized.

**Metavolcanics:** Green to yellow-brown grains that commonly have anomalously low birefringence occur pervasively as minor components in Bowser Basin sandstones. These grains include detrital chlorite and rare serpentine and were counted as metavolcanics.

**Sedimentary lithic fragments:** Sedimentary lithic fragments include mudstones, claystones and siliceous argillite. They form a continuum with low rank metasedimentary lithic fragments from which they are distinguished by lack of significant clay alignment. There is also a continuum between sedimentary lithic fragments and argillaceous chert. Sedimentary lithic fragments are distinguished by higher birefringence and generally lower resistance to compaction (i.e. usually compacted grains).

Figure 3-1: Photomicrographs of typical volcanic lithic and chert grains with poikilitic calcite cement.

No attempt has been made to distinguish intra-basinal from more distantly transported clasts. Locally derived mudstone rip-up clasts combine with provenance derived sedimentary lithic fragments in widely varying degrees in different samples, leading to wide variance in abundance throughout the section.

**Monocrystalline quartz:** Monocrystalline quartz is counted for single crystal quartz grains. Both single extinction (less than 5°) and undulatory extinction (greater than 5°) are common. Quartz grains composed of multiple crystals larger than 62 $\mu$m are counted as monocrystalline quartz as well, in order for this category to conform with $Q_m$ of Gazzi-Dickinson point counts.

**Polycrystalline quartz:** Polycrystalline quartz refers to all lithic quartz grains composed of more than 1 crystallite averaging between 30 and 62 $\mu$m. Chert combined with polycrystalline quartz are approximately equivalent to $Q_p$ of Gazzi-Dickinson point counts.

**Feldspar:** Feldspar was counted for any low birefringence monomineralic grain displaying twinning, cleavage near 90°, or evidence of replacement characteristic of feldspars. Twinning type was noted where present, but estimations of plagioclase to potassium feldspar ratios depended on examination of sodium cobaltinitrite stained reference sections.

**Replaced grains (alterites):** A grain was counted as replaced or "alterite" if replacement was too complete to allow confident assignment to original grain type. Replacement is commonly by carbonate, megaquartz, microcrystalline quartz, chlorite, illite, sericite or opaques. Replacement counts are presented as percent of the total grain count in the results section, but are not included in $Q_mFL_t$ or $Q_tFL$ calculations.

## RESULTS

The results of the point-counts are summarized in table 3-1. All of the samples are rich in chert and/or volcano-lithic fragments, and relatively lacking in monocrystalline quartz, except for two samples of Skeena Group green sandstones.

Table 3-1: Point count results for sandstones in the northern Bowser Basin. Abbreviations are described in caption for figure 3-2. The table is arranged with samples in stratigraphic order, starting with oldest at the base.

**PETROFACIES 3 (MIDDLE AND UPPER MCEVOY AND DEVILS CLAW FORMATIONS)**

| | QZmono | QZPc | F(p+k) | CHERT | VRF | SRF | MVRF | MRF | ALT |
|---|---|---|---|---|---|---|---|---|---|
| HOC 18-10 | 17.3% | 5.2% | 5.8% | 42.9% | 4.9% | 6.4% | 2.4% | 2.1% | 13.1% |
| HOC 18-6 | 3.8% | 5.0% | 3.1% | 59.6% | 12.3% | 6.9% | 3.5% | 4.7% | 1.2% |
| HOC 34-19 | 5.4% | 3.3% | 3.7% | 46.5% | 12.7% | 6.4% | 2.3% | 6.0% | 13.7% |
| HOC 35-23 | 4.4% | 6.8% | 2.4% | 52.7% | 11.9% | 9.5% | 1.7% | 5.8% | 4.8% |
| HOC 19-8 | 5.1% | 1.9% | 4.8% | 50.3% | 16.8% | 11.4% | 2.5% | 5.4% | 1.9% |
| GH7-40 | 13.0% | 6.5% | 5.1% | 46.9% | 5.8% | 6.8% | 3.8% | 9.6% | 2.4% |
| HOC 14-8 | 4.5% | 4.8% | 2.6% | 50.0% | 18.5% | 7.6% | 1.9% | 4.1% | 6.1% |
| *HOC 8-1 | 4.9% | 4.2% | 5.6% | 38.0% | 14.1% | 13.4% | 2.1% | 5.6% | 12.0% |
| HOC 12-10 | 4.8% | 2.9% | 5.2% | 46.8% | 19.4% | 9.4% | 3.2% | 2.6% | 5.8% |
| HOC 33-16 | 5.5% | 6.1% | 6.3% | 43.3% | 11.5% | 8.2% | 0.3% | 4.2% | 14.5% |

**PETROFACIES 2 (LOWER MCEVOY FORMATION)**

| | QZmono | QZPc | F(p+k) | CHERT | VRF | SRF | MVRF | MRF | ALT |
|---|---|---|---|---|---|---|---|---|---|
| HOC 19-5 | 7.5% | 2.9% | 3.3% | 47.4% | 26.5% | 5.2% | 2.3% | 1.3% | 3.6% |
| HOC 15-9 | 3.2% | 5.3% | 5.7% | 50.9% | 27.0% | 4.2% | 0.0% | 1.1% | 2.8% |
| HOC 16-1 | 4.3% | 7.4% | 6.3% | 42.8% | 25.8% | 2.7% | 0.0% | 0.7% | 10.0% |
| HOC 33-7 | 5.0% | 6.0% | 4.6% | 51.0% | 22.7% | 0.3% | 2.3% | 1.7% | 6.3% |

**PETROFACIES 1 (CURRIER FORMATION)**

| | QZmono | QZPc | F(p+k) | CHERT | VRF | SRF | MVRF | MRF | ALT |
|---|---|---|---|---|---|---|---|---|---|
| HOC 14-1 | 18.0% | 2.7% | 13.0% | 27.0% | 29.3% | 3.7% | 4.7% | 0.0% | 1.7% |
| HOC 8-11 | 12.1% | 3.3% | 9.1% | 13.4% | 32.2% | 2.3% | 3.3% | 3.3% | 21.2% |
| HOC 8-8 | 4.2% | 3.8% | 7.5% | 20.0% | 39.6% | 14.2% | 3.8% | 1.7% | 5.4% |
| HOC 15-7 | 7.5% | 4.9% | 16.7% | 13.1% | 35.1% | 8.9% | 2.3% | 0.3% | 11.1% |
| HOC 30-8 | 8.6% | 1.5% | 22.8% | 10.5% | 41.7% | 5.2% | 4.0% | 1.9% | 3.7% |
| HOC 30-6 | 2.9% | 1.9% | 11.1% | 27.9% | 42.5% | 5.1% | 1.3% | 0.3% | 7.0% |
| HOC 30-3 | 4.1% | 0.3% | 10.4% | 14.2% | 59.0% | 4.7% | 2.5% | 0.3% | 4.4% |
| HOC 27-1 | 7.2% | 1.4% | 23.8% | 17.5% | 22.4% | 2.0% | 0.6% | 1.7% | 23.3% |
| HOC 22-6 | 5.4% | 2.4% | 2.7% | 42.2% | 34.8% | 10.8% | 0.0% | 0.0% | 1.7% |

**SAMPLES THAT DO NOT FIT PETROFACIES AS DESCRIBED IN TEXT**

| | QZmono | QZPc | F(p+k) | CHERT | VRF | SRF | MVRF | MRF | ALT |
|---|---|---|---|---|---|---|---|---|---|
| HOC 19-2 | 0.6% | 2.6% | 6.4% | 15.2% | 59.7% | 5.5% | 1.9% | 1.3% | 6.8% |
| HOC 17-7 | 10.6% | 1.6% | 16.0% | 14.7% | 38.8% | 2.5% | 0.9% | 0.3% | 15.6% |
| HOC 13-3 | 8.7% | 2.0% | 13.4% | 22.1% | 24.1% | 8.1% | 7.3% | 1.2% | 13.1% |

**SKEENA GROUP AT MOSQUE MOUNTAIN**

| | QZmono | QZPc | F(p+k) | CHERT | VRF | SRF | MVRF | MRF | ALT |
|---|---|---|---|---|---|---|---|---|---|
| HOC 30-12 | 39.2% | 13.7% | 9.6% | 13.2% | 7.3% | 3.2% | 2.3% | 5.6% | 5.8% |
| HOC 30-10 | 32.8% | 13.2% | 12.0% | 1.9% | 5.0% | 0.3% | 8.8% | 8.5% | 17.4% |

The most striking result of the point-counts is the identification of three distinct grain type populations, named herein petrofacies 1, 2 and 3, each characterizing a particular stratigraphic interval. Composition of the petrofacies is described in the following section and is followed by interpretation of provenance. Inherent in the provenance interpretations is the assumption that provenance controls sandstone composition. Most researchers have concluded that provenance exerts the strongest control over composition, and provenance interpretations have been made accordingly. However, other factors including climate, relief, transport processes, alluvial storage, recycling and burial diagenesis clearly are capable of influencing composition. Consideration is given to these other factors and their likely effects on compositions of the studied sandstones in a separate section following the petrofacies descriptions and interpretations.

### *Petrofacies 1*

Petrofacies 1 (P1) is present in Currier and older undivided Bowser Lake Group rocks, and is dominated by volcanic lithic fragments, with subequal to minor chert, low monocrystalline quartz ($< 10\%$ except in samples #14-1 and 8-11), and about 10-25 % feldspar (Fig. 3-2). Volcanic lithic fragments typically have trachytic texture with more or less aligned lathe-like plagioclase phenocrysts set in an aphanitic groundmass, and are variously fresh to chloritized. Quartz and vitric shards are generally absent from volcanic lithic fragments, although some euhedral monocrystalline quartz of possible volcanic origin occur. In the two samples with the greatest concentration of quartz (samples 14-1 and 8-11), mono- and polycrystalline quartz were point-counted separately by the methods outlined by Basu et al. (1975), to better characterize the origin of quartz. Non-undulatory monocrystalline quartz dominated other types by at least a factor of four to one, and polycrystalline quartz was mostly composed of much greater than 4 crystallites per grain.

Chert in P1 only rarely contains definitive radiolarian or sponge spicule ghosts, and therefore an origin from devitrified volcanics for a portion of the chert in P1 can not be discounted. The total volcanic signal may thus include some portion of the chert and quartz grains, and therefore may be

Figure 3-2: Composition of Petrofacies 1. Detrital modes of nine grain types plotted against percent of sample. Qm= monocrystalline quartz; $Q_{pc}$= polycrystalline quartz (crystallites between 30 and 62 $\mu$m); $F_{(p+k)}$= total feldspar; CH= chert (crystallites less than 30 $\mu$m); VRF= volcanic lithic fragments; SRF= sedimentary lithic fragments not including chert; MRF= metamorphic lithic fragments; MVRF= metavolcanics including chlorite and serpentine; ALT= altered grain (unrecognizable origin).

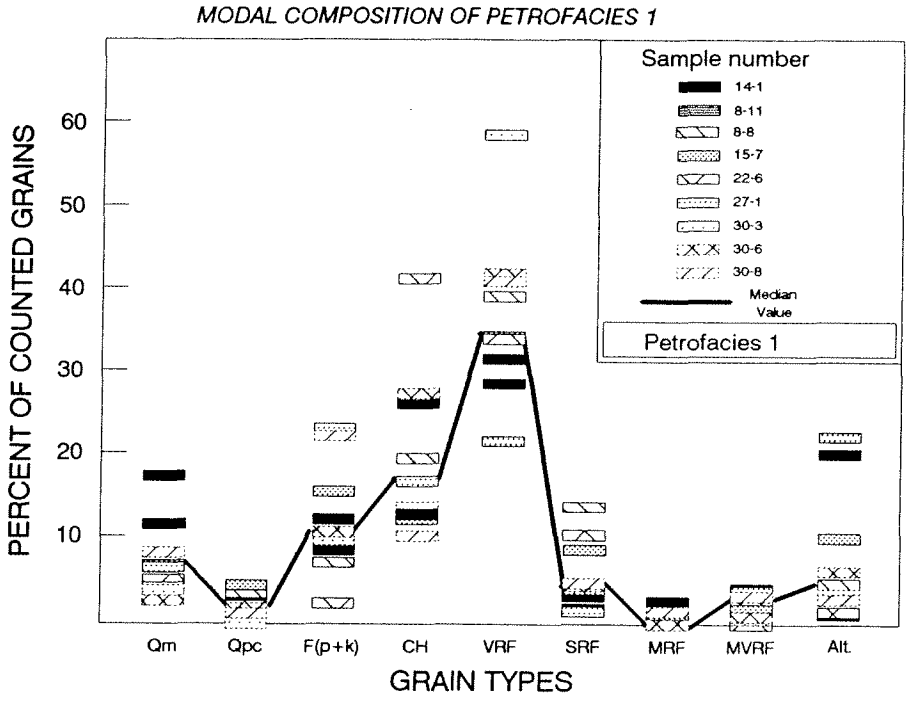

greater than the volcanic lithic fragments alone suggest. Unaltered mafic minerals are notably absent, except for biotite in more or less chloritized tabular grains.

Metamorphic fragments are rare in P1, and are limited to slatey grains from low grade metapelites.

Chromian spinel is a notable accessory mineral in P1 sandstones. It is easily identified based on dark reddish brown (nearly opaque in some cases) color and isotropic properties in thin section. Chromian spinel commonly occurs in ocean floor peridotites, olivine basalts and dunites and is often preserved during the alteration of ocean floor rocks (Hekinian, 1982). It has also been reported as the dominant heavy mineral in sandstones sourced from ophiolites (Stattegger, 1987). Chromian spinel grains from selected sandstones were further analysed by microprobe and yielded compositions similar to spinels from alpine-type peridotites associated with marginal basin origin (Chapter 4). Zircon is rare in the Bowser Basin, although zircon is usually the most abundant type of accessory heavy mineral grain in sandstones. Typically less than one zircon grain occurs for every five to ten chromian spinels. Serpentine with an anastomosing network texture typical of alteration from olivine (Shelley, 1975), and in some cases containing small (less than 10 micrometre), dispersed chromian spinel crystals, has also been identified as an accessory mineral in some P1 sandstones.

Feldspar exhibits the most pronounced variation in P1. Most arkosic samples are located towards the south and east edge of the study area, which may reflect proximity to a rugged source area. Feldspar composition supports a proximal source to the southeast. Potassium feldspar is absent from samples in the northern and central portion of the study area, but is present in minor quantities near the eastern margin of the basin. Potassium feldspar is a common component of many island arc suites, but is rare in ocean floor basalts. Concentration of potassium feldspar in the most arkosic samples supports their proximity to an island arc source. Much lower feldspar and exceptionally high chert content is found in sample 22-6. This sample comes from a wave reworked marine bar sand topped by a shell lag. The relatively more mature composition is attributed to mechanical abrasion by wave reworking and thus

provides an example of the effects of intense reworking on the composition of P1 sandstones.

*Provenance interpretation*

The composition of petrofacies 1, dominated by volcanic lithic fragments and sub-equal or lesser amounts of chert (some of undoubted biogenic origin), points to an oceanic provenance. Two types of oceanic source rocks are inferred from grain composition observations. The observations that quartz is uncommon, feldspar is largely plagioclase, biogenic chert is relatively abundant, and chromian spinel, serpentine and biotite occur as accessory minerals point to a peridotite, other ultramafic or basaltic oceanic terrane such as uplifted sea floor. Support for sea floor involvement can be found in the fact that much of the volcanic lithic content is more or less altered to chlorite, which is a common trait of ocean floor volcanics (Hekinian, 1982). Localized arkosic samples, as well as a minor fresh volcanic lithic component, suggest a volcanic island arc source in addition to the inferred ocean crust source. Similar quartz-poor, feldspathic to arkosic sands derived from an oceanic island arc occur in Central America (Lundberg, 1991). Although modal quartz values are consistently low, most of the non-chert quartz in the northern Bowser Basin is monocrystalline, and some is euhedral. This composition of quartz is comparable to volcanic sands described by Girty *et al.* (1988), and therefore provides further support for a volcanic source.

The commonly altered nature of the volcanic lithic fragments indicates the volcanic signal of P1 is largely derived from extrabasinal eroded and transported paleovolcanics (Zuffa, 1985). No clear intrabasinal neovolcanic signal was identified in the sandstones, suggesting active volcanism was absent or minor during P1 time. Contrary evidence for active volcanism in Currier rocks is provided by drill cores which have encountered several thin tuffaceous layers. However, these tuffs are fine grained and may represent long distance aerial transport (Gulf Canada Resources Limited, open file reports, 1984, 1987). The paleovolcanic signal is consistent with a provenance of uplifted sea floor and (mostly) inactive island arcs. Concentration of more arkosic samples on the southeastern margin of the study area may point approximately to the location of the inferred arc. In that direction, good candidates for an

older arc source include the Hogem Batholith and related calc-alkaline plutons. The Hogem batholith is a large intrusive body of mostly calc-alkaline Late Triassic and Early Jurassic age rocks (Garnett, 1978). Similar arc sources that may have contributed sediment to the Bowser Basin from the northwest include the Hotailluh Batholith (Moffat *et al.*, 1988). Suitable ocean floor rocks include the Cache Creek Group in the Atlin terrane to the north as originally suggested by Eisbacher (1981), and Slide Mountain terrane rocks lying farther to the northeast.

Red chert, which is absent from northern Bowser Basin conglomerates, is common in radiolarian cherts that formed above open ocean crust (Jones and Murchey, 1986; Sedlock and Isozaki, 1990). The association of red chert and spreading centers is supported by experimental demonstrations that chert turns red when heated above 230° to 290°C in the presence of oxygen (Rick, 1978). Biogenic chert colors that occur in the Bowser Basin may also be characteristic of particular sea floor depositional settings. Grey and green chert are associated with oceanic island arcs, and black chert is associated with continental margins, where argillaceous continent detritus dilutes siliceous material and cherts commonly grade to claystone (Jones and Murchey, 1986).

### *Petrofacies 2*

Petrofacies 2 (P2) occurs in lower McEvoy Formation sandstones and is dominated by volcanic lithic grains, but is also rich in chert and low in feldspar (Fig. 3-3). P2 has little or no metamorphic content, and accessory grains include rare petrified wood and coal spar, in addition to numerous argillaceous intrabasinal sedimentary lithic fragments. The high volcanic lithic content and lack of metamorphic indicators are similar to P1 (Currier Formation and older strata), but the high chert content is similar to younger McEvoy and Devils Claw formations sandstones (described below as petrofacies 3). Because of P2's stratigraphic position and composition, it can best be considered a transitional petrofacies between the volcanic lithic rich P1 sandstones of the Currier Formation and older strata, and the chert rich sandstones of upper McEvoy and Devils Claw formations.

Figure 3-3: Petrofacies 2 composition. Plotted parameters are the same as in figure 3-4.

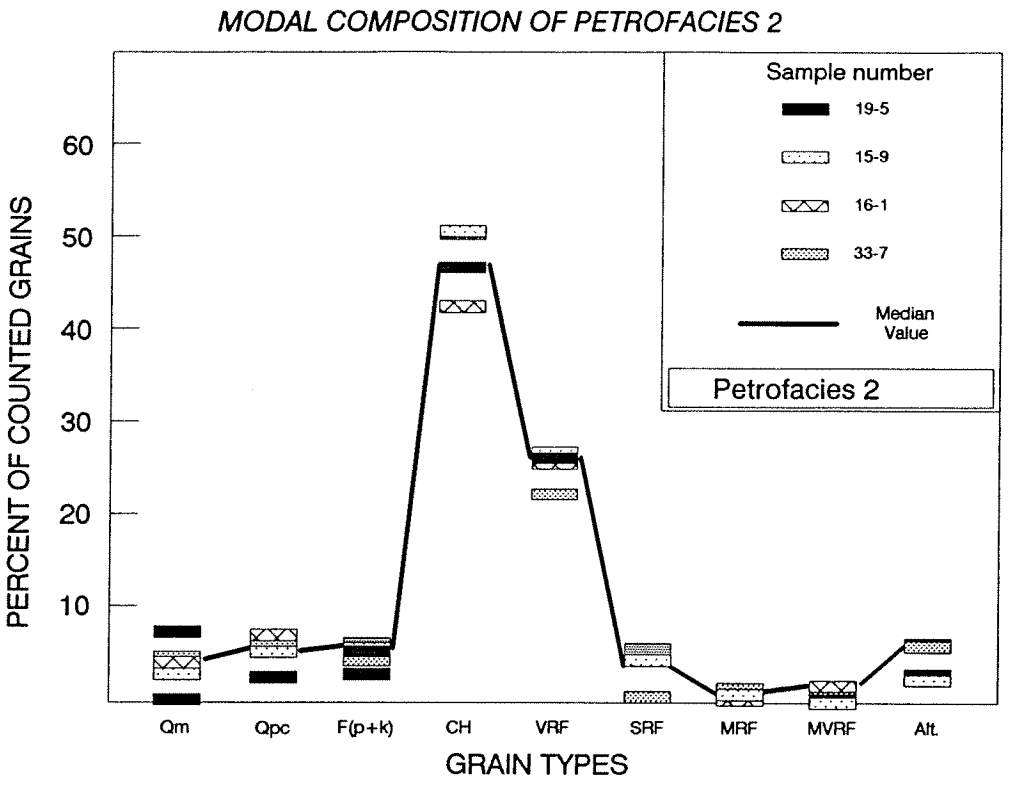

*Provenance interpretation*

Petrofacies 2 is similar in composition to P1 with a high volcanic lithic content, low quartz, and little or no metamorphic signal. P2 differs from P1, however, in having a higher chert content. P2 is therefore compositionally more mature than P1, which suggests recycled P1 as a source. Accessory grains such as coal spar and petrified wood occur rarely in P2, indicating erosion of previously lithified sediments, and are consistent with a recycled P1 provenance. Because P2 lacks a metamorphic input, and is restricted to lower McEvoy Formation strata, metamorphic terrane unroofing apparently commenced during mid-McEvoy time.

### *Petrofacies 3*

Petrofacies 3 (P3) occurs in sandstones from the middle McEvoy Formation through at least the middle to upper Devils Claw Formation. It is characterized by >40% chert, <20% volcanic lithic fragments, and a small but significant component (<10%) of metamorphic lithic fragments (Fig. 3-4). Feldspar content drops compared to P1 to less than 6% of total grains, but like P1, only plagioclase feldspar is present in most samples. Monocrystalline quartz is more abundant than in P1, and commonly has euhedral outlines with few inclusions characteristic of volcanic origin (and sometimes embayments and rarely with negative crystal inclusions which can indicate a volcanic origin as well; Scholle, 1982).

Volcanic lithic fragments have a trachytic texture like P1, and are the same size and texture as other grains, and only rarely appear fresh. Most are extensively chloritized, as are accessory biotite grains. Glass shards are very rare components (only one clearly identified), and easily altered mafic minerals are absent except in easternmost areas. The volcanic grains may therefore be described as derived from an extrabasinal paleovolcanic source (Zuffa, 1985).

Metamorphic lithic fragments occur more commonly in P3 than in P1 and are mostly metapelites, derived from slates and phyllites (Fig. 3-5). Other grains can also be considered part of

Figure 3-4: Petrofacies 3 composition. Plotted parameters are the same as in figure 3-4.

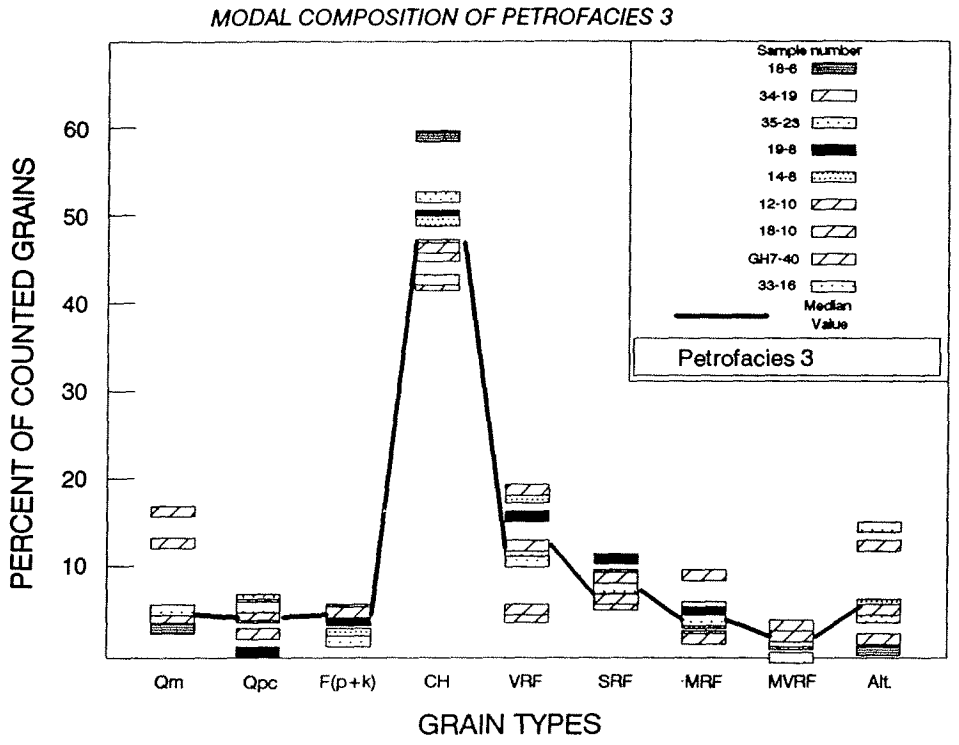

Figure 3-5: Metamorphic grain from P3, probably from either a phyllite or schist. Plain and cross polar transmitted light micrographs. Grain is approximately 350 $\mu$m long dimension.

the total metamorphic provenance signal. Some polycrystalline quartz grains have more than 10 stretched crystallites with sutured contacts (Fig. 3-6), which are very good indicators of phyllite, schist or higher grade metamorphic provenance (Scholle, 1982). Muscovite, which is abundant in metamorphic terranes, is present in P3 as an accessory mineral that is commonly partially chloritized (Fig. 3-7).

Accessory grains of chromian spinel are only found in some P3 sandstones. In samples that contain chromian spinels, the composition is very similar to that of P1 chromite, based on microprobe study (Chapter 4, this thesis). Accessory grains of serpentine, some with an irregular anastomosing network typical of olivine replacement (Shelley, 1975), have also been identified in some sandstones.

*Provenance interpretation*

Petrofacies 3 is similar to P1 in that both are lithic rich, but substantial differences are present, implying some changes in provenance. Primarily, P3 has a much higher chert and lower volcanic lithic content. Total quartz (combination of monocrystalline quartz, polycrystalline quartz, and chert equivalent to $Q_t$ of Dickinson and Suczek, 1979) is close to 70%, and most of the total quartz is chert (45-60%). Volcanic lithic fragments are pervasively chloritized and less common (5-20%) than in P1. Relatively high total quartz content suggests in part a recycled sedimentary provenance. The high chert content, pervasive volcanic lithic component and accessory chromian spinel, serpentine and chloritized biotite suggests the origin of the recycled sediments was a sea floor and island arc provenance, much like that for P1. Most likely P3 is in part recycled alluvial facies equivalent to marine and deltaic facies preserved in P1, and in part first cycle sediments from the same sea floor source rocks.

Interpreting P3 exclusively as recycled P1 is not sufficient, however, to account for other components of the grain composition. The clear metamorphic signal composed of polycrystalline quartz grains with more than ten sutured, stretched crystallite contacts per grain, increased metapelite grain abundance and rare accessory muscovite indicates a metamorphic terrane as part of P3's provenance. Volcanic lithic fragments are less common than P1, as expected if P2 is partly recycled P1, and

Figure 3-6: Polycrystalline quartz grain of probable metamorphic origin. Grain is approximately 550 $\mu$m in long dimension.

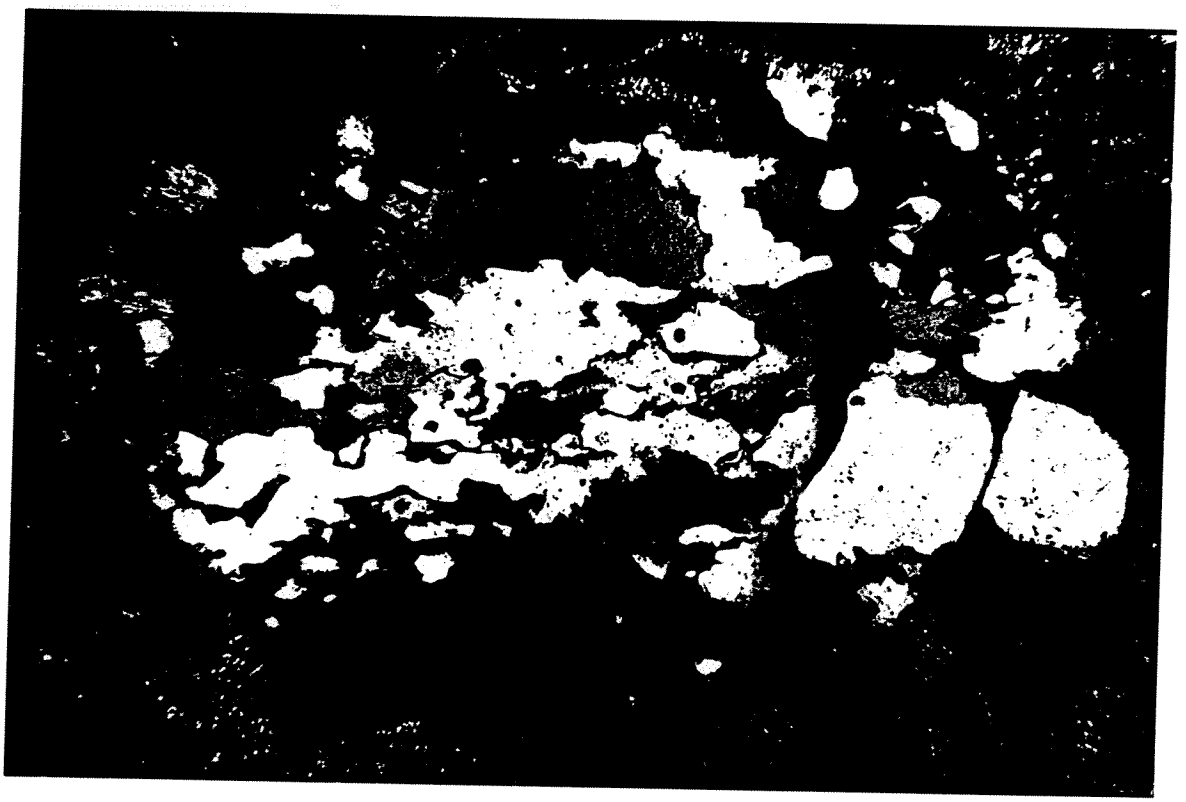

Figure 3-7: Muscovite grain (crossed polarized light) from Petrofacies 3. Grain is approximately 300 $\mu$m long dimension

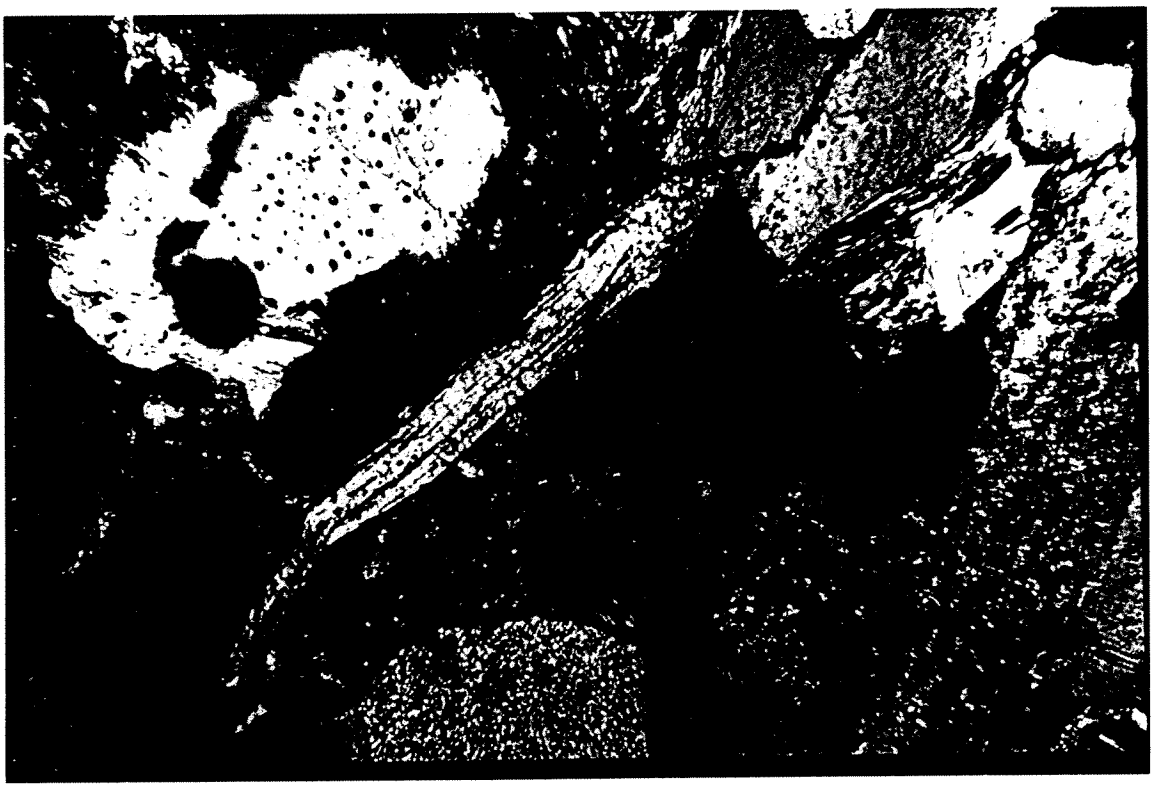

the volcanic lithic grains are mostly attributable to a paleovolcanic source like P1. However, the presence of rare volcanic lithic fragments with included glass shards and quartz, and euhedral monocrystalline quartz of probable volcanic origin, suggests minor input from active, probably siliceous, volcanic sources not evident in P1.

Considered together, the grain composition of P3 indicates a provenance terrane consisting of unroofed metasedimentary facies (including at least slates, phyllites and schists) mixed with both first cycle and recycled oceanic lithosphere facies. Uplift of previously deeply buried rocks is supported by collection of a single calc-alkaline quartz diorite pebble (2 cm by 6 cm) from an otherwise oligomict chert pebble conglomerate of the upper McEvoy Formation. Indications within P3 of uplift and active acid magmatism in the provenance are supported by the presence of increasingly coarse, thick and abundant chert pebble and cobble conglomerate up through the McEvoy and Devils Claw Formations.

As with P1, the Cache Creek Group and Slide Mountain Assemblage along with magmatic arc rocks associated with the Hogem or related batholiths are likely candidates for source. Potassium-argon ages from the Hogem batholith, and stocks to the east of it, indicate early to mid- Cretaceous resumption of increasingly sialic volcanism (Garnett, 1978). The recycled and metamorphic components may reflect uplift associated with dissection and emergence of the Jurassic island arc.

Three McEvoy and Devils Claw Formation samples were counted that do not fit in P3 or P2 and warrant individual consideration. Each of these samples is enriched in volcanic lithic fragments and relatively depleted in chert compared to P3 or P2, but also differ significantly from P1.

Sample 19-2 is the most volcanic-rich sandstone in either the McEvoy or Devils Claw Formations. It was collected in a basal pebble-granule conglomerate layer of the McEvoy Formation. This basal conglomerate has been correlated to both the north and south of sample 19-2's location, and may represent a tectonic pulse associated with inception of McEvoy/Devils Claw deposition (Cookenboo, 1989) in an analogous manner to the Cadomin Formation of the Blairmore Group in the Western Canada Sedimentary Basin (Varley, 1984).

Sample 17-7, collected from eastern-most McEvoy strata (at Distingue Mountain east of the Skeena River), has a significant accessory mafic mineral assemblage. Another sampled sandstone from the same vicinity that was too fine grained to point-count shows a similar mafic assemblage. Sandstones from this locale are closest to the provenance (as indicated by current directions) of any other P2 or P3 samples, and may be compositionally less mature as result.

Sample 13-3 is the stratigraphically highest sandstone examined from the Devils Claw Formation. This sample is from a grey-green sandstone with accessory fine grained muscovite and rare glaucony grains (possibly glauconitic minerals based on petrography and SEM-EDS- lack of x-ray diffraction data renders glauconitic mineral determination uncertain; Odin and Fullagar, 1988). Sample 13-3 is also unusual among sandstones from the study area because it contains potassium feldspar. This sample may suggest a younger volcanic/tectonic pulse, but further investigation of the upper Devils Claw Formation is needed to be certain of its implications.

Two samples of quartz-rich sandstone were counted. Both are from micaceous green sandstones typical of the Skeena Group (Tipper and Richards, 1976), and both were collected from the northeastern ridge of Mosque Mountain, stratigraphically above volcanic lithic rich fluvial sandstones of P1. These sandstones carry a very strong metamorphic provenance signal. Muscovite is common, as are polycrystalline quartz grains with aligned sutured crystallite boundaries and in some samples included fine grained mica (sericite). Some of these grains are interpreted as schists and phyllites (Scholle, 1982). Medium sized quartz grains were sufficiently abundant to warrant counting and plotting on a diamond discrimination diagram as described by Basu *et al.* (1975). The quartz plots within the middle and upper metamorphic provenance among sands derived from garnet through sillimanite rank metamorphics, which is consistent with the presence of schistose grains and muscovite.

## OTHER INFLUENCES ON PETROFACIES COMPOSITION

To this point, interpretation of sandstone petrofacies has assumed provenance alone controls composition. However, as alluded to earlier, composition actually depends on the interplay of factors as diverse as

facies exposed in the provenance, climate, relief, transport processes, alluvial storage, recycling and burial diagenesis. The point-count characterization of sandstone is a combination of signals from each of these diverse factors and extracting the provenance signal alone can be a perilous exercise. Most researchers have concluded that the strongest individual signal is generally provenance, but that other factors can mimic provenance variations is amply demonstrated by reports of first cycle quartz arenites and sub-arenites produced in modern humid tropical environments (Dutta and Suttner, 1986).

That humid weathering controls on sandstone composition are not limited to tropical climates has been shown by work in the southeastern United States and California (Grantham and Velbel, 1988; Girty, 1991). Basu (1985) demonstrated humid climate is reflected in increased compositional maturity for both plutonic and metamorphic provenances. Similarly, preferential destruction of labile grains with increased burial depth, chemical weathering, mechanical abrasion (as in reworked shallow marine sands) or recycling are well established (Blatt, 1982).

All these diverse factors can be divided into two classes distinguished by effect on composition: first, an "additive" class consisting only of provenance facies and diagenesis (in which grains have been altered so completely they are counted as another grain type); and second, a "destructive" class consisting of all the other factors, which each tend to preferentially destroy labile grains. Because an attempt is made during counting to recognize alterites, the assumption is made that the "additive" class is entirely composed of provenance signal. The provenance signal then becomes less labile grain rich through exposure to the "destructive" class of factors. That some alterites are not recognized as such in the counts is suggested by the elevated monocrystalline quartz values for two quartz cemented P1 sandstones (i.e., some quartz cement was counted as quartz grains), however, this is believed not to be a serious defect. By making the assumption that provenance signal becomes less strong in labile grains through time, two logical tests can be applied to the previously made provenance interpretations.

1) If the petrofacies more affected by a particular "destructive" factor has more labile grains than a less affected petrofacies, provenance changes must contribute to the difference.

2) If a compositionally more mature petrofacies has types of labile grains not present in a less mature petrofacies, provenance control is indicated.

Passing the above tests permits confidence that qualitative differences between petrofacies reflect provenance changes rather than variations induced by "destructive" factors:

In order to apply these two tests, decisions must be made as to which grains are relatively more stable and which petrofacies has been exposed to the more severe action of each. Qualitative ranking of relative stability is all that can be accomplished, because quantitative data for specific lithic grain types is mostly lacking. Although monocrystalline quartz can be assumed to be most stable grain type in the medium sand fraction (Blatt *et al.*, 1980), relative stability between chert and volcanic lithic grains are less well known, because little is presently known about relative chemical and mechanical stability of chert versus fine grained volcanics. Grain size certainly plays a role, as shown most convincingly by the oligomict chert pebble composition of the conglomerates compared to the high volcanic lithic fragment content of co-eval sandstones. As grain size is reduced, chert becomes less stable relative to volcanic lithic fragments (and volcanic lithic fragments become important components of sandstone). Despite being relatively unstable at very fine or finer grain size, at medium sand size chert is assumed to be relatively more stable than volcanic lithic grains. Metamorphic lithic fragments are considered less stable than either chert or volcanic lithic fragments. Polycrystalline quartz grains (with sutured crystallites) are relatively more stable than other metamorphic grains, and therefore make good markers for metamorphic provenance. Qualitatively, metapelites, sedimentary lithic fragments, chloritized volcanic lithics, and feldspar are all considered here to be the most labile fraction, with volcanic lithic probably somewhat more stable, and monocrystalline quartz and chert the most stable fraction.

Given the assumed relative stabilities of the major grain types, (Fig. 3-8) the proportion of stable grains increases upwards in the succession.

Consideration will be given below to each of the "destructive" factors. Based on stratigraphic relationships and sedimentologic interpretations, each petrofacies with more or less confidence can be

ranked in relation to each destructive factor.

The highest confidence can be assigned to relative burial effects. The Currier and older Bowser Lake Group rocks are stratigraphically beneath the McEvoy and Devils Claw Formations, and therefore are assumed to have experienced greater burial alteration. The validity of this assumption is supported by the independent observation that in the older sandstones pressure solution effects including stylolites and spaced cleavage are pervasive.

Applying test #1 with respect to burial effects, P1 was most deeply buried and P2 next most deeply buried, but compositional stability is in the order P3 > P2 > P1; therefore, provenance differences, not burial diagenesis, are accepted as accounting for differences between P1, P2 and P3.

Similarly, P1 is the petrofacies likely to be most affected by abrasion because of its partially shallow marine depositional character. Choosing between P2 and P3 as likely more affected by abrasion is difficult because both are fluvio-deltaic deposits, but an increase in conglomerate in P3 bearing strata may suggest less transport and therefore less abrasion for P3. Again, as with relative burial depth, the petrofacies most affected by abrasion is the most labile, leading to the conclusion that provenance changes rather than abrasion account for changes in composition. The same reasoning applies to relief in the source area, if conglomerate composition of associated strata can be read as an indication of source area relief. P1 strata (Currier and older Bowser Lake Group rocks) are less than 3% conglomerate (in stratigraphic thickness), the McEvoy Formation is approximately 6% conglomerate, and the Devils Claw Formation is nearly 50% conglomerate.

Figure 3-8: Relative stability of grain types assumed in this study.

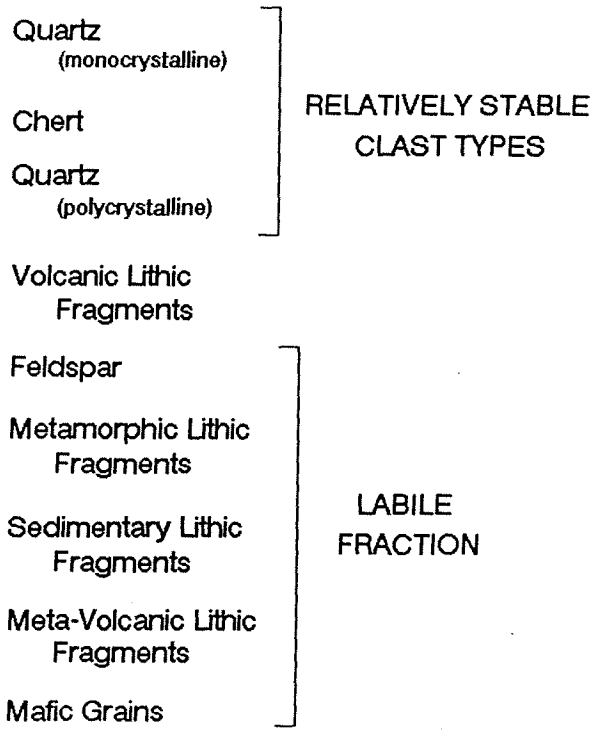

Climate is also difficult to evaluate quantitatively, but three factors suggest seasonally humid conditions prevailed throughout Currier, McEvoy and Devils Claw time. First, at least thin seams of coal occur throughout the section as does petrified wood with conspicuous development of annual rings. Conspicuous tree rings are botanical evidence of seasonal climate (Creber and Chalconer, 1985) and coal is clear evidence of humid climate. Second, deposition occurred on the western continental margin adjacent to the ocean and west of mountains, a geographical position that is likely to be humid outside the tropics. Finally, macroflora species composition remained quite stable throughout the Currier to Devils Claw section (MacLeod and Hills, 1990), supporting the persistence of a similar climate during deposition of all examined stratigraphic units. Given evidence for climatic stability, climatic changes are discounted as a cause of changing grain compositions.

Labile metamorphic indicators not seen in P1 or P2 appear in the otherwise compositionally most mature P3. P3 therefore passes test #2 by possessing labile grains not seen in the other petrofacies, although P3 is otherwise compositionally most mature. This leads to acceptance of the conclusion that provenance changes are indicated by the appearance of metamorphic indicators in P3.

In summary, all the "destructive" signals seem to be contra-indicated as root causes of compositional changes. This conclusion follows from application of the two tests described earlier in this section and consideration of independent geological evidence applicable to these rocks. Provenance changes as interpreted from the grain composition can therefore be accepted with reasonable confidence as the cause of petrofacies variations through time.

Therefore three successive stages of provenance evolution (Fig. 3-9) are interpreted based on the petrofacies compositions: 1) during P1 deposition, first cycle detritus was eroded from uplifted oceanic lithosphere and island arc facies; 2) during P2 time first cycle and recycled sea floor and island arc facies were eroded; and 3) during P3 time further uplift led to erosion of metamorphic, minor plutonics, and acid volcanic arc strata in addition to continued erosion of first cycle and recycled oceanic lithosphere and island arc facies.

Figure 3-9: Evolution of provenance as interpreted from the succession of petrofacies.

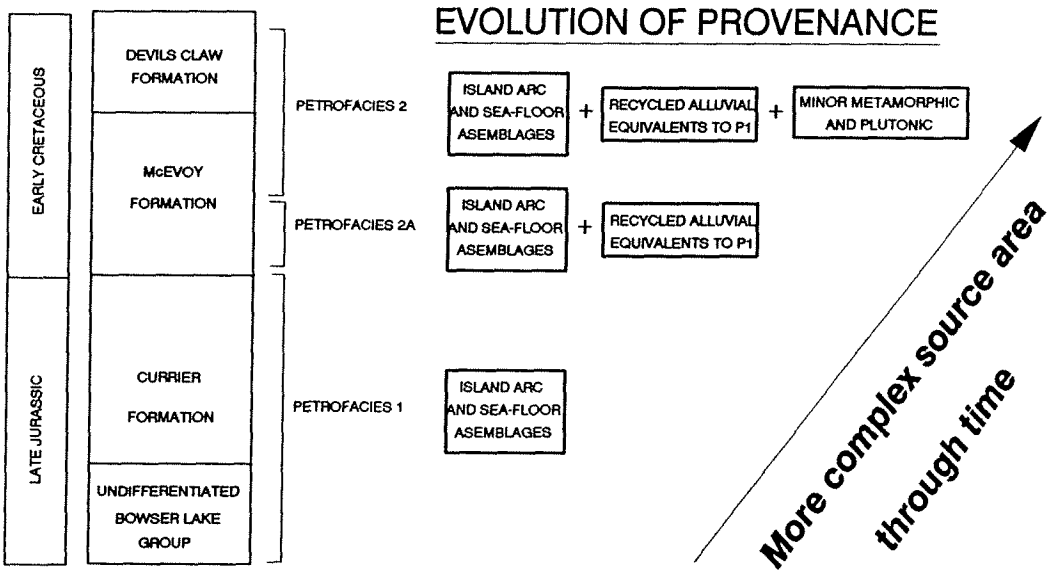

## PROVENANCE TECTONIC SETTING

Point-count categories were regrouped in order to plot the grain composition data on Dickinson-Suczek diagrams (Fig. 3-10; modified from Dickinson, 1985). Percentages for each parameter were then calculated for the three petrofacies, and mean sample values were plotted on Dickinson and Suczek (1979) type tectonic provenance discrimination diagrams yielding results consistent with the interpretations made above. Petrofacies 1 (Qt=34%, F=14%, L=52%; Qm=9%, F=14%, Lt=77%) plots in the magmatic arc field of the $Q_tFL$ and $Q_mFL_t$ diagrams. Petrofacies 2 (Qt=62%, F=5%, L=33%; Qm=5%, F=5%, Lt=89%) and petrofacies 3 (Qt=64%, F=5%, L=31%; Qm=7%, F=5%, Lt=88%) plot in the recycled orogen provenance field of those same diagrams, as expected from the provenance interpretations. P1 is very much borderline to the magmatic arc field, however, and is only slightly within the volcanic rather than plutonic field. On the $Q_mFL_t$ diagram, both petrofacies plot more completely within their appropriate fields, probably reflecting the postulated volcanic origin for some of the chert in P1. The volcanic greater than plutonic signal, and increasing ratio of chert to quartz implied from the diagrams for P1 and P3, respectively, are entirely appropriate based on grain compositions.

On the $Q_mPK$ diagram (not shown), P1 plots within the family of Circum-Pacific volcanoplutonic suites, as might be anticipated from the Bowser Basin's position within the circum-Pacific orogenic belt of the Cordillera. P3 plots in the field of increasing maturity/stability from continental provenances, which reflects the addition of metamorphic and plutonic provenance terranes to recycled P1 sediments.

## DISCUSSION

The following discussion examines implications from this study at three scales: 1) a local scale which relates the changing grain compositions through time to Bowser Basin tectonics; 2) a Cordilleran-wide scale which places this study in perspective with other information relating to Cordilleran orogenic

Figure 3-10: Ternary diagrams of sandstone composition. After Dickinson and Suczek (1979).

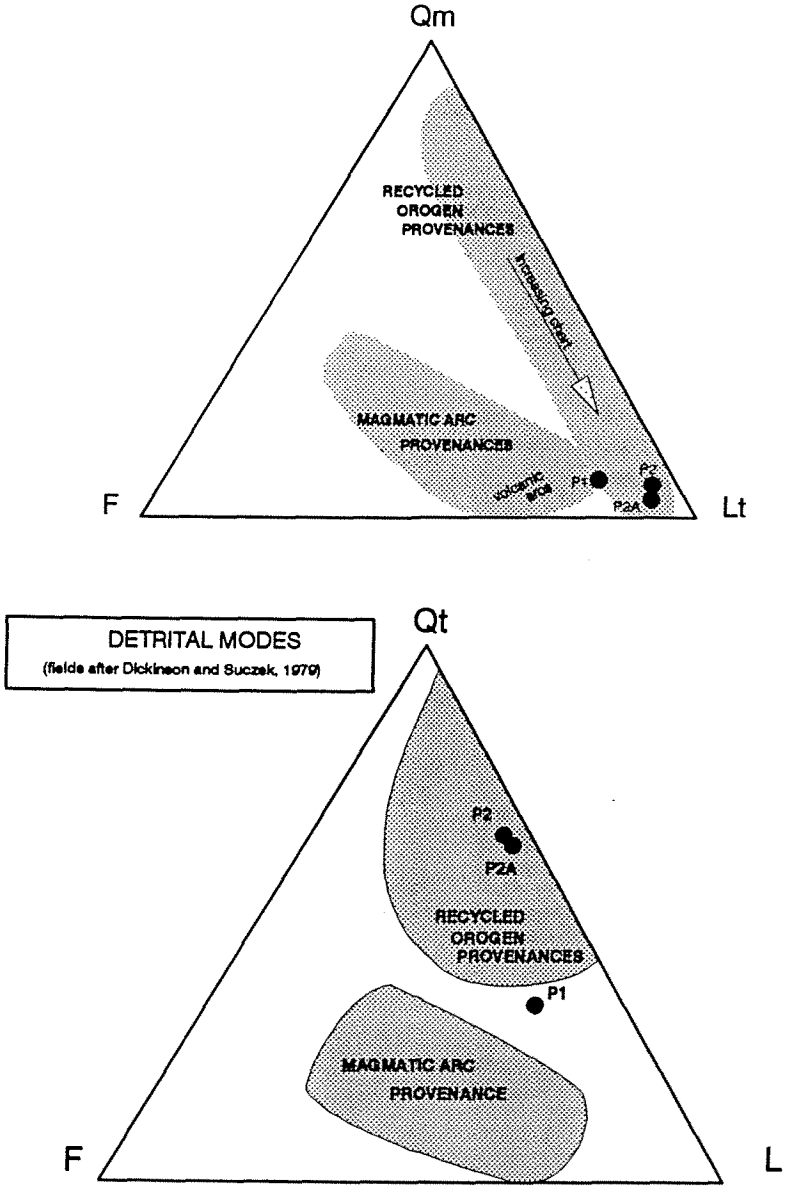

development; and 3) a world-wide scale which relates the filling of the Bowser Basin to rifting of the Atlantic and break up of Pangea.

*Bowser Basin tectonic implications*

Petrofacies described in this study both support and expand upon earlier conclusions concerning the provenance of Bowser Basin sediments. Eisbacher (1981) concluded, based on the oligomict chert composition of conglomerate clasts, that ocean floor facies of the Cache Creek Group exposed in the Atlin terrane north and east of the Bowser Basin were the most likely source for Bowser Basin sediments. This study supports the conclusion that the Bowser Basin sediments were derived from oceanic suites. The sandstone grain compositions demonstrate that sea floor and island arc igneous suites were also present in the provenance, and that the igneous suites were probably inactive ("ancient" at the time of their erosion). Uplift and erosion of both sea floor and island arc suites probably implies obduction onto the North American continental margin by the Early or Middle Jurassic, soon after initiation of rifting of the Atlantic Ocean. Such an obducted island arc and associated sea floor provenance is sufficient to describe the entire source of Currier Formation and older Bowser Lake Group rocks.

For the younger rocks of the McEvoy and Devils Claw Formations, however, the sandstone compositions document a more complex provenance. At least part of the ocean floor source in P2 and P3 is recycled sediment, eroded presumably from alluvial equivalents to Currier and older Bowser Lake Group strata, and the additional input of unequivocal metamorphic grains necessitates erosion of a metamorphic terrane for part of the provenance. In other words, provenance of McEvoy and Devils Claw strata was a mixture of oceanic facies, recycled oceanic facies and minor unroofed metamorphic facies with associated magmatic activity. The most likely source for the metamorphic signal is unroofing of the Omineca Geanticline and the timing of that unroofing, at least in the vicinity of the northern Bowser Basin, most likely was not before middle McEvoy deposition (first occurrence of P3).

The amount of material eroded can be estimated roughly from the extent and thickness of preserved Bowser Basin strata. The Bowser Basin covers roughly 50 000 square kilometres today

(Wheeler and McFeely, 1987), and restoring 35% to 40% post-depositional compressional deformation (Moffat, 1985; Evenchick, 1991), suggests the area at the time of deposition was in excess of 70 000 square kms. True stratigraphic thickness is between 5 and 10 kms (Chapter 2), and porosity is virtually absent, therefore, at minimum, a source area the size of the present day Bowser Basin would have been eroded to a depth of roughly 7 to 14 kms. Modern sediment budget studies suggest that such an estimate significantly under-represents the total eroded material from the Bowser Basin provenance. For example, as much as 40% of Yukon River sediment load may have by passed the Yukon delta and shelf to be deposited more than 300 kms north in the Chukchi Sea (Nelson and Creager, 1977). If similar sediment bypass conditions held for the Bowser Basin, then the eroded material could have covered an area the size of the present day Bowser Basin, eroded to a depth of between 10 and 20 kms.

Erosion of pre-existing sedimentary strata is inferred from the high content of chert in P2 and P3, along with a smaller recycled volcanic lithic signal. The most obvious source for recycled sands of this composition are up-dip equivalents of Currier and older Bowser Lake Group rocks. Preserved facies of sediments associated with P1 are shallow marine and deltaic. Alluvial equivalents are unknown, and may have been eroded to produce the recycled signal in P2 and P3 sandstones. An angular unconformity recording erosion of Bowser Lake Group rocks has been reported beneath Sustut Group rocks east (depositionally up-dip) of the Bowser Basin (Eisbacher, 1981), suggesting erosion of these rocks is likely to have contributed to P2 and P3.

The oligomict chert composition of the conglomerate clasts contrasts markedly with the varied and changing composition of the sandstones. Chert is the clast type least susceptible to mechanical abrasion during transport, and lack of less stable clast types in the conglomerates may reflect some distance of transport. Estimation of the minimum distance of transport can be made considering the lack of less stable clast types in the conglomerates in comparison with modern rivers. Chert gravel in rivers draining plutonic and metamorphic rocks of the Black hills of South Dakota, for example, dominates over other lithic types after less than 15 kilometres transport (Plumley, 1948). Extrapolation of these data suggests lithic gravels other than chert may be virtually eradicated from gravels that receive as little

as 25 kilometres transport under similar conditions. Direct application of these distances to the Bowser Basin is probably not valid, due to its dominantly volcanic rather than plutonic/metamorphic source, and the likely differing conditions of climate and source area relief. However, 25 kilometres of stream transport as a minimum estimate is revealing, and probably is the minimum necessary to account for the oligomict chert composition. Conglomerate textures also support at least moderate transport distances, because the pebbles and cobbles are well to very well rounded. Unlike volcanic lithic gravels, volcanic sands can dominate the sediment load of very long rivers. Examples of major modern rivers dominated by volcanic lithics include the Fraser, Colville, Columbia, Magdelena, and Yukon rivers (Potter, 1979). All of these modern volcanic lithic dominated rivers occur in the circum-Pacific region (Potter, 1979), the same as the rivers that fed the Bowser Basin.

Petrofacies documented in this study also shed light on relationships between deposits in the northern and southern parts of the basin. P1 is volcanic lithic rich, as are the Ashman, Trout Creek, and younger Bowser Lake Group rocks in the southern Bowser Basin (Tipper and Richards, 1976; Richards, pers. comm. 1991 - unpublished sandstone thin section analyses). Richards' data suggest that chert-rich sandstone is encountered earliest in the southern Bowser Basin in Kitsun Creek rocks of the lower Skeena Group (?Hauterivian -Albian; Tipper and Richards, 1976). Higher in the Skeena Group (?Albian), micaceous green sandstones compositionally similar to samples 30-10 and 30-12 carry a strong metamorphic signal and abundant potassium feldspar. If the entry of metamorphic grains occurred approximately contemporaneously throughout the Bowser Basin and elsewhere in the western Canadian Cordillera (see next subheading below), then the Skeena Group green sandstones may be approximately contemporaneous with P3. Support for this idea may be found in the composition of the sample 13-3, the highest Devils Claw sandstone examined. As mentioned earlier, this grey-green sandstone contains both fine grained muscovite and the first potassium feldspar seen in the Devils Claw or older sandstones.

Ages of the studied strata based on marine invertebrates and palynology appear consistent with this interpretation. The Currier and older Bowser Lake Group strata are dated as Late Jurassic and perhaps in part earliest Cretaceous, largely contemporaneous with upper Ashman Formation and younger

Bowser Lake Group facies dated as Late Jurassic in the southern Bowser Basin (Tipper and Richards, 1976). The lower McEvoy (P2) are dated by palynology as late Barremian to Aptian age (Moffat *et al.*, 1988; Rouse, pers. comm., *in* Cookenboo and Bustin, 1989). The middle McEvoy through the middle Devils Claw interval has been dated as middle to late Albian by palynology, and the upper Devils Claw as latest Albian to Cenomanian (Moffat et al., 1988; and Rouse, pers. comm., 1989). Micaceous green sandstones of the Skeena Group exposed on the Skeena arch near the southern margin of the Bowser Basin and farther south in the Chilcotin-Nechako region were also deposited in the mid-Cretaceous (mid to late Albian for the Chilcotin-Nechako region- Hunt, 1992; and Albian, or possibly as old as Aptian to Barremian for the Skeena Arch region- Palsgrove and Bustin, 1991). Both P3 and Skeena green sandstones show the first significant metamorphic provenance terrane signals in their respective parts of the basin.

### *Implications for Cordilleran tectonics*

Lithic-rich sandstones similar to those of the northern Bowser Basin characterize Mesozoic sandstones from Cordilleran basins. Out of Dickinson and Suczek's (1979) list of 88 separate sandstone compositions from around the world, only 5 are chert and 2 volcanic lithic rich (>30%) , but 4 of 5 chert and both volcanic lithic rich sandstones are from Mesozoic Cordilleran basins (in part, of course, a result of sample bias). More recent studies and data sets not included in Dickinson and Suczek (1979) strengthen the conclusion that the lithic rich sandstones are characteristic of Mesozoic Cordilleran basins. The widespread extent and commonalty of character between these chert and volcanic lithic rich sandstones has implications for Cordilleran tectonics.

Even an incomplete listing of occurrences of chert rich sandstones demonstrates that chert is pervasive in northern Cordilleran sandstones during the Cretaceous. Chert-rich sandstones were reported in Dickinson and Suczek (1979) from the mid-Cretaceous Virginia Ridge Formation in the Methow Basin (Cole, 1973; Tennyson and Cole, 1978), Lower Cretaceous Blairmore Group (Mellon, 1967) of the Western Canada Sedimentary Basin (WCSB); and the Upper Triassic Vester Formation of Oregon

(Dickinson and Suczek, 1979). Chert and quartz rich sandstones are also reported from the Late Jurassic-Early Cretaceous Kootenay Group (Gibson, 1985) and Early Cretaceous Gates and Moosebar Formations (Carmichael, 1983; Leckie, 1983), of the WCSB. These Lower Cretaceous sandstones from the WCSB generally lack an abundant volcanic lithic fraction. By the early to mid-Cretaceous, chert and/or quartz dominated sandstones are ubiquitous in Canadian Cordilleran basins.

Gates Formation sandstones contain grains of low to medium rank metamorphics (Leckie, 1983), suggesting provenance from a metamorphic terrane during the Albian. Metamorphic and plutonic indicators are generally absent from Kootenay Group sandstones (Gibson, 1985). The first clear indications of a metamorphic provenance in the WCSB closely parallels the Skeena Group green sandstone (Albian, at least in part) and McEvoy Formation (?Albian) in the Bowser Basin.

Sandstones dominated by volcanic lithic fragments in the northern Cordillera have been reported from a number of basins. Included in these reports are Middle Blairmore Group sandstones of the Lower Cretaceous WCSB (Mellon, 1967), the Methow and Tyaughton intermontane basins and possibly the melange belt of the North Cascades (Garver, 1989). This report adds Late Jurassic to earliest Cretaceous sandstones of P1 in the northern Bowser Basin. Unpublished data (Richards, pers. comm. 1991) indicate Late Jurassic sandstones in the southern Bowser Basin are also dominanted by volcanic lithic fragments.

Although specific source areas for lithic sandstones have been the subject of considerable speculation, in general most authors have argued for a source west of the WCSB and east of the Intermontane Belt, in an area centering around the Omineca geanticline. In some samples, the same rocks may be sources for detritus shed both to the east and west. This study has suggested the Hogem Batholith and associated island arc volcanics as possible sources for Bowser Basin sandstones. The Hogem batholith has also been suggested as part of the source of the Gates Formation east of the Omineca geanticline (Leckie, 1983).

The Omineca Geanticline apparently cored an extensive land mass marginal to North America that provided a source for clastics in all directions. The land mass apparently began shedding oceanic

lithosphere and island arc detritus into the northern Bowser in the Middle Jurassic.

Changes in sandstone composition provide insight into the tectonic history of this Omineca geanticline landmass. The first detritus shed was volcanic lithic rich, reflecting ocean floor and arc sources. Some of those first sediments are preserved in P1 in the Bowser Basin, but others were recycled by uplift in the Early to mid-Cretaceous. These recycled sediments accumulated both in the Bowser Basin west of the source, and the WCSB east of the source.

The source area tectonic regime deduced from P1 grain composition requires erosion of an undissected arc and obducted of oceanic lithosphere. The extrabasinal and paleovolcanic signal (and lack of neovolcanic indicators) among the volcanic lithic grains suggests that the arc source was ancient (at least largely inactive) at the time of its erosion. Arc volcanics surrounding (and presumably beneath) Bowser Basin clastics further support proximity to an older arc. The volcanic lithic signal is more pronounced in sediments west of the Omineca geanticline than in the WCSB, suggesting that the arc was out-board of the obducted sea-floor terrane, and that the obducted ocean floor may have actually been back-arc seafloor. Uplift and erosion of such ancient island arc and associated sea-floor probably occurred by obduction of marginal basin and fringing island arc suites onto the western margin of North America prior to the Middle Jurassic. A model involving Early Jurassic closure of marginal seas (not a unique solution) is illustrated in figure 3-11. Obduction of oceanic and island-arc strata of the Slide Mountain assemblage, compatible with this model, occurred northeast of the Bowser Basin by the late Early Jurassic (Hansen, 1992). A compatible history of Early to Middle Jurassic obduction for Slide Mountain and Quesnellia rocks on to North America (Murphy, 1989), and Middle to Late Jurassic obduction of Cache Creek terrane on to Quesnellia (Mortimer *et al.*, 1989) also has been described in the southern Canadian Cordillera.

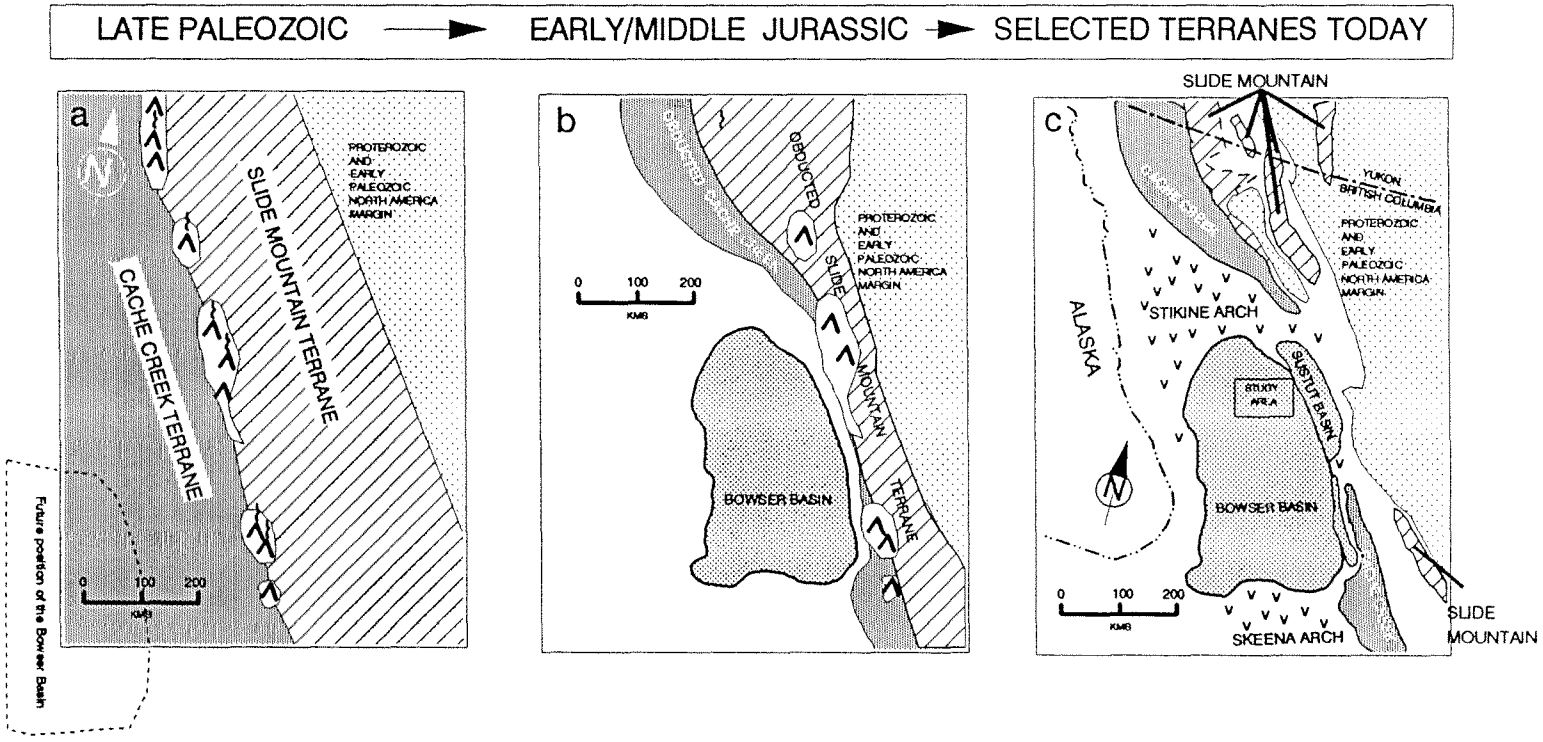


**Figure 3-11: Model of Cordilleran tectonic development consistent with interpretation of provenance.**

a) Late Paleozoic reconstruction of western North American margin, based on Bowser Basin provenance considerations. Note the marginal sea is fringed by active island arcs.

b) By the Early to Middle Jurassic, fringing island arcs and associated marginal seas have been closed by obduction onto the western margin of North America. Note that the island arc is no longer active.

c) Terranes as they appear today in the Canadian Cordillera. Obducted terranes are discontinuous erosional remnants of their Mesozoic extents.

Added to the source area during the Early to mid- Cretaceous are metamorphic and plutonic indicators, as well as indications of active acidic volcanism and minor plutonics, reflecting the first actual unroofing of rocks belonging to the Omineca Crystalline Belt and dissection of the P1 island arc. The unroofing is first recorded in the WCSB by the Gates Formation (middle Albian), for which the Hogem batholith plutonics are a suggested source (Leckie, 1983). In the Bowser Basin, first unroofing is recorded in the middle McEvoy (Early Cretaceous - possibly middle Albian) and Skeena Group (?Hauterivian to Albian). As in the Gates Formation, unroofing of the Hogem batholith or related plutons is a possible contributing source for P2.

*Implications to rifting of Pangea and the opening of the Atlantic*

The widespread occurrence of chert and volcanic lithic rich sandstones in Mesozoic Cordilleran basins, although rare elsewhere in the world, suggests a commonalty of origin in response to unusual conditions. It is proposed that these lithic sands were sourced from an extensivearea of ophiolite and island arcs obducted shortly after North America began rifting from Pangea in the Early to Middle Jurassic (Hay et al., 1981). A latest Triassic to earliest Jurassic change in North American plate motion (Ekstrand and Butler, 1989) preceded the initial rifting of Pangea and opening of the Atlantic Ocean. On the western margin of North America, the initial rifting of the Atlantic appears to be recorded by the obduction of the expansive area of marginal sea floor and island arcs that formed the provenance for Bowser Basin sands. The occurrence of similar Jura-Cretaceous lithic suites throughout the Cordillera suggests that closure of marginal seas and obduction of fringing island arcs was a widespread process associated with initial rifting of the Atlantic. Remains of these marginal seas and island arc are preserved in the elongate outcrop occurrences of Cache Creek, Slide Mountain and Bridge River rocks stretching from Washington through British Columbia and into the Yukon.

# CONCLUSIONS

1) Sandstones of the northern Bowser Basin exhibit changing grain composition in successive stratigraphic units.

2) Currier Formation and older Bowser Lake Group sandstones belong to a volcanic lithic rich suite termed petrofacies 1 (P1) in this report. P1 is interpreted as the product of obducted marginal sea-floor and island arc provenance terranes.

3) Sandstones in the lower McEvoy Formation are chert rich, with lesser volcanic lithic fragments. These sandstones are assigned to petrofacies 2 (P2), which is interpreted as the product of first cycle and recycled sea-floor and island arc provenance.

4) Upper McEvoy and Devils Claw Formation sandstones are chert rich with lesser volcanic lithic fragments, and also show for the first time in the northern Bowser Basin a metamorphic (phyllite/schist) and minor plutonic provenance signal. These sandstones are termed petrofacies 3 (P3) in this report, and are interpreted as the product of first cycle and recycled sea-floor and island arc provenance, with additional exposed metamorphic and plutonic facies.

5) Chert and volcanic lithic rich sandstones similar to the northern Bowser Basin petrofacies characterize Mesozoic basins located adjacent to and within the Canadian cordillera. The composition and widespread nature of these sandstones suggests uplift and erosion of a large area of island arc and marginal sea floor presumably obducted to the western margin of North America as a consequence of initiation of rifting of the Atlantic ocean in the Early to Middle Jurassic.

# REFERENCES

Basu, A., 1985. Influence of climate and relief on compositions of sands released at source areas. *In* Zuffa, G. G. (*ed.*), Provenance of Arenites. D. Reidel Publishing Company, p. 1-18.

Basu, A., Young, S. W., Suttner, L. J., James, W. C. and Mack, G. H., 1975. Re-evaluation of the use of undulatory extinction and polycrystallinity in detrital quartz for provenance interpretation. Journal of Sedimentary Petrology, v. 45, p. 873-882.

Blatt, H. 1982. Sedimentary Petrology. W. H. Freeman and Company. 564 p.

Blatt, H., Middleton, G. and Murray, R., 1980. Origin of Sedimentary Rocks, 2nd ed.,: Prentice-Hall, Inc., Englewood Cliffs, New Jersey, 782 p.

Carmichael. S. M. M., 1983. Sedimentology of the Lower Cretaceous Gates and Moosebar Formations, northeast coalfields, British Columbia. Ph.D. thesis, University of British Columbia, Vancouver, British Columbia. 285 p.

Cheeney, R. F., 1983. Statistical methods in geology. George Allen Unwin, Boston, 169 p.

Cole, M. R., 1973. Petrology and dispersal patterns of Jurassic and Cretaceous sedimentary rocks in the Methow River area, north Cascades, Washington. PhD thesis University of Washington, 110 p.

Coney, P. J., Jones, D. L., and Monger, J. W. H., 1980. Cordilleran suspect terranes. Nature, v. 288, p. 329-333.

Cookenboo, H. O., 1989. Lithostratigraphy, palynostratigraphy, and sedimentology of the northern Skeena Mountains and their implications to the tectonic history of the Canadian Cordillera. MSc. thesis, University of British Columbia, Vancouver British Columbia. 131 p.

Cookenboo, H. O., and Bustin, R. M., 1989. Jura-Cretaceous (Oxfordian to Cenomanian) stratigraphy of the north-central Bowser Basin, northern British Columbia: Canadian Journal of Earth Sciences, v. 26, p. 1001-1012.

Cordey, F., Mortimer, N., Dewever, P., and Monger, J. W. H., 1987. Significance of Jurassic radiolarians from the Cache Creek terrane, British Columbia. Geology, v. 15, p. 1151-1154.

Creber, G. T. and Chalconer, W., 1985. Tree growth in the Mesozoic and Early Tertiary and the reconstruction of Palaeoclimates. Palaeogeography, Palaeoclimatology, Palaeoecology, v. 52, p. 35-60.

Dickinson, W. R., 1985. Interpreting provenance relations from detrital modes of sandstones. *In* Zuffa, G. G. ed., Provenance of Arenites: D. Reidle, Dordrecht, p. 333-361.

Dickinson, W. R. and Suczek, C. A., 1979. Plate tectonics and sandstone compositions. American Association of Petroleum Geologists Bulletin, v. 63, p. 2164-2182.

Dutta, P. K. and Suttner, L. J., 1986. Alluvial sandstone composition and paleoclimate, II. Framework mineralogy. Journal of Sedimentary Petrology, v. 56, p. 346-358.

Eisbacher, G. H., 1974. Sedimentary and tectonic evolution of the Sustut and Sifton Basins, north-central British Columbia. Geological Survey of Canada Paper 73-31, 57 p.

Eisbacher, G., 1981. Late Mesozoic - Paleogene Bowser Basin molasse and Cordilleran tectonics, western Canada, *In* Miall, A. D. (ed.), Sedimentation and Tectonics. Geological Association of Canada, Special Paper 23, p. 125-151.

Ekstrand, E. J. and Butler, R. F., 1989. Paleomagnetism of the Moenave Formation: Implications for the Mesozoic North American apparent polar wander path. Geology, v. 17, p. 245-248.

Evenchick, C. A., 1991. Geometry, evolution and tectonic framework of the Skeena fold belt, north central British Columbia. Tectonics, v. 10, p. 527-546.

Garnett, J. A., 1978. Geology and mineral occurrences of the southern Hogem Batholith, British Columbia Department of Mines and Petroleum Resources Bulletin, No. 70, 75 p.

Garver, J. I., 1989. Tectonic significance of polymodal compositions in melange sandstones, western melange belt, North Cascade Range, Washington - Discussion. Journal of Sedimentary Petrology, v. 58 p. 1046-1050.

Gibson, D. W., 1985. Stratigraphy, sedimentology and depositional environments of the coal-bearing Kootenay Group, Alberta and British Columbia. Geological Survey of Canada Bulletin 37, 108 p.

Girty, G. H., 1991. A note on the composition of plutoniclastic sand produced in different climatic belts. Journal of Sedimentary Petrology, v. 61, p. 428-433.

Girty, G. H., Mossman, B. J. and Pincus, S. D., 1988. Petrology of Holocene sand, peninsular ranges, California and Baja Norte, Mexico: Implications for provenance-discrimination models. Journal of Sedimentary Petrology, v. 58, p. 881-887.

Grantham, J. H. and Velbel, M. A., 1988. The influence of climate and topography on rock-fragment abundance in modern fluvial sands of the southern Blue Ridge Mountains, North Carolina. Journal of Sedimentary Petrology, v. 58, p. 219-227.

Green, G. M., 1991. Detailed sedimentology of the Bowser Lake Group, northern Bowser Basin, British Columbia. Current Research, Part A, Geological Survey of Canada Paper 91-1A, p. 187-195.

Gulf Canada Resources Limited 1984. Mount Klappan property. British Columbia Ministry of Energy, Mines and Petroleum Resources, Open File Report 111.

Gulf Canada Resources Limited 1987. Lost Fox property. British Columbia Ministry of Energy, Mines and Petroleum Resources, Open File Report 723.

Hansen, V. L., 1992. *P-T* evolution of the Teslin suture zone and Cassiar tectonites, Yukon, Canada: evidence for A- and B-type subduction. Journal of Metamorphic Geology, v. 10, p. 239-263.

Hawkins, J. W. Jr., 1980. Ophiolites. Proceedings International Ophiolite Symposium, Cyprus, 1979. p. 244-254.

Hay, W. W., Barron, E. J. , Sloan, J. L. and Southam, J. R., 1981. Continental drift and the global pattern of sedimentation. Geologische Rundschau, v. 70, p. 302-313.

Hekinian, R. 1982. Petrology of the ocean floor. Elsevier Oceanography Series. v. 33. Elsevier Scientific Publishing, Amsterdam. 407 p.

Hunt, J. A., 1992. Stratigraphy, maturation and source rock potential of Cretaceous strata in the Chilcotin-Nechako region of British Columbia. MSc. thesis, The University of British Columbia. 448 p.

Jones, D. L. and Murchey, B., 1986. Geologic significance of Paleozoic and Mesozoic radiolarian chert. Annual review of Earth and Planetary Sciences. v. 14, p. 455-492.

Leckie, D. A., 1983. Sedimentology of the Moosebar and Gates Formations (Lower Cretaceous). Ph.D. Thesis, McMaster University, 515 p.

Lundberg, N., 1991. Detrital record of the early Central American magmatic arc: Petrography of intraoceanic forearc sandstones, Nicoya Peninsula, Costa Rica. Geological Society of America Bulletin, v. 103, p. 905-915.

MacLeod, S. E., and Hills, L. V., 1990. Conformable Late Jurassic (Oxfordian) to Early Cretaceous strata, northern Bowser Basin, British Columbia: A sedimentological and paleontological model. Canadian Journal of Earth Sciences, v. 27: 988-998.

Malloch, G. S., 1914. Groundhog coal field. Summary report of the Geological Survey Department of Mines. p. 69 to 101.

Mellon, G. B., 1967. Stratigrphy and petrology of the Lower Cretaceous Blairmore and mannville Groups, Alberta foothills and plains. Alberta Research CouncilBulletin, v. 21, 270 p.

Moffat, I. W., 1985. The nature and timing of deformational events and organic and inorganic metamorphism in the northern Groundhog Coalfield: implications for the tectonic history of the Bowser Basin. Ph.D thesis, University of British Columbia, Vancouver, B.C.

Moffat, I. W., Bustin, R. M., and Rouse, G. E., 1988. Biochronology of selected Bowser Basin strata: tectonic significance. Canadian Journal of Earth Sciences, v. 25, p. 1571-1578.

Mortimer, N., van der Heyden, P., Armstrong, R. L., and Harakal, J., 1989. U-Pb and K-Ar dates related to the timing of magmatism and deformation in the Cache Creek terrane and Quesnellia, southern British Columbia. Canadian Journal of Earth Sciences, v. 27, p. 117-123.

Murphy, D., C., 1989. Crustal paleo-rheology of the southwestern Canadian Cordillera and its influence on the kinematics of Jurassic convergence. Journal of Geophysical Research, v. 94, p. 15723-15739.

Nelson, H. and Creager, J. S., 1977. Displacement of Yukon-derived sediment from Bering Sea to Chukchi Sea during Holocene time. Geology, v. 5, p. 141-146.

Odin, G. S. and Fullagar, P. D., 1988. Geological significance of the glaucony facies. *In* Odin, G. S. (*ed.*) Green Marine Clays: Developments in Sedimentology 45, Elsevier, New York. p. 295-392.

Palsgrove, R. J. and Bustin, R. M., 1991. Stratigraphy, sedimentology and coal quality of the Lower Skeena Group, Telkwa Coalfield, Central British Columbia, NTS 93L/11. British Columbia Ministry of Energy, Mines and Petroleum Resources, Paper 1991-2, 60 p.

Pollock, S. G., 1987. Chert formation in a volcanic arc. Journal of Sedimentary Petrology, v. 57, p.75-87.

Potter, P. E., 1978. Petrology and chemistry of modern big river sands. Journal of Geology, v. 86, p. 423-449.

Rick, J. W., 1978. Heat-altered cherts of the lower Illinois Valley; an experimental study in prehistoric technology. Northwestern University Archeological Program Prehistoric Records, v. 2 p.

Ricketts, B. A. and Evenchick, C. A., 1991. Analysis of the Middle to upper Jurassic Bowser Basin, northern British Columbia. Current Research, Part A, Geological Survey of Canada Paper 91-1A, p. 65-73.

Samson, S. D., McClelland, W. C., Patchett, P. J., Gehrels, G. E. and Anderson, R. G., 1989. Evidence from neodymium isotopes for contributions to Phanerozoic crustal genesis in the Canadian Cordillera. Nature, v. 337, p. 705-709.

Scholle, P., 1982. A color illustrated guide to constituents, textures, cements, and porosities of sandstone and associated rocks. American Association of Petroleum Geologists Memoir 28. 201 p.

Sedlock, R. L. and Isozaki, Y., 1990. Lithology and biostratigraphy of Fransiscan-like chert and associated rocks in west-central Baja California, Mexico. Geological Society of America Bulletin. v. 102, p. 852-864..

Shelley, D., 1975. Manual of optical mineralogy. Elsevier, New York, p. 239.

Stattegger, K., 1987. Heavy minerals and provenance of sands: modeling of lithological end members from river sands of northern Austria and from sandstones of the Austroalpine Gosau Formation. Journal of Sedimentary Petrology, v. 57. p. 301-310..

Sugitani, K., Sano, H., Adachi, M., and Sugisaki, R., 1991. Permian hydrothermal deposits in the Mino Terrane, central Japan: implications for hydrothermal plumes in an ancient ocean basin. Sedimentary Geology, v. 71, p. 59-71.

Tennyson and Cole, 1978. Tectonic significance of upper Mesozoic Methow-Pasayten sequence, nor theastern Cascade Range, Washington and British Columbia. *In* Mesozoic paleogeography of the western United States. Society of Economic Paleontologists and Mineralogists Pacific Section Pacific Coast Paleogeography Symposium 2, p. 499-508.

Tipper, H. W. and Richards, T. A., 1976. Jurassic stratigraphy and history of north-central British Columbia. Geological Survey of Canada, Bulletin 270, 73 p.

Varley, C. J., 1984. Sedimentology and hydrocarbon distribution of the Lower Cretaceous Cadomin Formation. *In* Koster, E. H., Steel, R. J., (*eds.*,) Sedimentology of gravels and conglomerates. Memoir 10, Canadian Society of Petroleum Geologists, p. 175-187.

Wheeler, J. O., and McFeely, P., 1987, Tectonic assemblage map of the Canadian Cordillera and adjacent parts of the United States of America. Geological Survey of Canada, Open File 1565.

Zuffa, G. G., 1985. Optical analyses of arenites: influence of methodology on compositional results. *In* Zuffa, G. G. (*ed.*), Provenance of Arenites. D. Reidel Publishing Company, p. 165-189.

# CHAPTER 4

# DETRITAL CHROMIAN SPINEL COMPOSITIONS USED TO RECONSTRUCT THE TECTONIC SETTING OF PROVENANCE: IMPLICATIONS FOR OROGENY IN THE CANADIAN CORDILLERA

## ABSTRACT

Detrital chromian spinel is an important accessory mineral in northern Bowser Basin sandstones. Microprobe analyses show that Bowser Basin detrital chromian spinels have Cr/(Cr+Mg) between 0.21 and 0.89; $Mg/(Mg+Fe^{2+})$ between 0.24 and 0.70; and $Fe^{3+}/(Fe^{3+} + Al + Cr)$ values below 0.12. Comparison with spinels from the literature on ultramafic rock types indicates that the detrital spinel compositional range closely matches spinels from alpine-type peridotites emplaced by obduction of marginal basin crust and island arc complexes. Furthermore, Bowser Basin spinels are compositionally distinct from spinels derived from mid-ocean ridges, stratiform ultramafic complexes or Alaskan-type peridotites.

Based on a study of detrital spinels, it is concluded that the Bowser Basin provenance included extensive alpine-type peridotite that originated as marginal basin lithosphere, and that there is no evidence for mid-ocean ridge derived material in the provenance. This provenance interpretation agrees with earlier interpretations which related chert pebbles in the Bowser Basin to chert-rich strata of the Cache Creek terrane and is consistent with the interpretation, based on detrital modes analysis, which calls for an obducted oceanic crust and island arc provenance. The chromian spinel chemistry adds, however, the important tectonic details that mid-ocean ridge derived lithosphere, Alaskan-type peridotites, and stratiform complexes were not exposed in the provenance, and that erosion of the source area occurred prior to any regional greenschist or higher grade metamorphic events. Thus microprobe compositional analysis of detrital spinels adds important detail to the provenance interpretation that is not

available through detrital modes analysis alone. The conclusion that marginal basin lithosphere rather than mid-ocean ridge derived material was the sediment source has important implications to the tectonic history of the Canadian Cordillera. It suggests that the obducted provenance terranes were closely associated with North America. The success of microprobe analysis of detrital chromian spinel from the northern Bowser Basin suggests that similar methods could be profitably used in other basins derived from complex accreted terranes.

## INTRODUCTION

Sandstone provenance studies utilize a broad array of techniques that conceptually fall into two basic approaches. The most widely used approach involves characterization of the bulk composition of the sandstone, typically by point-count determination of modes for detrital framework grains. Data from such studies are commonly plotted on ternary diagrams following the methods of Dickinson and Suczek (1979) or others, and the ternary plots are used to interpret the tectonic setting of the provenance (e.g., recycled orogen versus magmatic arc versus continental block). The success of bulk characterization methods, and especially detrital modes analysis, in relating sands and sandstones to particular provenance tectonic settings is demonstrated by their widespread application and stems directly from their use of the major components of sandstone as the basis of the provenance interpretation. However, when used alone, detrital modal analysis yields sandstone provenance interpretations that are potentially ambiguous because many factors other than type of source rock exposed in the provenance affect the final composition of sandstones. These factors include climate, relief, transport mechanisms and post-burial intrastratal solution. Well-documented cases of both ancient and recent first cycle quartz arenites derived from humid tropical areas highlight the potential influence that factors other than source rock composition play in determining the final composition of sandstones (Franzinelli and Potter, 1983; Suttner and Dutta, 1986). This ambiguity has been demonstrated statistically by Molinaroli *et al.* (1991), who used discriminant function analysis of data from Dickinson *et al.* (1983) to show that the detrital modes approach leads to a correct prediction of the tectonic setting of the provenance in only 75 to 85% of the cases. In order to increase confidence in provenance interpretations and simultaneously

add detail unavailable from conventional detrital modes analyses, a second approach (outlined below) to sandstone provenance analysis is employed with increasing frequency.

This second approach utilizes a single (or at most a few) mineral which can be related by appearance, composition or other distinguishing feature to a well-defined petrogenesis. Methods that exploit such an approach are extremely diverse. Examples include petrographic classification of quartz grains (Basu *et al.*, 1975), compositional analysis of feldspars (Trevena and Nash, 1981) or heavy minerals, and laboratory methods of radiogenic decay or fission track dating of detrital zircons (c.f. Smith and Gehrels, 1991; Ross and Parrish, 1991). However, the advantages and disadvantages of this second approach are also diverse. For example, the quartz grain classification method of Basu *et al.* (1975) distinguishes plutonic from metamorphic terranes based on relative abundances of undulatory and polycrystalline grain types, but no quartz types uniquely indicate a single provenance. Lack of a unique linkage between quartz grain type and a particular provenance leads to ambiguities due to potentially mixed provenance terranes, and this method does not address a possible volcanic origin at all. Alternatively, feldspars and heavy mineral suites are susceptible to differential degrees of weathering and intrastratal solution (Pettijohn, 1975) which can mask or even obliterate the provenance signal. Dating detrital zircons can successfully determine the age of the provenance, but may not reveal much about the tectonic setting of the provenance simply because zircons are common to many petrologic associations. Despite their limitations, each of these methods can add important detail and confidence to provenance interpretations based on bulk composition techniques.

This study uses electron microprobe compositional analysis of detrital chromian spinel to determine tectonic setting of provenance. Compositional analysis of chromian spinel is routinely applied in petrologic studies of spinel-bearing mafic and ultramafic rocks (e.g. Irvine, 1973; Dick and Bullen, 1984; Hawkins and Melchior, 1985; Nixon, *et al.*, 1990), because chromian spinel composition is a sensitive indicator of parental melt conditions. Chromian spinel also is unusually stable chemically compared to other ultramafic minerals, and may be the only mineral unaltered by sub-greenschist facies serpentinization common to sea floor environments (Hekinian, 1982). Detrital chromian spinel is

important to provenance studies for the same reasons that led to the widespread utilization of spinels in petrologic studies of mafic and ultramafic rocks. Chromian spinel's unusual chemical stability ensures preservation of the compositional signature after burial in sedimentary strata, in contrast to most other mafic minerals which alter rapidly at near surface conditions. For provenance studies, chromian spinel offers the further advantages of mechanical stability (lack of cleavage and high degree of hardness; Bowie, 1967), and ease of recognition in both transmitted and reflected light petrography (medium to dark red-brown, yellow-brown or green-brown color, high relief, low reflectivity, and isotropic nature).

Despite chromian spinels wide use in petrologic studies, its use in provenance studies has been limited. Previous use of chromian spinel chemistry to aid provenance interpretations include a study by Utter (1978), who used the morphology and composition of detrital chromite to relate Proterozoic placer sands in South Africa to an Archean greenstone origin. In Japan, detrital chromian spinel chemistry has been used to relate serpentine sandstones to adjacent peridotites (Arai and Okada, 1991). Other applications of detrital chromian spinel studies include heavy mineral concentrate exploration for deposits of diamonds and other economic minerals (Pasteris, 1984; Mitchell, 1991).

The provenance of sandstones examined in this study is of central importance, both in a spatial and a temporal sense, to understanding the history of accretion in the Canadian Cordillera. The examined sandstones are from strata exposed in the northern Bowser Basin, located in the Intermontane belt of the Cordillera (Fig. 4-1), and were deposited during the Late Jurassic and Early Cretaceous, when much of the accretion of the Cordillera occurred. Earliest provenance interpretations in the Bowser Basin associated the abundance of chert pebbles with chert-rich rocks of the Cache Creek Group (Malloch, 1914). This interpretation is reinforced by identification of sandstones as having chert- and volcanic-lithic rich compositions, and paleocurrent measurements suggesting a northerly and northeasterly sediment source (Eisbacher, 1974; Cookenboo, 1989).

Figure 4-1: Location of the study area in the Intermontane Belt of the Canadian Cordillera. Terrane boundaries and Alaskan type peridotites after Wheeler and McFeeley (1987).

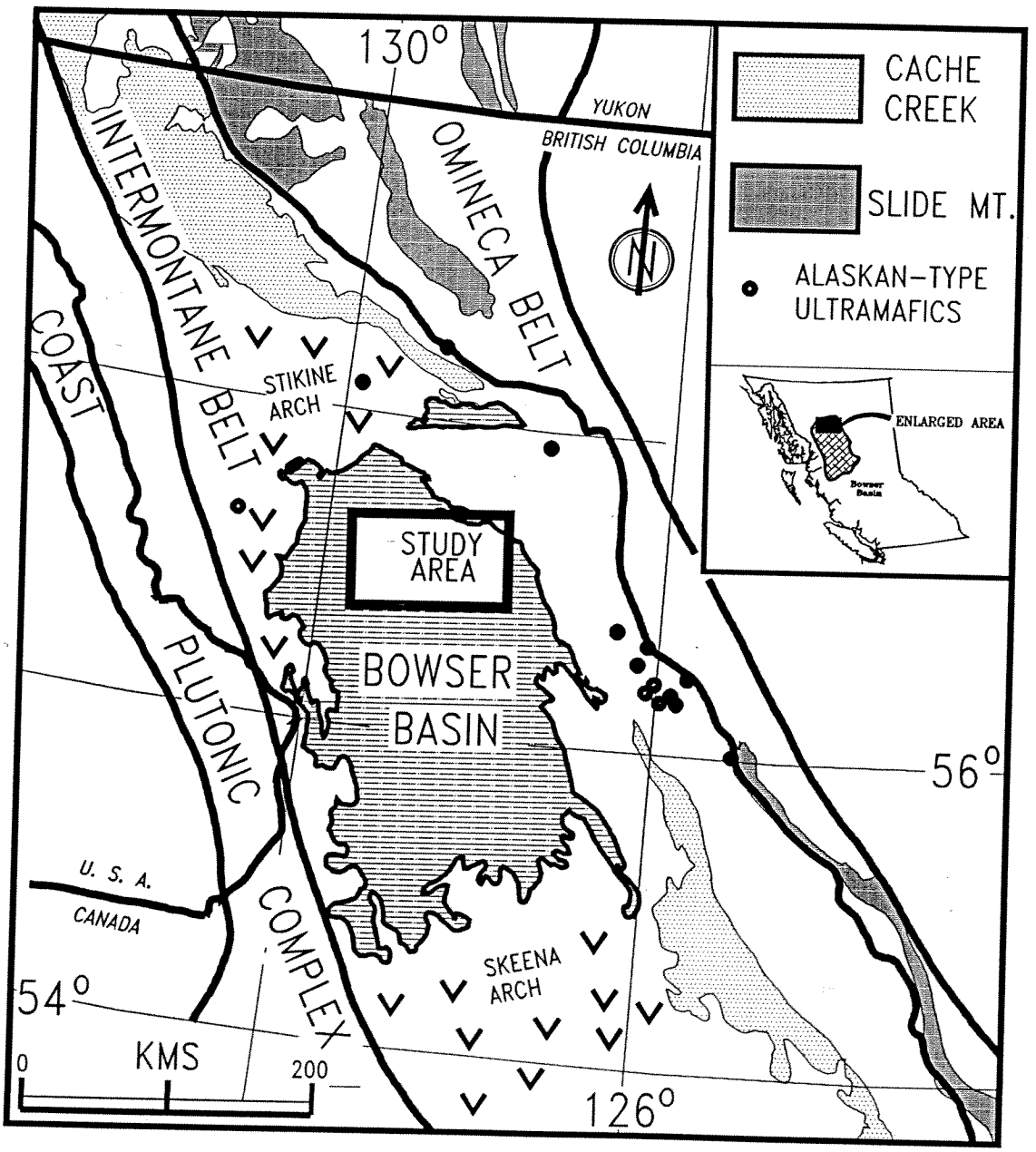

Framework grain detrital modes established that the provenance tectonic setting evolved from primarily an island arc and oceanic crust terrane to a combined terrane of island arc, oceanic crust, recycled sediments, metapelites, and minor plutonic rocks (Chapter 3). Stable isotope analysis of Bowser Basin shales suggests a similar evolution of provenance from nearly juvenile oceanic crust to increasingly continental values during the Early through Late Jurassic interval (Samson *et al.*, 1989). Chromian spinel compositions have the potential to provide a more detailed understanding of provenance tectonic setting, especially as relates to the type of oceanic lithosphere, and therefore can potentially both strengthen provenance interpretations based on detrital modal analyses, and add detail to the accretionary history of the Cordillera.

## METHODS

Routine thin section examination and point-count analyses revealed that chromian spinel occurs as an accessory mineral ($<1\%$) in all stratigraphic units. Samples containing relatively higher concentrations of chromian spinel were selected during thin section analysis for microprobe study. Seven sandstones were chosen as representative of the four stratigraphic horizons exposed in the study area (fig 4-2), and a total of 124 grains were analyzed from these seven chosen sandstones.

Major and minor element compositional data for chromian spinels were obtained from polished thin sections using a fully automated, four spectrometer Cameca SX-50 scanning electron microprobe employing the PAP matrix correction routine (Pouchou and Pichior, 1984). Analyses were made with an accelerating voltage of 15 kV, a beam current of 30 nA, and a spot size of 2 $\mu$m; TAP, LiF, and PET were used as the analyzing crystals. Peak counting times were 30 seconds for Si, Al, Ti, Cr, Fe, Mn, Mg, and Ca and 15 seconds for Zn, V, and Ni; background times were half of peak times. Analysis of standards as unknowns was done at the beginning, middle and end of analytical runs to ensure proper calibration throughout. All Fe is expressed as $Fe_2O_3$, and atomic concentrations of ferric and ferrous iron were calculated assuming ideal spinel stoichiometry. The assumption of ideal stoichiometry is routinely made in petrographic studies of spinel-bearing rocks (c.f. Dick and Bullen, 1984; Hawkins and

Figure 4-2: Stratigraphic column of the northern Bowser Basin. Horizons sampled are marked with an asterisk.

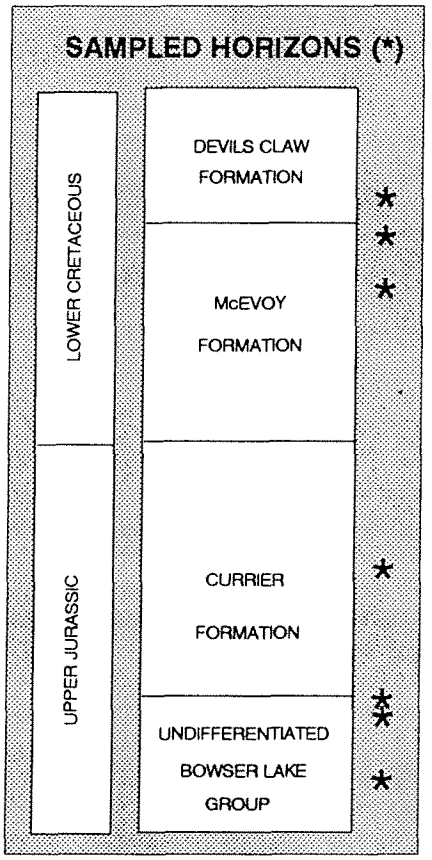

Melchior, 1985; Duncan and Green, 1987; Nixon *et al.*, 1990), and has been shown to be reasonable for a wide range of natural and synthetic chromian spinel compositions when checked by wet chemistry and Mossbauer spectra investigations (Osborne *et al.*, 1981). Atomic ratios are used herein, unless weight per cent oxide is specified. The notation Cr# is used for atomic ratios of Cr/Cr+Al and Mg# is used for atomic ratios of $Mg/Mg+Fe^{2+}$ following the common practise in petrologic literature (c.f. Dick and Bullen, 1984).

Most grains were analyzed twice, once in the core and once near the rim. The only exceptions were grains too small to permit separate analysis of core and rim. Core to rim variations were measured both to identify grains that may have partially re-equilibrated during mineral growth or in response to metamorphic events, and to check whether significant compositional gradients may have been established by low temperature alteration, weathering or post-depositional diagenetic processes.

## PETROGRAPHIC DESCRIPTIONS

Chromian spinel grains examined in this study generally are medium to dark red-brown (and in a few cases nearly opaque) in transmitted light. Less commonly, yellowish-brown grains occur, and one dark greenish-brown grain was observed. The range of spinel colors suggests a relatively broad range of Cr and Al substitution (Bernier, 1990). Chromian spinels are most abundant in fine to very fine grained sandstones, and in some samples are concentrated in thin laminae which are also enriched in other heavy mineral grains such as zircon. Typical grains are between 75 to 150 $\mu$m across. Grain margins commonly exhibit conchoidal fractures, suggesting mechanical breakage, but some grains are subhedral, suggesting preservation of the original crystal boundaries. Grains are generally visually homogeneous and show no obvious signs of zoning. Several serpentine grains with red-brown spinel inclusions were noted. A few spinel grains contain inclusions of olivine ($OF_{92-94}$).

## RESULTS

Detrital spinels measured in this study exhibit a wide variation in major element concentrations

(representative analyses presented in table 4-1). Cr# ranges between 0.21 and 0.89, with most Cr# above 0.35. Only four out of 124 grains measured had Cr# less than 0.30. Mg concentration generally decreases, and Fe increases, with increasing Cr#. Mg# ranges between 0.24 and 0.70. $Fe^{3+}$ concentration is consistently low. The maximum $Fe^{3+}/(Fe^{3+}+Cr+Al)$ in the measured spinels is 0.12. Core to rim variations are minor, and no consistent trends were noted.

The elements Ti, Mn, V, Zn, and Ni generally occur in only trace amounts (less than 1.0 wt % oxide). Ti is the most abundant of these minor elements, but even $TiO_2$ concentrations generally are low, and more than 90% of measured grains have $TiO_2$ concentrations less than 0.25%. All of the more $TiO_2$ enriched grains occur in the youngest stratigraphic units sampled (upper McEvoy and lower Devil Claw formations). A single exceptionally $TiO_2$-rich grain (4.2 wt % oxide), which also contains very high total Fe (58.6 wt % oxide), also occurs in the upper McEvoy Formation. This grain plots outside the compositional limits on all the discriminant diagrams discussed in the following section (figures 4-3, 4-4, and 4-5).

In my detrital grains, V and Zn concentrations consistently are below 0.50 wt. % oxide, and Ni concentrations are less than 0.25 wt. % oxide. One exceptional grain has Zn concentration of 0.57 wt. % oxide in its rim (V in this grain's rim is 0.35 wt. % oxide). This grain, like the high $TiO_2$ grain discussed above, is from the upper McEvoy Formation.

*Type of ultramafic source*

Major element concentrations of chromian spinels from a variety of types of ultramafic complexes around the globe have been arranged into fields on several discriminant diagrams, each of which represent one face of the spinel compositional prism (Irvine, 1974; Dickey, 1975; Basu *et al.*, 1975; Wilson, 1982; and Dick and Bullen, 1984). By comparison with these fields, the type of ultramafic source of the detrital spinels can be determined. However, it must be noted that occurrence within a field on any one diagram alone does not necessarily imply a match of the detrital spinels with a particular origin. Because variation occurs between three trivalent and two divalent cations, there is

TABLE 4-1: Representative analyses of detrital spinels from the northern Bowser Basin. Ideal spinel stochiometry was assumed in calculation of $Fe^{2+}$ and $Fe^{3+}$ atomic ratios. Cr# equals atomic ratio of Cr/(Cr+Al) and Mg# equals atomic ratio of Mg/(Mg+$Fe^{2+}$)

| | REPRESENTATIVE ANALYSES | | | | | |
|---|---|---|---|---|---|---|
| | 1 | 2 | 3 | 4 | 5 | 6 |
| $SiO_2$ | 0.01 | 0.85 | 0.05 | 0.02 | 0.03 | 0.07 |
| $Al_2O_3$ | 33.79 | 34.66 | 28.38 | 23.02 | 22.46 | 9.62 |
| $TiO_2$ | 0.06 | 0.04 | 0.08 | 0.11 | 0.12 | 0.30 |
| $Cr_2O_3$ | 30.87 | 29.74 | 40.11 | 43.04 | 42.78 | 53.45 |
| $Fe_2O_3$ | 19.88 | 19.13 | 16.40 | 22.30 | 21.48 | 28.75 |
| MnO | 0.08 | 0.12 | 0.09 | 0.11 | 0.09 | 0.16 |
| MgO | 14.60 | 14.63 | 13.81 | 11.72 | 11.39 | 8.02 |
| CaO | 0.00 | 0.05 | 0.00 | 0.03 | 0.10 | 0.02 |
| ZnO | 0.18 | 0.26 | 0.19 | 0.28 | 0.31 | 0.11 |
| $V_2O_3$ | 0.12 | 0.10 | 0.27 | 0.24 | 0.28 | 0.12 |
| NiO | 0.19 | 0.19 | 0.07 | 0.02 | 0.03 | 0.05 |
| TOTAL | 99.78 | 99.77 | 99.45 | 100.89 | 99.07 | 100.67 |
| *Atomic Ratios* (stoichiometric calculations based on 4 O) | | | | | | |
| Al | 1.19 | 1.22 | 1.02 | 0.85 | 0.85 | 0.39 |
| Ti | 0.00 | 0.00 | 0.00 | 0.00 | 0.00 | 0.01 |
| Cr | 0.72 | 0.70 | 0.97 | 1.07 | 1.08 | 1.45 |
| $Fe^{2+}$ | 0.35 | 0.35 | 0.37 | 0.45 | 0.46 | 0.59 |
| $Fe^{3+}$ | 0.09 | 0.08 | 0.01 | 0.08 | 0.06 | 0.15 |
| Mg | 0.65 | 0.65 | 0.63 | 0.55 | 0.55 | 0.41 |
| Mn | 0.00 | 0.00 | 0.00 | 0.00 | 0.00 | 0.01 |
| Cr# | 0.65 | 0.36 | 0.49 | 0.56 | 0.56 | 0.79 |
| Mg# | 0.38 | 0.65 | 0.63 | 0.54 | 0.54 | 0.41 |

overlap among fields on some plots, although the fields may be largely distinct on other plots.

A ternary plot of Cr, Al and $Fe^{3+}$ (Fig. 4-3) is useful for distinguishing alpine-type peridotites from Alaskan-type and stratiform peridotite complexes, as demonstrated by Dick and Bullen (1984). In alpine-type peridotites, Cr increases with increasing $Fe^{3+}$, but $Fe^{3+}$ concentrations overall remain quite low. Both stratiform and Alaskan-type complexes exhibit, in part, much higher concentrations of $Fe^{3+}$ than the alpine-type peridotites, and greater scatter of $Fe^{3+}$ concentrations relative to Cr concentrations. For my spinels, chromium concentration increases with increasing $Fe^{3+}$ concentrations, and overall $Fe^{3+}$ concentrations remain low (Fig. 4-3), consistent with an Alpine-type peridotite origin (Dick and Bullen, 1984). High $Fe^{3+}$ spinels, which distinguish many stratiform complexes are entirely lacking from my data set (Irvine, 1974; Wilson, 1982; Dickey, 1975; and Dick and Bullen, 1984).

The importance of Fe-rich spinels in ultramafic bodies formed by fractional crystallization in the crust (Alaskan-type peridotites and stratiform complexes) is emphasized in figure 4-4, a plot of $Fe^{3+}/(Fe^{3+}+Cr+Al)$ versus Mg#. Except for a single grain which is considered separately later, the data from this study also plots entirely within the field of alpine-type peridotites (Irvine, 1974) in this diagram. The field for Alaskan-type complexes plots entirely outside the range of sampled grains, and therefore can be excluded as a significant contributor to the detritus. The stratiform field from Irvine (1974) partially overlaps the alpine-type peridotite field (Fig. 4-5), but none of the detrital grains exhibit the high $Fe^{3+}$ compositions that distinguish at least some stratiform complex chromian spinels (Irvine, 1974; Haggerty, 1979; Wilson, 1982; and Dick and Bullen, 1984) from alpine-type peridotites [exclusively low $Fe^{3+}$: $Fe^{3+}/(Fe^{3+} + Al + Cr)$ less than approximately 0.12]. Although contribution of minor portions of low $Fe^{3+}$ stratiform spinels is cannot be completely ruled out, such an explanation requires ad-hoc assumptions of only low $Fe^{3+}$ stratiform spinels being contributed, and therefore significant contribution from stratiform source is unlikely. Taken together, the Mg# versus $Fe^{3+}/(Fe^{3+}+Al+Cr)$ and Cr - Al - $Fe^{3+}$ ternary plots demonstrate that detrital chromian spinels from the northern Bowser Basin have close affinities to alpine-type peridotites and exclude Alaskan-type peridotites and stratiform complexes as major sediment sources.

Figure 4-3: Ternary plot of the major trivalent cations in chromian spinels. Solid circles are values from the detrital spinels in this study. For comparison, dark-gray fill covers nearly 300 spinel analyses from an Alaskan-type peridotite (Tulameen complex), after Nixon, *et al.* (1990). Hatching denotes field for chromian spinels of mantle melting origin, including ultramafic xenoliths, abyssal dunites, spinel and plagioclase peridotites, and alpine-type peridotites (Basu *et al.*, 1975; and Dick and Bullen, 1984). Stippled field shows compositional range of stratiform complex spinels derived by fractional crystallization, including data from the Bushveld, Rhum, Stillwater, Hartley (Great 'Dyke'), and Marum stratiform complexes (Duke, 1982; Wilson, 1982; and Dick and Bullen 1984).

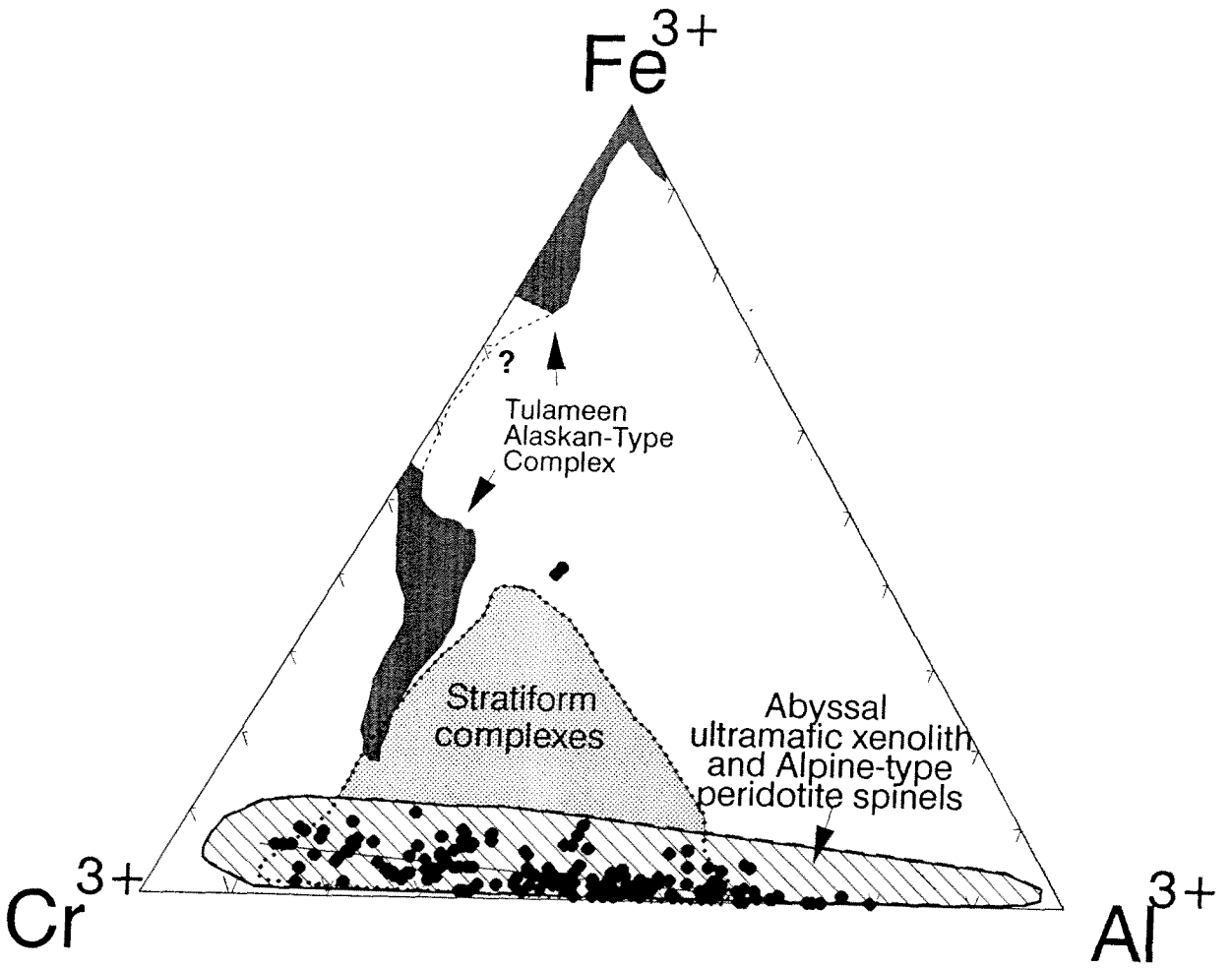

Figure 4-4: Plot of $Mg/(Mg+Fe^{2+})$ against ratio of trivalent cations $Fe^{3+}/(Fe^{3+}+Al+Cr)$ for detrital spinel data set compared to worldwide occurrences from Irvine (1974).

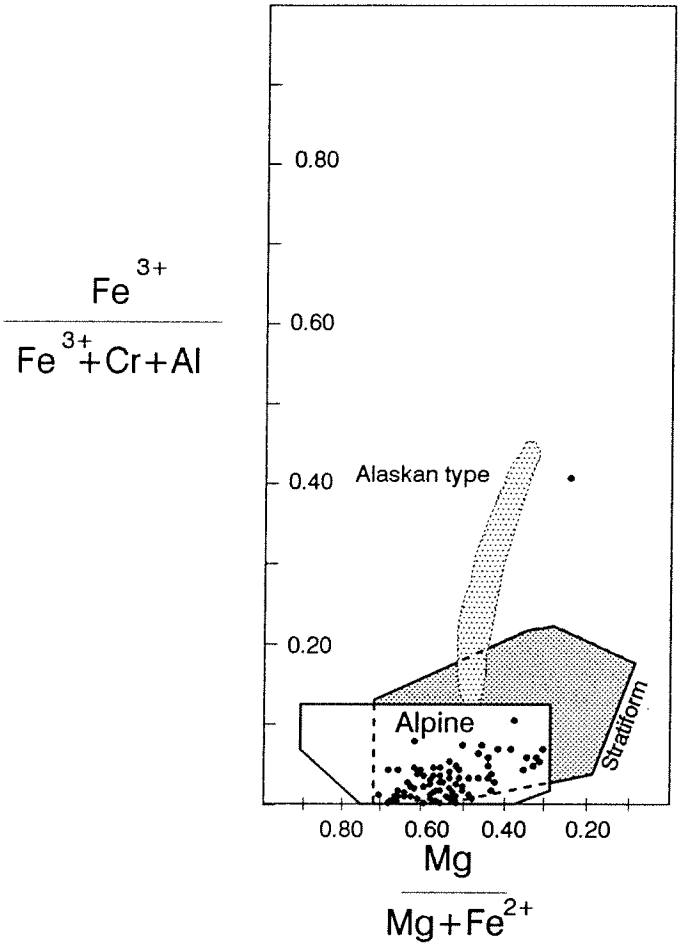

Figure 4-5: Cr/(Cr+Al) versus Mg/(Mg+$Fe^{2+}$). Fields include mid-ocean ridge-derived chromian spinels (abyssal peridotites, dunites and basalts; Dick and Bullen, 1984); Bowser Basin detrital spinel data set (data points marked by filled circles); and field for alpine-type peridotites.

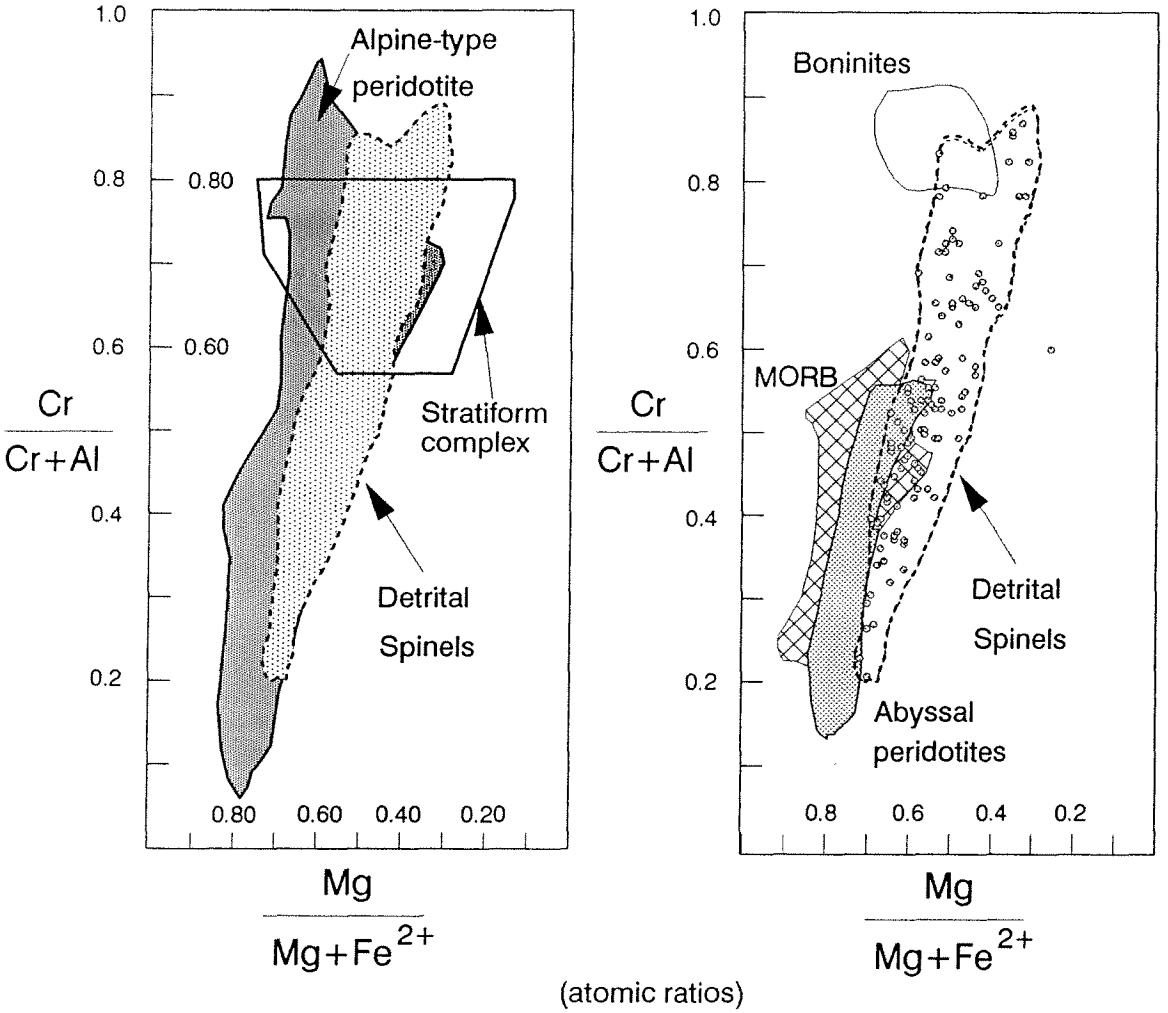

*Origin of the alpine-type peridotite source*

The origin of the alpine-type peridotite source can be constrained by consideration of the Cr# versus Mg# plot (Fig. 4-5). Chromian spinels formed at mid-ocean ridges in both peridotites and basalts are restricted to Cr# less than 0.60, and typically have high Mg#s (many 0.70 to 0.85; Dick and Bullen, 1984). In contrast, spinels in back-arc basin basalts tend to have lower Mg# for a given Cr#, and associated island-arc spinels exhibit Cr# in excess of 0.60 (Dick and Bullen, 1984; Fig. 4-6). The detrital spinels span a much greater range of Cr# compositions than abyssal spinels, and therefore abyssal rocks are excluded as the only source. A better match to spinel chemistry in this study comes from some very large and complex alpine-type peridotites because they exhibit a broad range of Cr#, including values both below and above the abyssal limit of 0.60 . These large ophiolites, which include the Samail in Oman (Pallister and Hopson, 1981), the New Caledonian (Nicolas and Prinzhofer, 1983) and Josephine peridotites, the Bay of Islands Complex (Dick and Bullen, 1984) and the Kanuti Ophiolite in Alaska (Loney and Himmelberg, 1989), are thought to have a "complex multi-stage melting history not found at mid-ocean ridges" (Dick and Bullen, 1984, p. 73). These ophiolites, and by inference the detrital chromian spinels in this study, likely originated from a complex of marginal basin lithosphere and island arc-associated rocks. Such a tectonic setting and complex melting history suggests a provenance in proximity to a continental margin.

The possibility exists that the detrital spinels could be a mixture of mid-ocean ridge-derived seafloor with more depleted marginal basin and island arc suites. Two aspects of the detrital spinel compositions, however, suggest that a mid-ocean ridge derived abyssal source did not contribute (at least significantly) to the sampled strata in the northern Bowser Basin. High alumina spinels (Cr#= 0.10 to 0.30) are common in abyssal peridotites, dunites, and basalts (Dick and Bullen, 1984), but are almost entirely lacking among my detrital spinels (only four grains out of 124 measured less than 0.30, lowest Cr#=0.21). High Mg#s (0.70 to 0.85 out of a range from 0.55 to 0.85) are also common in spinels from abyssal peridotites and basalts (Dick and Bullen, 1984), but like high alumina spinels also are missing from my detrital spinels (highest Mg#= 0.70). The lack of both high Al and high Mg

Figure 4-6: Cartoon illustrating typical spinel compositions from different sea-floor (potential alpine-type ophiolite) and continental crust origins. No scale implied.

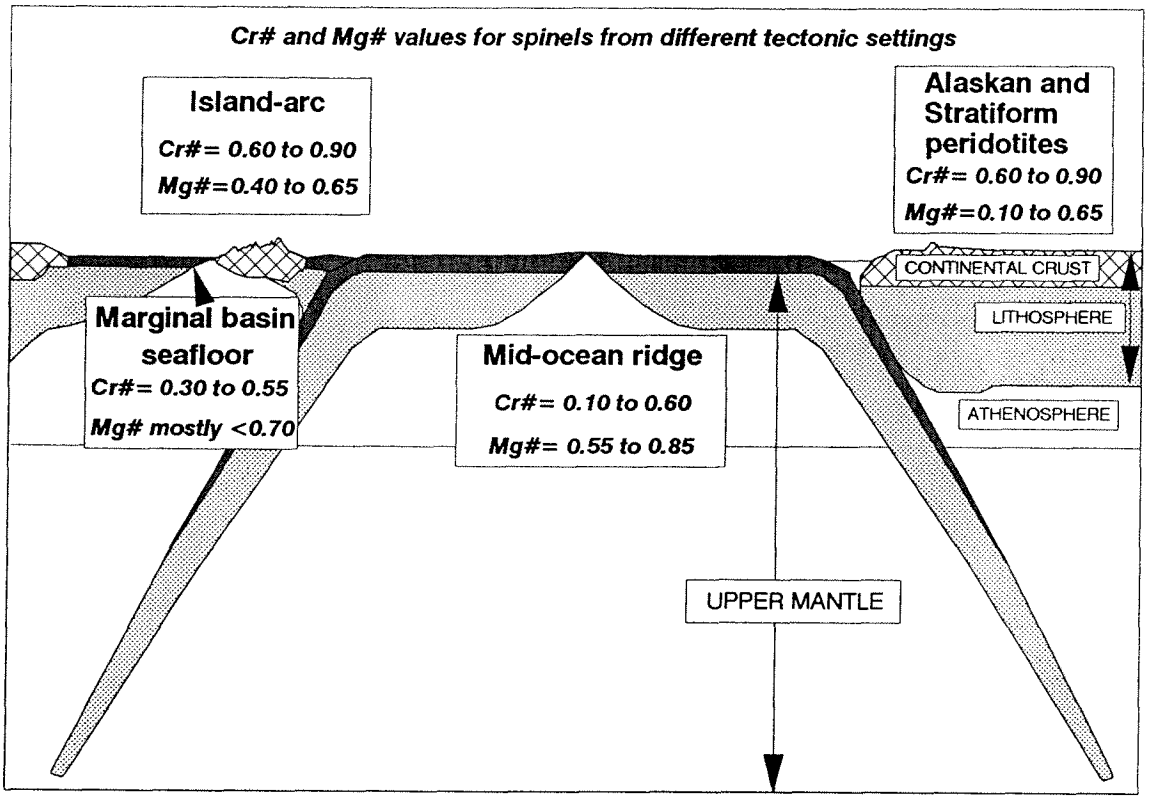

spinels, which are the best indicators of mid-ocean ridge origin, strongly suggests that northern Bowser Basin spinels did not originate from a mid-ocean ridge source. The generally lower Mg# of my spinels suggests that they crystallized at lower temperatures than normal mid-ocean ridge basalts (MORB) or peridotite (Hawkins and Melchior, 1985) because Mg concentration in chromian spinels decreases with lower temperatures of formation and increased partial melting (Hill and Roeder, 1974). One scenario for increased partial melt is increased water content, and a subducted slab associated with marginal basin/island arc development can provide the source for such elevated water content. Therefore, fluids evolved from subducted lithosphere may have contributed to the chemical signature of the ophiolite provenance as preserved in the detrital spinels.

A modern analog for my detrital spinels may in part occur in rocks of the Marianas Trough. Back-arc basin rocks in the Marianas Trough contain spinels with moderate Cr#s (0.30 to 0.55) and Mg#s (maximum Mg#= 0.73; average Mg#= 0.62; Hawkins and Melchior, 1985). Like my detrital spinels, the Marianas Trough spinels lack the very high Al and Mg examples common to abyssal suites. High Cr spinels (Cr# greater than 0.60) are lacking in the Marianas Trough suites, but do occur in spinels from Marianas island arc volcanics, including boninites (Cr#= 0.73 to 0.89; Bloomer and Hawkins, 1987). Obduction of a complex of rock suites similar to Marianas back-arc crust and island arc volcanics (including boninites) satisfactorily explains the compositional variation of my detrital spinels.

The single exceptionally $TiO_2$ rich spinel, mentioned earlier in the results section, deserves consideration. Such high $TiO_2$ chromian spinels (4.2 wt. % oxide) are uncommon, but have been reported from late stage wehrlites of the Samail ophiolite (Pallister and Hopson, 1981). This grain is therefore consistent with the interpreted input from a complex alpine peridotite source, and may further reflect addition of more evolved, late stage ophiolitic material to the provenance.

Spinel chemistry can record exposure to greenschist and higher grade metamorphism by development of compositional zoning, changes in major element chemistry, and addition of significant

(less than approximately 1.0 weight per cent oxide) concentrations of certain trace elements. Major element changes most clearly indicative of metamorphism include enrichment of $Fe^{3+}$, commonly in opaque ferritchromite rims, which can begin during greenschist metamorphism, and development of very high Cr (Cr# greater than 0.90) and very low Al (Cr# less than 0.05) compositions during greenschist and higher grades of metamorphism (Evans and Frost, 1975; Whittaker and Wadkinson, 1983). Neither compositional zoning nor very high Cr, Al or $Fe^{3+}$ content spinels occur among my detrital spinels. The generally low levels of Ni, Zn, and V combined with lack of significant core to rim variations and lack of very high Cr, Al or $Fe^{3+}$ spinels suggests erosion of the obducted alpine-type peridotite source occurred prior to any greenschist or higher grade regional metamorphic events. Lack of any consistent or appreciable core to rim variation trend also mitigates against the possibility of alteration of the spinels after deposition.

The same type of ultramafic source appears to have been the source of Bowser Basin sediments throughout accumulation of the sampled strata. No clear changes in spinel chemistry have been identified from the base to the top of the examined strata. Several subtle changes, however, suggest that a greater variety of source rocks became exposed through time. All spinels with $TiO_2$ concentrations greater than 0.25% were recovered from upper McEvoy Formation strata (Fig. 4-7), as well as a single grain with Zn concentration of 0.57 wt. % in its rim (V in grain's rim is 0.42 wt. %). Zn concentrations above 0.50% are commonly associated with sulfide mineralization (Bernier, 1990), suggesting that this single grain may record some localized metasomatic activity within the provenance. The slightly more variable compositions that occur in the McEvoy Formation are consistent with exposure of additional source rocks in basically the same source area. A similar conclusion that sediment source rocks became more varied through time is evident from the sandstone framework grain detrital modal study (Chapter 3).

Figure 4-7: $TiO_2$ versus $Cr_2O_3$ plot, demonstrating the restriction of high $TiO_2$ values to sandstones from the McEvoy Formation (petrofacies 2). Dashed line has a value of 0.25 wt. % $TiO_2$.

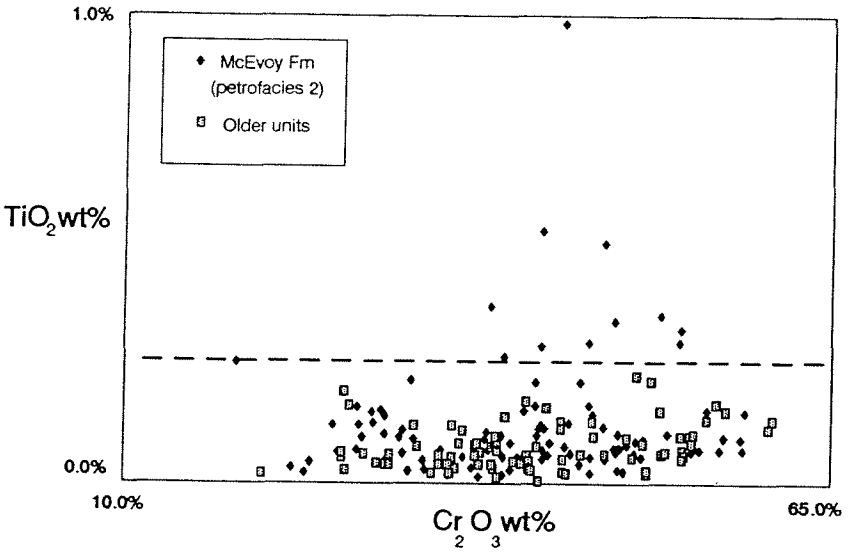

## PROVENANCE: CANDIDATES IN THE CANADIAN CORDILLERA

The earliest provenance interpretations for the northern Bowser Basin concluded that the most likely source was oceanic rocks of the Cache Creek terrane, based on the abundance of chert pebbles in conglomerates and paleocurrent direction indicators implying input from the north and east (Malloch, 1914; Eisbacher, 1974; Cookenboo, 1989). More detailed interpretation of provenance based on detrital modal analysis of the sandstones demonstrates that ocean floor and island arc terranes contributed to the Currier Formation and undivided Bowser Lake Group strata, with additional contribution from dissected arc and low to medium grade metapelites evident in the younger McEvoy and Devils Claw Formations (Chapter 3). Provenance interpreted from the detrital chromian spinel study is entirely consistent with the conclusions reached from the detrital modal analysis, but adds details significant to tectonic reconstructions of the Cordillera. In addition to confirming that island arc and oceanic crustal rocks were involved in the provenance, it is inferred from the detrital spinel compositions that the oceanic terrane was obducted marginal basin crust, and that the obducted material was eroded prior to any regional metamorphic events affecting the source area.

Several possible sources of chromian spinel exist to the north and east of the Bowser Basin, the direction of provenance indicated by paleocurrents. Alaskan-type peridotite bodies are scattered among rocks north and east of the Bowser Basin (Fig. 4-1), but these potential sources of chromian spinel can be eliminated as significant contributors because this type of peridotite contains $Fe^{3+}$-rich spinels unlike any found in the detrital spinel suite. Two oceanic terranes containing peridotites are also present to the north and east (Fig. 4-1 and Fig. 4-8c): 1) the Cache Creek terrane (Mississippian to Lower Jurassic; Wheeler, *et al.*, 1991) composed mainly of MORB-like tholeiitic and alkaline basalt rocks generally of open ocean affinities (Wheeler and McFeely, 1987); and 2) the Slide Mountain terrane (Devonian to Upper Triassic; Wheeler, *et al.*, 1991) composed of rocks with marginal basin and island arc affinities (Wheeler and McFeely, 1987). Both terranes contain alpine-type ophiolites, but few spinel analyses are presently available from either the Slide Mountain or Cache Creek groups. Based on its marginal basin

Figure 4-8: A model illustrating closure of marginal seas and fringing island arcs after initiation of rifting of the Atlantic Ocean in the Early Jurassic. Obduction and later erosion of such marginal basin crust and island arcs suites are the likely source for the chromian spinels of the northern Bowser Basin. 4-8a): Late Paleozoic reconstruction of western North American margin, based on Bowser Basin provenance considerations. Note the marginal basin is fringed to the west by active island arcs. 4-8b): By Early to Middle Jurassic, fringing island arcs and associated marginal seas have been closed by obduction onto the western margin of North America. Note that the island arc is no longer active. 4-8c): Terranes as they appear today in the Canadian Cordillera. Obducted terranes are discontinuous erosional remnants of their inferred Mesozoic extents.

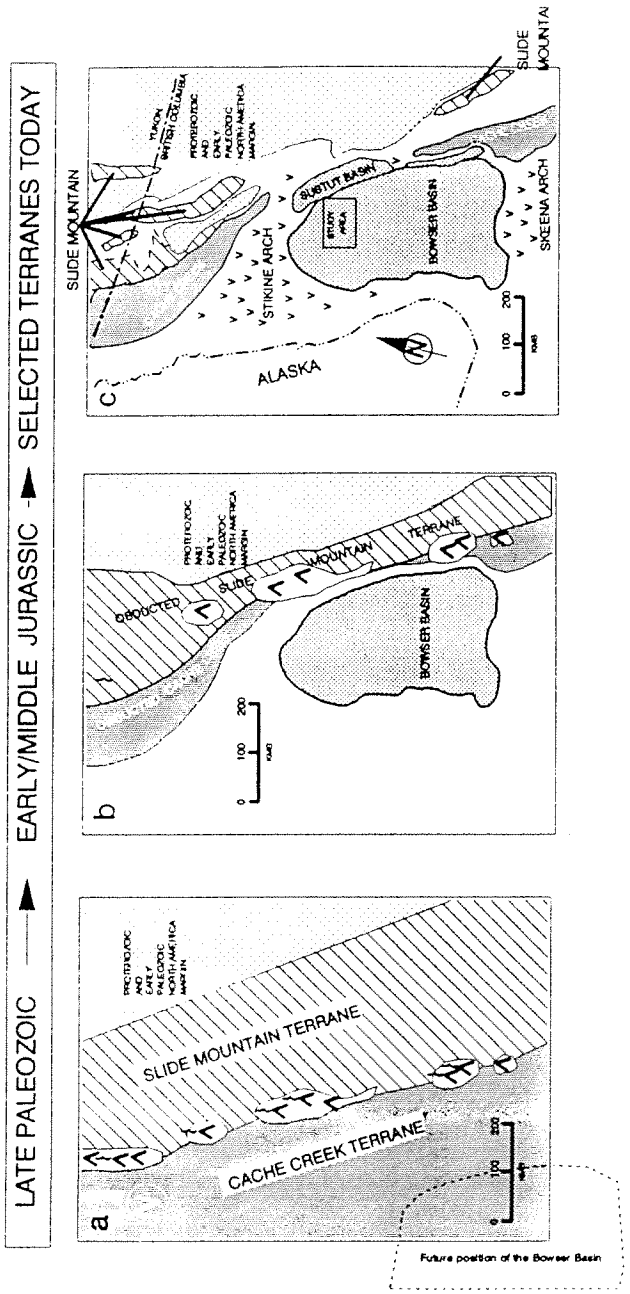


Figure 4-8: Model of Cordilleran tectonic development consistent with interpretation of provenance.

a) Late Paleozoic reconstruction of western North American margin, based on Bowser Basin provenance considerations. Note the marginal sea is fringed by active island arcs.

b) By the Early to Middle Jurassic, fringing island arcs and associated marginal seas have been closed by obduction onto the western margin of North America. Note that the island arc is no longer active.

c) Terranes as they appear today in the Canadian Cordillera. Obducted terranes are discontinuous erosional remnants of their Mesozoic extents.

and island arc affinities, the Slide Mountain terrane appears to be a potential source for part of the Bowser Basin sediments. Specifically, the Slide Mountain assemblage may have contributed Cr-rich spinels to the detrital spinels similar to those reported from the Redfern amphibolite in southeastern British Columbia (Radloff, 1989). At first examination, the more abyssal affinities of the Cache Creek Group would seem to render it incompatible with the detrital spinel chemistry. However, the Cache Creek terrane is only in part mid-ocean ridge-derived, and other parts have island arc and marginal-basin affinities that would make them suitable sources for the detrital spinels (Wheeler *et al.*, 1991). Chromian spinel compositions from Cache Creek Group north of the Bowser Basin near Atlin have Cr#s between 0.23 to 0.89; Mg#s 0.36 to 0.68 (Ash, written communication, 1993) and are comparable to my detrital spinels. Other Cache Creek chromian spinel analyses from five unaltered cores from Mt. Sydney-Williams (Cr#s from 0.31 to 0.53 and Mg#s from 0.48 to 0.73) and Murray Ridge and Chromian Peak (43 km north of Mt. Sydney-Williams; Cr#s from 0.54 to 0.91) southeast of the Bowser Basin also fit the detrital data set (Whittaker and Wadkinson, 1981; Whittaker, 1982; Whittaker and Wadkinson, 1983). No high Al-high Mg spinels (Cr# less than 0.20; Mg# greater than 0.75) which most clearly indicate a mid-ocean ridge origin have been reported from the Cache Creek. These variable spinel compositions support the conclusion that at least parts of the Cache Creek Group have close affinities to marginal basin lithosphere and would be suitable provenance for Bowser Basin sediments.

The detrital spinel compositions help to clarify understanding of the processes of accretionary tectonics that formed the Cordillera. From the detrital spinels, it is clear that obducted marginal seafloor and island arcs shed large quantities of detritus into the northern Bowser Basin from at least the Late Jurassic (Oxfordian and younger) through the mid-Cretaceous (Aptian or Albian; MacLeod and Hills, 1990; Cookenboo and Bustin, 1989). The spinel chemistry indicates that portions of marginal basin lithosphere and island arc volcanics formed from mantle with a higher degree of partial melting at lower temperatures compared to mantle at mid-ocean ridges. Such a chemical environment is expected in marginal basin floor formed above a subducting slab (e.g. Marianas Basin; Hawkins and Melchior, 1985), probably due to its enrichment in water derived from the subducting slab, and possibly because of

repeated cycles of melting. Because northern Bowser Basin sediments lack the low Cr# and high Mg# spinels typical of abyssal seafloor, mid-ocean ridge derived spinels appear to be absent from the source area. Based on the conclusion that the sediments in the Bowser Basin originated as marginal basin lithosphere, the process of accretionary tectonics in the provenance of the northern Bowser Basin probably involved accretion of terranes that were proximal to North America. A model consistent with these data (Fig. 8a, 8b, and 8c) calls for closure of marginal seas, and emplacement of remnants of those seas and associated island arcs on to the western margin of North America during or before the Middle Jurassic. Timing of this closure event may be associated with the latest Triassic to earliest Jurassic change in plate motion recorded in paleomagnetic studies of North America (Ekstrand and Butler, 1989), which in turn is related to the initiation of Atlantic rifting.

## CONCLUSIONS

1) Alpine-type peridotite is part of the Bowser Basin provenance.

2) Chromian spinel chemistry is similar to those alpine-type peridotites derived from complex mantle melting histories such as are believed to have been emplaced by obduction of marginal basin lithosphere and island arc complexes.

3) Lack of high Al and high Mg spinels, which commonly occur in abyssal basalts and peridotites, implies that mid-ocean ridge derived lithosphere did not contribute detritus significantly to the examined Bowser Basin strata. Lack of mid-ocean ridge contribution, combined with clear evidence for obducted marginal basin and island arc ultramafic suites, suggests the tectonic processes affecting Bowser Basin provenance involved accretion and obduction of fringing marginal seas and island arcs onto the western margin of North America, rather than closure of true open oceans.

4) Erosion of the source of Bowser Basin sediments occurred prior to any regional greenschist or higher grade metamorphic events affecting the provenance.

5) The detrital chromian spinels lack high $Fe^{3+}$ examples that typically occur in Alaskan and stratiform type peridotite complexes, suggesting that such peridotites did not contribute significantly to Late Jurassic and Early Cretaceous sediments in the northern Bowser Basin. This implies that Alaskan-type peridotites which are exposed today in the likely source area north and east of the of the study area were probably not exposed until after Bowser Basin sedimentation.

6) The ability of detrital chromian spinels to be used to discriminate plate boundary conditions for provenance suggests that methods used in this study may have broader application and could help elucidate the process of accretionary tectonics if applied in other Cordilleran basins, where an ultramafic source is suspected.

# REFERENCES

Arai, S. and Okada, H., 1991. Petrology of serpentine sandstone as a key to tectonic development of serpentine belts. Tectonophysics, v. 195, p. 65-81.

Basu, A. R. and MacGregor, I. D., 1975. Chromite spinels from ultramafic xenoliths. Geochimica et Cosmochimica Acta, v. 39, p 937-945.

Basu, A., Young, S. W., Suttner, L. J., James, W. C. and Mack, G. H., 1975, Re-evaluation of the use of undulatory extinction and polycrystallinity in detrital quartz for provenance interpretation. Journal of Sedimentary Petrology, v. 45, p. 873-882.

Bernier, L. R., 1990, Vanadiferous zincian-chromian hercynite in a metamorphosed basalt-hosted alteration zone, Atik Lake, Manitoba. Canadian Mineralogist, v. 28, p. 37-50.

Bloomer, S. H. and Hawkins, J. W., 1987, Petrology and geochemistry of boninite series rocks from the Mariana trench. Contributions to Mineralogy and Petrology, v. 97, p. 361-377.

Bowie, S. H. U., 1967, Microscopy: Reflected Light, *In* J. Zussman ed., Physical Methods in Determinative Mineralogy. Academic Press, New York.

Cookenboo, H. O., 1989, Lithostratigraphy, palynostratigraphy, and sedimentology of the northern Skeena Mountains and their implications to the tectonic history of the Canadian Cordillera. [unpublished MSc. thesis]: The University of British Columbia. 131 p.

Cookenboo, H. O., and Bustin, R. M., 1989, Jura-Cretaceous (Oxfordian to Cenomanian) stratigraphy of the north-central Bowser Basin, northern British Columbia. Canadian Journal of Earth Sciences, v. 26, p. 1001-1012.

Dick, H. J. B., and Bullen, T., 1984, Chromian spinel as a petrogenetic indicator in abyssal and alpine-type peridotites and spatially associated lavas. Contributions to Mineralogy and Petrology, v. 86, p. 54-76.

Dickey, J. S. 1975. A hypothesis of origin for podiform chromite deposits. Geochimica et Cosmochimica Acta, v. 39, p. 1061-1074.

Dickinson, W. R. and Suczek, C. A., 1979. Plate tectonics and sandstone compositions: American Association of Petroleum Geologists Bulletin, v. 63, p. 2164-2182.

Dickinson, W. R., Beard, L. S., Brakenridge, G. R., Erjavec, J. L., Ferguson, R. C., Inman, K. F., Knepp, R. A., Lindberg, F. A., and Ryberg, P. T., 1983, Provenance of North American

Phanerozoic sandstones in relation to tectonic setting. Geological Society of America Bulletin, v. 94, p. 222-235.

Duke, J. M., 1982. Ore deposits models 7. Magmatic segregation deposits of chromite. Geoscience Canada, v. 10, p. 15-24.

Duncan, R. H. and Green, D. H., 1987, The genesis of refractory melts in the formation of oceanic crust. Contributions to Mineralogy and Petrology. v. 97, p. 326-342.

Eisbacher, G., 1974, Evolution of successor basins in the Canadian Cordillera, *In* Dott, R. H., and Shaver, R. H., eds., Modern and Ancient Geosynclinal Sedimentation. Society of Economic Paleontologists and Mineralogists, Special Publication 19, p. 274-291.

Ekstrand, E. J. and Butler, R. F., 1989, Paleomagnetism of the Moenave Formation: Implications for the Mesozoic North American apparent polar wander path. Geology, v. 17, p. 245-248.

Evans, B. W. and Frost, B. R. 1975. Chrome-spinel in progressive metamorphism - a preliminary analysis. Geochimica et Cosmochimica Acta, v. 39, p. 959-972.

Franzinelli, E. and Potter, P. E., 1983, Petrology, chemistry, and texture of modern river sands, Amazon River system. Journal of Geology, v. 91, p. 23-39.

Haggerty, S. E., 1979. Spinels in high pressure regimes. In Boyd, F. R. and Meyer, O. A. (*eds.*), The mantle sample: inclusions in Kimberlites and other volcanics. Proceedings of the second international kimberlite conference, v. 2, p. 183-196..

Hawkins, J. W. and Melchior, J. T., 1985, Petrology of Mariana Trough and Lau Basin basalts. Journal of Geophysical Research, v. 90, p. 11431-11468.

Hekinian, R. 1982. Petrology of the ocean floor. Elsevier Oceanography Series. v. 33. Elsevier Scientific Publishing, Amsterdam. 407 p.

Irvine, T. N., 1974, Petrology of the Duke Island ultramafic complex, southeastern Alaska. Geological Society of America Memoir 138, 240 p.

Loney, R. A. and Himmelberg, G. R., 1989, The Kanuti Ophiolite, Alaska. Journal of Geophysical Research, v. 94, p. 15,869-15,900.

MacLeod, S. E., and Hills, L. V. 1990. Conformable Late Jurassic (Oxfordian) to Early Cretaceous strata, northern Bowser Basin, British Columbia: A sedimentological and paleontological model. Canadian Journal of Earth Sciences, v. 27: 988-998.

Malloch, G.S., 1914. Groundhog coal field. Summary report of the Geological Survey Department of Mines. p. 69 to 101.

Mitchell, R. H., 1991. Kimberlites and Lamproites: Primary sources of diamond. Geoscience Canada v. 18, p. 1-16.

Molinaroli, E., Blom, M. and Basu, A., 1991, Methods of provenance determination tested with discriminant function analysis. Journal of Sedimentary Petrology, v. 61, p. 900-908.

Nicolas, A. and Prinzhofer, A., 1983, Cumulative or residual origin for the transition zone in ophiolites; structural evidence. Journal of Petrology, v. 24, p. 188-206.

Nixon, G. T., Cabri, L. J. and LaFlamme, J. H. G., 1990, Platinum-group-element mineralization in lode and placer deposits associated with the Tulameen Alaskan-type complex, British Columbia. Canadian Mineralogist, v. 28, p. 503-535.

Osborne, M. D., Fleet, M. E. and Bancroft, G. M., 1981, $Fe^{2+}$ -$Fe^{3+}$ ordering in chromite and Cr-bearing spinels. Contributions to Mineralogy and Petrology, v. 77, p. 251-255.

Pallister, J. S. and Hopson, C. A. 1981, Samail ophiolite plutonic suite: field relations, phase variation, cryptic variation and layering, and a model of a spreading ridge magma chamber. Journal of Geophysical Research, v. 86, p. 2593-2644.

Pasteris, J. D., 1984, Use of indigenous kimberlite minerals, particularly spinels, in the evaluation of diamond potential. *In* Petruk, W. (*ed.*), Symposium on Process Mineralogy III: applications in metallurgy, coal, concrete, smelting, and exploration. Department of Energy, mines, and Resources, Ottawa, p. 157-179.

Pettijohn, F. J. 1975, Sedimentary rocks. 3rd ed., Harper and Row, New York, 628 p.

Pouchou, J. L., and Pichoir, F., 1984. A new model for quantitative analysis: Part I. Application of the analysis of homogeneous samples. La Recherche Aerospatiale, v. 5, p. 47-65.

Radloff, J. K., 1989, Origin and obduction of the ophiolitic Redfern Complex on the Omineca-Intermontane Belts boundary, western Cariboo Mountains, British Columbia. [unpublished MSc. thesis]: The University of British Columbia. 178 p.

Ross, G. M., and Parrish, R. R., 1991, Detrital zircon geochronology of metasedimentary rocks in the southern Omineca Belt, Canadian Cordillera. Canadian Journal of Earth Sciences, v. 28, p. 1254-1270.

Samson, S. D., McClelland, W. C., Patchett, P. J., Gehrels, G. E. and Anderson, R. G. 1989. Evidence

from neodymium isotopes for contributions to Phanerozoic crustal genesis in the Canadian Cordillera. Nature, v. 337, p. 705-709.

Smith, M. T., and Gehrels, G. E., 1991, Detrital zircon geochronology of Upper Proterozoic to Lower Paleozoic continental margin strata of the Kootenay arc: implications for the early Paleozoic tectonic development of the eastern Canadian Cordillera. Canadian Journal of Earth Sciences, v. 28, p. 1271-1284.

Suttner, L. J. and Dutta, P. K., 1986, Alluvial sandstone composition and paleoclimate, I. Framework mineralogy. Journal of Sedimentary Petrology, v. 56, p. 329-345.

Trevena, A. S. and Nash, W. P., 1981, An electron microprobe study of detrital feldspar. Journal of Sedimentary Petrology, v. 51, p. 137-150.

Utter, T. 1978, The origin of detrital chromites in the Klerksdorp Goldfield, Witwatersand, South Africa. Neues Jahrb. Mineralogies Abh., v. 133, p. 191-209.

Wheeler, J. O., and McFeely, P., 1987, Tectonic assemblage map of the Canadian Cordillera and adjacent parts of the United States of America. Geological Survey of Canada, Open File 1565.

Wheeler, J. O., Brookfield, A. J., Gabrielse, H., Monger, J. W. H., Tipper, H. W., and Woodsworth, G. J. (compiler), 1991, Terrane map of the Canadian Cordillera. Geological Survey of Canada Map 1713A, scale 1:2 000 000.

Whittaker, P. J., 1982, Chromite occurrences in ultramafic rocks in the Mitchell Range, British Columbia. *In* Current Research. Part A, Geological Survey of Canada, Paper 82-1A p. 239-245.

Whittaker, P. J. and Wadkinson, D. H. 1981, Chromitite in some ultramafic rocks of the Cache Creek Group, British Columbia, *In* Current Research. Part A, Geological Survey of Canada, Paper 82-1A p. 239-245.

Whittaker,P. J., D. H. Wadkinson, 1983, Origin of chromite in dunitic layers of the Mt. Sydney-Williams ultramafic rock complex, British Columbia, in M. J. Gallagher, ed., Metallogeny of basic and ultrabasic rocks. Institute of Mining and Metallurgy, London p. 217-228.

Wilson, A. H., 1982. The geology of the Great 'Dyke', Zimbabwe: the ultramafic rocks. Journal of Petrology, v. 23, p. 240-290.

# CHAPTER 5

# DIAGENESIS AND PORE WATER EVOLUTION IN GROUNDHOG COALFIELD STRATA, NORTHERN BOWSER BASIN

## ABSTRACT

Pore water evolution in the northern Bowser Basin of Brititsh Columbia has been studied by integrating data from sandstone cement paragenesis, mudstone concretion geochemistry, and organic maturation. This study suggests that diagenesis in shallow marine, deltaic, and coastal plain siliciclastic sediments such as occur in the northern Bowser Basin can be explained by the interaction of seawater moving through sandstones mixing with acid waters derived from dewatering of interbedded organic rich muds. Sandstones examined in this study are chert and volcanic lithic arenites and wackes derived from island arc and sea floor terranes.

Sandstone cement paragenesis includes seven discrete cement stages. From earliest to latest the cement stages are: 1) pore lining chlorite; 2) pore lining to pore filling illite; 3) pore filling kaolinite; 4) oil migration through some of the remaining connected porosity; 5) quartz cement; 6) chlorite dissolution; and 7) calcite cement. These seven stages of cement record pore water evolution (in the sandstones), which is interpreted as an advection controlled process. Pore water chemistry interpreted from the cementation history suggests seawater was the initial pore fluid. Seawater composition changed during transport through the sandstones, first by loss of $Mg^{2+}$ and $Fe^{2+}$ to chlorite precipitation (stage 1). Dewatering of interbedded organic rich mudstones probably added $Mg^{2+}$ and $Fe^{2+}$ to partially buffer the loss to chlorite cementation. Acids produced during breakdown of organic matter mixed into sandstone pore fluids due to further compaction of the muds, leading to reduction of initial alkalinity. Reduction in alkalinity, in turn, favors change from chlorite to illite precipitation (stage 2), and finally to kaolinite (stage 3). Pore waters reached their peak acidity at the time of oil migration (stage 4). Chlorite dissolution (stage 5) and quartz precipitation (stage 6) occurred when pores were filled by these acid fluids. Fluid inclusions in fracture filling quartz cements contain petroleum, high-pressure methane, and

methane-rich aqueous solutions. Homogenization temperatures from primary two phase inclusions are consistent with quartz cementation during progressive heating between approximately 100° and 200°C. Following quartz precipitation, alkaline pore waters were re-established, as evidenced by late stage calcite cementation (stage 7).

Mineralogy of mudstone concretions is mostly siderite and ferroan dolomite, consistent with formation in the methanogenic zone of early diagenesis in organic rich siliciclastics. C isotope ratios range from +1 to +5 per mil, consistent with formation during later rather than earlier methanogenesis. O isotope ratios suggest precipitation from initial meteoric to brackish waters at least as depleted as -10 per mil SMOW, although the possibility of later re-equilibration cannot be eliminated.

Pore water evolution in the mudstones is interpreted as a diffusion controlled process, with initial fluids dominated by meteoric waters from a cool, temperate climate. Organic diagenesis leads to high dissolved carbonate in the muds. Carbonate combined with $Fe^{2+}$ and $Mg^{2+}$ presumably derived, at least in part, from dissolution of mafic minerals.

Organic maturation, as measured by vitrinite reflectance, records steep paleogeothermal gradients, and high maximum basin temperatures. Forward modelling suggests that the steep thermal gradients and high maximum temperatures were sufficient to account for the interpreted pore water history. The modelling fits best with paleogeothermal gradients of 60° to 65°C/km. Such high geothermal gradients suggest the Bowser Basin accumulated above oceanic crust in a back-arc basin.

## INTRODUCTION

Diagenesis of siliciclastic rocks is controlled by temperature, solute characteristics and, to a lesser degree, pressure of the contained pore fluids. Temperature, pressure, and solute characteristics in turn relate to sediment and basin geologic history. Analysis of diagenetic effects with the goal of recovering information about the pore fluids is, therefore, a potentially powerful approach to understanding the origin and development of siliciclastic basins. Unfortunately, the complexity of pore fluids makes

unambiguous determination of temperatures and solute characteristics difficult. Ambiguity in diagenetic interpretations can, however, be reduced by integrating observations and analyses from multiple lines of evidence.

Three lines of diagenetic evidence used in the diagenetic study described in this chapter are sandstone cement paragenesis, mudstone concretion geochemistry, and organic matter maturation. Each of these data sets records a different aspect of diagenesis in a siliciclastic succession. Sandstone cement paragenesis, for example, records changing compositions of pore fluids controlled by advection, and may allow inferences regarding depositional conditions and later tectonic or metamorphic events. Mudstone concretion geochemistry, in contrast, records conditions of pore fluids that are dominantly affected by diffusion processes, and may allow inferences about depositional processes and organic matter content. The diagenesis of organic matter, which is primarily controlled by thermal exposure after burial, permits inferences concerning the maximum temperatures affecting sediments.

The siliciclastic succession examined is the Bowser Basin, which is one of a series of Jura-Cretaceous intermontane basins in the Canadian Cordillera. Methods employed in this study include petrographic and geochemical study of sandstone paragenesis and mudstone concretions, and vitrinite reflectance studies of organic matter. The various diagenetic observations are integrated to form the basis of a basin maturation model which is described in a later section. This model has implications to the depositional history and tectonic development of the Bowser Basin and other sedimentary basins of the Canadian Cordillera. These implications are discussed in the final section of this chapter.

## SANDSTONE CEMENT PARAGENESIS

Different mineralogies of cement precipitate in response to changing composition, temperature and pressure of the pore fluids. The paragenetic sequence for cements described herein has been established by petrographic examination of representative samples collected from all stratigraphic horizons exposed in the study area. Examined samples include very fine, fine and medium grained sandstones. Original depositional textures and cement paragenesis are obscure in most samples, which are severely compacted. Rare samples in which abundant early cementation has occurred, however,

preserve depositional textures and cement paragenesis. The paragenetic sequence described below is based on examination of mostly medium grained sandstones in which intergranular cements are exceptionally well preserved. More severely compacted sandstones were excluded from consideration during initial establishment of the paragenetic sequence. Following establishment of the paragenetic succession, more severely compacted sandstones were then examined, and importantly, did not contradict the established paragenetic sequence. The sandstone cement paragenetic sequence is summarized below (Fig. 5-1). A more detailed description of each cementation stage and its implied pore water condition follows this summary.

1) Isopachous chlorite cement formed on grain surfaces. Crystals are 10 to 25 $\mu$m long, and line pores in continuous coats with individual crystals oriented perpendicular to the grain surface.

2) Illite cement occurs as pore-lining or pore-filling cement inside some pores earlier lined by authigenic chlorite.

3) Kaolinite cement occurs as pore-filling cement in some sandstones previously lined by chlorite, illite, or both chlorite and illite.

4) Pore filling reservoir bitumen ("dead oil"), as determined by micro-Fourier transform infrared analysis, occurs in some chlorite lined pores.

5) Chlorite dissolution follows oil migration in sandstones that still have interconnected porosity. Chlorite dissolution is either partial or complete, and is in part contemporaneous with quartz cement (see below).

6) Quartz cement occurs as syntaxial overgrowths, or micro- and macro-crystalline pore filling cements. Macro-crystalline quartz cement fills fractures during this stage.

Figure 5-1: Stages of sandstone cementation in the northern Bowser Basin.

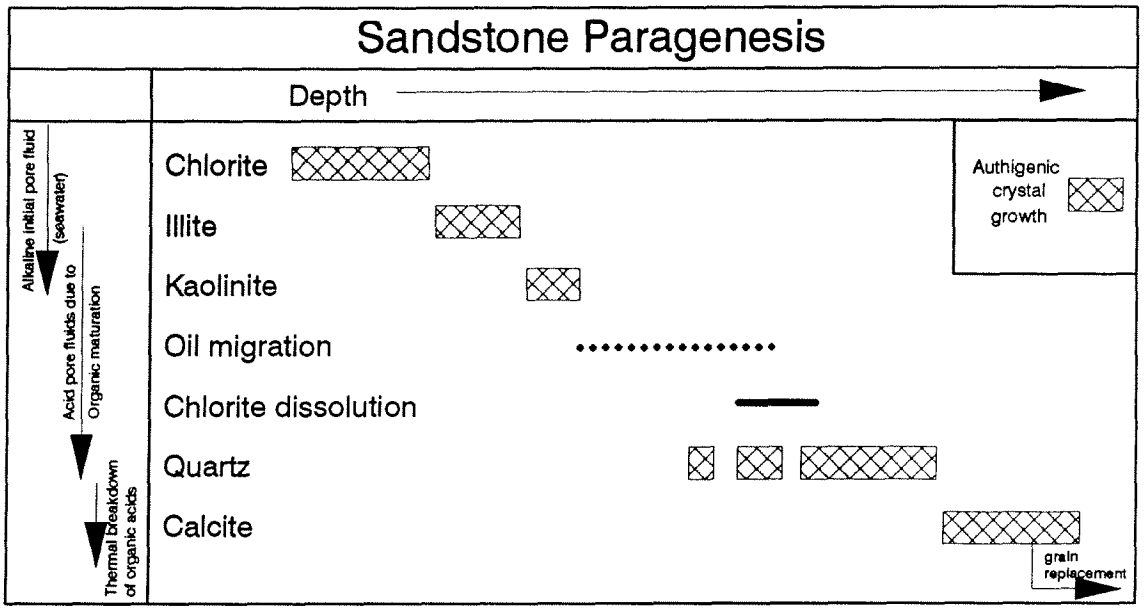

Hydrocarbon fluid inclusions in fracture filling quartz cements indicate that oil migration in part was contemporaneous with the quartz cementation stage.

7) Calcite occurs as a late stage pore filling cement, commonly with poikilitic texture, and as late stage grain replacement cement. Calcite also fills fractures, either alone or as a successor to earlier quartz cement in (presumably) reactivated fractures.

Not all of the stages of cementation summarized above occur in a single sandstone, but the order of the cements is consistent throughout the examined sample suite. For example, the combination of isopachous chlorite and calcite is present only in some thin sections, but where present, the chlorite cement always precedes the calcite. Similarly, reservoir bitumen never precedes chlorite cement, and quartz cements consistently post-date both chlorite and reservoir bitumen. Calcite never precedes quartz, reservoir bitumen, or chlorite cements.

Although cement stages are never observed out of order, some cement stages are commonly absent from particular sandstones. For example, isopachous chlorite cement is only rarely followed by reservoir bitumen, and is more commonly followed by calcite cement. Observed cement stages may vary across individual thin sections. For example, chlorite cement may have formed isopachous coats that completely occlude some pore throats, and in those pores no subsequent cementation or dissolution occurred. Elsewhere in the same thin section, pore throats were not completely blocked, and chlorite dissolution occurred. Subsequent calcite cement in such samples occurs either directly on grain surfaces, or upon a partially formed coat of chlorite, depending on the extent of chlorite dissolution.

The paragenetic sequence listed above is an ideal sequence of diagenetic stages that is more complete than the cementation record preserved in any individual sandstone. By considering all the cement stages listed above together, however, a more complete record of pore water evolution can be derived. The petrographic appearance of each cementation stage is described below, and the pore water chemistry implied by each stage is discussed in the following section.

## *CHLORITE CEMENTATION STAGE*

Chlorite cement forms continuous isopachous coats as much as 25 $\mu$m thick, of light green to yellow-green (transmitted light) crystals oriented perpendicular to grain surfaces (Fig. 5-2). The cements form regardless of substrate composition, as demonstrated by equal thickness of cements around grains irrespective of mineralogy. In some pores, chlorite has clearly grown out into the pore space and crystals display regular crystal shape. In other pores, although crystal orientation remains perpendicular, the interior surface of the chlorite cement is irregular, suggesting subsequent dissolution by pore waters. Chlorite cements subjected to later dissolution are commonly very thin in parts of a thin section, and may be altogether absent in still other parts where dissolution was apparently complete.

Chlorite cement forms early, as demonstrated by its formation directly on grain surfaces, and isopachous habit which implies growth into empty pore space. However, some compaction preceded chlorite cementation, as evidenced by the common occurrence of long grain contacts, and general lack of tangential contacts.

Pyrite framboids occur rarely in association with isopachous chlorite cements of the northern Bowser Basin. In some samples, the framboids are clearly located against grain surfaces and therefore, in those samples at least, preceded chlorite cementation (Fig. 5-3). Pyrite framboids are well known to form soon after burial (c.f. Gautier and Claypool, 1984) in response to the low oxygen-high sulfate pore conditions characteristic of the sulfate reducing zone (Berner, 1980). Such conditions are usually restricted to the upper few metres of organic rich sediments (Gautier and Claypool, 1985). The association of chlorite cement with pyrite framboids supports early formation of the chlorite.

### *Chlorite cementation stage pore water chemistry*

Precipitation of chlorite cement during the earliest sandstone cementation stage has implications regarding initial pore fluid composition. Laboratory experiments demonstrate that

Figure 5-2: Authigenic chlorite coats on sandstone clasts of varying compositions in plane polarized light. Qtz= quartz; VRF= volcanic rock fragment; Ch= chert. Scale bars are 50 $\mu$m.

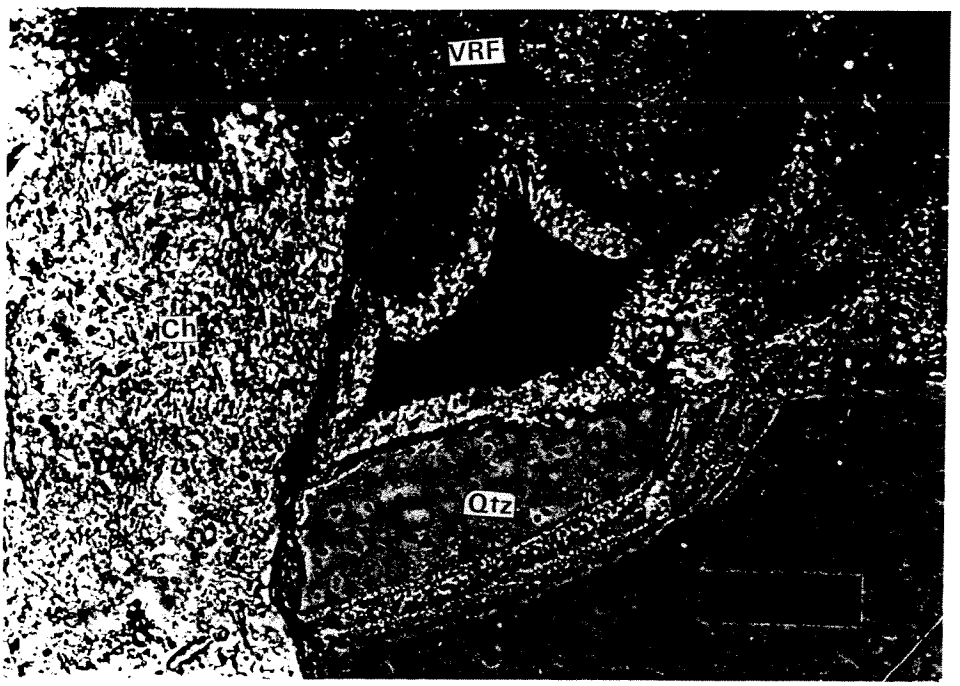


Figure 5-3: Sketch of a microscope view of isopachous chlorite cement with earlier pyrite framboids. After the chlorite cementation stage, compaction of the pore space caused the chlorite cement to break away from parts of the grain surfaces. In the top left quadrant, 60 $\mu$m of overlap in the chlorite cement occurs (in the form of a small reverse fault). In the lower right quadrant, compression of the pore space caused the chlorite cement and pyrite framboids contained within it o fold out from the grain surface into the remaining pore space. Pore-filling poikilitic calcite cement precipitated after the chlorite cementation stage. A and B are optically distinct crystals that both continue beyond the illustrated pore space.

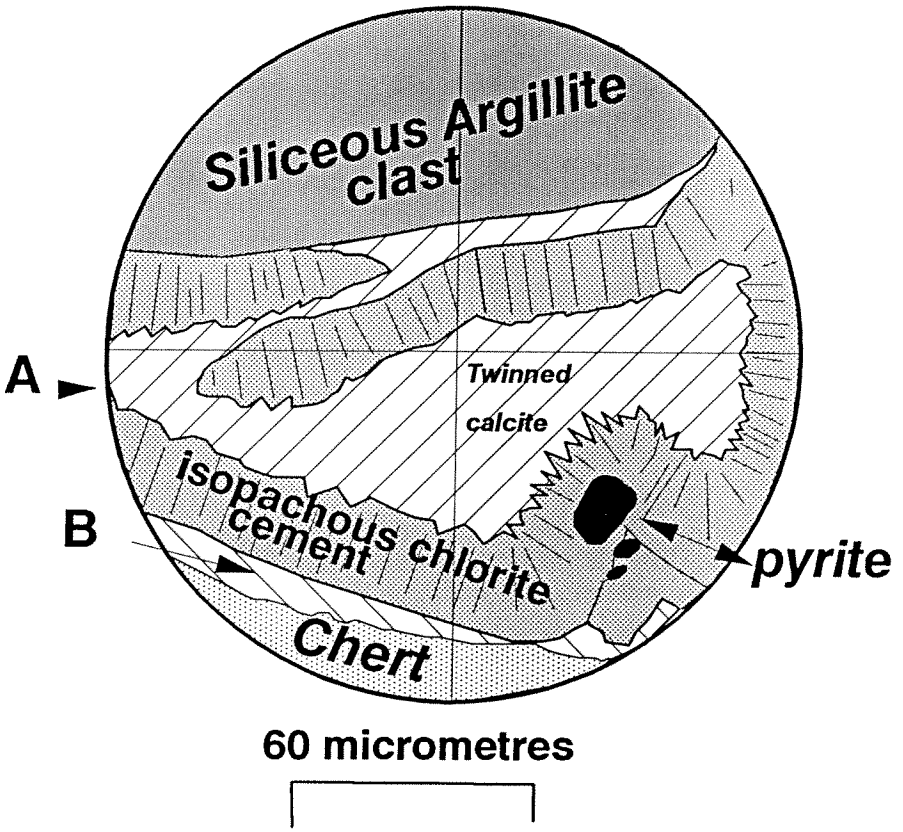

precipitation of chlorite cement requires pore solutions enriched in $Fe^{2+}$ and $Mg^{2+}$ (Small *et al.*, 1992). $Mg^{2+}$ activities must be relatively high or precipitation of other authigenic clays (illite or kaolinite) is favoured (Fig. 5-4; Jahren and Aagaard, 1989). In addition, chlorite precipitation suggests basic waters, because chlorite is unstable when exposed to warm acidic solutions (Foscolos, 1985). This instability is demonstrated in the laboratory by the common use of weak acid at 80° to 100°C to remove chlorite from clay mineral mixtures in order to facilitate XRD identification of clay minerals (Foscolos, 1985), and in oil fields by the success of injection of weak acids in dissolving chlorite cements (Almon and Davies, 1981). The relationship of chlorite stability to $H^+$ activity is shown quantitatively in the phase diagram in figure 5-4 (Jahren and Aagaard, 1989). The most likely source of large volumes of basic water is seawater, which is typically buffered between pH 8.0 and 8.4 (Brownlow, 1979), and chlorite cements are commonly associated with marine or brackish water deposits (Thomas, 1981). Normal seawater is also a source of abundant $Mg^{2+}$. $Fe^{2+}$ is not abundant in seawater, but concentrations rise near the mouths of major rivers, as demonstrated by the tendency of iron-rich green marine clays to precipitate in shallow marine waters near river mouths (Odin and Masse, 1988). Another potential source for both $Fe^{2+}$ and $Mg^{2+}$ ions is the breakdown of Fe-Mg silicates. A combination of river and Fe-Mg silicates sources probably contributed solutes to Bowser Basin pore waters because the sediments were derived in part from erosion of mafic and ultramafic rocks (Chapters 3 and 4), and were deposited in shallow marine, deltaic, and fluvio-deltaic settings (Chapter 2).

Temperatures during formation of chlorite cements can be constrained only within a broad range. Textural evidence in this study demonstrates that chlorite cementation occurred early, and therefore temperatures must have been relatively low. Compacted textures in chlorite cemented sandstones, however, suggest that precipitation did not initiate immediately following deposition. Initial temperatures of formation were therefore somewhat elevated from depositional temperature and therefore were probably above 15° to 25°C. An upper end to the chlorite cementation temperature range of roughly 80° to 100°C is implied by subsequent oil migration (see discussion under oil migration heading later). Chlorite precipitation is also limited by the production of acid waters due to the maturation

Figure 5-4: Phase diagram showing that chlorite precipitation is favoured by relatively high Mg2+ and low H+ activities in solution compared to illite or kaolinite. After Jahrens and Aagaard (1989).

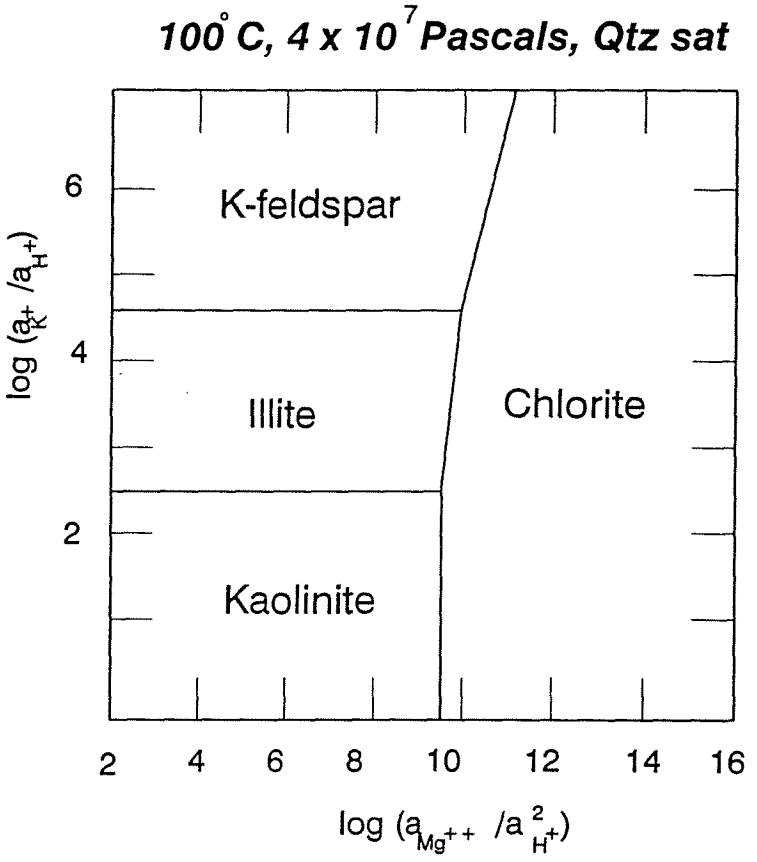

of organic matter, which initiates and peaks at approximately 80° to 100°C (Surdam and Crossey, 1985; Surdam and MacGowan, 1987). In summary, the pore water chemistry deduced for the chlorite cement stage implies a basic, $Mg^{2+}$ and $Fe^{2+}$ rich solution at temperatures above 15° and below about 90°C. Such a pore fluid is compatible with derivation from normal seawater that has elevated $Fe^{2+}$ and (perhaps) $Mg^{2+}$ concentrations.

The interpreted temperature range (above 15°C and below 90°C) is reasonable based on precipitation temperatures of authigenic chlorite reported in the literature. Examples from the literature include clays structurally similar to chlorite which precipitate in warm shallow seas at the sediment water interface (Odin and Masse, 1988), and authigenic chlorites from the North Slope of Alaska that formed in sandstones never exposed to temperatures greater than approximately 60°C (Smosna, 1988). In these North Slope sandstones, chlorite cementation precedes quartz overgrowths and later calcite pore-filling cements (Smosna, 1988). Further examples include subarkoses and sublitharenites of the Spindle Field, Colorado, that contain a similar sequence of early chlorite cement followed by quartz and then calcite cements (Pittman, 1988). Authigenic chlorites formed between 70° and 160°C also have been described from the North Sea by Jahren and Aagaard (1989).

### *ILLITE CEMENTATION STAGE*

Illite occurs as either a pore lining or pore filling cement in some chlorite cemented sandstones. Illite is distinguished from chlorite in thin section by lack of green color in plane polarized light and higher birefringence in cross polarized light, and in SEM analysis by characteristic filamentous and ribbon-like crystal shapes of illite. Energy dispersive spectrometry of the wavy pore-filling cements confirms the occurrence of $K^+$ and lack of $Mg^{2+}$ which supports the mineral identification as illite.

Textural relationships demonstrate that illite consistently forms following chlorite cementation. Some samples with illite also contain later pore-filling quartz cement, but illite has not been noted in any sample with reservoir bitumen. Illite, therefore, follows chlorite cement and precedes quartz cement.

*Illite Cementation Stage Pore Water Chemistry*

Illite precipitation is favoured over chlorite under conditions of higher $H^+$ activity and lower $Mg^{2+}$ activity (Fig. 5-4; Jahren and Aagaard, 1989). As shown by the phase diagram in figure 5-4, $K^+$ activity need not increase to move a fluid from the chlorite stability field to either the illite or kaolinite stability fields. Illite cementation following chlorite can be explained by a relatively simple model of pore water evolution. Some combination of lowering $Mg^{2+}$ concentrations and increased acidity is all that is required. Assuming that seawater was the starting pore fluid as inferred above, $Mg^{2+}$ concentration should be reduced as a direct result of chlorite cementation. As formation temperatures rise due to continued burial, the alkaline character of normal seawater should become more acidic due to production of organic acids associated with organic maturation. $K^+$ originally present in seawater is subsequently available to precipitate as authigenic illite.

Illite precipitation may be limited by $K^+$ available from seawater, because the provenance of northern Bowser Basin sandstones does not favor increasing $K^+$ concentrations in the pore fluids (Chapters 3 and 4). Bowser Basin provenance consists of largely unmetamorphosed oceanic terranes, which generally lack many common $K^+$ bearing mineral phases such as K-feldspar or muscovite. $K^+$ bearing phases in Bowser Basin sediments derived from those oceanic terranes are largely limited to uncommon biotite, and therefore only limited sources of $K^+$ are available to authigenic clays from origins other than seawater.

## *KAOLINITE CEMENTATION STAGE*

Authigenic kaolinite occurs in some Bowser Basin sandstones previously cemented by chlorite or illite. Kaolinite is recognized petrographically in this study based on its vermiform habit, and birefringence lower than illite. Kaolinite forms as pore filling cement inside pores already lined by chlorite or illite, which is strong petrographic evidence that kaolinite precipitation occurred subsequent to illite or chlorite cementation. Kaolinite is also commonly associated with reservoir bitumen in the pores, which is consistent with kaolinite precipitating after the illite cementation stage described above, and

prior to or contemporaneous with the oil generation and migration stage described below.

### *Kaolinite Cementation Stage Pore Water Chemistry*

Kaolinite precipitation is the next stage in the evolution of pore water that began as seawater, and subsequently precipitated first chlorite and then illite. Pore water in this evolutionary process first loses $Mg^{2+}$ and $Fe^{2+}$ during chlorite precipitation, and then $K^+$ during illite precipitation. Acidity in the pore waters increases simultaneously, due to creation of organic acids associated with the breakdown of organic matter. The trends of decreasing $Mg^{2+}$ and $K^+$ combine with increasing $H^+$ activity and together lead to pore water conditions favouring kaolinite precipitation (Fig. 5-5).

## *OIL MIGRATION STAGE*

Opaque pore filling material occurs in some pores and fractures that were earlier lined with isopachous chlorite cement. Micro-Fourier transform infrared analysis (mFTIR) demonstrates that the opaque material is reservoir bitumen (dead oil) that has lost most of its aliphatic components (probably due to post-migration thermal degradation; Fig. 5-6). The oil migrated into pores which were already lined with thick coats of chlorite cement (Fig. 5-7a), indicating that oil migration followed chlorite cementation, but preceded any significant chlorite dissolution. Reservoir bitumen also occurs in fractures in some northern Bowser Basin mudstones (Fig. 5-7b), including fractures in silicified wood, where hydrocarbons are preserved in fluid inclusions in quartz cements, as described later.

### *Oil migration stage pore water chemistry*

Generation and migration of oil occurs as a result of organic maturation processes that are constrained to relatively narrow temperature ranges. Oil generation initiates after suitable organic matter has been exposed to sufficient heat for a sufficient length of time (thermal exposure), and

Figure 5-5: Three successive cements in Bowser Basin sandstones occur as a result of changing pore water chemistry described in this phase diagram from Jahren and Aagaard (1989). Pore water chemistry starts near position 1, with high $Mg^{2+}$ and relatively low $H^+$ activities, as expected for fluids derived from seawater. Reduction in $Mg^{2+}$ activity due to chlorite cementation, and increase in dissolved acids derived from processes of organic matter maturation shift pore water chemistry towards position two, as recorded by precipitation of illite subsequent to chlorite (see text for descriptions). Position three is reached in some pores, where kaolinite is precipitated following or contemporaneous with oil migration.

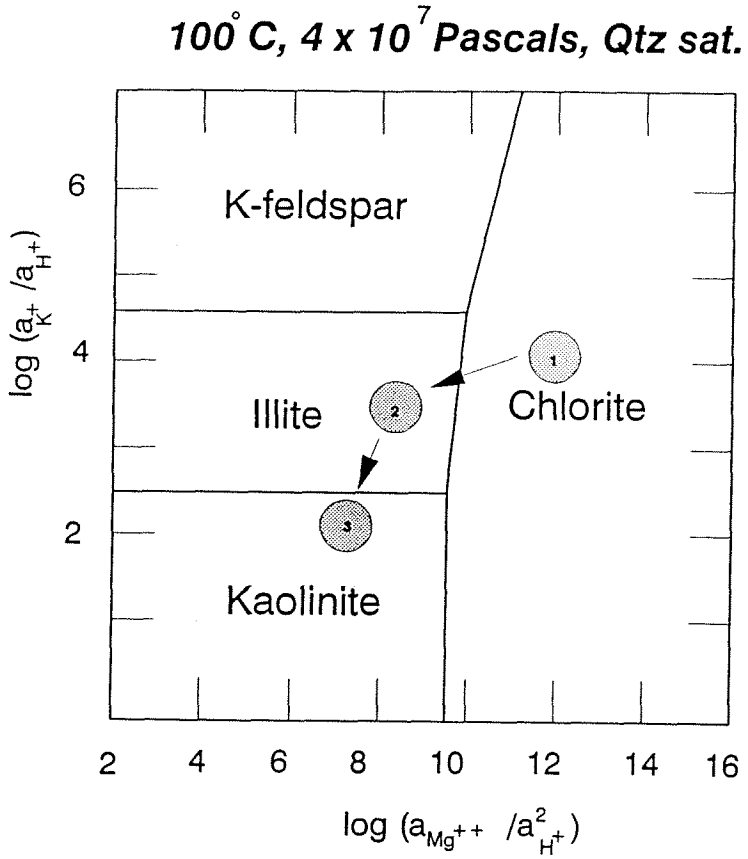

Figure 5-6: Micro-Fourier transform infrared analysis plots of opaque material in pores and fractures of Bowser Basin sandstones demonstrates that the material is organic matter with very low aliphatic component. Loss of aliphatics is typical of dead oil, otherwise referred to as reservoir bitumen.

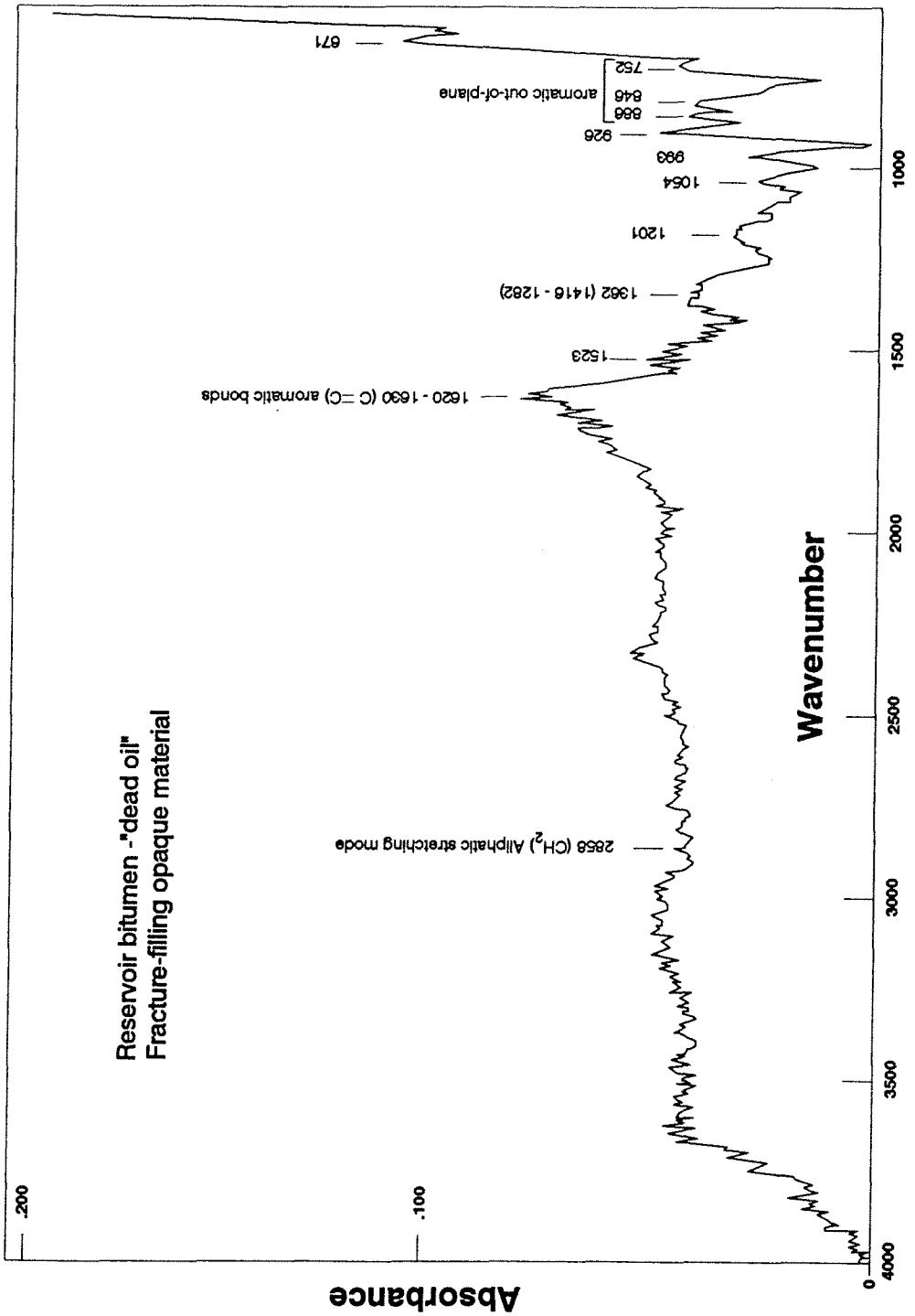

Figure 5-7: Chlorite cemented sandstone saturated with reservoir bitumen: a) oil in intergranular porosity; b) oil in chlorite cemented microfracture. Scale bars are 100 $\mu$m.

intense oil generation initiates between temperatures of approximately 60° to 130°C (Hunt, 1979). Oil generation is essentially complete in most sediments at temperatures below 150°C (Hunt, 1979), although light oil, condensate and methane production commonly continues to 180°C (Tissot and Welte, 1984). Vertical oil migration may cause the hydrocarbons to move into cooler sandstones, but it seems reasonable to assume that the oil migration stage occurred at temperatures of approximately 90° to 130°C. The chlorite cementation stage occurred entirely prior to oil migration and can be restricted, therefore, to temperatures below approximately 80° to 90°C. Illite and kaolinite precipitation follow chlorite cementation in some pores and probably occur simultaneously with initial oil migration as pore waters became less alkaline. Textural observations are consistent with such an interpretation because some chlorite lined pores are filled with illite that is dark brown in plain polarized light, suggesting that the illite is coated by migrating oil. Overlap of oil migration with illite and kaolinite precipitation is chemically reasonable because illite, kaolinite, and oil migration are all associated with increasingly acid pore water conditions (Carothers and Kharaka, 1978; Jahren and Aagaard, 1989).

### *CHLORITE DISSOLUTION STAGE*

Chlorite cement dissolution is evident in many northern Bowser Basin sandstones. The clearest evidence for chlorite dissolution is observed in thin sections in which some pores are completely occluded with thick isopachous chlorite cements, whereas pores elsewhere in the same thin section completely lack (or have only thin) chlorite cements. Such sandstones are interpreted to have experienced an early stage of chlorite precipitation that closed some pores completely, but left other pores partially open. Acidic waters subsequently moved through the remaining connected pores, leading to dissolution of chlorite cement. Dissolution could not occur in pores that were completely occluded during early chlorite cementation, presumably because acid waters could not permeate through the blocked pore spaces. The result is that some pores are filled with chlorite and other pores in the same sandstone lack chlorite altogether. Chlorite dissolution occurred prior to quartz and calcite cementation, because both quartz and calcite cements occur in pores with all or part of the earlier cement removed.

Quartz occurs rarely as the final pore filling cement inside a reservoir bitumen coating which is in turn inside pore-lining isopachous chlorite cement (Fig. 5-8). Some of these pores that contain chlorite, reservoir bitumen, and quartz cements are missing continuous chlorite coats. Incomplete chlorite coats are unusual, and only occur where quartz is present in addition to reservoir bitumen. This relation of quartz with incomplete chlorite coats implies chlorite dissolution occurred after oil migration, but before or at the same time as quartz cementation.

### *Chlorite dissolution stage pore water chemistry*

The inference of basic waters for the chlorite cementation stage described earlier suggests a simple and plausible explanation for the chlorite dissolution stage: the pore waters change from basic to acidic. Such a change to acidic conditions continues the trend of decreasing alkalinity inferred for the illite, kaolinite, and oil migration stages described above.

## *QUARTZ CEMENTATION STAGE*

Quartz cements occur as syntaxial overgrowths and micro- or megacrystalline pore-filling cements. Quartz overgrowths in some pores form smooth crystal faces, and rarely grow into pore-filling cements. Micro- or megacrystalline textures appear to depend at least in part, on the substrate. Megacrystalline quartz cements tend to form either on coarsely crystalline quartz grain surfaces, or on other earlier cements. The coarsely crystalline quartz cements tend to be clear and contain only rare and small fluid inclusions. Micro-crystalline pore-filling quartz cements generally occur in contact with chert grains.

The relative timing of the quartz cement stage is interpreted petrographically from the observation that quartz cement occurs in some pores inside thick isopachous chlorite cements. As mentioned earlier, quartz also rarely occurs upon reservoir bitumen lined isopachous chlorite

Figure 5-8: Authigenic quartz fills a pore lined first by isopachous chlorite cement and then coated by oil. This relation demonstrates that quartz cementation followed oil migration in the sandstones. Chlorite cement in this field of view is irregular, suggesting chlorite has been partially dissolved. Partially to completely dissolved chlorite cements are commonly closely associated with quartz cements, suggesting that the acid conditions favouring quartz cementation lead to dissolution of chlorite. Scale bar is 50 $\mu$m.

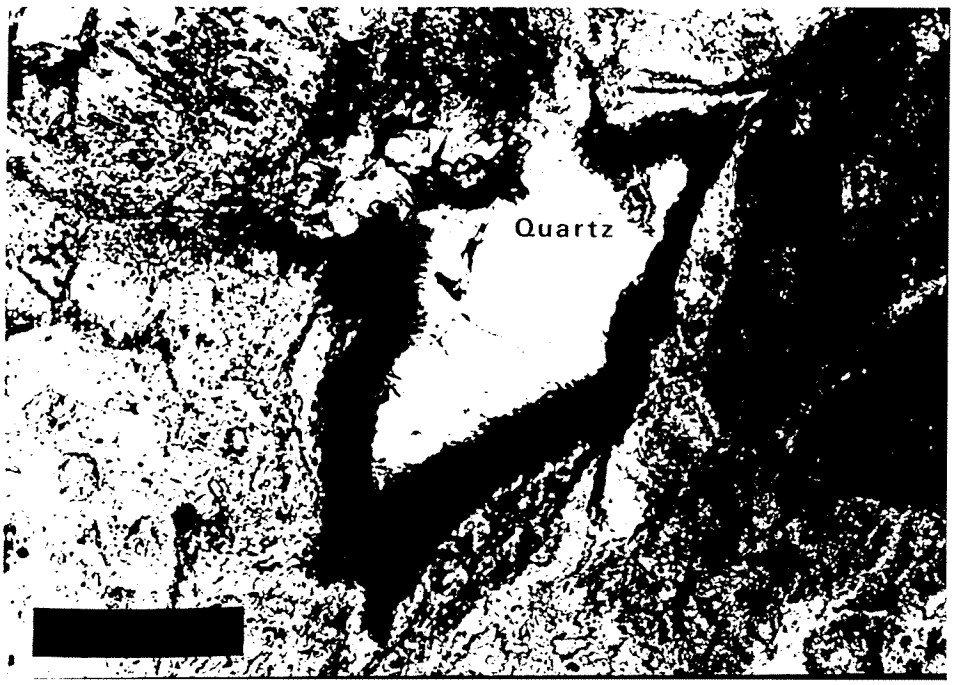

grain coats. In fractures containing both quartz and calcite cements, textural relations consistently indicate quartz cementation preceded calcite cementation. Quartz cementation, therefore, followed oil migration, and preceded calcite cementation.

*Fluid inclusions in fracture-filling quartz cements*

Quartz cements occur in fractures as well as in sandstone pore spaces. Fluid inclusions preserved in the fracture-filling cements are larger and more varied than those in pore-filling cements. Quartz crystals as large as 7 cm across occur in some fractures, and some contain fluid inclusions up to 10 $\mu$m (although rarely greater than 5 $\mu$m) in largest dimension. Observations of fluid inclusions in fracture filling quartz cements provide independent constraints on pore fluid composition and evolution.

Crushing quartz fracture filling cements releases abundant bubbles. The large size and abundance of bubbles demonstrates that high pressure gas is contained in some of the fluid inclusions. Solubility characteristics of the bubbles are useful for qualitative identification of contained gas phases (Roedder, 1974). The bubbles persist in immersion oil, but they dissolve rapidly in kerosene. Dissolution in kerosene is rapid for bubbles less than 5 $\mu$m in diameter, and takes less than two seconds for bubbles up to 10 $\mu$m in diameter. Larger bubbles with lower surface area to volume ratios dissolve more slowly until they reach diameters less than 10 $\mu$m, at which point they disappear rapidly. Relating bubbles to individual source inclusions is difficult. However, growth zones with many primary single phase, dark gray gas filled inclusions commonly release large numbers of bubbles. In one such growth zone, a large, dark grey single phase inclusion with an irregular shape formed a bubble that dissolved rapidly. Bubbles also appear when crushing zones of two phase, liquid-rich inclusions, and after crushing the formerly two phase inclusions are single phased, suggesting that the bubbles released originated as the vapor phase of the two phased inclusions.

Quartz cement from fractures in silicified wood, which is common in fine grained facies, was examined petrographically and on a USGS-type heating and freezing stage. Silicification of the wood began early, as demonstrated by the uncrushed cell walls and fine cellular detail preserved in the wood.

Early silica cementation within fossil wood cells probably depends on chemical conditions related to biogenic degradation within the cell spaces, and those chemical conditions may be largely unrelated to pore water conditions in associated sandstones (Hesse, 1990). Subsequent to the earliest, intercellular cements, however, quartz fracture filling cement formed, which are likely related to advection of pore fluids. This cement precipitated in a distinct succession of layers that becomes relatively younger towards the middle of the fracture. The earliest fracture filling cements occur on fracture walls, and have well shaped crystal faces projecting into the fractures. Fluid inclusions in this early fracture fill cement are generally small, and include both clear, single phase aqueous inclusions, and yellow-brown to dark brown coloured (Fig. 5-9a) one or two phase hydrocarbon inclusions (aqueous inclusions are almost always clear, and brown inclusions are almost certainly hydrocarbons; Roedder, 1974). Opaque reservoir bitumen ("dead oil") covers the interior crystal face surfaces of some of these early quartz crystals (Fig. 5-9b).

A younger phase ("medial phase") of quartz cement occurs inside the earliest fracture cement. This medial phase consists of several layers of quartz crystals which contain two phase aqueous inclusions with irregular to smooth shapes, some of which occur in distinct growth zones. In one primary growth zone, homogenization temperatures ($T_h$) for two phase aqueous inclusions with consistent liquid to vapour ratios (L/V) were measured by temperature cycling. Nine such inclusions from the same growth zone, each less than 3.5 $\mu$m in diameter with smooth but irregular shape and containing "dancing" bubbles, yielded $T_h$ between 90.5° and 97.3°C (plus or minus 1.5°C). Due to the small size of the inclusions, final melting could not be directly observed, but reappearance and unhindered movement of the vapor bubble upon heating was determined by using a freeze/refreeze temperature cycling technique. Final melting ($T_m$) determined for the same set of inclusions yielded temperatures between +4.5° and +24.2°C (dropped to +22.8° in repeat run of highest $T_m$ inclusion). Because $T_m$ is above 0°C, final melting is assumed to be final melting of clathrate. A larger inclusion with apparently smaller L/V did not homogenize to much higher temperatures (+120°C), and therefore is assumed to have leaked. $T_m$ for this larger inclusion was +1.9°C, consistent with clathrate melting

under lower pressures than the smaller, consistent $T_h$ inclusions. Three fluid inclusions from another medial phase quartz crystal yielded less consistent $T_h$, but still suggestive of low temperature homogenization. $T_h$ for these three inclusion were between 92° and 102°C.

Single phase inclusions, which are gas filled based on their dark gray appearance`s (resulting from low refractive index; Roedder, 1974; 1984) also occur in medial phase quartz crystals. Some of these darker inclusions are clearly primary, and some that have irregular but smooth walled shape occur in the previously described growth zone along with the measured inclusions discussed above with consistent L/V and $T_h$. Single phase gas inclusions from other, probably later, primary growth zones have well developed negative crystal shapes. Late in the medial phase, many large irregular shaped primary hydrocarbon inclusions formed, apparently as a single event.

The youngest quartz cement in the examined fracture ("late stage") precipitated adjacent to the crystals containing the large hydrocarbon inclusions mentioned above, and consists of clear quartz. Late stage fluid inclusions include primary two phase aqueous inclusions with smooth walls, which tend to exhibit somewhat poorly developed negative crystal shape. Single phase gas inclusions with good negative crystal shapes are also common in the same growth zones. In one growth zone, primary, liquid-rich, two-phase, aqueous inclusions with consistent L/V ratios yielded $T_h$ between 141° and 162°C. The measured inclusions vary in shape from moderately irregular to negative crystal shape, and the two largest inclusions are over 7 $\mu$m in each dimension. Six primary two phase inclusions (negative crystal faces) from a different growth zone with apparently consistent L/V ratios yielded rather inconsistent $T_h$, ranging from 161° to 194°C.

*Fluid inclusion implications to pore water evolution*

Crushing quartz cements demonstrates that high pressure gas is abundant, and the gas is probably methane due to the bubbles' rapid solution into kerosene (Roedder, 1974). Many bubbles

Figure 5-9: a) Hydrocarbon fluid inclusions (see arrows) in a single crystal of quartz cement from a fracture in silicified wood. The inclusions formed in a single growth zone near the edge of this crystal, and are shown in a micrograph combining three successively deeper focus levels. The largest inclusions in the picture are 5 to 7 $\mu$m across; b) Hydrocarbon fluid inclusions, and opaque bitumen (arrows) between quartz crystal surfaces. Fracture is 175 $\mu$m wide in silicified wood.

emerged from zones with abundant single phase inclusions, and one bubble was observed to emerge from an individual dark gray single phase inclusion, which clearly indicates that the single phase inclusions contain methane. In addition, methane occurs pervasively in organic rich sediments, (Roedder, 1984; Hanor, 1987) which strongly supports the suggestion that the high pressure gas released during crushing is methane. Complete dissolution of even very large bubbles (formed by coalescence of many smaller bubbles) suggests that little or no $CO_2$ (or other gas species) is mixed with the methane. Although necking of inclusions at reduced temperatures can isolate vapor bubbles that were originally in solution, the occurrence of many single phase gas inclusions with good negative crystal shapes in the same primary growth zones as two-phase inclusions with consistent L/V ratios strongly suggests that methane was trapped both as a separate phase and in aqueous solution (Bodnar *et al.*, 1985). Observations of liquid-rich two phase inclusions during crushing were more ambiguous, but suggest that many (most or all) of the aqueous two phase inclusions probably also contain a high pressure methane vapor phase. Methane adds many difficulties to quantitative microthermometry measurements in fluid inclusions, including affecting melting temperatures of saline solutions and forming a clathrate that is difficult to see in very small inclusions (Hanor, 1980). However, the most serious difficulty is probably the potential for *in-situ* production of excess methane by post-trapping thermal breakdown of acids or hydrocarbons (Hanor, 1980). Valuable qualitative information is available, however. $T_m$ of aqueous solutions were +1.9° to +24.2°C, indicating formation of a methane clathrate. Consistent $T_h$ from medial phase primary inclusions suggests minimum trapping temperatures greater than 97°C. Less consistent $T_h$ from late phase cements suggest higher trapping temperatures, probably in excess of 161°C to 194°C.

### *Quartz cementation stage pore water chemistry*

Silica precipitation is favoured by acidic pore waters (Friedman, *et al.* 1974; 1992). Increasingly acidic pore water conditions were established during oil migration as demonstrated first by the illite cementation stage and then the subsequent chlorite dissolution stage. The quartz cementation stage in sandstones follows chlorite dissolution and may be explained as a simple continuation of the trend of increasingly acidic pore water conditions. The temperature range for the quartz cementation

stage is constrained at the low end by temperatures attributed to the onset of oil generation/migration, and the generation of pore water acidity probably occurred between 80° to 130°. Primary hydrocarbon inclusions demonstrate that fracture filling quartz cements in silicified wood precipitated in part contemporaneously with oil migration. The fluid inclusions also demonstrate the occurrence of abundant methane in the pore waters, both as a separate gas phase and in solution in aqueous fluids. $T_h$ for selected primary two phase inclusions suggests that quartz formed contemporaneously with oil migration formed at temperatures near 100°C. Late quartz formed after oil migration, probably at temperatures closer to 200°C ($T_h$ between 141° and 194°C: minimum trapping temperatures higher dependent on pressure correction). Organic acids are destroyed by thermal reactions between 120° and 200°C, leading to loss of pore water acidity, and presumably terminating quartz cementation (Surdam and Crossey, 1985).

*CALCITE CEMENTATION STAGE*

Authigenic calcite occurs in pores and fractures as coarsely crystalline or poikilitic textured cement. Poikilitic crystals are up to several millimetres across, completely surrounding detrital grains, and are usually twinned. Textural relationships demonstrate that calcite formed after both chlorite and quartz cement stages. Calcite cementation appears to have continued to great depth in the northern Bowser Basin. Some sandstones from lower stratigraphic levels (undivided Bowser Lake Group and Currier Formation) are calcite cemented and replaced to such a degree that calcite forms more than 30% of the rock volume (visual estimate). In these sandstones, original depositional textures are obscured, but it appears that most of the calcite occurs as grain replacement and that replacement followed extensive compaction. Other sandstones from higher stratigraphic levels (upper McEvoy and Devils Claw Formations) commonly have extensive poikilitic calcite pore-filling cements. In contrast to the sandstones with extensive replacement cements from lower stratigraphic levels, the pore-filling cements preserve and visually outline the grain contacts. The grain contacts are dominated by pressure solution features, suggesting that calcite cements which occur in these pore-filling cements also followed significant burial. However, these sandstones are from the younger stratigraphic units and therefore were

never buried as deeply as those sandstones dominated by grain replacement calcite cements.

*Calcite cementation stage pore water chemistry*

Calcite precipitation as a late stage cement implies return of alkaline pore water conditions such as prevailed during the early chlorite cement. However, unlike the alkaline waters that led to chlorite cementation, pore waters during the late calcite cementation stage were probably not replenished by relatively unaltered seawater. $Mg^{2+}$ concentrations during the late stage calcite cementation were significantly lower than in seawater, because dolomite precipitation is thermodynamically favoured over calcite at elevated temperatures unless $Mg^{2+}$ concentrations are very low relative to $Ca^{2+}$ (Hardie, 1987). Pore filling calcite cementation is assumed to have initiated at temperatures near 200°C, because it followed quartz cementation which occurred up to at least 200°C. At such elevated temperatures, acids generated during organic maturation have been thermally broken down (Carothers and Kharaka, 1978). Calcite becomes less soluble with rising temperatures, and therefore late stage calcite precipitation is expected to continue as long as formation temperatures rise. Extensive late stage calcite grain replacement as experienced in the older strata supports the re-establishment of alkaline pore waters, because silica solution (necessary for silicate grain replacement) requires alkaline conditions (Friedman, *et al.*, 1974; 1992).

The source of the $Ca^{2+}$ is unclear. $Ca^{2+}$ could remain from connate seawater incorporated with the sediments during or shortly after deposition, and only during late stage diagenesis be able to precipitate with the return of alkaline pore water chemistry. Alternatively (or additionally), $Ca^{2+}$ could be released from minerals in the sediments. The provenance of the Bowser Basin sediments, which includes mafic and ultramafic rocks of oceanic and island arc origin (Chapters 3 and 4), suggests the sediments may have contributed to $Ca^{2+}$ in the pore waters. $Ca^{2+}$ occurs in plagioclase feldspar in such rocks, and is further taken up from seawater in large amounts during some types of hydrothermal alteration (Seyfried, *et al.*, 1988). Probably $Ca^{2+}$ is released from feldspars into pore fluids during late stage diagenesis in the Bowser Basin. A further potential source of $Ca^{2+}$ could be dissolution of

biogenic carbonate buried with the sediments. No primary carbonate beds have been identified within the Bowser Basin siliciclastic succession, and shelly fauna is rare to absent above the lower Currier Formation, and therefore this source of $Ca^{2+}$ is presumably relatively minor.

*SUMMARY OF PORE WATER EVOLUTION*

Sandstone pore water evolution in the northern Bowser Basin can be adequately described by interaction of three factors: 1) initial fluid composition dominated by seawater; 2) dissolution of unstable siliciclastic sediments leading to mobilization of Mg, Fe, Si, and Ca; and 3) organic matter maturation leading first to the production of acids and later to thermal breakdown of the acids. Interaction of these three factors results in evolution of pore water that can be described in four successive stages summarized in figure 5-10 and below:

Stage 1) Alkaline pore waters interact with mafic and ultramafic detritus in Bowser Basin sediments leading to elevated $Fe^{2+}$ and $Mg^{2+}$ concentrations. Precipitation of authigenic chlorite is favoured from these alkaline, Fe and Mg-rich pore waters at temperatures below approximately 90°C.

Stage 2) Pore waters become less alkaline due to breakdown of organic matter, leading first to illite precipitation, which depletes $K^+$ supplied from seawater. Kaolinite precipitation occurs following $K^+$ depletion in sandstones that have not been completely occluded by pore filling cements.

Stage 3) Pore waters become increasingly acidic as a result of continued generation of organic acids. Oil migration, chlorite dissolution and quartz

Figure 5-10: Four stages of pore water chemistry shown as a function of changing cation concentrations due to rock-water interactions, and alkalinity due to organic maturation.

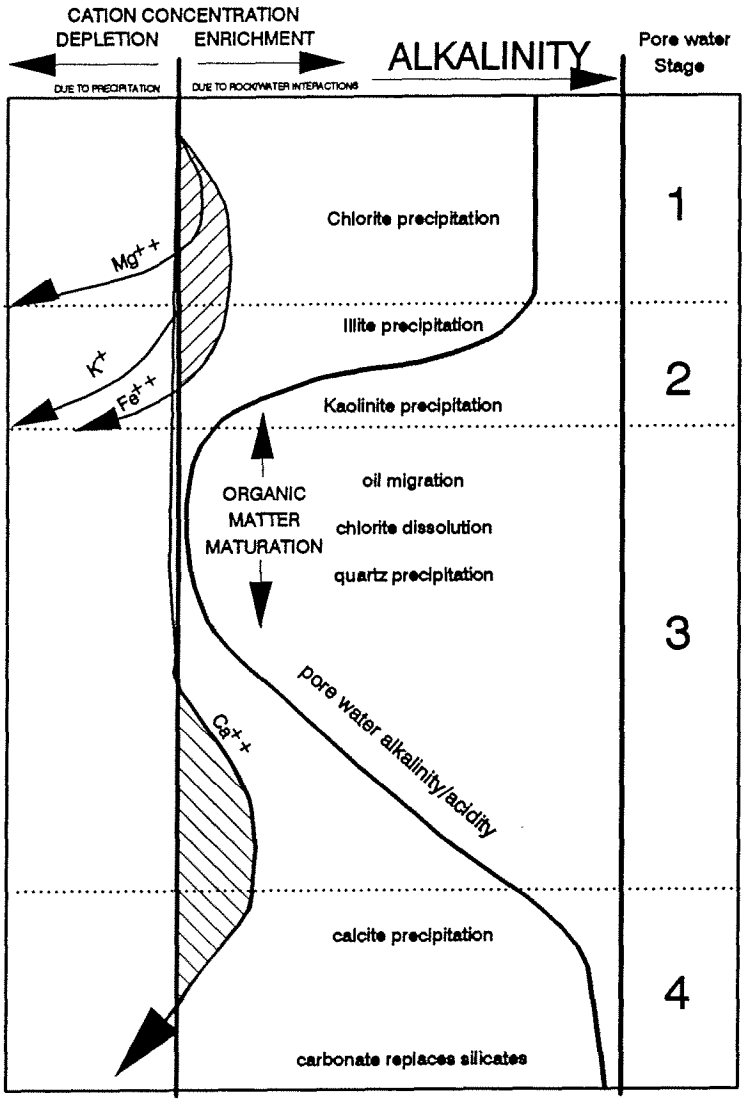

precipitation occurred under these acid water conditions. Acid waters probably initiated at temperatures between approximately 80$^{o}$ and 130$^{o}$C, and persisted to temperatures near 200$^{o}$C.

Stage 4) Pore water acidity is eliminated due to thermal degradation of organic acids. Thermal breakdown of organic acids in oil field waters begins at approximately 120°C, and is complete by approximately 200°C (Carothers and Kharaka, 1978). Calcite cementation follows re-establishment of alkaline pore waters at temperatures in excess of 200°C.

The four stages of pore water evolution described above record advection in Bowser Basin sandstones. When compaction and cementation combine to completely occlude pores, advection ceases and the record of sandstone cement paragenesis is terminated. As long as advection continues, replenishment of pore fluids is required. During the earliest stage of pore water evolution, replenishment was probably dominated by relatively unaltered seawater, which is the most likely source of large volumes of $Mg^{2+}$ and $K^{+}$ rich alkaline fluid. The later stages of pore water evolution, in contrast, are increasingly affected by dewatering of interbedded organic-rich mudstones. Mixing of waters derived from the mudstones with seawater is initially recorded by increasing acidity of pore waters. This increasing acidity leads to the succession of authigenic clay cements preceding oil migration. By stage three in the pore water evolution, waters derived from the mudstones clearly dominate advection through the sandstones. Stage four, however, records a return to more alkaline conditions, and may thus record re-establishment of external recharge by seawater or, perhaps more likely, meteoric waters as the dominant pore fluid. Stage four pore waters probably moved through the sediments only after dewatering of the mudstones due to compaction was largely complete.

## PORE WATER EVOLUTION AND GREYWACKE GENESIS

A general model for pore water evolution that explains a broad variety of sandstone cement histories can be developed from the interpreted controls on cement paragenesis in the Bowser Basin.

Varying grain composition, pH of depositional waters, organic matter content, and rate of burial within geologically reasonable limits permits prediction of pore water evolution paths leading to diverse cementation histories. For example, initial acidic meteoric waters might yield an initial cementation stage of kaolinite, rather than chlorite as in the Bowser Basin. If located in an intracratonic basin, which would typically have more abundant $K^+$ bearing species, an initial illite or K-feldspar stage is more likely. Low primary production or slow sedimentation rate could reduce the amount of buried organic matter compared to the Bowser Basin. This could eliminate the acid water stage associated with thermal maturation, and thus eliminate oil migration, chlorite dissolution, and quartz cementation. The different cementation histories outlined above will result in pseudo-matrix rich sandstones with the widely variable authigenic clay, quartz, carbonate, and organic matter content that typifies greywackes.

## ECONOMIC IMPLICATIONS OF PORE FLUID EVOLUTION

The changes from alkaline to acidic and back to alkaline pore fluid chemistry have several important implications to economic mineral potential in the Bowser Basin. First, hydrocarbon potential is low, although the acidic pore water stage clearly records that oil and gas generation occurred, and furthermore, sandstones saturated with bitumen (dead oil) prove that oil pooled in reservoir rocks. However, fluid inclusions in quartz and the subsequent alkaline pore fluid stage both attest to later formation temperatures greatly in excess of the oil window. Vitrinite reflectance data discussed later in this chapter confirm that maximum temperatures reached roughly 250°C to 315°C (depending on stratigraphic position), which greatly exceeds the oil death line of roughly 165°C (Tissot and Welte, 1984). Multiple stages of structural deformation followed sediment accumulation in the Bowser Basin (Moffat and Bustin, 1993), and the preservation of saturated bitumen reservoirs may imply that the oil was thermally degraded prior to compressional deformation. Gas reservoirs that could have survived post-oil migration thermal exposure would likely have been breached by later structural deformation. Remaining hydrocarbon potential may be limited to gas from coal, because there is presently little data to suggest whether adsorbed methane might survive post-generation structural deformation.

Although the high temperatures implied by the later alkaline pore fluid stage make hydrocarbon potential low, the change from acidic to alkaline conditions at temperatures near 200°C suggests potential for accumulation of economic metals may be high. Gold is relatively soluble in acidic solutions and therefore potentially mobilized as either a chloride or sulphide complex. Solubility drops by a factor of as much as 30 times at 200°C when pH is changed from 6.0 to 9.4 (Seward, 1973). Such a variation in pH occurred in the Bowser Basin between the quartz and calcite cementation stages, and therefore metals mobilized by acid pore fluids may have been precipitated simultaneous with the initiation of calcite precipitation. Thus, if gold or other acid soluble metals were present in the sediments at the time of burial, then the diagenetic pore water evolution of the Bowser Basin appears to be an effective method of mobilization and concentration.

## MUDSTONE PORE WATER EVOLUTION

Authigenic carbonate occurs in resistant yellow-brown weathering concretions or concretionary layers in mudstones of the northern Bowser Basin. Concretions commonly exceed 10 cm in diameter, and some layers are more than 1 m thick. The concretions are lithified, have homogeneous black to dark gray interiors, but lack concentric layering. When cut and polished, finely detailed sedimentary structures such as trace fossils and laminations can be observed. Fossil leaves, and less commonly shells, are very well preserved on the outer surfaces of many concretions, but similar preservation is rare in the interior of the concretions.

Authigenic layers with an early diagenetic origin are described in the literature from many sedimentary basins (Raiswell, 1971; Gautier and Claypool, 1984). Like these examples from the literature, authigenic layers in the northern Bowser Basin are assumed to have a diagenetic origin, and thus may record information relevant to the pore water history of the mudstones. The concretions are further assumed to have precipitated from the inside out over time, in a manner similar to that of authigenic carbonates described in other clastic basins. Because the concretions formed in the mudstones during diagenesis, their record of pore water chemistry should generally reflect the pore water evolution

determined for the sandstones. However, whereas advection controlled pore water circulation in the sands, dewatering compaction probably controlled fluid movement in the muds, and therefore some differences in pore water chemistry may also be expected.

Authigenic carbonates vary in thickness and abundance with stratigraphic level. In shallow marine mudstones of the undivided Bowser Lake Group, (the lowest stratigraphic level examined), authigenic layers consist of poorly lithified concretions or bands of concretions typically less than 6 cm thick, and usually separated vertically by more than 10 m of mudstone. Up section, coincident with the appearance of organic rich deltaic facies, authigenic layers are more common and better developed. Well lithified ovoid concretions 10 to 20 cm in diameter occur in layers commonly separated vertically by less than 5 m of strata. Continuing up section, the concretion layers become more continuous and more closely spaced vertically. Within the upper portion of the Currier Formation, some layers have grown together into continuous resistant beds up to 10 cm thick. In the overlying McEvoy Formation, some continuous authigenic layers exceed 1 m in thickness. Raiswell (1988) suggested that the thickness and degree of continuity of authigenic carbonates layers is in part controlled by the temporal continuity of deposition. Discontinuous sedimentation is needed to give continuous authigenic layers time to develop. If such a relation holds in the Bowser Basin, then the increasing abundance, thickness, and continuity of authigenic layers higher in the section suggests that sedimentation became more intermittent, commensurate with changes from shallow marine to deltaic, and finally to fluvio-deltaic depositional environments.

Nine concretions from Bowser Basin strata were sampled for mineralogical and geochemical analysis. The stratigraphically lowest sample analyzed (concretion sample 22-13) was collected from deltaic black shales deposited 110 metres above marine shell beds near the transition from undivided Bowser Lake Group strata to the Currier Formation. Six of the nine analyzed concretions were collected within the lower delta plain deposits of the lower Currier Formation, one from higher in the Currier Formation, and one from the overlying McEvoy Formation. Each of these concretions was in turn sampled three, or rarely four, times from the middle to the rim. This sampling pattern was designed to

detect changes in pore water chemistry that may have occurred during the growth of the concretion. The samples were analyzed by XRD to determine mineralogy, and acid dissolution/gas chromatography-mass spectrometry to determine C and O stable isotope ratios.

Carbonate minerals identified in the concretions are siderite, ferroan dolomite (ankerite), and calcite. Concretions in which two carbonate minerals occur contain siderite and ferroan dolomite. Siderite probably formed prior to ferroan dolomite, based on siderite's greater abundance in the interior of two of the examined concretions. Mostly ferroan dolomite concretions with only minor siderite exhibit no trends of changing mineralogical abundance from core to rim. Ferroan dolomite also occurs alone in two other analyzed concretions. Calcite occurs in one monomineralic concretion, and may have formed either late, after the ferroan dolomite, or early before the formation of siderite.

Siderite precipitation requires anoxic pore waters depleted in sulfate (Curtis, 1967), and commonly occurs very early in diagenesis (Gautier and Clatpool, 1984). Siderite concretions analyzed in this study occur in mudstones associated with thick lower delta-plain coals (Chapter 2). In lower delta plain environments of the Mississippi River, early siderite concretions form in the upper few metres of sediment (Coleman, 1982). The occurrence of siderite cores inside ferroan dolomite concretions suggests that siderite also may have begun precipitating very early in the northern Bowser Basin mudstones.

The concretions have a thick (up to 1 to 2 cm) yellow-brown weathering rind on their surfaces, presumably derived from oxidized Fe out of the ferroan dolomite structure. Ferroan dolomite is probably the most widespread authigenic cement in the basin, as well as among analyzed samples, because a similar yellow-brown weathering rind occurs in most well developed carbonate layers in outcrop. Ferroan dolomite, like siderite, is an authigenic mineral characteristic of the methanogenic zone of early diagenesis. Given the inferred very early diagenesis origin for the siderite concretions, and the fact that ferroan dolomite follows siderite (in some concretions at least), it is concluded that ferroan dolomite was probably a later rather than earlier precipitation product of the methanogenic zone.

## *CARBON AND OXYGEN STABLE ISOTOPES*

Carbon and oxygen stable isotope ratios were determined for ten of the examined concretions, in an attempt to better understand the source of the authigenic carbonate and the temperatures at which it formed. Carbon isotope ratios in authigenic carbonates primarily reflect the source of the carbon. During the earliest stages of diagenesis in organic rich muds, isotopically light carbon is released by bacterial degradation of organic matter, because bacteria preferentially consume the lighter carbon isotopes first. As a result, very early authigenic carbonates tend to have very light $d^{13}C$ values. Carbonates formed in the aerobic and sulfate reducing zones of North Sea sandstones, for example, have $d^{13}C$ values ranging from -35 to -20‰ (Kantorowicz, *et al.*, 1987). As diagenesis progresses, bacteria are forced to consume progressively heavier carbon, and authigenic carbonates become progressively heavier as a result (Gautier and Claypool, 1985).

Carbon isotope values in authigenic carbonates from northern Bowser Basin mudstones are restricted to a relatively narrow set of values, with most $d^{13}C$ values occurring between +0.8 and +6.0‰ PDB. Such values are considerably heavier than most very early formed authigenic carbonates from mudstones, and are typical of later stages of methanogenesis. The C isotope ratios, therefore, support a later rather than earlier origin for the concretions within the methanogenic stage of early diagenesis. The $d^{13}C$ ratios also suggest authigenic carbonate precipitation in the muds occurred concurrently with precipitation of authigenic clays in the sandstones, because authigenic clays were being precipitated in sandstones during early diagenesis (as described in the sandstone paragenetic cement section of this chapter).

Kantorowicz *et al.* (1987) concluded that ferroan carbonate cements with the positive $d^{13}C$ ratios characteristic of late methanogenesis, correlate well with later hydrocarbon generation. Clearly oil was generated in northern Bowser Basin sediments, because dead oil remains in some sandstones (as discussed earlier). Therefore, organic matter capable of generating oil must have remained in the muds after bacterial activity ceased. Kantorowicz *et al.*'s (1987) association of positive $d^{13}C$ ratios with oil

generation is, therefore, supported in the rocks of the northern Bowser Basin.

Oxygen isotope ratios were also determined for the mudstone concretions from the northern Bowser Basin. $d^{18}O$ values in authigenic carbonates are a function of temperature and the $d^{18}O$ ratio of the pore fluid at the time of precipitation. Additional factors that affect resultant $d^{18}O$ values include the mineralogy of the carbonate, and the concentrations of other dissolved ions that may occur in the pore fluid. The fractionation effects attributable to different minerals encountered in this study can be accounted for by use of experimentally derived fractionation equations in carbonate species-water systems (calcite: Friedman and O'Neil, 1977; siderite: Carothers *et al.*, 1988; ferroan dolomite: Fisher and Land, 1986; Longstaffe, 1989). However, little data is available concerning fractionation effects in complex solutions such as might be expected in actual pore waters. The effect of other ions in solution on fractionation in reactions, therefore, remains unknown, and interpretations made in this chapter regarding O isotope data are made with the caveat that such effects are not accounted for. Even with such a caveat, the $d^{18}O$ data are inherently ambiguous due to their dependence on both formation temperature and the $d^{18}O$ composition of the pore waters. If neither temperature of formation or pore water $d^{18}O$ composition can be tightly constrained, as is the case in the Bowser Basin, then interpretations must remain somewhat speculative. There are three different models of plausible pore water compositions, and some important inferences concerning Bowser Basin pore water evolution can be reached. The three models are described below:

1) The *-10 ‰ SMOW meteoric model* assumes a meteoric origin for pore fluids in the muds at the time of concretion precipitation. This model further assumes that the meteoric water was isotopically similar to modern meteoric water which precipitates in the cool humid temperate climate of western British Columbia and southern Alaska (-16‰ to -10‰ SMOW; Yurtsever, 1975; Gat, 1980). Such values are in accord with climatic and paleogeographic reconstructions that point to a cool humid temperate climate on the western margin of North America for Bowser Basin sediments (Chapters 2 and 3). Notably this meteoric model is inconsistent with a low latitude position for the Bowser Basin during or shortly after deposition, as suggested from some paleomagnetic and paleontologic studies. Such a low latitude origin

would imply meteoric $d^{18}O$ ratios of -4‰ or higher, and would be more closely consistent with the 0‰ seawater model described later.

The -10‰ SMOW meteoric model is geologically plausible for the northern Bowser Basin because of the paleogeographic considerations alluded to earlier, and because of the abundance of coal and plant remains preserved in the sediments. -10‰ is at the high end of likely meteoric recharge values, and yields a maximum set of temperatures for plausible meteoric waters. Such a maximum meteoric temperature is convenient for comparison with the other models, and also takes into account the tendency of pore waters to become isotopically heavier after burial (Hanor, 1987). -10‰ SMOW is also a reasonable model for initial brackish waters in the muds, for example if the meteoric water mixed with $d^{18}O$ ratio of -16‰ SMOW mixed with approximately 1/3 seawater by volume.

This meteoric pore water model contrasts with the seawater origin inferred for the sandstones based on the paragenetic cement succession described earlier. This contrast may reflect the dominance of diffusion processes during burial and dewatering of the muds, at the same time that advection recharged by seawater dominates diagenetic processes in the sandstones.

2) The *0‰ seawater model* assumes an unevolved seawater origin for the pore fluids. This model is geologically plausible if seawater (or tropical rain water) dominates pore fluids in the muds, and if this seawater is largely unaltered by dissolution of detrital minerals or breakdown of plant material within the sediments. Given the relatively high temperatures this model points to, as discussed below, an assumption that detrital dissolution is unimportant and that plant derived carbon is not contributed in significant amounts is difficult to support geologically.

3) The *+4‰ evolved seawater model* assumes a seawater origin for the pore fluids, and accounts for the geologically likely condition of the pore fluid becoming isotopically heavier after burial. The magnitude of the shift to positive $d^{18}O$ values is uncertain, but most mafic and ultramafic rocks such as form at least part of the provenance for Bowser Basin sediments (Chapters 3 and 4) have $d^{18}O$ values between +5 and +7‰ (Brownlow, 1979). +4‰ $d^{18}O$ for the pore waters, therefore, makes a reasonable model that

accounts for dissolution by such detrital grains. Given the chemically unstable nature of most detrital material derived from mafic and ultramafic terranes, and the relatively high temperatures implied by this model (as discussed below), this +4‰ SMOW evolved seawater model is probably more plausible geologically than the 0‰ SMOW seawater model described above for pore fluids that were originally derived from seawater.

The three pore fluid $d^{18}O$ models outlined above yield three distinct temperature ranges for equilibrium precipitation of each of the different authigenic carbonate mineralogies. For siderite cements, which range in $d^{18}O$ values from +11.5‰ to +15.0‰ SMOW, the indicated temperature ranges are approximately 60° to 80°C assuming the -10‰ SMOW meteoric model; 140° to 180°C for the 0‰ SMOW seawater model; and 190° to 260°C for the +4‰ SMOW evolved seawater model (Fig. 5-11). The -10‰ SMOW meteoric model is the only model to yield geologically reasonable precipitation temperatures, given the presumed methanogenic zone origin of the siderite cements, if we assume that the $d^{18}O$ values reflect original values and not open system re-equilibration values acquired some time well after concretion precipitation. The high temperatures yielded by both the 0‰ and +4 ‰ SMOW seawater models are only plausible assuming re-equilibration at high temperatures. However, due to the high temperatures apparently reached in the Bowser Basin following deposition (Bustin, 1984; and discussion later in this chapter), neither seawater model can be eliminated from consideration based on the siderite $d^{18}O$ values alone.

Ferroan dolomite cement $d^{18}O$ values indicate higher temperature ranges for each model than the temperatures deduced from the siderite $d^{18}O$ values. $d^{18}O$ values for most of the concretions, which were collected in deltaic strata of the lower Currier Formation, range from 9‰ to 13‰ SMOW. The core of concretion sample 22-13, collected from the top of the undivided Bowser Lake Group at the transition from marine to deltaic strata, yielded higher $d^{18}O$ ratios of 16.1‰. The 9 to 13‰ . $d^{18}O$ range corresponds to a temperature range of approximately 75° to 110°C for the -10‰ SMOW meteoric model; 190° to 280°C for the 0‰ SMOW seawater model; and 290° to in excess of 400°C for the +4 evolved seawater model (fig 5-12). As was the case for the siderite $d^{18}O$ values, the only model to

Figure 5-11: Range of concretion $d^{18}O$ ratios in siderite cement and their equilibrium formation temperature assuming three different pore water isotope composition models. The three models are described in text.

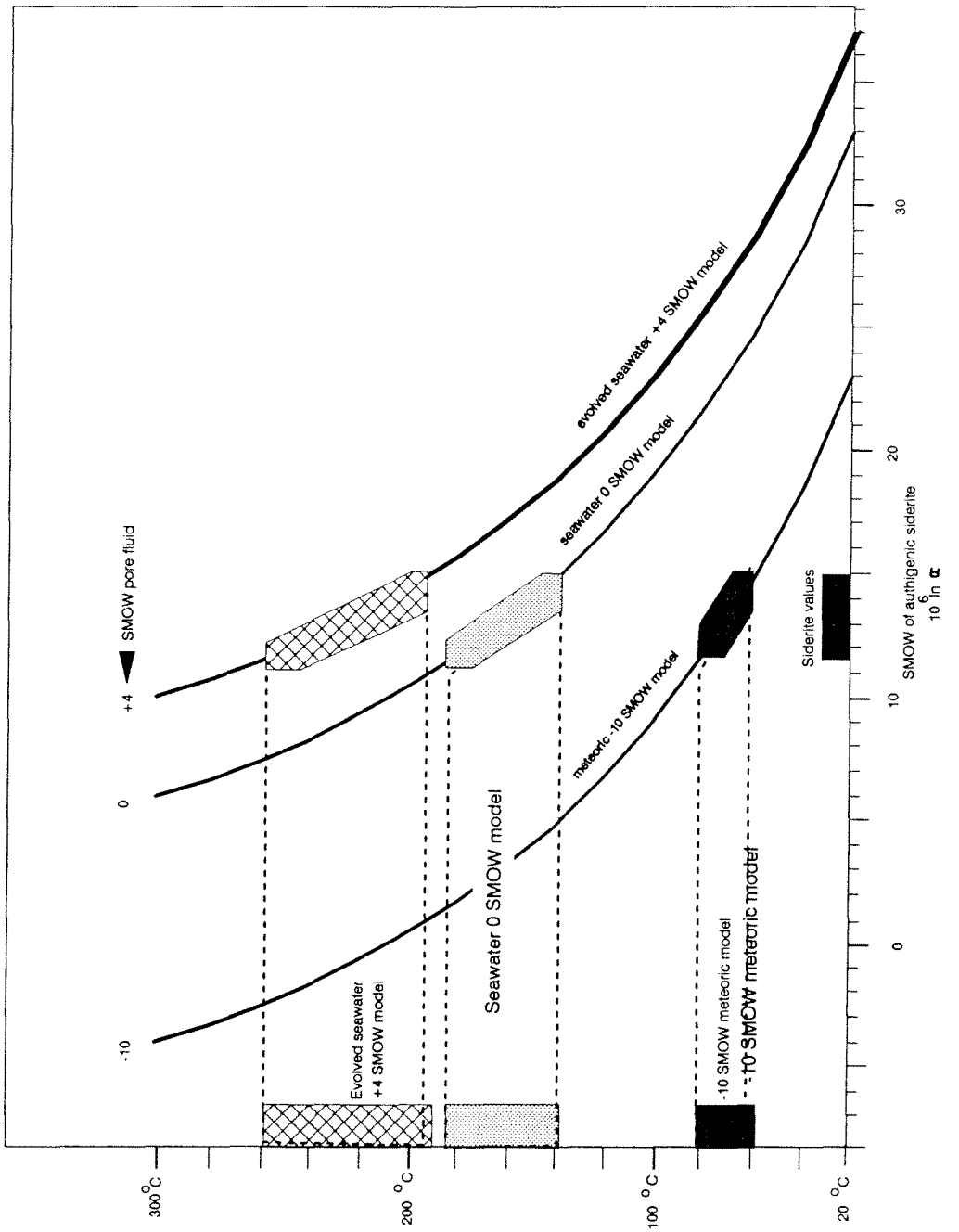

Figure 5-12: Range of concretion $d^{18}O$ ratios in ferroan dolomite cement and their equilibrium formation temperature assuming three different pore water isotope composition models. The three models are described in text.

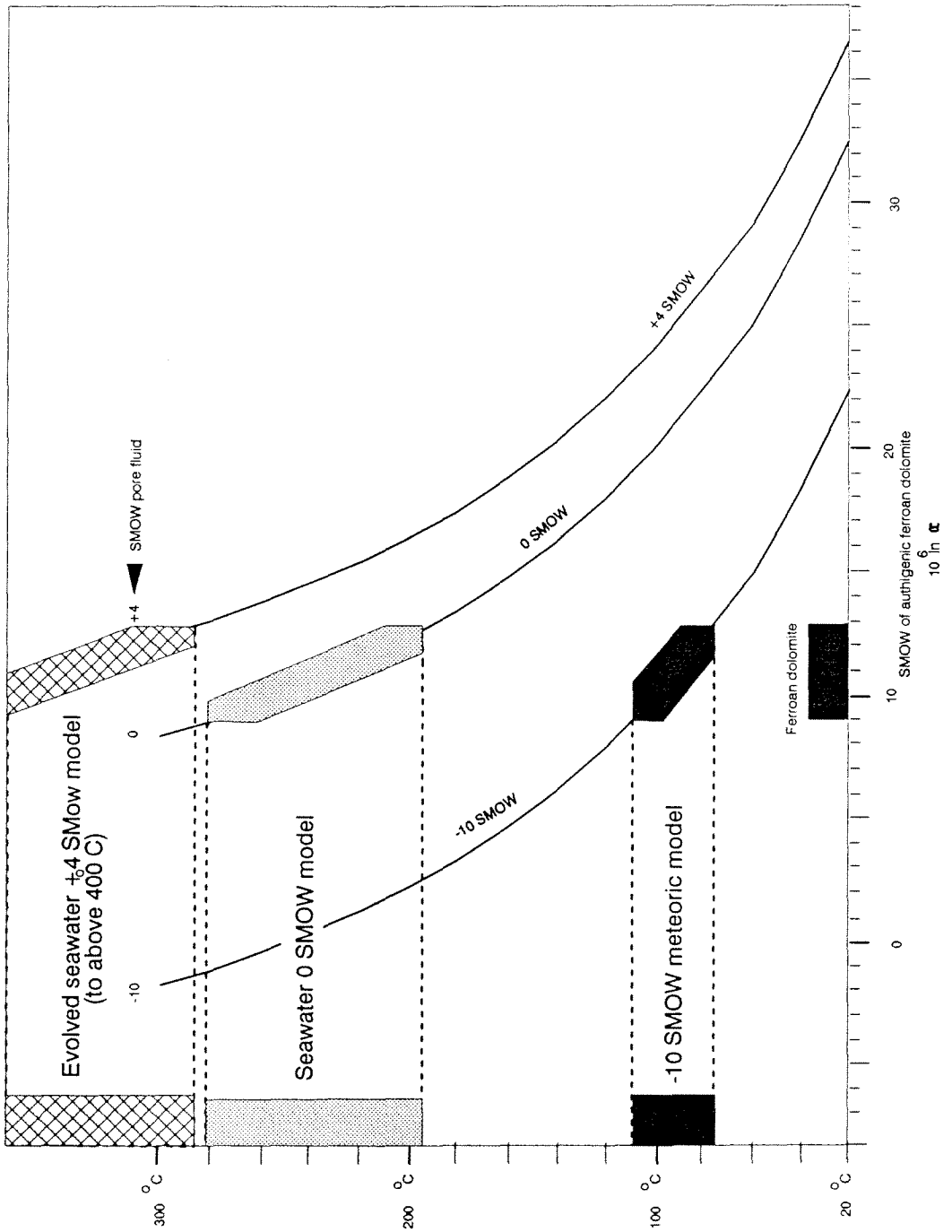

yield geologically reasonable formation temperatures is the -10‰ SMOW meteoric model. The +16‰ SMOW value for the core of sample 22-13 is interpreted using this model as either indicating concretion formation initiated at a somewhat lower temperature of about 50°C from similar -10‰ SMOW pore water or that some seawater mixed with meteoric water (brackish water), raising the $d^{18}O$ of the pore fluid. Pore water $d^{18}O$ of -7‰ would raise predicted equilibrium precipitation temperature to 70°C. Because this sample was collected just above shell-bearing marine beds, the seawater mixing explanation appears most likely.

The 0‰ SMOW seawater model is tenable for ferroan dolomite cements only if re-equilibration occurred during deepest burial (maximum temperatures generally believed to be less than approximately 300°C; Bustin, 1984; and discussion later this chapter). The +4‰ SMOW evolved seawater model is barely tenable even assuming re-equilibration at the highest postulated formation temperatures. Unlike with the -10‰ SMOW meteoric model, the +16‰ SMOW core value for sample 22-13 is not readily explicable under either of these models.

The higher temperatures indicated for ferroan dolomite compared to siderite cements are consistent with the -10‰ SMOW meteoric model, but are largely uninterpretable under the other models. Assuming that temperatures predicted by the -10‰ SMOW meteoric model are correct, siderite precipitation occurred at temperatures between 60° and 80°C, and ferroan dolomite precipitation followed at temperatures of 75° to 110°C (Fig. 5-13). These temperature ranges are at least partially within the methanogenic zone, and the change from siderite to ferroan dolomite follows the trend of relatively more siderite in the cores than near the rim indicated by two of the concretions.

The much higher formation temperatures for ferroan dolomite compared to siderite precipitation derived from the two seawater models is not readily explicable based on any obvious geologic process. Under these models, siderite would have re-equilibrated over a broad range of temperatures

Figure 5-13: Comparison of predicted temperatures for siderite, ferroan dolomite and calcite concretion cements, assuming different modelled pore water compositions.

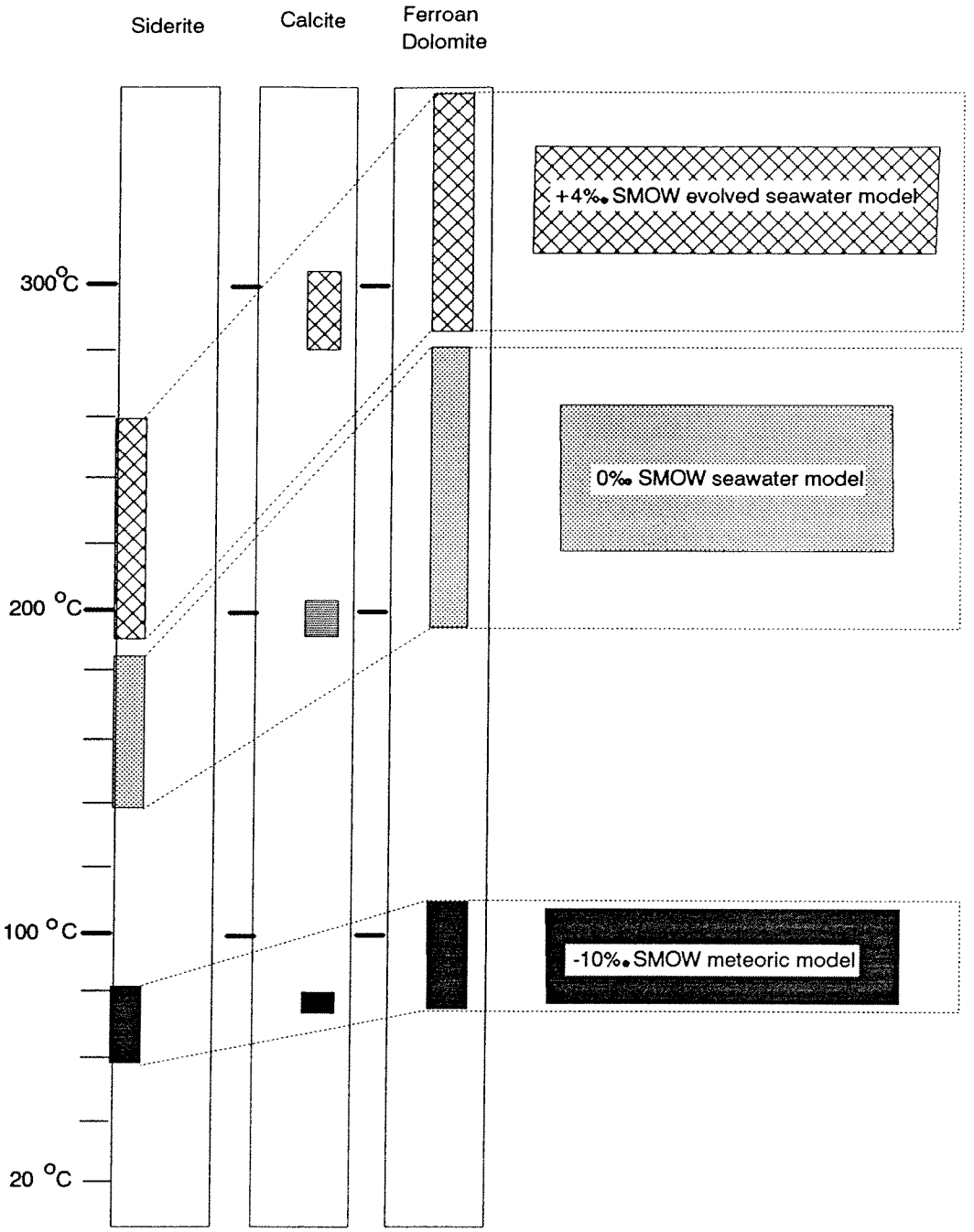

from 10° to perhaps 100°C below the even broader range of ferroan dolomite re-equilibration temperatures (Fig. 5-13). There is no obvious geologic reason for siderite to re-equilibrate at significantly lower temperatures than the ferroan dolomite, especially where siderite occurs in cores of ferroan dolomite concretions. The entirely ferroan dolomite sample 22-13 is also inexplicable under these models. Assuming the 0‰ SMOW seawater model, the ferroan dolomite core of sample 22-13 must have re-equilibrated at approximately 150°C, and the rim ($d^{18}O$=12.9‰ SMOW) at approximately 195°C.

One calcite concretion was analyzed for O isotopes. This concretion was collected from the McEvoy Formation, approximately 500 to 1000 m stratigraphically above the other discussed samples. Assuming the parameters of the -10‰ SMOW meteoric model, precipitation occurred between 75° and 80°C (Fig. 5-14). As with siderite and ferroan dolomite, the other models yield significantly higher pore fluid temperatures (190° to 200°C for 0‰ SMOW seawater, and 280° to 300°C for the +4‰ SMOW evolved seawater model). Given the lack of other analyzed concretions with either similar mineralogy or stratigraphic origin, more specific discussion of this sample is unwarranted, other than to note that re-equilibration is required to explain any but the -10‰ SMOW meteoric model for calcite as well as siderite or ferroan dolomite.

The -10‰ SMOW meteoric model is the only one of the three models that yields geologically reasonable precipitation temperatures. Meteoric water from a cool temperate climate, is therefore, required to explain the origin of the analyzed concretions, if the $d^{18}O$ values approximate values at the time of precipitation. Both of the seawater models require re-equilibration of the authigenic carbonates at near maximum burial temperatures to explain observed $d^{18}O$ values. Because of the high temperatures the Bowser Basin strata were exposed to after burial, re-equilibration cannot be excluded as a possibility. However, re-equilibration fails to explain the observed core to rim variations and the lower siderite compared to ferroan dolomite temperatures, and therefore is a very unsatisfactory explanation. The superior ability of the -10‰ SMOW meteoric model to explain all the observed $d^{18}O$ data indicates that

Figure 5-14: Range of concretion $d^{18}O$ ratios from calcite cement and their equilibrium formation temperature assuming three different pore water isotope composition models. The three models are described in text.

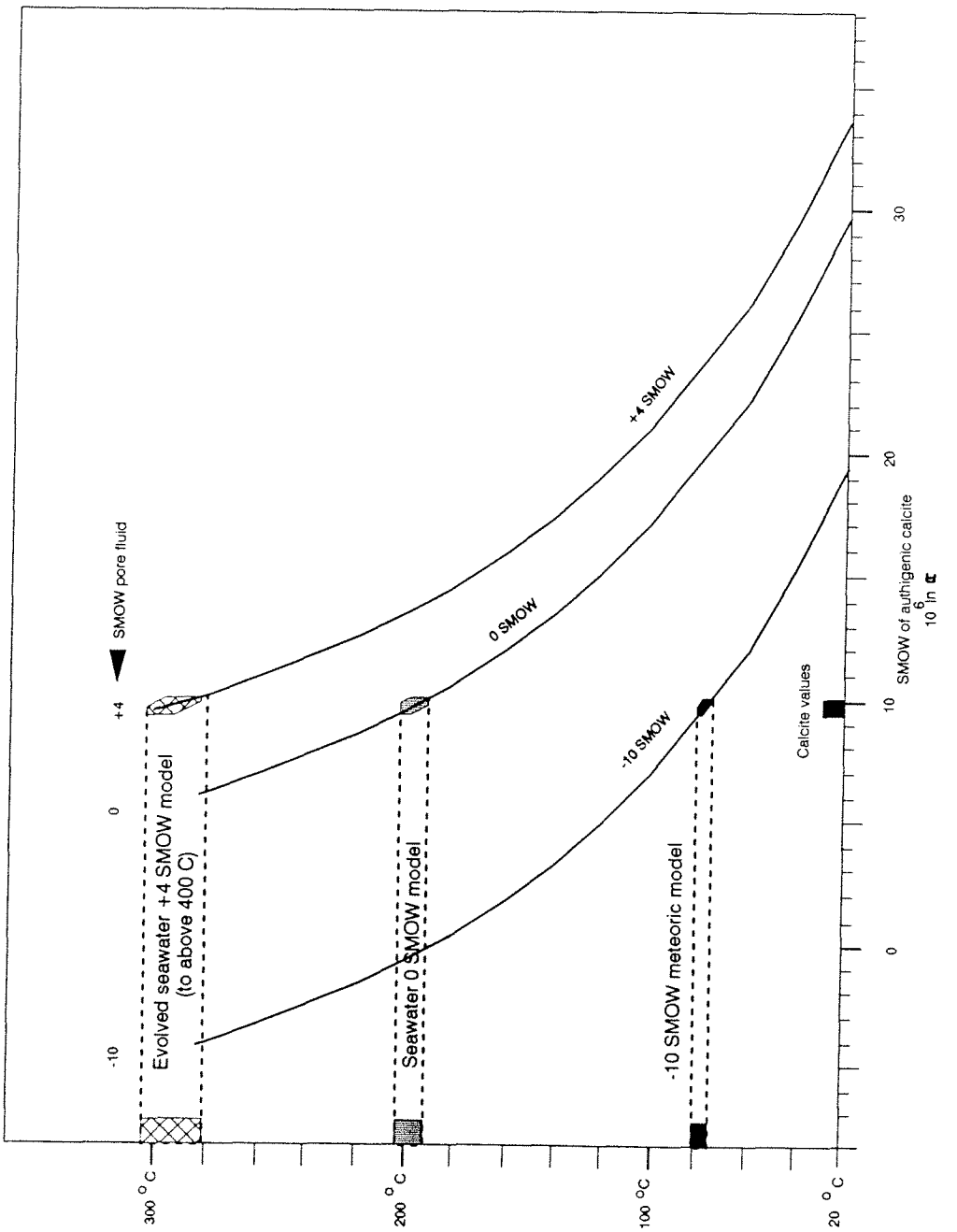

cool temperate meteoric waters controlled mudstone pore fluid compositions in the Bowser Basin during early diagenesis. Meteoric water in muds is also consistent with the coal and flora found in association with the mudstones. In fact, the -10‰ SMOW meteoric model favoured in this discussion may assume starting pore fluid $d^{18}O$ values that are too high. Meteoric waters as low as -16‰ SMOW, which yield initial ferroan dolomite and siderite precipitation at temperatures of 20° to 30°C are consistent with observations of very early initiation of concretion growth reported from some modern deltas (Tye and Coleman, 1989).

### *COMPARISON OF EARLY DIAGENESIS IN SANDSTONES AND MUDSTONES*

Authigenic cements precipitated during early diagenesis differ between the mudstones and sandstones of the northern Bowser Basin. For example, authigenic carbonates precipitated as concretions in mudstones, and authigenic clays precipitated in sandstones. Although the differences in cement mineralogy between mudstones and sandstones are striking, some similarities in the pore waters are suggested. Mg and Fe are important elemental components both of the chlorite cements in the sandstones, and of the ferroan dolomite cements in the mudstones. In addition, relatively alkaline waters are required for either chlorite or carbonate cement stability. However, some chemical conditions must be different to cause chlorite to precipitate in the sandstone at nearly the same time that ferroan dolomite is precipitating in the mudstone. One possible factor is that sulfate may inhibit dolomite formation (Baker and Kastner, 1981), although that point is questioned by Hardie (1987). Perhaps sulfate concentrations were higher in the sandstones, in which seawater (an excellent source of sulfate) was being replenished by advection. Alternatively (or in addition to), $HCO_3^-$ (and $CO_3^{2-}$) concentrations were probably higher in the mudstones, because this is where the organic matter was being consumed by bacteria. Higher $HCO_3^-$ concentration clearly favors carbonate precipitation.

The difference between pore fluids in the sandstones and mudstones is further emphasized by the $d^{18}O$ ratios in the mudstone concretions, which strongly favor meteoric (and in at least one sample brackish) water as the original pore fluid in the muds. This striking difference in pore water for the

muds and sands during early diagenesis probably reflects the fundamental difference in groundwater transport processes that prevail in the different lithologies. Diffusion and dewatering dominate in muds and advection, possibly recharged by seawater, dominates in sands. Hence cementation in the muds appears to record a unidirectional expulsion of meteoric waters whose chemistry is largely controlled by breakdown of organic matter, while cementation in the sands records mixing of meteoric waters driven out of the muds with connate saline waters. Similar replacement of marine or brackish waters by meteoric waters in a marginal marine succession is recorded by strongly negative $d^{18}O$ (-8.3‰ to -18.2‰) values in early formed carbonate concretions in sandstones from Scotland (Wilkinson, 1993).

## ORGANIC DIAGENESIS

Vitrinite reflectance (random in oil: $Ro_{rand}$) was measured from coals and carbonaceous mudstones from each stratigraphic unit within the study area to provide a maximum temperature for diagenesis. The data set shows that the oldest strata have the highest reflectance values, and that values become markedly lower in progressively younger strata (Fig. 5-15). The lowermost strata, consisting of the marine undivided Bowser Lake Group, yield vitrinite reflectance values in excess of $Ro_{rand}$= 4.1%, that is equivalent to a coal rank of anthracite and meta-anthracite (Bustin, *et al.*, 1990). The Currier Formation yields $Ro_{rand}$ values between 2.8% and 4.1%. The thickest and most economically interesting coals in the Currier Formation occur in the lower part of the unit, and have $Ro_{rand}$ values between 3.1% and 4.1%, that corresponds to anthracite rank. McEvoy Formation $Ro_{rand}$ values span the range between 1.9 and 2.9%, equivalent to semianthracite coal rank (Bustin, *et al.*, 1990). Like the Currier Formation, the McEvoy Formation tends to exhibit lower $Ro_{rand}$ values upward in the formation. The Devils Claw Formation yields $Ro_{rand}$ values between 1.1% and 1.8%, equivalent to medium and low volatile bituminous coal.

### *BASIN MATURATION MODELLING*

A thermal maturation model that employs Arrhenius type equations to represent organic maturation was to used to determine maximum temperatures in the basin. This model is a forward

Figure 5-15: Vitrinite reflectance increases significantly with stratigraphic depth, implying a steep thermal gradient.

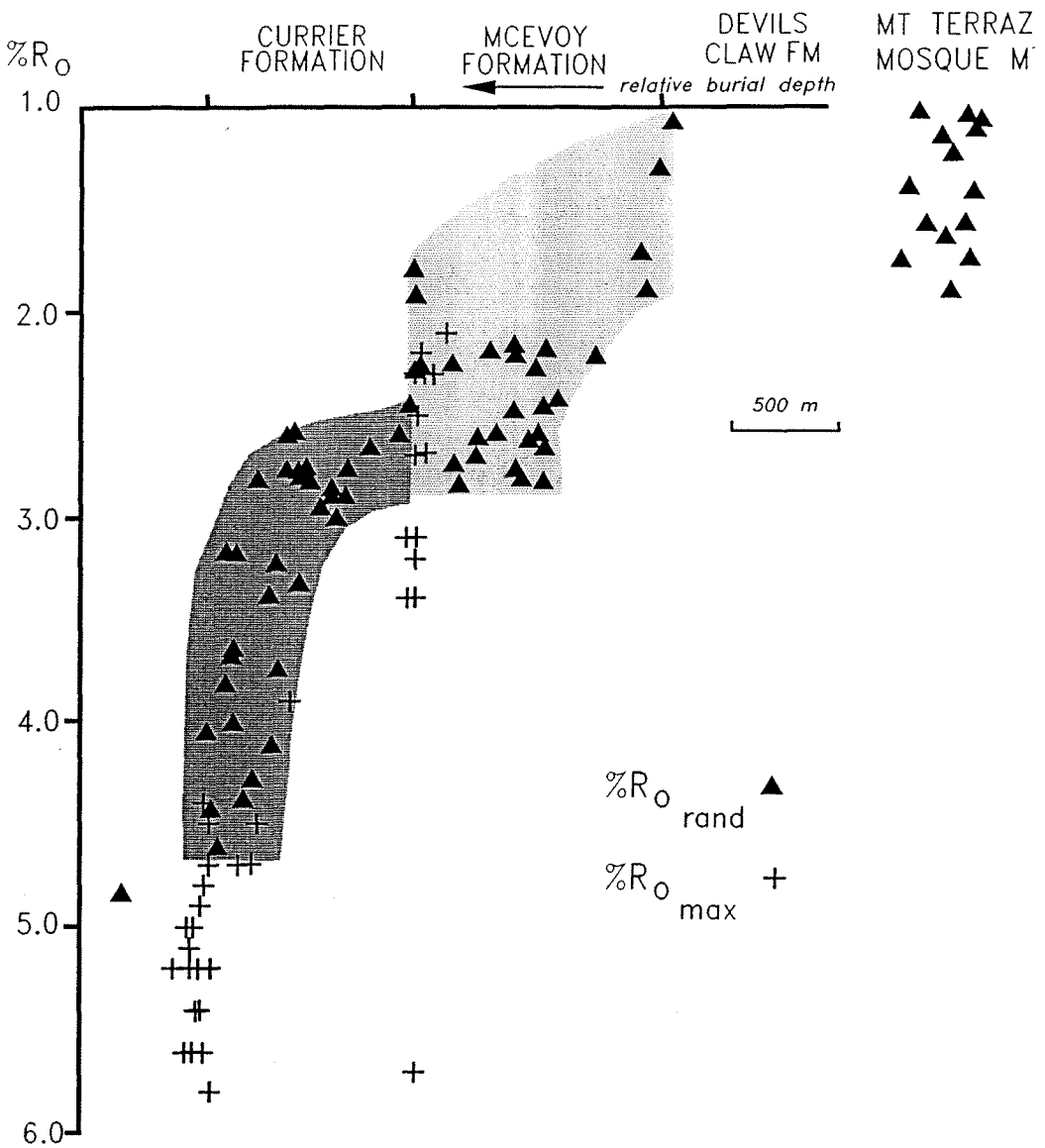

modelling type that requires input based on assumptions of paleogeothermal gradient and burial history (Chonchawalit, 1993). Output is in the form of predicted vitrinite $Ro_{rand}$ values. When output values approximate the measured values, then the assumptions used are concluded to be a plausible model of paleogeothermal gradient and burial history.

## *PARAMETERS OF THE FAVOURED PALEOGEOTHERMAL GRADIENT AND BURIAL HISTORY MODEL*

The paleogeothermal gradient and burial history model used in this analysis is constrained by geologic parameters derived from a combination of stratigraphic (Cookenboo, 1989 and Appendices 1, 2, and 3), lithofacies (Chapter 2), paleontologic (Appendix 1), provenance (Chapters 3 and 4), and diagenetic data (this chapter). Stratigraphic data, as summarized in chapter 1 (based on Cookenboo and Bustin, 1989; Cookenboo, 1989; and Appendixes 1, 2, and 3) yields the following estimated thicknesses for units in the study area: 1000 m for the Currier Formation; 1000 m for the McEvoy Formation; and 600 m for the Devils Claw Formation. Lithofacies demonstrate progressive shallowing of the marine basin fill to near sea-level by the end of undivided Bowser Lake Group deposition, and subsequent accumulation of Currier, McEvoy, and Devils Claw formations near sea-level.

Paleontologic data described in Appendix 1 are the basis for ages used in this model: Currier Formation was deposited between the Oxfordian (Late Jurassic) and the Earliest Cretaceous (Berriasian); the McEvoy Formation was deposited during the latest Barremian or Aptian to the mid to late Albian (mid-Cretaceous); and the Devils Claw Formation in latest Albian or earliest Cenomanian (Late Cretaceous) time (Bustin and Moffat, 1983; Moffat *et al.*, 1988; MacLeod and Hills, 1990; Cookenboo *et al.*, 1991). Numerical ages for the stages are taken from (Palmer, 1983).

Provenance analysis (Chapters 3 and 4) constrains the basin to some type of oceanic setting because the basin was filled by detritus derived from island arc volcanics and marginal basin lithosphere, and because that detritus was derived from the east (to northeast). In other words, the Bowser Basin was outboard of obducted oceanic terranes, and therefore also likely accumulated in an oceanic terrane. The

paleogeothermal gradient favoured for this setting is 65°C/km, similar to some western Pacific marginal basins(e.g. the central Sumatra basin with a gradient of 65° to 90°C/km; North, 1985), and higher than most continenetal values. Simulations using lower geothermal gradients are also reported here as a test of the validity of the model.

The pore water evolution determined from sandstone cement paragenesis and concretion geochemistry is consistent with progressive burial leading to steadily increasing formation temperatures from burial to over 200°C, which provides the final constraint for the thermal maturation model. This constraint is that the thermal model should use a linear, constant geothermal gradient. In other words, there is no need to postulate a separate thermal event sometime late in basin evolution.

The depth to which the Devils Claw Formation was buried is one further geologic parameter that must be considered. This depth is difficult to estimate, because strata that buried the Devils Claw Formation are now eroded entirely away. The depositional thickness of these eroded strata has been the subject of much speculation (Bustin, 1984, Bustin and Moffat, 1989), because the thickness controls the maximum depth to which Bowser Basin sediments were buried. Bustin (1984) used approximately 1500 m of post-Devils Claw burial by strata equivalent to the Sustut Group that are presently exposed east of the basin (Eisbacher, 1981), and high geothermal gradients (in excess of 50°C/km) to account for the high rank coals in the Groundhog Coalfield. Bustin and Moffat (1989) demonstrated that an additional 2000 m (beyond the 1500 m accounted for by Sustut Group equivalents) of burial were required to achieve anthracite rank coals in the Currier Formation at more nearly typical continental geothermal gradients of 30 to 40°C/km. Fifteen hundred metres of post Devils Claw burial is favoured in the thermal model in this study, because: 1) 1500 m is compatible with known thickness of Sustut Group sediments deposited prior to Late Cretaceous erosion of the Bowser Basin (Eisbacher, 1974); and 2) 1500 m is compatible with preservation of significant intergranular porosity in upper McEvoy Formation sandstones until after late stage calcite cementation (Galloway, 1974; Trevena and Clark, 1986).

Due to the uncertainties in actual burial depth, models assuming deeper burial were also run,

and are described later.

*RESULTS OF BASIN MATURATION MODELLING*

The best fit of the calculated values to measured vitrinite reflectance values from the northern Bowser Basin is the model run using 65°C/km as the geothermal gradient and assuming 1500 m of burial of the Devils Claw Formation (see burial history curve Fig. 5-16). Selected model runs using 65°C/km and lower geothermal gradients and yielding output in the form of calculated vitrinite reflectance values are illustrated in figure 5-17. Calculated maximum temperatures for the best fit run (65°C/km) are 215°C for basal McEvoy Formation and deeper stratigraphic horizons. Temperatures in excess of 200°C were inferred from the pore water evolution described earlier, and therefore this model generally agrees with sandstone paragenesis observations. The maximum temperature reached by the upper McEvoy or lower Devils Claw Formation horizon is 155°C. Lower formational temperatures than predicted by the sandstone cements can be explained as the result of vertical migration of pore fluids from greater depths. Geothermal gradients less than 60° to 65°C/km are insufficient to explain measured vitrinite reflectance values assuming 1500 m of post Devils Claw Formation burial. For example, the 50°C/km run predicts semianthracite ($Ro_{rand}$ = 2.4%) in the lower Currier coal measures (Fig. 5-17), in contrast to actual ranks of anthracite and meta-anthracite. Notably, the 65°C/km geothermal gradient run matches observed vitrinite reflectance values in the upper stratigraphic horizons as well as in the lower units. This matching at all stratigraphic levels is lacking in runs described below.

Maturation model runs using a geothermal gradient of 40°C/km, but assuming 5000 m burial of the Devils Claw Formation (instead of 1500 m used above) results in anthracite in lower Currier and below, which is compatible with measurements. However, the 40°C/km and 5000 m burial run also predicts anthracite occurs in the upper McEvoy/basal Devils Claw, which is incorrect. 3000 m burial and 40°C/km yields compatible reflectance values in the upper McEvoy/basal Devils Claw Formation,

Figure 5-16: Burial history curve, assuming ages, stratigraphic thickness, and burial depths of favoured maturation model.

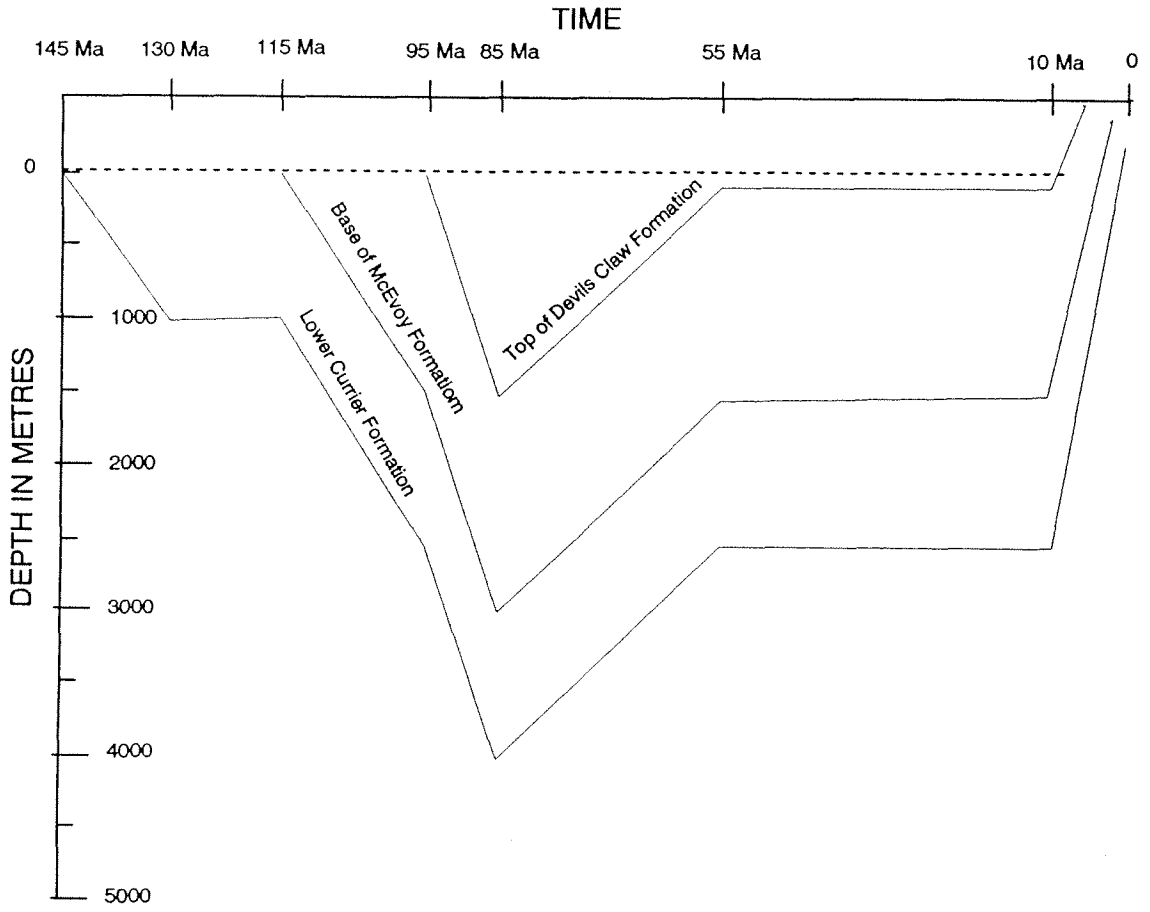

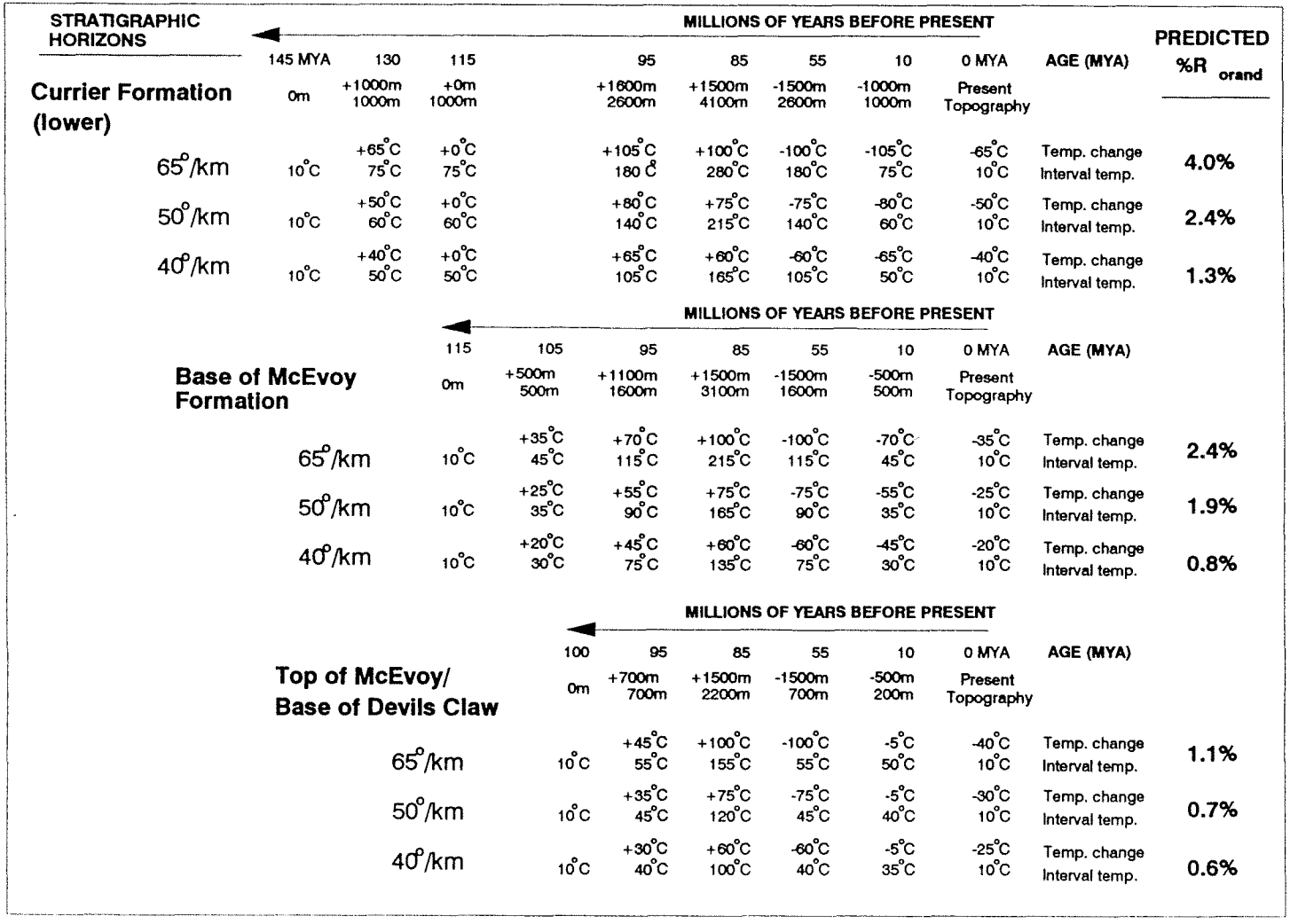

| STRATIGRAPHIC HORIZONS | MILLIONS OF YEARS BEFORE PRESENT | | | | | | | | | | PREDICTED %R orand |
|---|---|---|---|---|---|---|---|---|---|---|---|
| | 145 MYA | 130 | 115 | 95 | 85 | 55 | 10 | 0 MYA | AGE (MYA) | |
| **Currier Formation (lower)** | 0m | +1000m 1000m | +0m 1000m | +1600m 2600m | +1500m 4100m | -1500m 2600m | -1000m 1000m | Present Topography | | |
| 65°/km | 10°C | +65°C 75°C | +0°C 75°C | +105°C 180°C | +100°C 280°C | -100°C 180°C | -105°C 75°C | -65°C 10°C | Temp. change Interval temp. | 4.0% |
| 50°/km | 10°C | +50°C 60°C | +0°C 60°C | +80°C 140°C | +75°C 215°C | -75°C 140°C | -80°C 60°C | -50°C 10°C | Temp. change Interval temp. | 2.4% |
| 40°/km | 10°C | +40°C 50°C | +0°C 50°C | +65°C 105°C | +60°C 165°C | -60°C 105°C | -65°C 50°C | -40°C 10°C | Temp. change Interval temp. | 1.3% |

| | MILLIONS OF YEARS BEFORE PRESENT | | | | | | | |
|---|---|---|---|---|---|---|---|---|
| | 115 | 105 | 95 | 85 | 55 | 10 | 0 MYA | AGE (MYA) |
| **Base of McEvoy Formation** | 0m | +500m 500m | +1100m 1600m | +1500m 3100m | -1500m 1600m | -500m 500m | Present Topography | |
| 65°/km | 10°C | +35°C 45°C | +70°C 115°C | +100°C 215°C | -100°C 115°C | -70°C 45°C | -35°C 10°C | Temp. change Interval temp. |
| 50°/km | 10°C | +25°C 35°C | +55°C 90°C | +75°C 165°C | -75°C 90°C | -55°C 35°C | -25°C 10°C | Temp. change Interval temp. |
| 40°/km | 10°C | +20°C 30°C | +45°C 75°C | +60°C 135°C | -60°C 75°C | -45°C 30°C | -20°C 10°C | Temp. change Interval temp. |

| | MILLIONS OF YEARS BEFORE PRESENT | | | | | | |
|---|---|---|---|---|---|---|---|
| | 100 | 95 | 85 | 55 | 10 | 0 MYA | AGE (MYA) |
| **Top of McEvoy/ Base of Devils Claw** | 0m | +700m 700m | +1500m 2200m | -1500m 700m | -500m 200m | Present Topography | |
| 65°/km | 10°C | +45°C 55°C | +100°C 155°C | -100°C 55°C | -5°C 50°C | -40°C 10°C | Temp. change Interval temp. |
| 50°/km | 10°C | +35°C 45°C | +75°C 120°C | -75°C 45°C | -5°C 40°C | -30°C 10°C | Temp. change Interval temp. |
| 40°/km | 10°C | +30°C 40°C | +60°C 100°C | -60°C 40°C | -5°C 35°C | -25°C 10°C | Temp. change Interval temp. |

Figure 5-17: Maturation model runs with assumed paleogeothermal gradients of 40°C/km, 50°C/km, and 65°C/km for three stratigraphic horizons.

but predicts the deepest modelled horizon (500 m below the Currier Formation) does not even reach semianthracite rank.

The results of the computer maturation simulation are resistant to changes in timing within geologically reasonable bounds. Changes in timing of burial and uplift have negligible influence on the model output, because $Ro_{rand}$ is related to the highest temperatures reached by a stratigraphic unit and therefore termination of burial effectively stops $R_{orand}$ increase. Runs using alternative age assignments similar to those suggested by leaf fossil studies (MacLeod and Hills, 1990) also do not differ significantly in final $R_{orand}$.

### *IMPLICATIONS FOR DIAGENETIC HISTORY*

The thermal maturation model yields geothermal gradients and maximum temperatures consistent with the proposed pore water evolution. Most importantly, maximum temperatures deduced from the maturation model exceed the minimum temperatures inferred for the late stage of calcite cementation (in excess of 200°C). The compatibility of the diagenetic history with the maturation model does not exclude other possible explanations, but it does permit confidence that the preferred models of both maturation and diagenetic history are geologically reasonable histories for the northern Bowser Basin.

### *IMPLICATIONS OF MATURATION MODEL TO REGIONAL TECTONICS*

The maturation model used above implies that the geothermal gradient must be higher than normal continental crustal averages to result in the high maturation gradient that occurs in the northern Bowser Basin. Low gradients will not produce anthracite, except with very deep burial, and if burial is that deep, low gradients would cause the entire preserved stratigraphic column to be anthracite. The compatibility of a high geothermal gradient with both the maturation model and previously determined independent geologic data strongly supports accepting the favoured basin development model.

A high geothermal gradient is consistent with the inferred accumulation of the Bowser Basin

sediments in an oceanic or back-arc basin (Chapter 4) west of the North American continental margin. Similar basins in the southwest Pacific typically have high heat flows. The proposed high heat flow also fits well with other basins in Cordillera. Maturity gradients (and coal ranks) for Mesozoic strata in the Western Canada Sedimentary Basin (WCSB) are lower than in comparable aged strata of the Bowser Basin, but increase westward towards the mountains (Bustin, 1991). This trend of increasing geothermal gradient continues further west to the Bowser Basin. Heat flow also increases westward, roughly doubling from 40 $mW/m^2$ in the Foreland Belt to approximately 80 $mW/m^2$ in the Intermontane Belt (Sweeney, *et al.*, 1992). Increasing geothermal gradient and heat flow are probably due to variation in type of basement, because Paleozoic and older North American continental crust thins from the craton towards the deformed belt, and probably changes to oceanic crust farther west (Thompson, 1989). Sediment accumulation in the Bowser Basin occurred above this oceanic crust outboard of North America. The Bowser Basin sediments were therefore subjected to high geothermal gradients following deposition.

## CONCLUSIONS:

1) Pore water evolution of the northern Bowser Basin is recorded in the paragenetic sequence of sandstone cements. That sequence of cements records the following diagenetic stages: i) early isopachous chlorite cement; ii) illite cementation; iii) kaolinite cementation; iv) oil generation and migration; v) chlorite dissolution; vi) quartz cementation; and vii) late stage calcite pore-filling and grain replacement cement.

2) Pore water chemical conditions inferred from the sandstone cement paragenesis suggest that chlorite precipitated from an alkaline fluid such as seawater. The initial seawater probably was enriched in Fe and Mg due to dissolution of mafic minerals.

3) The progression of sandstone cement stages was primarily controlled by changes in pore fluid pH, and secondarily by rock-water interactions. Acidity increased in pore waters at the time of oil migration as a result of thermal maturation of organic matter. Illite, kaolinite, and quartz cements precipitated from

these increasingly acidic pore waters. Precipitation of illite removed $K^+$ from solution (rock-water interaction), favoring the change from the illite to kaolinite cement stage. Acid water conditions also caused chlorite dissolution. Calcite cementation began after the thermal breakdown of organic acids led to reduced acidity in the pore waters, probably at temperatures in excess of 200°C.

4) Pore fluids in the mudstones were strongly depleted relative to seawater in $d^{18}O$ during methanogenesis as recorded in authigenic carbonate concretions. The highly negative $d^{18}O$ values suggest that meteoric waters (i.e., fresh or brackish) from cool temperate climates were the primary source of the pore waters in the mudstones.

5) Maturation modelling assuming heating of the sediments due to deposition and progressive burial in a high geothermal gradient regime such overlying back-arc crust accounts for measured vitrinite reflectance data. There is no need for later thermal events associated with structural deformation or tectonic events to explain the diagenetic history of the northern Bowser Basin, although such thermal events cannot be excluded.

# REFERENCES

Almon, W. R., and Davies, D. K. 1981. Formation damage and the crystal chemistry of clays. *In* F. J. Longstaffe (ed.), Clays and the resource geologist; Mineralogical Association of Canada Short Course Handbook, v. 7, p. 81-103.

Baker, P. A., and Kastner, M., 1981. Constraints on the formation of sedimentary dolomite. Science, v. 213, p. 214-216.

Bodnar, R. J., Reynolds, T. J., and Kuehn, C. A., 1985. Fluid-inclusion systematics in epithermal systems. *In* Berger, B. R., and Bethke, P. M., *(eds.)* Geology and geochemistry of epithermal systems. Reviews in Economic Geology v. 2, p. 73-97.

Brownlow, A. H., 1979. Geochemistry. Prentice-Hall, Inc. Englewood Cliffs, New Jersey. 498 p..

Bustin, R. M., 1984. Coalification levels and their significance in the Groundhog Coal field, north-central British Columbia. International Journal of Coal Geology, v. 4, p. 21-44.

Bustin, R. M. 1991. Organic maturity in the western Canada sedimentary basin. International Journal of Coal Geology, v. 19, p. 319-358..

Bustin, R. M., and Moffat, I. 1983. Groundhog Coalfield, British Columbia: reconnaissance stratigraphy and structure. Bulletin of Canadian Petroleum Geology, 31: 231-245.

Bustin, R. M., and Moffat, I, W., 1989. Semianthracite, anthracite and meta-anthracite in the central Canadian Cordillera: their geology, characteristics and coalification history. International Journal of Coal Geology, v. 13, p. 303-326.

Bustin, R. M., Barnes, M. A., and Barnes, W. C., 1990. Determining levels of organic diagenesis in sediments and fossils fuels. *In* McIlreath, I. A. and Morrow, D. W. (*eds.*) Diagenesis. Geoscience Canada Reprint Series 4, p. 205-226.

Carothers, W. W., Adami, L. H., and Rosenbauer, R. J., 1988. Experimental oxygen isotope fractionation between siderite-water and phosphoric acid liberated $CO_2$. Geochimica and Cosmochimica Acta, v. 52, p. 2445-2450.

Carothers, W. W., and Kharaka, Y. K., 1978. Aliphatic acid anions in oilfield waters-implications for the origin of natural gas. American Association of Petroleum Geologists Bulletin, v. 62, p. 2431-2441.

Chonchawalit, A., 1993. Basin analysis of Tertiary strata in the Pattani basin, Gulf of Thailand. Ph.D.

thesis, The University of British Columbia, 366 p.

Cookenboo, H. O., 1989. Lithostratigraphy, palynostratigraphy, and sedimentology of the northern Skeena Mountains and their implications to the tectonic history of the Canadian Cordillera. MSc. thesis, University of British Columbia, Vancouver British Columbia. 131 p.

Cookenboo, H. O., and Bustin, R. M., 1989. Jura-Cretaceous (Oxfordian to Cenomanian) stratigraphy of the north-central Bowser Basin, northern British Columbia: Canadian Journal of Earth Sciences, v. 26, p. 1001-1012.

Eisbacher, G. H., 1974. Sedimentary and tectonic evolution of the Sustut and Sifton Basins, north-central British Columbia. Geological Survey of Canada Paper 73-31, 57 p.

Eisbacher, G. H., 1981. Late Mesozoic-Paleogene Bowser Basin Molasse and Cordilleran tectonics, Western Canada. *In* A D. Miall (*ed.*), Sedimentation and Tectonics in Alluvial Basins. Geological Association of Canada, Special Paper 23, p. 123-151.

Fisher, R. S., and Land, L. S., 1986. Diagenetic history of Eocene Wilcox sandstones, south-central Texas. Geochimica and Cosmochimica Acta, v. 50, p. 551-561.

Foscolos, A. E., 1985. Catagenesis of argillaceous rocks. *In* McIlreath, I. A. and Morrow, D. W. (*eds.*) Diagenesis. Geoscience Canada Reprint Series 4, p. 177-188.

Friedman, G. M., Amiel, A. J., and Schneidermann, N. A., 1974. Submarine cementation in reefs: example from the Red Sea. v. 44, p. 816-825.

Friedman, G. M., Sanders, J. E., and Kopaska-Merkel, D. C., 1992. Principles of sedimentary deposits. Maxwell Macmillan Company, Toronto. 717 p.

Friedman, I., and O'Neil, J. R., 1977. Compilation of stable isotope fractionation factors of geochemical interest. *In* . Fleischer, M. (*ed.*), Data of Geochemistry, sixth edition. United States Geological Survey Professional Paper 440-kk, 12 p.

Galloway, W. E., 1974. Deposition and diagenetic alteration of sandstone in northeast Pacific arc-related basins: implications for graywacke genesis. Geological Society of America Bulletin, v. 85, p. 379-390.

Gat, J. R. 1980. The isotopes of hydrogen and oxygen precipitation. *In* Handbook of Environmental Isotope Geochemistry Fritz, P. and Fontes, J. Ch., (*eds*), v. 1, p 21-48.

Gautier, D. L., and Claypool, G. E., 1984. Interpretation of methanic diagenesis in ancient sediments by analogy with processes in modern diagenetic environments. *In* McDonald, D. A., and Surdam,

R. C., (*eds.*) Clastic Diagenesis. American Association of Petroleum Geologists Memoir 37, p. 111-123.

Hanor, J. S., 1980. Dissolved methane in sedimentary brines: potential effect on the PVT properties of fluid inclusions: Economic Geology, v. 75, p. 603-609.

Hanor, J. S., 1987. Origin and migration of subsurface brines. Society of Economic Paleontologists and Mineralogists. Short Course Notes v. 21, 247 p.

Hardie, L. A., 1987. Dolomitization: a critical view of some current views. Journal of Sedimentary Petrology, v. 57, p. 166-168.

Hesse, R. 1990. Silica diagenesis: origin of inorganic and organic replacement cherts. *In* McIlreath, I. A. and Morrow, D. W. (*eds.*) Diagenesis. Geoscience Canada Reprint Series 4, p. 253-275.

Hunt, J. M., 1979. Petroleum Geochemistry and Geology. W. H. Freeman and Company, San Francisco. 617 p.

Jahren, J. S. and Aagaard, P., 1989. Compositional variations in diagenetic chlorites and illites, and relationships with formation-water chemistry. Clay Minerals, v. 24, p. 157-170.

Longstaffe, F. J., 1989. Stable isotopes as tracers in clastic diagenesis. *In*: Hutchinson, I. E. (*ed.*), Short Course in Burial Diagenesis, Mineralogical Association of Canada Short Course Series, v. 15, p. 201-277.

MacLeod, S. E., and Hills, L. V. 1990. Conformable Late Jurassic (Oxfordian) to Early Cretaceous strata, northern Bowser Basin, British Columbia: A sedimentological and paleontological model. Canadian Journal of Earth Sciences, v. 27: 988-998.

Moffat, I. W., and Bustin, R. M., 1993. Deformational history of the Groundhog Coalfield, northeastern Bowser Basin, British Columbia: styles, superposition and tectonic implications. Bulletin of Canadian Petroleum Geology, v. 41, p. 1-16.

Moffat, I. W., Bustin, R. M., and Rouse, G. E. 1988. Biochronology of selected Bowser Basin strata: tectonic significance. Canadian Journal of Earth Sciences, v. 25, p. 1571-1578.

North, F. K., 1985. Petroleum Geology. Allen and Unwin, London. 607 p.

Odin, G. S. and J. P. Masse, 1988. The verdine facies from the Senegalese continental shelf. *In* Odin, G. S. (*ed.*) Green Marine Clays. Developments in sedimentology v. 45. Elsevier, New York, p. 83- 106.

Palmer, A. R., 1983. The decade of North american geology 1983 geological time scale. Geology, v. 11, p.503-504.

Pittman, E. D., 1988. Diagenesis of Terry Sandstone (Upper Cretaceous), Spindle Field, Colorado. Journal of Sedimentary Petrology, v. 58, p. 785-800.

Raiswell, R., 1971. The growth of Cambrian and Liassic concretions. Sedimentology, v. 17, p. 147-171

Raiswell, R., 1988. Chemical model for the origin of minor limestone-shale cycles by anaerobic methane oxidation. Geology, v. 16, p. 641-644.

Roedder, E., 1974. Composition of Fluid Inclusions. United States Geological Survey Professional Paper 440JJ, 164 p.

Roedder, E., 1984. Fluid Inclusions. *In* Ribbe, P. H., (*ed.*), Reviews in Mineralogy, Mineralogical Society of America, v. 12, 644 p.

Seyfried, W. E., Bendt, M. E., and Seewald, J. S., 1988. Hydrothermal alteration processes at mid-ocean ridges: constraints from diabase alteration experiments, hot-spring fluids, and compositions of the oceanic crust. Canadian Mineralogist, v. 26, p. 787-804.

Small, J. S., Hamilton, D. L., and Habesch, S., 1992. Experimental simulation of clay precipitation within reservoir sandstones 1: Techniques and examples. Journal of Sedimentary Petrology, v. 62, p. 520-529.

Smosna, R., 1988. Low-temperature, low-pressure diagenesis of Cretaceous sandstones, Alaskan North Slope. Journal of Sedimentary Petrology, v. 58, p. 644-655.

Surdam, R. C. and Crossey, L. J., 1985. Mechanisms of organic/inorganic interactions in sandstone/shale sequences. *In* Gautier, D. L., Kharaka, Y. K., and Surdam, R. C. (*eds.*) Relationship of organic matter and mineral diagenesis. Society of Economic Paleontologists and Mineralogists short course v. 17, p. 177-232.

Surdam, R. C., and MacGowan, D. B., 1987. Oilfield waters and sandstone diagenesis. Applied Geochemistry, v. 2, p. 613-619.

Sweeney, J. F., Stephenson, R. A., Currie, R. G., and DeLaurier, J. M., 1992. Tectonic Framework Part C. Crustal Geophysiscs. *In* Gabrielse, H., and Yorath C. J. (*eds.*), Geology of the Cordilleran Orogen in Canada. Geological Society of America's Geology of North America, v. G-2, p. 39-58.

Thomas, J. B., 1981. Classification of clay minerals in tight gas sandstones: case studies in which clay

minerals are crucial to drilling fluid selection, formation evaluation, and completion techniques. *In* F. J. Longstaffe (ed.), Clays and the resource geologist; Mineralogical Association of Canada Short Course Handbook, v. 7, p. 104-118.

Tissot, B. P. and Welte, D. H., 1984. Petroleum Formation and Occurrence. Springer-Verlag, New York,. 699 p.

Trevena, A. S., and Clark, R. A., 1986. Diagenesis of sandstone reservoirs of Pattani Basin, Gulf of Thailand. American Association of Petroleum Geologists Bulletin, v. 70, p. 299-308.

Tye, R. S. and Coleman, J. M., 1989. Depositional processes and stratigraphy of fluvially dominated lacustrine deltas; Mississippi delta plain. Journal of Sedimentary Petrology, v. 59, p. 973-996.

Wilkinson, M. 1993. Concretions of the Valtos Sandstone Formation of Skye: geochemical indicators of palaeo-hydrology. Journal of the Geological Society, London, v. 150, p. 57-66.

Yurtsever, Y. 1975. Worldwide survey of stable isotopes in precipitation. Rep. Sect. Isotope Hydrology, International Atomic Energy Agency, 40 p.

# CHAPTER 6

## CONCLUDING REMARKS

Lithofacies, provenance, and diagenetic studies (chapters 2, 3, 4, and 5) support a deep basin fill model of Bowser Basin development. This model suggests the sediments themselves may have largely controlled the tectonic development of the Bowser Basin until after deposition of the youngest preserved strata (Devils Claw Formation). By this model, Bowser Lake Group sedimentation began in a deep marine basin, possibly of typical oceanic depths (3000 to 4000 m), and sediments built up to near sea-level, forming a shelf by the Late Jurassic. Sediments exposed in the study area accumulated above the shelf and deeper marine basin fill. Accommodation space was created by subsidence primarily due to the combined action of sediment compaction and isostatic adjustment. The major conclusions from each chapter that pertain to this basin model are reviewed below, and later discussed in relation to a collapsed margin model of Cordilleran accretion.

Lithofacies successions demonstrate that Bowser Basin sediments accumulated as fill in a pre-existing deep oceanic basin. North of the study area, Bathonian and Callovian (Middle Jurassic) basinal and slope clastics (Ricketts, 1990) overlie Bajocian (Middle Jurassic) and older deep marine clastic and volcaniclastic equivalents to arc volcanic rocks exposed along the Stikine Arch. Similar Lower to Middle Jurassic oceanic arc volcanics and basinal sediments are exposed on the western (Lewis, *et* al., 1993), southern (Tipper and Richards, 1976) and eastern margins of the Bowser Basin. Within the study area, more than 3000 m of Oxfordian (Upper Jurassic) to Albian (Lower Cretaceous) sediments accumulated, overlying the deep marine sediments exposed to the north. Lithofacies associations described in this study indicate that these sediments accumulated in shelf, deltaic and alluvial coastal plain environments. Notably, all the sediments in the study area are interpreted to be near sea-level deposits.

Accumulation of more than 3000 m of shelf, delta, and coastal plain deposits requires creation of near sea-level sediment accommodation space. Because sediments exposed in the study area accumulated over deep basinal fill, sediment compaction and isostatic subsidence of the basin must have

contributed to the accommodation space. The amount of subsidence attributable to sediment compaction and isostatic subsidence largely depends on the initial depth of the oceanic basin, which is poorly constrained. Calculations were made of sediment compaction and isostatic subsidence assuming various initial depths for the Bowser Basin (Chapter 2). These calculations suggest that by filling a pre-existing basin with initial depths of 3000 to 4000 m (typical of modern open ocean, back-arc and interarc basins; Shupe, 1992), accommodation space sufficient to contain the entire preserved near sea-level sedimentary record exposed in the study would be created by compaction and isostatic adjustment. Initial depths of 2000 m result in roughly 2000 m of compaction and isostatic subsidence, enough to accommodate the marine shelf, lower delta plain and one half of the upper delta plain facies associations. Filling a 1000 m initial depth basin only accommodates 850 m of near sea-level deposits, enough to account for the shelf and part of the lower delta plain accumulation. A sediment-controlled model consistent with these calculations and the observed lithofacies can, therefore, explain the tectonic development of the Bowser Basin until after the youngest preserved strata (Devils Claw Formation) were deposited. By this sediment-controlled model, the entire sediment record preserved in the study area was accommodated by sediment compaction and isostatic adjustment resulting from filling a typical marine basin of 3000 to 4000 m initial depth. Alternatively, outside tectonic forces such as thrust loading (c.f. Ricketts *et al.*, 1993) or thermal subsidence must be invoked if initial water depths were less than 2000 m.

Sandstone provenance described in chapters 3 and 4 supports an oceanic setting for the Bowser Basin. Interpretation of framework grain modal analysis (chapter 3) suggests the provenance was obducted oceanic lithosphere and (at least mostly) inactive island arc volcanics. Recycled sediment and minor plutonic and metasedimentary indications not observed in Upper Jurassic sandstones appear in the Lower Cretaceous sediments, but the original (first cycle) sediment source remained the same island arc and oceanic lithosphere throughout the preserved strata. Microprobe analysis of detrital chromian spinels in the sandstones (chapter 4) supports an oceanic origin for the strata, and suggests that the obducted oceanic lithosphere originated in a marginal basin setting (suprasubduction zone) rather than at a mid-ocean ridge. Furthermore, erosion of the obducted oceanic strata probably occurred prior to any high

grade (greenschist) metamorphic events affected the source rocks.

In summary, the provenance was obducted island arc assemblages and marginal basin lithosphere. Current directions indicate the obducted source rocks were north and northeast of the study area (Eisbacher, 1981; Cookenboo, 1989), and therefore between the North American craton and the Bowser Basin. The setting of the Bowser Basin was seaward of obducted oceanic terranes. Accumulation of Bowser Basin sediments in a pre-existing basin of typical oceanic depths, as suggested by the lithofacies analysis in chapter 2, is reasonable given the oceanic provenance. Subsidence controlled by compaction/isostatic load as modelled in chapter 2 is compatible, therefore, with both the lithofacies and the provenance studies.

Diagenetic studies (chapter 5) are the basis of a model of pore water evolution for the Bowser Basin that is consistent with accumulation in a deep ocean basin. Pore fluid chemistry was interpreted from sandstone cement paragenesis and mudstone concretion geochemistry as a record of pore water evolution. Pore waters in the sandstones evolved from alkaline marine or brackish waters at or soon after burial, to acidic waters associated with organic maturation occurring interbedded mudstones (80° to 200°C), and back to alkaline waters after thermal breakdown of organic acids at temperatures above 200°C. Anthracite coals in the study area suggests a relatively high paleogeothermal gradient. Maturation modelling described in chapter 5 is compatible with a paleogeothermal gradient of 65°C/km, and maximum temperatures of slightly more than 300°C for the lower part of the exposed strata (500 m below the base of the Currier Formation). The progressive increase of temperature from initial burial to in excess of 200°C (as recorded by the pore water evolution), and peaking near 300°C (as recorded by vitrinite reflectance), suggests heating due to progressive burial in a high paleogeothermal gradient regime such as typifies oceanic settings.

Progressive burial in a high paleogeothermal gradient regime is compatible with the deep oceanic basin setting for the Bowser Basin postulated from the lithofacies and provenance considerations described earlier. Other settings with high paleogeothermal gradients, such as some continental rift

basins, could satisfy the maturation model in chapter 5, but lithofacies in such settings tend to change from older alluvial deposits to younger marine facies, rather than the deep to marginal marine and alluvial succession in the Bowser Basin. Sandstone compositions in continental rift basins are also likely to be incompatible with those of the Bowser Basin, because rift basins tend to have at least in part a cratonic provenance.

The model of Bowser Basin origin and tectonic development postulated earlier in this chapter is compatible with the multiple lithofacies, provenance and diagenetic conclusions of this thesis. The model is also compatible with a collapsed margin model of Cordilleran development. As put forward here, such a model for Cordilleran tectonic development suggests that marginal seas and fringing island arcs to the west of the North American craton accreted to the continental margin after the latest Triassic/earliest Jurassic change in plate motion (Ekstrand and Butler, 1989). Obduction of the island arcs and parts of the marginal basin lithosphere exposed the Bowser Basin provenance to erosion by the Middle Jurassic. Such a history of accretion has been described for the southern Canadian Cordillera, with the Slide Mountain and Quesnellia terranes obducting onto the continental margin during the Early and Middle Jurassic (Murphy, 1989), and the Cache Creek terrane obducting onto Quesnellia in the Middle and Late Jurassic (Mortimer *et al.*, 1990). Following obduction of eastern oceanic terranes, continued North American plate motion towards the Pacific Ocean (as recorded by the continued rifting of the Atlantic Ocean) requires an arc to the west of the Bowser Basin. The sandstone provenance for Gravina-Nutzotin sediments of southeast Alaska record such an active island arc west of the Bowser Basin during the Late Jurassic and Early Cretaceous (Cohen and Lundberg, 1988). The Coast Plutonic Complex (CPC) may be the magmatic record of the required arc to the west of the Bowser Basin, because portions of the CPC were forming above east dipping subduction during the Late Jurassic and Early Cretaceous (van der Heyden, 1989). Compressional deformation of the Bowser Basin began in the Late Cretaceous following deposition of the Devils Claw Formation (Moffat and Bustin, 1993), contemporaneous with major Late Cretaceous magmatic activity in the CPC (van der Heyden, 1989). By Campanian and Maastrichtian time (latest Cretaceous), the Bowser Basin was apparently uplifted and

shedding sediments to the east into the Sustut basin (Eisbacher, 1981; Bustin and McKenzie, 1989).

# REFERENCES

Bustin, R. M., and McKenzie, K. J., 1989. Stratigraphy and depositional environments of the Sustut Group, southern Sustut Basin, northcentral British Columbia. Bulletin of Canadian Petroleum Geology, v. 31, p. 231-245.

Cohen, H. A., and Lundberg, N., 1988. Sandstone petrology of the Seymour Canal formation (Gravina-Nutzotin Belt): Implications for the accretion history of southeast Alaska [abs.,]:. Geological Society of America Abstracts with Programs, v. 20, p. 163.

Eisbacher, G. H., 1981. Late Mesozoic-Paleogene Bowser Basin Molasse and Cordilleran tectonics, Western Canada. *In* A D. Miall (*ed.*), Sedimentation and Tectonics in Alluvial Basins. Geological Association of Canada, Special Paper 23, p. 123-151.

Ekstrand, E. J. and Butler, R. F., 1989, Paleomagnetism of the Moenave Formation: Implications for the Mesozoic North American apparent polar wander path: Geology, v. 17, p. 245-248.

Lewis, P. D., Thompson, J. F. H., Nadaraju, G., R. G. Anderson, and G. G. Johnson, 1993. Lower and Middle Jurassic stratigraphy in the Treaty Glacier area and geological setting of the Treaty Glacier alteration system, northwestern British Columbia. Geological Survey of Canada Current Research Part A, Paper 93-1A, p. 75-86.

Moffat, I. W., and Bustin, R. M., 1993. Deformational history of the Groundhog Coalfield, northeastern Bowser Basin, British Columbia: styles, superposition and tectonic implications. Bulletin of Canadian Petroleum Geology, v. 41, p. 1-16.

Mortimer, N., van der Heyden, P., Armstrong, R. L., and Harakal, J., 1990. U-Pb and K-Ar dates related to the timing of magmatism and deformation in the Cache Creek terrane and Quesnellia, southern British Columbia. Canadian Journal of Earth Sciences, v. 27, p. 117-123.

Murphy, D., C., 1989. Crustal paleo-rheology of the southwestern Canadian Cordillera and its influence on the kinematics of Jurassic convergence. Journal of Geophysical Research, v. 94, p. 15723-15739.

Ricketts, B. D. 1990, A preliminary account of sedimentation in the lower Bowser Lake Group, northern British Columbia, in Current Research, Part F, Geological Survey of Canada, Paper 90-1F, p. 145-150.

Ricketts, B. D., Evenchick, C. A., Anderson, R. G., and Murphy, D. C., 1993. Bowser Basin, northern British Columbia: constraints on the timing of initial subsidence and Stikinia-North America terrane interactions. Geology, v. 20, p. 1119-1122.

Shupe, J. F., 1992. Worlds oceans floors: Pacific Ocean and Indian Ocean. Graves, W. (*ed.*), map. National Geographic Society.

Tipper, H. W. and Richards, T. A., 1976. Jurassic stratigraphy and history of north-central British Columbia. Geological Survey of Canada, Bulletin 270, 73 p.

van der Heyden, P., 1989. U-Pb and K-Ar geochronometry of the Coast Plutonic Complex, 53°N to 54°N, British Columbia, and implications for the Insular-Intermontane superterrane boundary. Ph.D. thesis, the University of British Columbia, Vancouver British Columbia. 392 p.

# APPENDIX 1

## CONFORMABLE LATE JURASSIC (OXFORDIAN) TO EARLY CRETACEOUS STRATA, NORTHERN BOWSER BASIN, BRITISH COLUMBIA: DISCUSSION

MacLeod and Hills' (1990a) article entitled "Conformable Late Jurassic (Oxfordian) to Early Cretaceous strata, northern Bowser Basin, British Columbia: A sedimentological and paleontological model" makes an important contribution to understanding the complex geologic history of the northern Bowser basin. They have reported insightful sedimentologic descriptions and comprehensive plant macrofossil collections. Errors in stratigraphic nomenclature and incompleteness in their treatment of previously published paleontologic data, however, led them to propose revisions to the age and conformity of the strata that I feel warrants further discussion. I am pleased to have this opportunity to discuss these points in light of recent research in the area and to be allowed to relate my best understanding of the stratigraphic relationships.

Three specific concerns with MacLeod and Hills (1990a) that I wish to discuss are: (1) erroneous application of published stratigraphic nomenclature (for example, inadvertently assigning the Currier Formation type section to the McEvoy Formation); (2) incomplete discussion of previously published paleontologic data with direct bearing on the age of the strata (most importantly omission of reference to the late Oxfordian to early Kimmeridgian ammonite *Amoeboceras* recovered from within the coal measures, calling into question their conclusion that the Currier Formation is entirely Early Cretaceous); and (3) comparisons with plant macrofossils collected elsewhere in western Canada which do not always utilize the most current age estimates of those strata (at least five out of seven "Neocomian" and "Aptian" floras from outside the northern Bowser basin in Figure 9 from MacLeod and Hills (1990a) occur in stratigraphic units that extend into the early or middle Albian, calling into question their conclusion of a pre-Albian age for strata in the northern Bowser basin). In the following discussion, I will explore these points more completely, and then conclude by presenting my best resolution of the data, based on work by myself and Moffat *et al.* (1988), and my understanding of MacLeod and Hills' data.

**1) Errors in stratigraphic nomenclature**

The first point I will discuss is the misapplication of previously published stratigraphic names (Cookenboo and Bustin 1989). This point may be the most important in as much as, without consistency of usage, no comparison of work between authors can be meaningful. For this reason, formal descriptions, including type section localities were published in Cookenboo and Bustin (1989) for each of the formalized stratigraphic units. The location of the Currier type section described in Cookenboo and Bustin (1989, p. 1007) as "southwest of Mount Klappan between the headwaters of the Little Klappan River, Tahtsedle Creek, and Didene Creek (lat. 57°11'30''N, long. 129°0'50''W)" and shown in map view (Figure 2 of the same article) plots in the middle of "McEvoy" on MacLeod and Hills' (1990a) map (Fig. A1-1a). A map resulting from detailed field work in the area shows that McEvoy Formation strata are restricted to only the top of the ridge where the Currier Formation type section is located (Fig. A1-1b; Moffat, 1985). Although none of MacLeod and Hills' section locations are included in their recent article, additional photographs were presented by MacLeod and Hills (1990b) which clearly show that the Currier type section had been extensively sampled, but MacLeod and Hills (1990a, 1990b) incorrectly included those samples in their McEvoy floral collections. One effect of this error in stratigraphic nomenclature is to mix Currier and McEvoy plant collections, and thereby mask any age differences that may exist between the stratigraphic units. This mixing of stratigraphic units is compounded in MacLeod and Hills' (1990a) comparison of flora with other occurrences in western Canada. As shown in their Figure 9 (MacLeod and Hills 1990a, p. 996), the McEvoy and Devils Claw Formations are treated as one unit ("McEvoy-Devils Claw flora"), but as I have already remarked, plants collected from part of the Currier were included in their McEvoy flora. MacLeod and Hills (1990a, pp. 994, 995) conclude that "There are no floral breaks either within or between the Currier and McEvoy formations" and that "The conformable nature of the entire Jackson to Devils Claw stratigraphic sequence is further supported by the apparent continuity of macrofloras across the Currier-McEvoy boundary." Given their mixing of defined stratigraphic nomenclature, I feel such conclusions are unsupported. I believe this error may be traced to MacLeod and Hills' attempt to directly equate informal stratigraphic units developed by Gulf Canada Resources Limited (1984)

Figure A1-1: The location of the Currier Formation type section. Map A is from MacLeod and Hills (1990a) where the Currier type section plots in what are called "McEvoy" strata, and map B is a detail from field mapping by Moffat (1985). Mapped lithostratigraphic units are: Kdc= Devils Claw; Kmu= upper McEvoy; Kml= lower McEvoy; Jc= Currier; and Jj= Jackson.

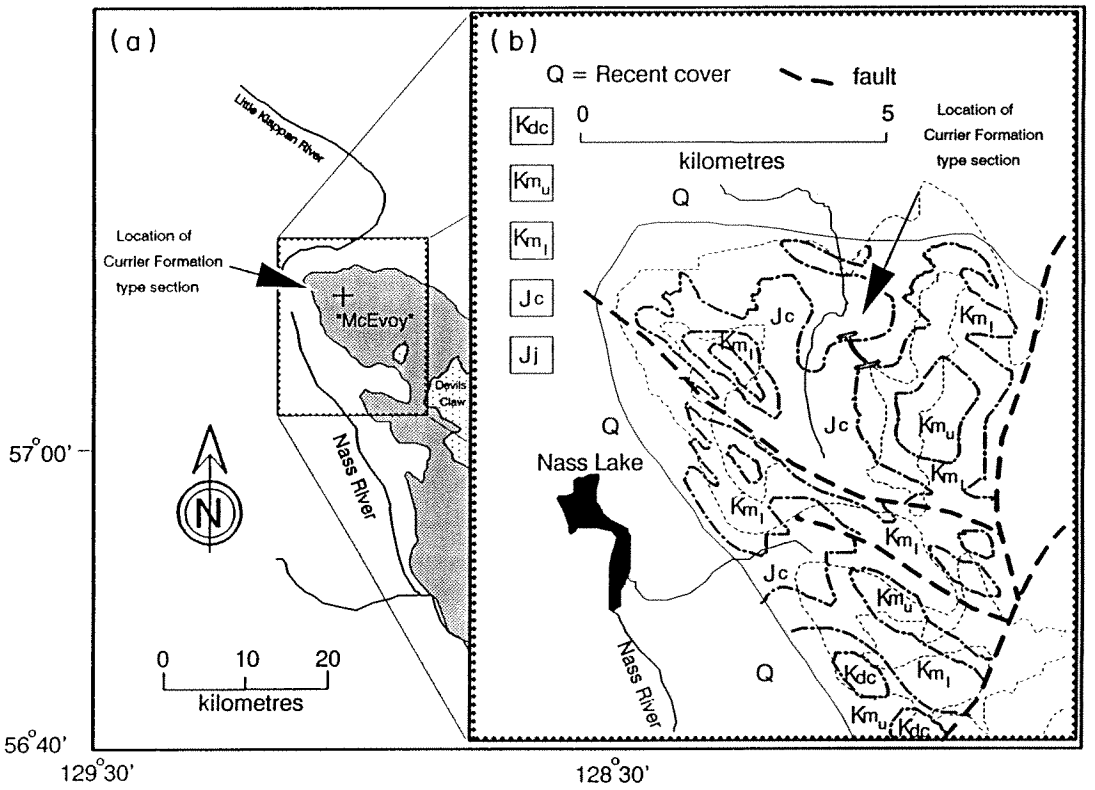

during their exploration of the Klappan coalfield to published formations (Cookenboo and Bustin 1989). Gulf used a similar four unit division of the stratigraphy, but the stratigraphic boundaries chosen as contacts were not equivalent to ours. Gulf's coal-bearing unit (referred to as the Klappan unit in unpublished coal reports; Gulf Canada Resources Limited 1984, 1987) started with the first thick coal and ended with the last thick coal. The Currier's contact with the McEvoy, however, was described as "...the appearance of thin- to thick- bedded light grey, fine sandstones of limited lateral extent, thick siltstones, shales, and occasional pebbly conglomerates, as well as a marked reduction in coal" (Cookenboo and Bustin 1989, p. 1005). The upper part of the Currier Formation, which is well exposed in the type section, in fact has few thick coals.

Coal-bearing strata that previously were treated as part of the informal upper Jackson unit (Moffat 1985; Moffat *et al.* 1988; Cookenboo and Bustin 1989) were included in the Currier Formation by MacLeod and Hills (1990a). The same revision in nomenclature (effectively lowering the basal contact of the Currier to include all of the coal-bearing strata (Fig. A1-2), some of which were previously included in the upper portion of the underlying Jackson unit) was anticipated by Cookenboo and Bustin (1990), leaving me in complete agreement regarding the most useful definition of the base of the Currier Formation. This lower part of the Currier Formation, which is poorly exposed in the type section, contains much of the coal, and may be more closely equated with Gulf's informal Klappan unit. Equating the informal Klappan unit with the Currier Formation as defined in Cookenboo and Bustin (1989) may have led MacLeod and Hills to inadvertently exclude the Currier type section (and presumably other equivalent strata) from the Currier Formation, and to include those strata in the McEvoy Formation. MacLeod and Hills' "Currier" designation therefore may correctly represent a consistent and mappable lithostratigraphic unit, but it is invalid because it incorrectly uses a previously defined formation name.

I wish to emphasize that differences I have pointed to between MacLeod and Hills' (1990a) stratigraphy and that found in earlier publications about the area (Cookenboo and Bustin 1989; Moffat et al. 1988) relate to nomenclature, specifically the misuse of defined stratigraphic names. I do not dispute their geologic descriptions or interpretations, rather I point out that in their comparison

Figure A1-2: Stratigraphic nomenclature used by various authors in the coal-bearing section of the northern Bowser basin.

<table>
<tr><th>Bustin and Moffat (1983)</th><th>Moffat (1985) Moffat et al. (1988)</th><th>Cookenboo and Bustin (1989)</th><th>This discussion and Cookenboo and Bustin (1990)</th><th>Discussion paper and MacLeod and Hills (1990)</th><th>Gulf Canada Resources Ltd. (1984, 1987)</th></tr>
<tr><td>Devils Claw unit</td><td>Devils Claw unit</td><td>Devils Claw Formation</td><td>Devils Claw Formation</td><td>Devils Claw Formation</td><td>Devils Claw</td></tr>
<tr><td>McEvoy unit</td><td>McEvoy unit</td><td>McEvoy Formation</td><td>McEvoy Formation</td><td rowspan="2">McEvoy Formation</td><td rowspan="2">Malloch</td></tr>
<tr><td rowspan="2">Currier unit</td><td>Currier unit</td><td>Currier Formation</td><td rowspan="2">Currier Formation</td></tr>
<tr><td>upper Jackson unit</td><td>? upper Jackson unit</td><td>Currier Formation</td><td>Klappan</td></tr>
<tr><td>Jackson unit</td><td>Jackson unit</td><td>Jackson unit</td><td>Ashman Formation</td><td>Jackson unit</td><td>Spatsizi</td></tr>
</table>

of results with previous work, they are in part referring to the same rocks by different names. I believe it is important to point this out, or great confusion may result among interested readers.

Perhaps renaming MacLeod and Hills' "Currier" the Klappan member of the lower Currier Formation would eliminate much of the stratigraphic confusion. Their usage of "McEvoy" should be discontinued because it includes both the upper strata of the Currier Formation and the strata that were actually defined as the McEvoy Formation.

**2) Omission of relevant paleontological data**

The second point I wish to raise is the omission in MacLeod and Hills (1990a) of relevant previously published paleontologic data. Perhaps the most significant omission is that of the recovery of the Late Jurassic ammonite *Amoeboceras* identified by P. Smith (personal communication, in Moffat and Bustin 1984) and H. Tipper (personal communication, in Moffat et *al.* 1988). The photograph reproduced in figure A1-3 was not included in the article by Moffat et *al.* (1988) because one reviewer suggested it added little. This ammonite was recovered from within the coal-bearing strata 20 m below the top of the informal Jackson unit, as the term was applied by Moffat (1985). A coal seam 1 to 1.5 m thick crops out immediately below, placing the strata within the Currier Formation, as used by MacLeod and Hills (1990a). Elsewhere in Canada, *Amoeboceras* occurs in the black shale facies of the Upper Bowser Lake Group (Tipper and Richards 1976), in the Upper Oxfordian Passage beds in the Fernie Group near Jasper, Alberta, and in the Upper Oxfordian green beds of the Fernie Group near Carbondale River, Alberta, where it is associated with *Buchia concentrica* (Frebold and Tipper 1970; Hall 1984). In the Arctic, *Amoeboceras* is known from strata only as young as the early Kimmeridgian (Frebold 1961), strongly suggesting the Currier is not entirely Early Cretaceous.

Seemingly dismissed by MacLeod and Hills (1990a) are previously reported palynomorph assemblages recovered from the McEvoy and Devils Claw Formations. Three assemblages, assigned a Barremian age (G. E. Rouse, personal communication, in Cookenboo and Bustin 1989), a middle Albian age (Moffat *et al.* 1988) and a Cenomanian age (G. E. Rouse personal communication, in Cookenboo and Bustin 1989) all contained angiosperm microflora (figured in Moffat *et al.* 1988). The oldest (Barremian) assemblage was recovered 35 m from the base of the McEvoy Formation

Figure A1-3: The upper Jurassic ammonite *Amoeboceras* recovered from the coal-bearing section in the northern Bowser basin (1.5x). The tabulate venter (not seen here) bears a serrated keel.

from rocks just above the Currier type section, and 200 m above the last sample of Jurassic dinoflagellates recovered from the Currier type section. Barremian palynomorphs 35 m above the base of the McEvoy Formation (and directly overlying the Currier type section) and a middle Albian palynomorph assemblage in the overlying Devils Claw Formation (Moffat *et al.* 1988) led to the suggestion that the McEvoy was Barremian to mid-Albian (Cookenboo and Bustin 1989). A suggested Cenomanian age for a palynomorph assemblage from higher in the Devils Claw Formation (G. E. Rouse, personal communication, *in* Cookenboo and Bustin 1989) led to an assigned age range of late middle Albian to Cenomanian for the Devils Claw Formation (Cookenboo and Bustin 1989). Based on published palynological assemblages, the McEvoy and Devils Claw Formations together range from Barremian to Cenomanian in age (Moffat *et al.* 1988; Cookenboo and Bustin 1989). This age range is older, in part, than "the Albian to Cenomanian age" MacLeod and Hills (1990a, p. 995) mistakenly attributed to Moffat et *al.* (1988) for these units. Further unpublished work has caused me to amend the range slightly to late Barremian or Aptian to latest Albian or Cenomanian.

**3) Comparisons with other plant macrofossil collections**

The third and final point concerns the ages of leaf collections from elsewhere in western Canada that MacLeod and Hills (1990a) compare to the Currier, McEvoy and Devils Claw flora. MacLeod and Hills (1990a) closely follow Bell (1956) who assigned Neocomian and Aptian ages to leaf fossil collections from a number of units. More recently published ages for the same stratigraphic units based on criteria other than plant macrofossils, including palynology, ammonites, trigonids, buchias, and K-Ar dates, have yielded a new perspective on the age of some of these units. Five of the seven stratigraphic units containing the floras (excluding the mixed Currier, McEvoy and Devils Claw floras) listed in Figure 9 of MacLeod and Hills (1990a) as being Aptian or Neocomian in age, extend to the early or middle Albian (specifically the Gething, Lower Blairmore, Jackass Mountain, Tantalus, and Skeena floras; Stott 1963, 1968, 1982; Jeletzky and Tipper 1968; Tipper and Richards 1976; Kleinspenh 1985; Lowey and Hills 1988).

The earliest and perhaps best documented claim that Bell's (1956) "Aptian" flora occurs in early

or middle Albian age strata was made by Stott (1963) for the Gates Formation in the WCSB. Stott (1968, pp. 76-77) later named 41 plant forms that were identified by Bell, D. C. McGregor, and F. M. Hueber as "Luscar (Aptian)" flora. Bell (1956, pp. 10-11: quoted in Stott 1968) concluded that "the extreme rarity of dicotyledons within it, together with the survival of many species occurring in the Kootenay flora, certainly favors the Aptian age.", but Stott showed conclusively that the Gates Formation overlies marine shales of the Moosebar, which contains marine fauna of middle Albian age. Jeletzky and Tipper (1968), writing about the Jackass Mountain Group, recognized the controversy about whether Bell's "Aptian" flora is really Aptian or Albian and concluded "In this report, the strata containing this flora will be considered Aptian fully realizing that some or all of these rock units may be middle or lower Albian in age." (Jeletzky and Tipper 1968, p. 47). Caldwell (1984) also recognized the "Aptian" flora age difficulty, and concluded "A survey of the literature conveys the impression that too great a reliance has been placed on the dominantly pre-Albian age suggested originally by the flora, despite an indistinguishable flora having been recovered from younger rocks of known Albian age." (Caldwell 1984, p. 187).

MacLeod and Hills' (1990a) conclusion that all of the McEvoy and Devils Claw Formations are pre-Albian in age rests largely on their assumption that leaf collections lacking angiosperm leaves are restricted to Aptian or older strata. Persistence until the late Albian of a flora lacking in angiosperms is well documented in northern Alaska (Smiley 1969a, 1969b; Spicer 1987). An estimated 10 000 specimens from 250 localities in the 3 000 m thick Nanushuk and Colville Groups of the north slope of Alaska were divided by Smiley (1969a, 1969b) into seven floral zones. The seven floral zones are dated by marine invertebrates and microfossils which were present in interbedded marine sediments. The two oldest floral zones range from middle Albian or older to late Albian in age and are dominated by pteridophytes, ginkgophytes, cycadophytes, and conifers. The first angiosperms appear in the third floral zone of late Albian to early Cenomanian age (Smiley 1969a; *Inoceramus dunveganensis* first occurs within the upper part of this floral zone). Angiosperms only become dominant components of the flora in the overlying fourth floral zone. A notable similarity with the McEvoy and Devils Claw Formations

is the intermittent occurrence of rare angiosperm palynomorphs in strata deposited before the first appearance of angiosperm leaves (May and Shane 1985). The occurrence of such a similar flora in other middle and late Albian rocks largely refutes MacLeod and Hills' argument that the composition of the Bowser basin flora precludes an Albian age for the McEvoy and Devils Claw Formations.

The difficulty in using plant macrofossils as a guide to age is partly due to the long-ranging nature of plant macrofossils. This long-ranging character is well demonstrated in MacLeod and Hills (1990a) Figure 4 which lists the worldwide and North American ranges of 16 "dominant plant fossils". As figured, only 4 species do not extend through the Albian. Furthermore, two of those four, *Sagenopteris williamsii* (Newberry) Bell and *Ctenis borealis* (Dawson), previously have been reported from the early Albian Gates Formation (Stott 1968). Contrary to MacLeod and Hills' (1990a, p. 994) statement that "Most of the 19 species that are common to both the Currier and McEvoy formations are also long-ranging, pre-Albian, Mesozoic taxa...", I conclude, based in part on their own data, that most or perhaps all sixteen species common to the Currier and McEvoy formations are long-ranging **through** the Albian.

Because the plant macrofossils are long-ranging, age assignments based on them must be based on paleofloristic abundance trends rather than extinction events. MacLeod and Hills demonstrate, based on their extensive macrofloral collections, that the Currier through Devils Claw floras are rich in cycadophytes and gingkophytes and contain only rare *Sagenopteris* leaves. Additionally, in all their floral collections no angiosperm leaves have been found. MacLeod and Hills (1990a) use these facts to suggest paleofloristic similarities to collections of leaves from the Western Canada Sedimentary Basin. Based on my understanding of the ages of these floras and the Alaskan North Slope flora described by Smiley (1969a, 1969b), I suggest that MacLeod and Hills' leaf collections are consistent with an age as young as middle or late Albian. A middle or late Albian age for part of the McEvoy and Devils Claw Formations is entirely consistent with the ages deduced from palynological data (including angiosperm pollen and dinoflagellate cysts figured in Moffat et *al.* 1988), and does not necessitate a reappraisal of the ages as MacLeod and Hills (1990a) propose.

Although MacLeod and Hills (1990a) assert that paleofloristic abundance trends suggest the McEvoy and Devils Claw are pre-Albian in age, I suggest that a better explanation of the paleofloristic trends they identify may be variations in climate. This seems especially likely because none of the "dominant plant macrofossils" demonstrably become extinct before the end of the Albian, and similar floras as young as late Albian are known. Vahkrameev (1978) recognized an abundant ginkgo and cycad flora, similar to that described by MacLeod and Hills, as indicative of a warm, temperate and humid climatic province. Perhaps the western margin of North America remained more temperate and humid (or perhaps simply less seasonal) longer into the Albian than did the Western Canada Sedimentary Basin, which was apparently separated from the Pacific during the Early Cretaceous by mountains of the mid-Columbian orogen (Stott 1982).

**My resolution of the data**

Considering the points I have raised, it seems incumbent upon me that I give my best resolution of the complete spectrum of published evidence bearing on the ages of the Currier, McEvoy and Devils Claw Formations. I will consider each unit separately, summarizing the data that I believe most relevant and trying, where possible, to achieve the most compatible interpretation of the varied data sets.

There are two apparently incompatible data sets that bear directly on the age of the Currier Formation. The ammonite *Amoeboceras* (Moffat *et al.* 1988) and dinoflagellates including *Nannoceratopsis sp., Pareodinia minuta, and Pareodinia* cf. *ceratophora* (Cookenboo and Bustin 1989), recovered from coal-bearing strata, suggest that the Currier is at least in part Late Jurassic. MacLeod and Hills (1990a) have produced specimens of *Buchia* from strata below the Currier, suggesting a Late Jurassic (Oxfordian to Tithonian) age, and the astariid bivalve *Herzogina*, previously known only from Neocomian strata, in the Currier Formation (MacLeod and Hills 1990a). Resolution of the paradox of latest Jurassic *Buchia* occurring stratigraphically below Kimmeridgian to Oxfordian ammonites appears possible in four ways: (1) some or all of the invertebrates and microfossils were mis-identified; (2) ammonite and dinoflagellate cysts were redeposited in younger strata; (3) age relations between Late Jurassic Buchias and *Amoeboceras* are less well known than previously thought; or (4) the

stratigraphy and structure is more complex than previously suspected. No evidence has been offered to suggest that any of the first three options apply. Given the complexity of the structure and stratigraphy in the northern Bowser basin, the fourth possibility seems most likely. Because the locations of the *Buchia* collections were not provided in MacLeod and Hills (1990a), suggestions to resolve this apparent contradiction may be premature, but perhaps the *Buchia* beds are not stratigraphically below all the coal-bearing strata and record a post- or late Currier marine transgression.

Resolution of the age of the Currier rests on several questions that are still open, but at present, it seems strongly indicated (based on the ammonite *Amoeboceras* and dinoflagellates recovered from the coal-bearing strata) that the Currier is in part Late Jurassic, and (based on the species of Buchias and *Herzogina*) may also be in part latest Jurassic and earliest Cretaceous.

The age of the McEvoy and Devils Claw formations can be resolved somewhat more satisfactorily by realizing that the "lower Blairmore-Luscar-Gething flora extends upward into rocks of middle Albian age." (Stott 1968, p. 77). A Barremian to middle Albian age for the McEvoy is consistent both with similar macroflora occurrences elsewhere in western North America and with published ages based on palynology. Palynomorphs recovered from the Devils Claw Formation are consistent with an age range of late middle Albian to latest Albian or Cenomanian.

Finally, I wish to give my view of the evidence for and against the existence of an unconformable contact between the Currier and McEvoy Formations. Cookenboo and Bustin (1989) suggested an age range of Oxfordian to Kimmeridgian or Tithonian for the Currier and Barremian to middle Albian for the McEvoy. MacLeod and Hills (1990a, p. 996) conclude that "The presence of *Herzogina* (Neocomian) near the base of the Currier Formation and a macroflora with a distinctly Early Cretaceous, pre-Albian age component in the Currier and overlying McEvoy and Devils Claw Formations eliminates the need for a major Kimmeridgian-Barremian [Kimmeridgian or Tithonian to Barremian is a more accurate representation of the proposal] unconformity in this area as proposed by Cookenboo and Bustin (1989)." I concur with MacLeod and Hills that their evidence fails to support an unconformity, but due to the long-ranging nature of the macroflora and the mixing of stratigraphic units by MacLeod and Hills, I believe that the data presented by MacLeod and Hills (1990a) are insufficient to

deny the existence of such an unconformity. Ammonite and palynological evidence for a Late Jurassic Currier and palynological evidence for a Barremian to Albian or Cenomanian McEvoy and Devils Claw is neither conclusively supported nor contradicted by the evidence MacLeod and Hills have so far presented. Even if the Currier is in part Neocomian as suggested by MacLeod and Hills' Buchias and *Herzogina*, the Currier may only be as young as the earliest Cretaceous (Berriasian), allowing most of the Neocomian for an hiatus or unconformity. The occurrence of such an unconformity is consistent with the well established regional unconformity known from Lower Cretaceous strata elsewhere in the Canadian Cordillera, both along the margins of the Bowser basin (Eisbacher 1974; Tipper and Richards 1976) and within the Western Canada Sedimentary Basin (Stott 1982). Because there is no compelling reason to change views, I elect to stand by the proposal that a unconformity **probably** separates the Currier and McEvoy Formations in the study area (although perhaps of somewhat briefer duration than Kimmeridgian or Tithonian to Barremian span originally proposed.).

# REFERENCES

Bell, W. A. 1956. Lower Cretaceous floras of western Canada. Geological Survey of Canada, Memoir 285.

Bustin, R. M., and Moffat, I. 1983. Groundhog Coalfield, British Columbia: reconnaissance stratigraphy and structure. Bulletin of Canadian Petroleum Geology, v. 31, p. 231-245.

Caldwell, W. G. E. 1984. Early Cretaceous transgressions and regressions in the southern interior plains. *In* The Mesozoic of middle North America. *Edited by* D. F. Stott and D. J. Glass. Canadian Society of Petroleum Geologists, Memoir 9, p. 173-203.

Cookenboo, H. O., and Bustin, R. M., 1989. Jura-Cretaceous (Oxfordian to Cenomanian) stratigraphy of the north-central Bowser Basin, northern British Columbia. Canadian Journal of Earth Sciences, v. 26, p. 1001-1012.

Cookenboo, H. O., and Bustin, R. M., 1990. Stratigraphy of coal occurrences in the Bowser Basin. *in* Geological Fieldwork 1989. British Columbia Ministry of Energy, Mines and Petroleum Resources, Paper 1990-1, p. 473-477.

Eisbacher, G. H. 1974. Sedimentary and tectonic evolution of the Sustut and Sifton Basins, north-central British Columbia. Geological Survey of Canada, Paper 73-31.

Frebold, H. 1961. The Jurassic faunas of the Canadian Arctic. Geological Survey of Canada, Bulletin 74.

Frebold, H., and Tipper, H. W. 1970. Status of the Jurassic in the Canadian Cordillera of British Columbia, Alberta, and southern Yukon. Canadian Journal of Earth Sciences, v. 7, p. 1-21.

Gulf Canada Resources Limited 1984. Mount Klappan property. British Columbia Ministry of Energy, Mines and Petroleum Resources, Open File Report 111.

Gulf Canada Resources Limited 1987. Lost Fox property. British Columbia Ministry of Energy, Mines and Petroleum Resources, Open File Report 723.

Hall, R. L. 1984. Lithostratigraphy and biostratigraphy of the Fernie Formation (Jurassic) in the southern Canadian Rocky Mountains. *In* The Mesozoic of middle North America. *Edited by* D. F. Stott and D. J. Glass. Canadian Society of Petroleum Geologists, Memoir 9, p. 233-247.

Jeletzky, J. A., and Tipper, H. W. 1968. Upper Jurassic and Cretaceous rocks of Taseko Lakes map area and their bearing on the geological history of southwestern British Columbia. Geological Survey

of Canada, Paper 67-54.

Kleinspenh, K. L. 1985. Cretaceous sedimentation and tectonics, Tyaughton-Methow Basin, southwestern British Columbia. Canadian Journal of Earth Sciences, v. 22, p. 154-174.

Lowey, G. W., and Hills, L. V. 1988. Lithofacies, petrography and environments of deposition, Tantalus Formation (Lower Cretaceous) Indian River area, west-central Yukon. Bulletin of Canadian Petroleum Geology, v. 36, p. 296-310.

MacLeod, S. E., and Hills, L. V. 1990a. Conformable Late Jurassic (Oxfordian) to Early Cretaceous strata, northern Bowser Basin, British Columbia: A sedimentological and paleontological model. Canadian Journal of Earth Sciences, v. 27, p. 988-998.

MacLeod, S. E., and Hills, L. V. 1990b. Conformable Late Jurassic (Oxfordian) to Early Cretaceous (Aptian) strata, northern Bowser Basin. Geological Association of Canada/Mineralogical Association of Canada Annual Meeting, Program with Abstracts, v. 15, p. A80.

May, F. E., and Shane, J. D. 1985. An analysis of the Umiat delta using palynological and other data, North Slope, Alaska. *In* Geology of the Nanushuk Group and related rocks, North Slope, Alaska. *Edited by* A. C. Huffman. United States Geological Survey, Bulletin 1614, p. 97-120.

Moffat, I. W. 1985. The nature and timing of deformational events and organic and inorganic metamorphism in the northern Groundhog Coalfield: implications for the tectonic history of the Bowser Basin. Ph.D thesis, University of British Columbia, Vancouver, B.C.

Moffat, I. W., and Bustin, R. M. 1984. Superposed folding in the northern Groundhog coalfield; evidence for polyphase deformation in the northeastern corner of the Bowser basin. *In* Current research, part B. Geological Survey of Canada, Paper 84-1B, p. 255-261.

Moffat, I. W., Bustin, R. M., and Rouse, G. E. 1988. Biochronology of selected Bowser Basin strata: tectonic significance. Canadian Journal of Earth Sciences, v. 25 p. 1571-1578.

Smiley, C. J. 1969a. Cretaceous floras of the Chandler-Colville region, Alaska: stratigraphy and preliminary floristics. American Association of Petroleum Geologists Bulletin, **53**:482-592.

Smiley, C. J. 1969b. Floral zones and correlations of Cretaceous Kukpowruk and Corwin Formations, northwestern Alaska. American Association of Petroleum Geologists Bulletin, v. 53, p.2079-2093.

Spicer, R. A. 1987. Late Cretaceous floras and terrestrial environment of northern Alaska. *In* Alaskan North Slope geology. *Edited by* I. Tailleur and P. Weimer. Society of Economic Paleontologists and Mineralogists, v. 50, p. 497-512.

Stott, D. F. 1963. Stratigraphy of the Lower Cretaceous Fort St. John Group, Gething and Cadomin Formations, Foothills of northern Alberta and British Columbia. Geological Survey of Canada, Paper 62-39.

Stott, D. F. 1968. Lower Cretaceous Bullhead and Fort St. John Groups between Smoky and Peace Rivers, Rocky Mountain Foothills, Alberta and British Columbia. Geological Survey of Canada, Bulletin 152.

Stott, D. F., 1982. Lower Cretaceous Fort St. John Group and Upper Cretaceous Dunvegan Formation of the Foothills and Plains of Alberta, British Columbia, District of Mackenzie and Yukon Territory. Geologic Society of Canada, Bulletin 328.

Tipper, H. W., and Richards, T. A. 1976. Jurassic stratigraphy and history of north-central British Columbia. Geological Survey of Canada, Bulletin 270.

Vachrameev, V. A., 1978. The climates of the northern hemisphere in the Cretaceous in light of paleobotanical data. Paleontological Journal, V. 12, 143-154.